POLITECNICO DI TORINO

Master's Degree Course in Automotive Engineering

Master's degree Thesis

Modelling and simulation of a hydraulic interconnected suspension system for automotive applications

Supervisors:
Prof. Alessandro Vigliani
Prof. Enrico Galvagno

Candidate:
Francesco Carlomagno

December 2020

Ai miei Genitori

Abstract

The design of a vehicle's suspension system has the main task to find the best trade-off between the handling capability of the vehicle and the ability to filter the road irregularities. Since the early stage of the automotive industry, different types of solutions have been introduced to maximize at same time both requirements and, one of these, are the passive interconnected suspensions that provide a linkage between the front and the rear axle.

This work proposes a fluid-mechanical interconnected suspension system with the aim to uncouple the pitch and heave modes from the roll and warp ones, and to realize a soft warp mode.

The initial part of the document presents a detailed description of the different archetypes presented up to now in the literature and in the industry, highlighting the tests and the results declared.

Afterwards, the main part of the thesis's project regarding the modelling of the fluid-mechanical system is illustrated: a physical model that replicate the whole interconnected suspension system is elaborated in Simscape environment.

The analysis of the system on the vehicle dynamics has been carried out in co-simulation environment between Simscape and Vi-CarRealTime package, where a comparison between a high-performance vehicle model in conventional configuration and with the interconnected suspensions is evaluated in standard manoeuvres and in lap time simulations.

Contents

1 Introduction

The present chapter is organized in five paragraphs where the first is dedicated to an introduction at the interconnected suspensions, for the purpose of introduce at the lector what the word 'interconnected' means and which are their features; in the second chapter are described the different solutions proposed by Universities and Industry. The third paragraph illustrate the interconnection modelling solutions exposed in literature while the fourth describe the results coming from tests or simulations published. Finally, this chapter ends with a paragraph dedicated to the introduction at present work and to its purposes.

1.1 Background

The suspension is a system that has two functions, the first is to isolate the vehicle body from road irregularities and the second is to control the relative motion, forces and moments between the tires and the sprung mass. These functions are explicated by mechanical linkages, restoring and damping element, such as springs and dampers.

The suspension system has a fundamental role in the definition of vehicle handling and ride behaviour. Generally, in a conventional suspension system these two requirements are opponent, such as to improve the handling is required high stiffness and high damping in order to minimize the tire vertical load variation, while to improve the comfort is required a softer setup to filter the excitations coming from the road surface. So, in this scenario, since the beginning of automotive industry have appeared the interconnected suspensions and more recently active/semi-active suspensions, in order to find a trade-off between these two objectives.

The interconnected suspensions are a system in which the displacement of a wheel induces a force on another wheel station [1], so their application allows to the designers to get a deeper control over the stiffness and damping of each suspension mode, instead of being completely defined by the single-wheel stiffness and damping. In general, these solutions are passive, so it means that no power must be supplied by a hydraulic or electric unit and no electronic control units are used.

The term suspension mode describes the simultaneous vertical motion of wheels (unsprung masses) relative to the vehicle body (sprung mass) [2]. For a vehicle it is possible to define four modes (Fig.1):

- *Heave*, when all wheels are in phase;
- *Pitch*, when the wheels of the same axle (front/rear) are in phase each other but out of the phase with wheels of the other axle;
- *Roll*, when wheels of the same side (right/left) are in phase each other but out of the phase with wheels of the other side;
- *Warp* or *articulation mode*, when the wheel of one diagonal are in phase each other but out of the phase with the wheels of the other diagonal.

To each of the mode some characteristics of the vehicle dynamics behaviour can be associated and a suspension that is able to decouple the different modes, so that for each mode is possible to assign a proper value of stiffness and damping, represent the optimal way to reach the trade-off between ride and handling.

Heave is the mode that carry the static load due to the mass of the vehicle and the aerodynamic downforce. In general, for all type of vehicle it is desired a slight rising rate for low wheel travel to improve the comfort, while a rigid progressive springing is preferable in case of highly loaded vehicle to avoid abrupt contact at end of suspension travel. In case of race cars, a rigid heave mode is always desirable, due the fact that aerodynamic downforces generation is very sensitive to ride heights variations.
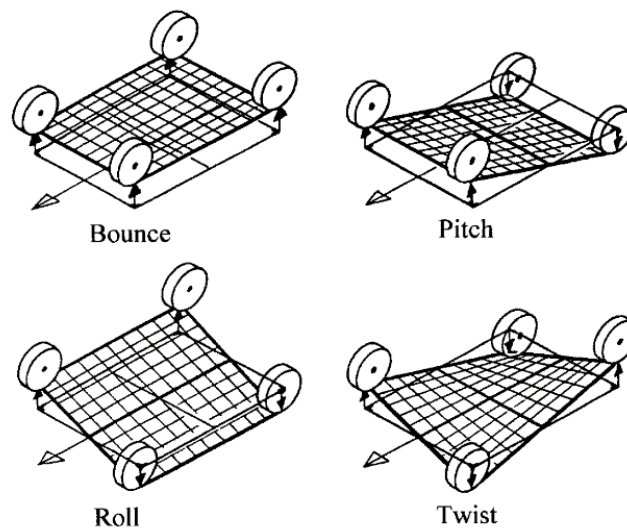

Fig. 1. Suspension modes [3]

10

Pitch is the mode that is activated when a vehicle is accelerating or decelerating due the fact that generally the suspensions are designed with the pitch centre below the centre of gravity of the vehicle and so the body tends to 'dive' or 'squat' (angular movements around y-axis of a vehicle) as a consequence of the inertial longitudinal acceleration. Pitch mode is the most suited to absorb road bumps and for this reason is strictly linked with the ride and comfort of the vehicle and so, in case of passenger car a quite soft configuration with a linear behaviour is preferred. For the race cars is still valid what said for heave mode.

Roll mode is the most important for car directional stability and handling performance. When a vehicle is in a cornering phase, the centrifugal force generates a moment that act on longitudinal axis of the vehicle body. The designers want a stiff roll mode with a linear and symmetric trend to eliminate the roll angle due the fact that it is uncomfortable and it is the cause of wheel camber variation and roll steer that reduce the contact area between the tire and the road and so, the capability of the tire to applicate a force on the road surface. Also, in case of vehicle with a high centre of gravity as the SUVs or commercial vehicles, a stiffer roll mode allows to reduce the roll-over risk.

Warp mode is quite different with respect the others. Indeed, it is activated only by road irregularities or by the presence of banking and inclination angle of the road surface; so, in case of an ideally perfectly flat road it is not present. An ideal warp mode should be free to move and totally unsprang, so that no spring or damper displacement must occurs. A stiff warp mode penalizes the handling and the grip capabilities of the tires because it induces vertical wheel load variation and avoid the tire to follow the road irregularities reducing the contact with the road surface (Fig.2). In a vehicle with a conventional suspension system the warp stiffness is the same of the roll stiffness, so it means that a vehicle in a cornering phase on an irregular road will be subjected to a non-controllable vertical load variations between the axles that will change its balance, inducing understeer or oversteer as function of road profile. Also to give better the idea, when a car with a stiff twist mode is parked on uneven ground, then the pair of diagonally opposite wheels that are on the high ground will carry most of the weight of the car, while the other pair of wheels will carry less weight. A soft twist-mode allows the four wheels contact patch to accommodate to any unevenness of the ground, and thus share the vertical loads that act on the car [3].
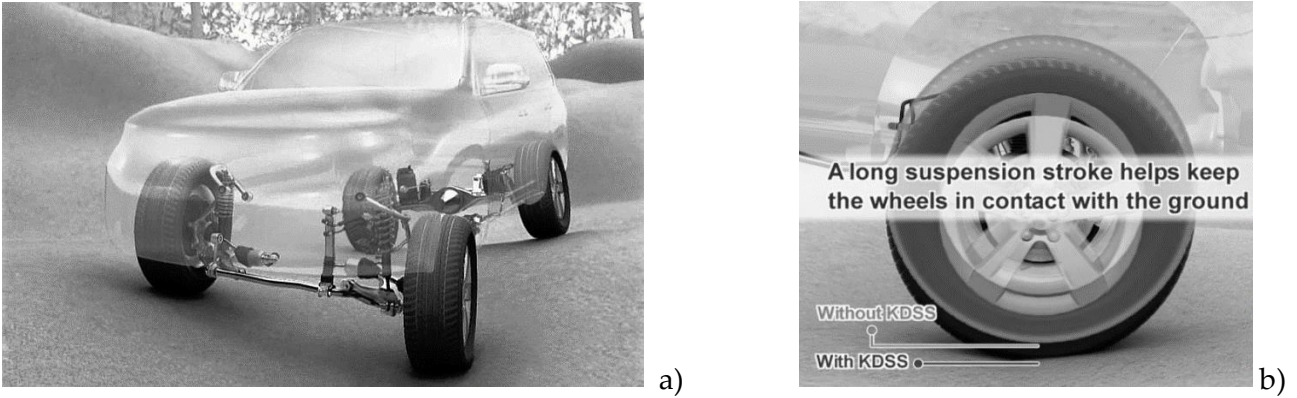
Fig.2 a) An off-road warp excitation. b) differences of the same vehicle provided ad not provided with the KDSS system capable to reduce warp stiffness: a soft warp mode allows to increase the wheel travel and as consequence the tire contact area with road surface. [4]

In normal vehicle operation is not possible to individuate a single mode of operation, but a combination of the four mode, so that the stiffness and the damping of each wheel is always the linear combination of the four different modes.

While layouts that allow to interconnect all vehicle corners are uncommon, some typologies of two-wheels interconnections are used in all vehicles. The interconnections typologies are divided by Ortiz [5] in:

- *Anti-synchronous interconnections*, made through *Z-bars*, that stiffen in-phase suspension motion;
- *Anti-oppositional interconnections*, by means of *U-bars*, that stiffen out-of-phase suspension motion;

In table 1 is possible to find the effects of these interconnections.

Type of interconnection	Type of wheel pairing		
	Same end (front/rear)	Same side (right/left)	Diagonally opposite
Anti-synchronous (Z-bar or third spring)	Stiffens pitch & bounce	Stiffens roll & bounce (e.g. Hydragas)	Stiffens bounce & warp
Anti-oppositional (U-bar or T-bar)	Stiffens roll & warp (e.g. anti-roll bar)	Stiffens pitch & warp	Stiffens roll & pitch

Table 1. Wheel pair interconnections developed by Ortiz [5]

1.2 Applications

Since the beginning of automotive industry different kinds of solutions to increase the ride and handling capabilities of the vehicles have been introduced: the interconnected suspensions are one of them. Referring to passive solutions, it is possible to individuate three typologies of interconnections:

- Mechanical;
- Hydro-pneumatic;
- Hydraulic.

1.2.1 Mechanical interconnections

Referring to front-rear interconnections, one of the most famous and earlier solution it is the suspension system installed on the Citroen 2 CV (Fig.3); this car has been built from 1948 to 1990 and it has become known for its simplicity, low maintenance costs and versatility. Both the front and the rear have been provided with two trailing arms connected each other through a bell-crank and push rod to a cylinder installed horizontally with respect the vehicle body. The coil springs gives the stiffness to the system, while the damping is given by friction dampers.
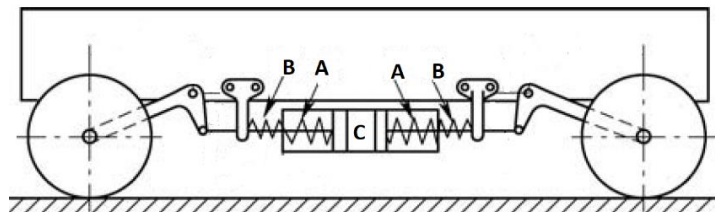

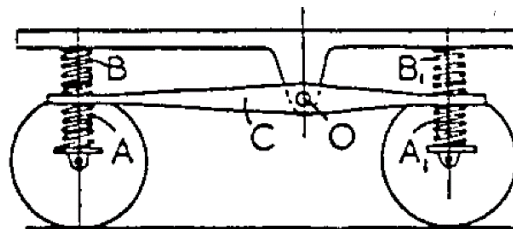Fig.3 Real scheme of 2 CV interconnected suspension [2]

Fig.4 Conceptual scheme of interconnection [9]

The benefit of these scheme is to have a soft pitch mode that improves the ride and the bump absorption capability and, at same time, a rigid heave mode that increase the load capacity. These results have been possible by the interconnection scheme, where front and rear wheels are connected to element C through two springs, A and B, of different stiffness. The A spring is

softer and allows to have a low pitch ride frequency, while B is stiffer in order to have a high load carry capability. As it possible to see from the conceptual scheme of Fig.4, in case of front bump the soft A spring is compressed at front and the rotation of the plate C compresses the A spring on the rear: the pitch motion is reduced. Also, working as a 'Z-bar', also the roll mode is stiffened, increasing the stability in corners.

In the 1968 the inventor William Allison proposed a front-rear interconnection using torsion bars (Fig.4). The vehicle is provided with simple trailing arms both at front and rear, but on each side a torsion bar (24 and 22 in the Figure) that link them is installed in order to stiffen the roll and the bounce mode.
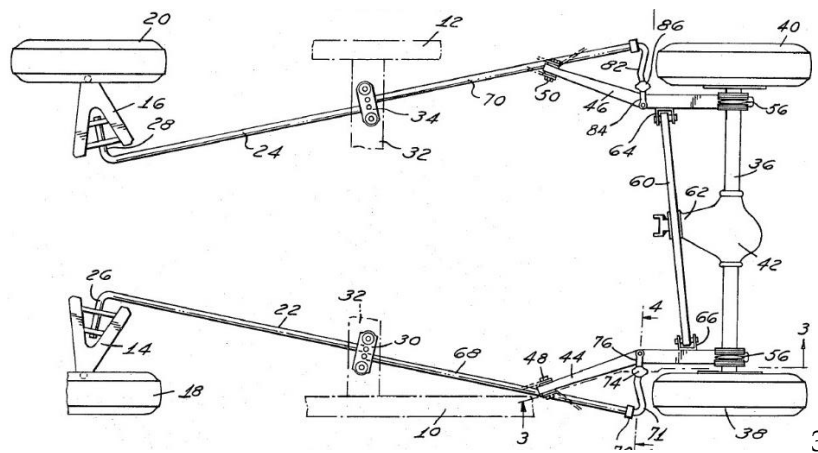

Fig. 4 The front-rear interconnection proposed by Allison [10]

Going to more recent applications, the anti-roll bar is a kind of two-wheels mechanical interconnection that is widespread in all kind of vehicle and it is possible to classify it as U-bar, due the fact that it acts when the wheels of the same axle moves out of phase, while, in case of in-phase motion, it has a null effect on the total stiffness of a single wheel. Its application is motivated by the fact that in a conventional suspension system with a damper-coil spring element for each vehicle corner, the designers decide the stiffness of the coil spring as function of the natural ride frequency desiderated (a common passenger car suspension has a front ride frequency from 1,2÷2,0 Hz, lower value could cause sickness while higher values bring to a unpleasant ride comfort), and then increase the roll stiffness by means of the roll bar to improve the stability in corners and the handling. The anti-roll bars in general are very simple, in fact the interconnection is realized through torsion bar activated by links jointed to suspension arms (Fig.5). In the last decades some active anti-roll bar that exploit hydraulic or electro-mechanic system have been introduced in premium cars.

Another type of two-wheel mechanical interconnection is what is called in motorsport environment 'third-element': it has a function of a Z-bar and connects the wheels on the same axle to stiffen the pitch and the heave mode. As stated before, in racecars there are completely different requirement to fulfil with respect passenger cars, indeed the comfort is no longer a requirement, but all choices are directed to the improvement of the performances and so, as in the case of high downforce race cars, an important aspect is to maintain a low ride heights variation as function of the speed, and for this reason the third springs is used. The third element can be actuated directly by the push/pull rods (Fig. 6a) or by a set of rods and a rocker arm (Fig. 6b).
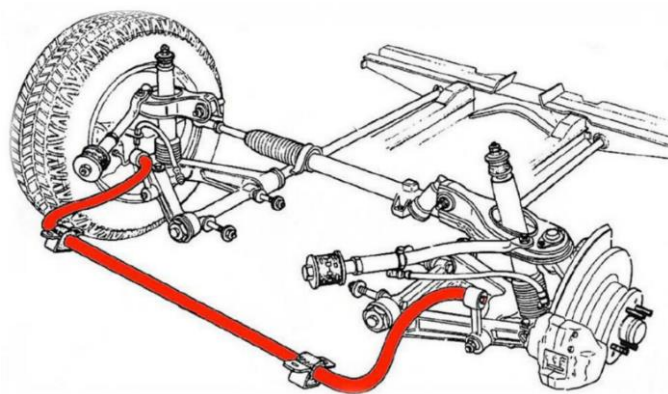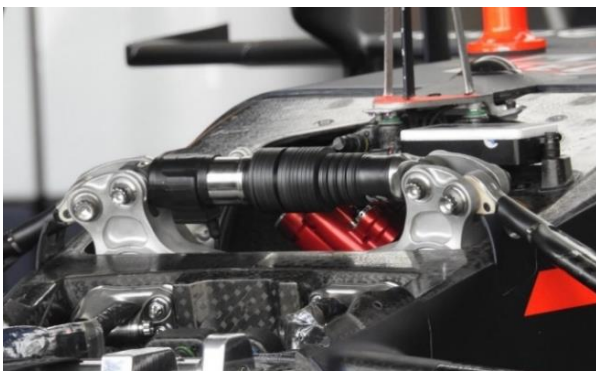

Fig. 5 Torsion bar [6]

a)

b)

Fig 6a) A typical F1 heave spring-damper installation with disc spring elements, Red Bull F1 team 2019 [7];
6b) A third spring-damper (black) actuated by rods and rocker arm mechanism [8].

Another interesting mechanical application is what is proposed by Mercedes AMG with the Project 1 road legal hyper-car, whose concept was presented in 2017. This car abandons the conventional scheme of a spring-damper system for each wheel in favour of a Z-bar and a T-bar for each axle to control respectively the pitch and the roll of the axle in an independent way (Fig. 7). Indeed, the bars are represented by two spring-damper system which activation is demanded to an appropriate rocker arm mechanism, that in case of symmetric wheel travel can compress the heave spring-damper while the point of actuation of the roll-spring damper are subjected to a rotation so that this element is not compress. The opposite happens in case of roll. This solution has the advantage to set two different springing and damping characteristic between roll and damping, increasing the freedom for the designers to optimize the performance of the vehicle, considering the different requirements for aerodynamics, handling and comfort.
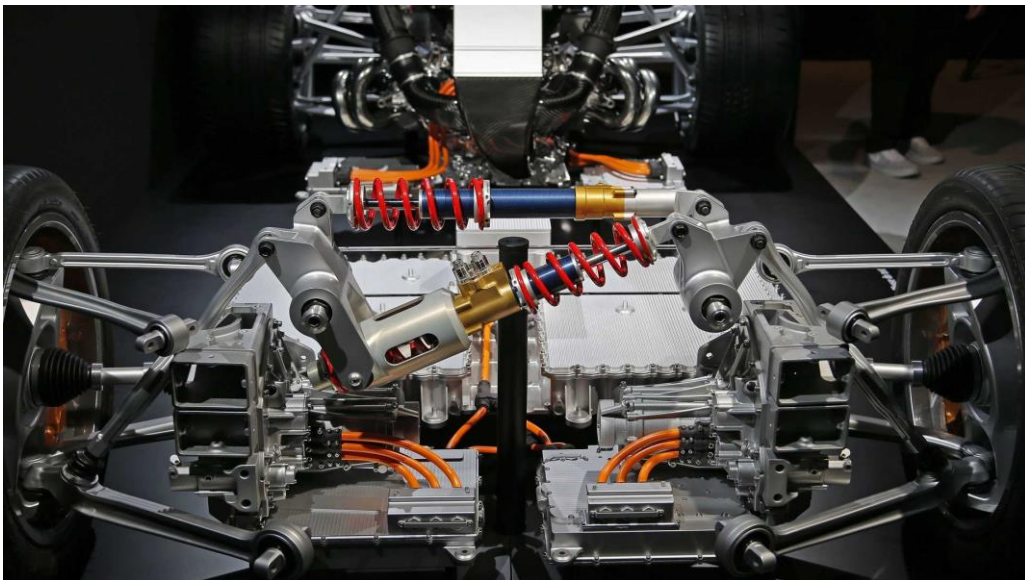

Figure 7 Mercedes-AMG Project 1 front suspension system, 2017. The horizontal element is the pitch spring-damper, while the oblique is the roll one [29].

1.2.2 Hydro-pneumatic interconnections

In the '70s Moulton introduce a new kind of interconnection between front and rear axle, using hydraulic connection pipes and pneumatic accumulators. The scope of this system is the same of the 2 CV suspension, so to reduce the stiffness of the pitch mode and improve the comfort in case of road irregularities. The system is made by a piston linked to suspension arm that act on cylinder fill with oil and connected with a pipe to the front axle wheel; a flexible membrane separates the cylinder from a pneumatic accumulator filled with high pressure gas.

The work modalities are represented in Fig. 8: in case of pitch or warp (front wheel up and rear wheel down) the oil goes from the front chamber to the rear chamber without acting on the membrane, so low stiffness is obtained; in case of bounce or roll (front and rear wheels both up or down) the oil can't flow between the two cylinders, then the it press against the lower side of the membrane which deflection is contrasted by the high pressure gas, so higher stiffness is obtained.
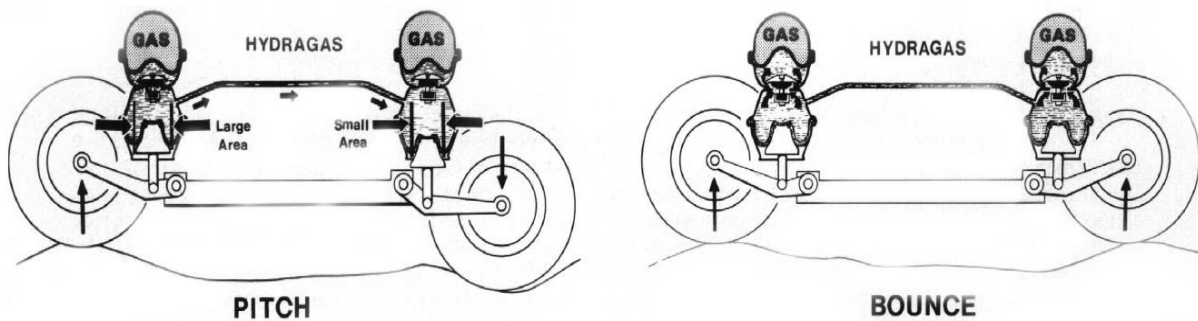

Fig. 8 Moulton's Hydragas behaviour on pitch and bounce mode [11]

Experimental tests, conducted by authors in [11] on different kinds of car segments to evaluate the vertical acceleration perceived by passengers with and without the Hydragas suspensions, have showed a significant improvement of ride performances at low frequencies of excitation, while, for higher frequencies (above 15 Hz) not a unique trend is evident.

1.2.3 Hydraulic interconnected suspension (HIS)

These types of interconnections are the most diffused in the different applications due to their greater flexibility in the vehicle packaging and installation.

The first concept dates back even in the 1927 with the idea of an American engineer called Hawley, who patent a system composed by double acting cylinders, in place of shock absorbers, connected on the same axle through pipes (Fig.8). The author's declared aim was to increase the energy absorption capability of the shock absorbers and to compensate the movement of one corner wheel with which of the other side wheel, reducing the roll motion [12].
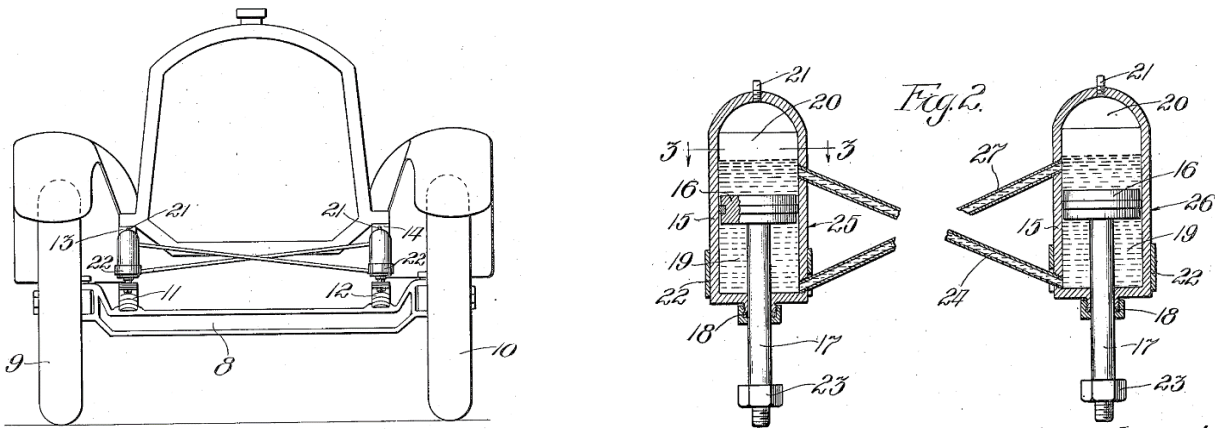

Fig. 8 Hawley's shock absorbers interconnection patent, 1927 [12]

More recently E. Zapletal proposed a new concept of suspension, called 'Balanced Suspension', that theoretically can fully decouple the suspension modes and to set in an independent way the stiffness and the damping of each mode. The system exploits hydraulic pipes to connect the front shock-absorbers to a mechanical central unit, that using specific linkages is able to guarantee an independent control of each mode, such as high roll stiffness and soft warp mode (Fig. 9).
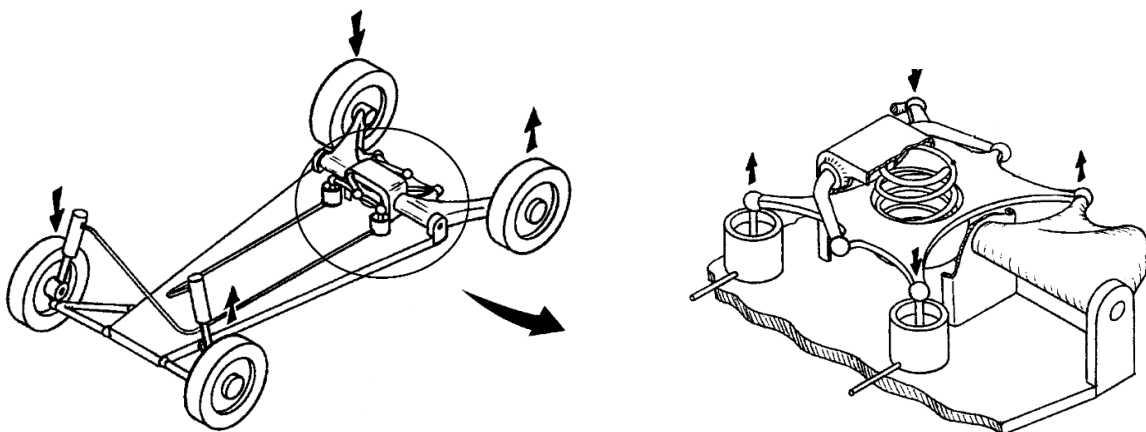

Fig.9 Balanced suspension proposed by E. Zapletal [3]

In 2002 J. Fontdecaba in [13] proposed a Hydraulic scheme that is able to decouple the modes and evaluated the potential benefits through experimental tests on a SUV. The system consists of four hydro-pneumatic accumulators actuated by suspension linkages that defines the stiffness and daming for roll mode; all accumulators are hydraulically connected by means of pipes to a hydraulic central unit, also provided with hydro-pneumatic accumulators, that is able to reduce the pitch and heave stiffness, and by a means of a iso-static valve, it is able to free the articulation motion.

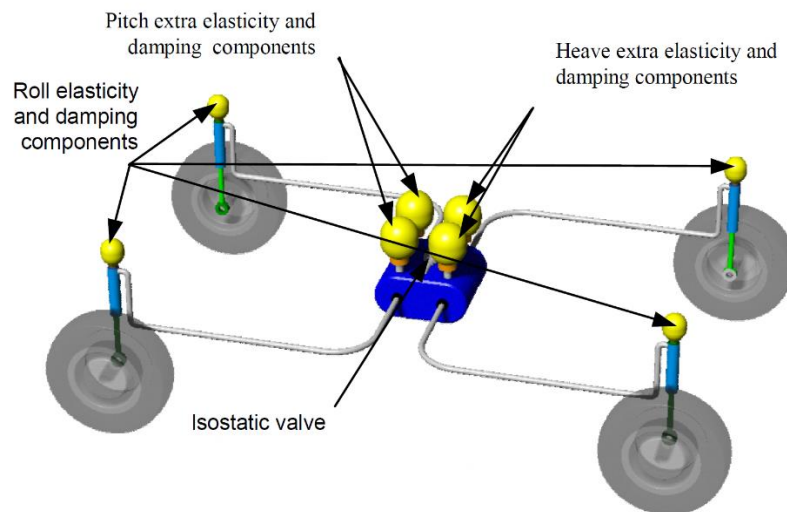The scheme of the system is illustrated in Fig. 10.

Fig. 10 Fontdecaba's suspension [13].

Smith and Walker, of the Cambridge University, presented in [14] a hydro-mechanical connection that ideally should be capable to decouple suspension modes. They substitute the classical shock-absorber with a hydraulic actuator activated by suspension rockers, that send oil to a central unit, where, by mechanical leverage called kinematic constraint mechanism (KCM), they are able to activate four spring-damper system, each one for each suspension mode (Fig. 14).

A similar concept was applied by the members of AMZ Formula Student team of ETH of Zurich for the 2017 race car design. They used a passive hydraulic system to fully decouple the suspension modes, by using hydraulic actuators connected on the suspension push rods that send fluid in four double acting hydraulic cylinders where
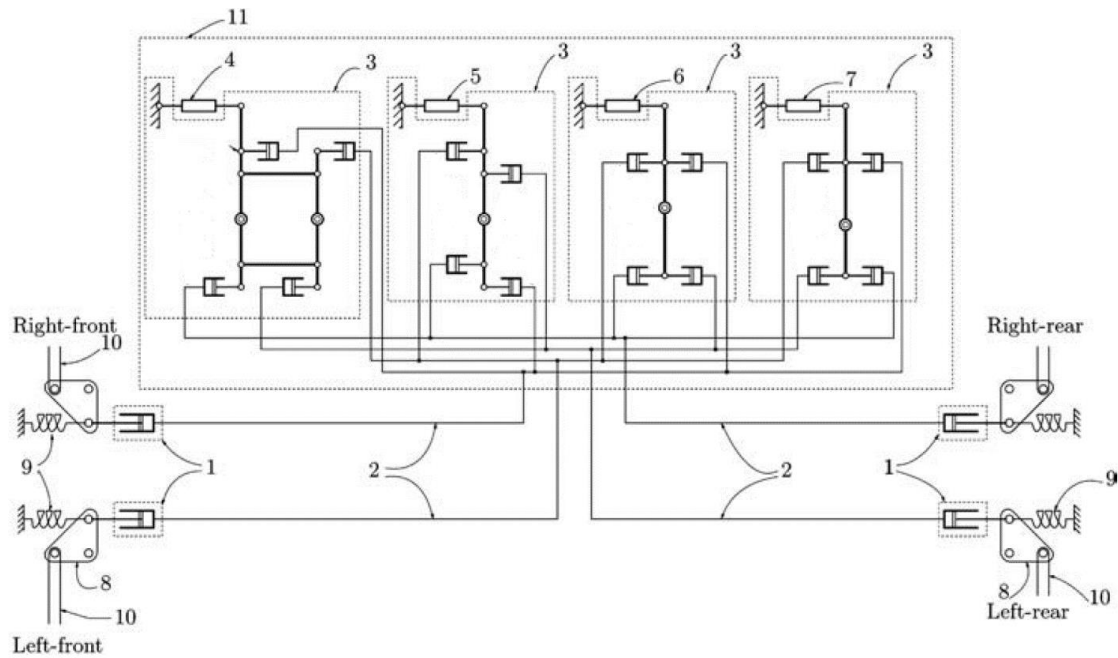
Fig. 14 Interconnection by means of kinematic constrain mechanism (1 acturator; 2 Hydraulic circuit; 3 KCM; 4-7 damper-spring elements for bounce, pitch, roll and warp; 8 rocker mechanism; 9 pre-load spring; 10 suspension rods; 11 central unit) [14]

pistons can move axially activating three air spring elements. The movement of the pistons is controlled by the pressure and the amount of oil sent by each wheel corners and by the kind of interconnection (Fig. 15a). Three translational spring-damper elements are used to control the springing and the damping of heave, pitch and roll mode while the warp mode is integrated in the roll element, where they substitute the warp element with a lever arm that is able to free the articulation mode cancelling the warp springing and that is used also to change the front-rear roll balance[15]. Furthermore, they install a rotational damper to suppress the warp oscillation coming from tires behaviour.

An interesting video of the system in action is available at [16].

A widely diffused application is the KDSS (Kinetic Dynamic Suspension System) developed by the australian Kinetic Pty LTD, nowadays acquired by Tenneco. This system is appeared in the late '00s and is still present on some SUVs of the Toyota group. It allows to engage and disengage the front and the rear anti-roll bar through a hydraulic system composed by two double acting cylinders (one for axle) improving both the performances on roads and on off-road condition (Fig. 16)
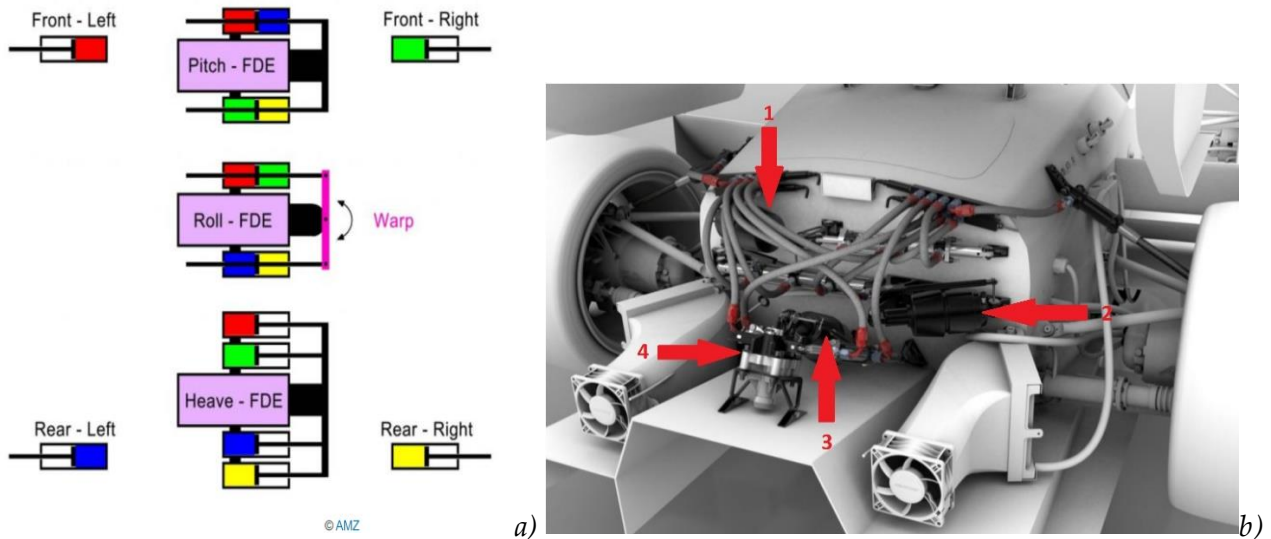
Fig 15 a) Schematic of hydraulic connection and spring-damper unit activation; b) Real system application (1 Pitch spring-damper, 2 heave spring-damper, 3 Roll spring-damper, 4 lever arm mechanism). [15]

In case of roll on flat road, the fluid remains still inside the circuit and the pressure of the oil is the same of which of pneumatic accumulators, so the anti-roll bars are engaged, improving handling capability and safety. In case of off-road, the movement of the wheels induce the oil to move from rear to front, pushing down the pistons that disengage the anti-roll bars, allowing a higher wheel travel and a better contact with the ground (Fig. 2). In case of small irregularities, the dampers inside the accumulators dampen the vibration increasing the ride performances.
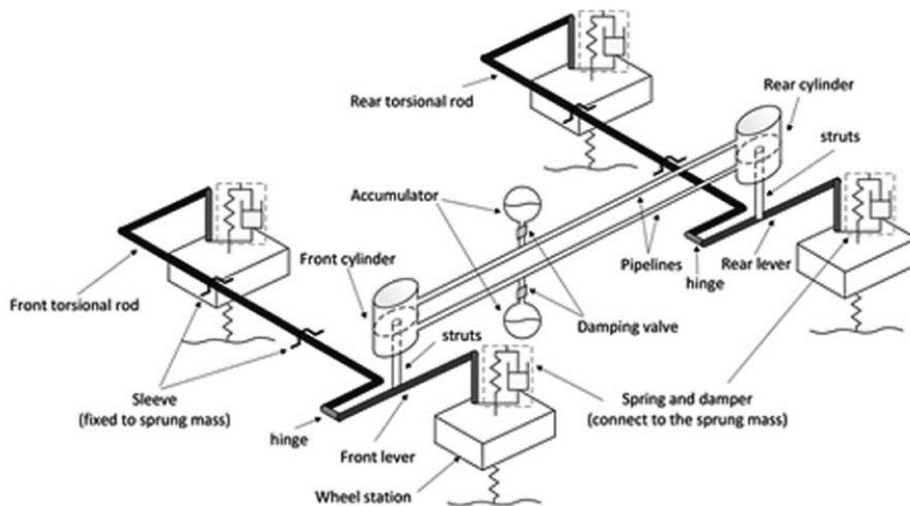

Fig. 16 KDSS suspension system [17]

The same company Kinetics Pty LTD has over 100 patents on different hydraulic interconnection schemes, including both interconnection in the roll plane and in the pitch plane. One of the most common schemes is the 'H2', an interconnection in the roll plane obtained with two side-symmetric hydraulic circuits, represented in the Fig.17:
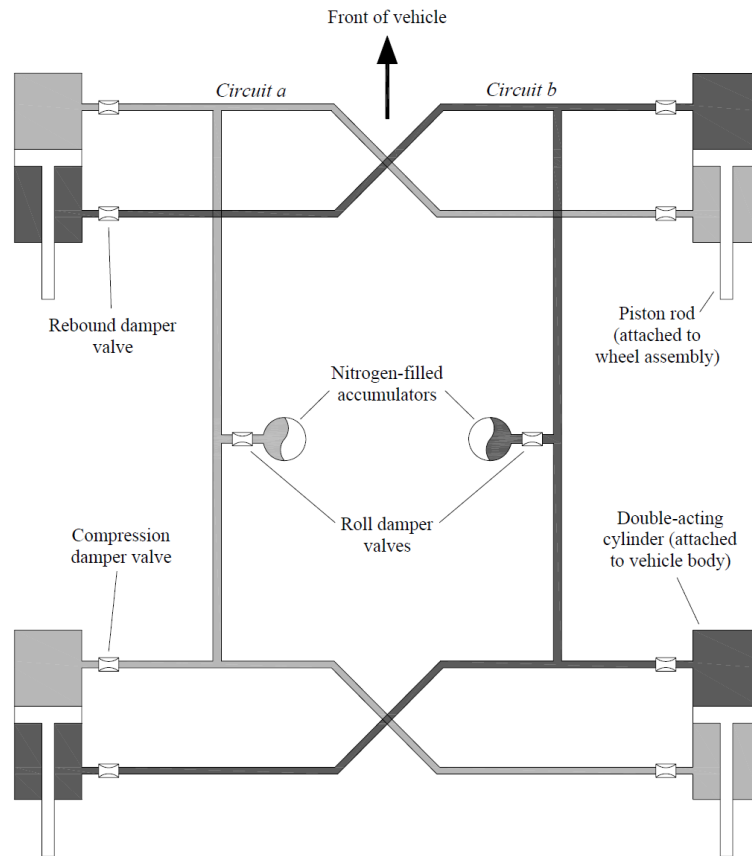

Fig. 17 H2 hydraulic arrangement [2]

The H2 kinetic configuration is composed by four double acting cylinders connected to wheels by suspension rods, ten damping valve, two nitrogen accumulators and pipes. Generally, the vehicle on which is installed can maintain the restoring elements to carry the weight of the body, but the damping is given by the compression and rebound valve integrated into the cylinders.

In heave mode the oil flows from the upper chamber of each cylinder to the lower chamber of the opposite side cylinder; due the presence of the rod, the volume of oil outgoing and ingoing are different, so the remaining volume flows through the roll valve into the accumulators, slightly contributing to heave damping.

In roll mode the top chambers of one side have outgoing flow, the bottom ingoing, while, in the other circuit the opposite situation; the only way where the displaced volume can go is into the

roll accumulators: the roll dynamic properties are given by the roll valve setting and the pressure of the nitrogen inside the accumulator.

In pitch and warp mode the flow is displaced by the different chambers and not inside the roll accumulators, so these modes are not affected.

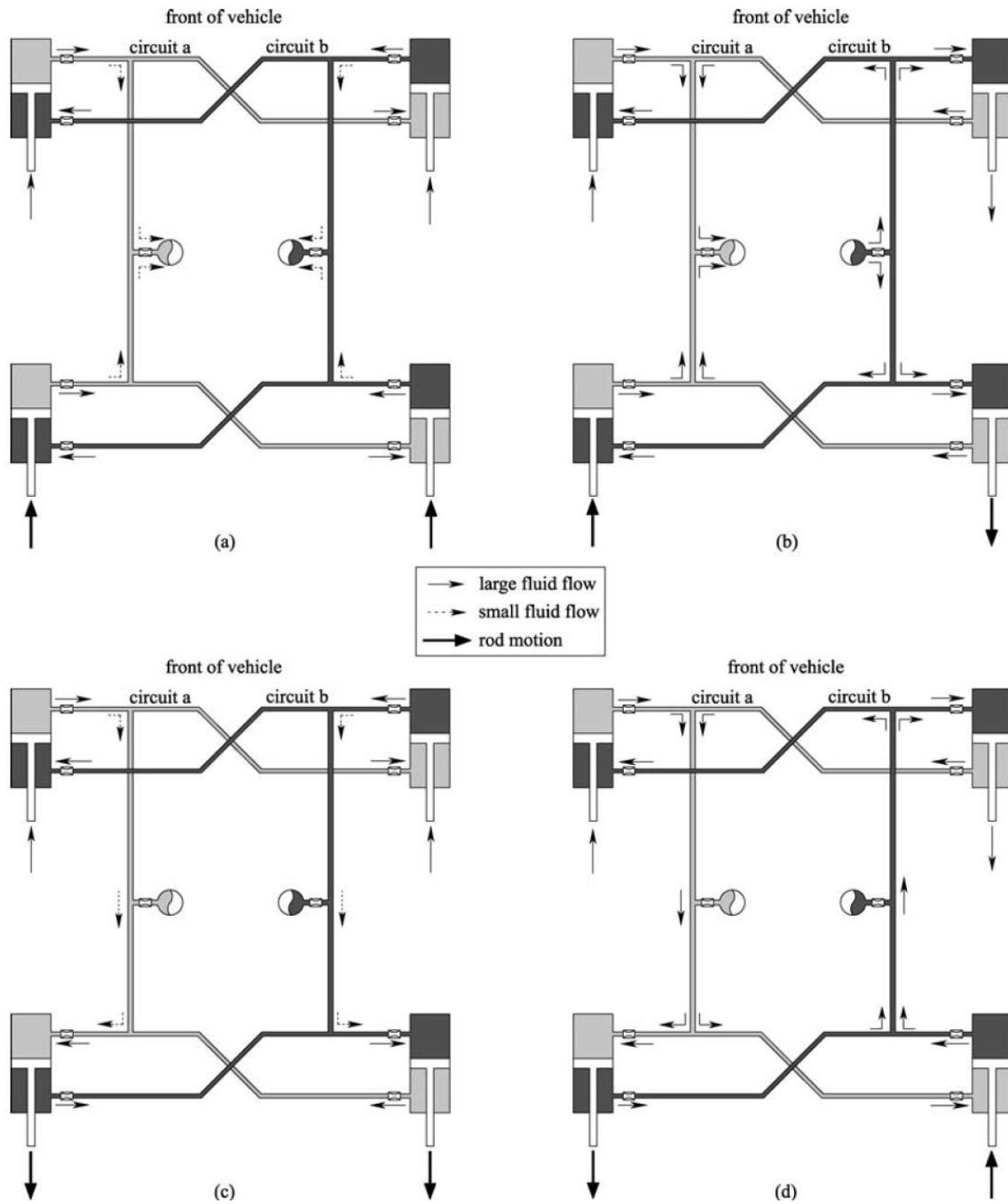A schematic illustration of what has been said above is in Fig.18.

Fig. 18 Ideally actuation in the different suspension mode: (a) heave, (b) roll, (c) pitch, (d) warp. [2]

Based on the H2 configuration, McLaren has developed a semi-active suspension system called 'Pro-active Chassis Control', installed on more extreme passenger cars starting from 2017 thanks to the collaboration with the company Tenneco. The main differences with H2 layout of Fig. 17 are that there are four accumulators instead of two, and, that the bound and rebound dampers' rates are continuously adjustable by means of a needle valves and solenoids electronically controlled.

This solution has different benefits: increase of roll stiffness, so better performances and stability in corners without penalize the comfort; soft articulation mode, so the road surface irregularities have not effects on the vertical load distribution to all vantage of a neutral dynamic behaviour. The overall scheme layout is presented in Fig. 19.
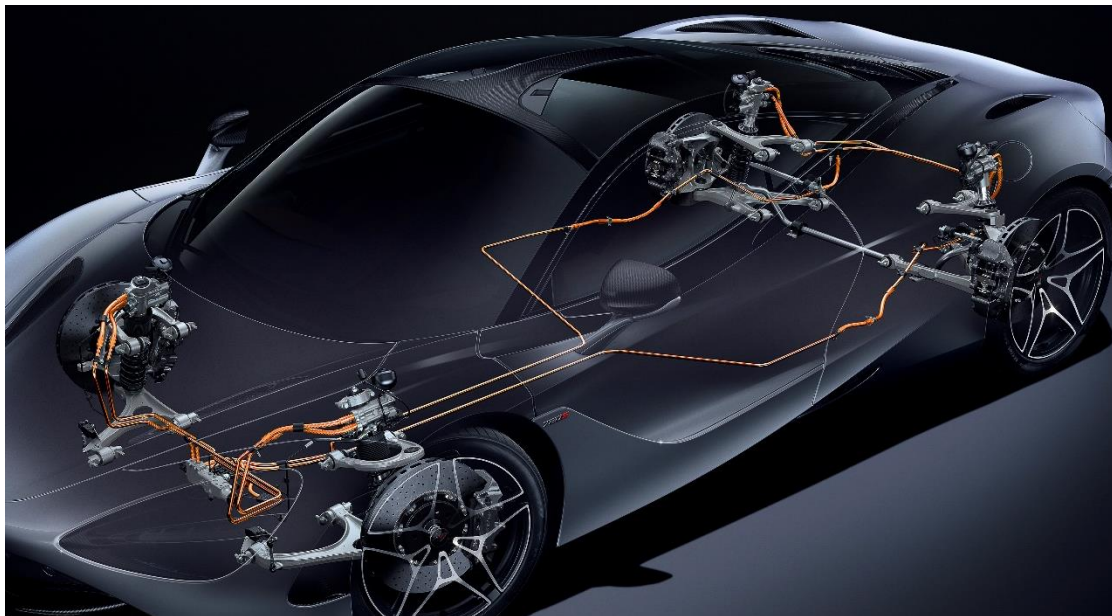

Fig. 19 McLaren hydraulic interconnection applied on 720S [18].

Just as a mention, interconnection configurations between front and rear were also present in the most acclaimed racing championships. Citroen and Mitsubishi developed hydraulic interconnected suspension respectively for the World Rally car series and for the Dakar Rally series, but due the huge advantages given by these systems, starting from 2006 were banned.

In 2013 interconnected suspensions appeared also in F1 with the name "FRICS" (Front Rear InterConnected Suspension). This system has become famous with the Mercedes W05 but also other teams, as Red Bull, have it. It was developed in order to increase the pitch stiffness in order to reduce the ride height variations: aerodynamics designer could optimize the downforces around a small window of ride heights, reducing compromises, as done in the '90s with active suspensions. The system was banned in 2014 due its complexity and because judged as an 'active' aerodynamic component.

1.3 Proposed Modelling in Literature

1.3.1 Ideal interconnection Modelling

The advantage of an ideal passive decoupling scheme on the vehicle dynamics was explained by J. Fontdecaba in [13] using a simple mathematical formulation. In fact, neglecting for the moment the damping, the type of interconnection etc, the stiffness of each suspension mode can be linked with the wheel displacements (assuming x_{fr} front right, x_{fl} front left, x_{rr} rear right, x_{rl} rear left) with:

$$(F_{fr} + F_{fl} + F_{rr} + F_{rl} = K_H(x_{fr} + x_{fl} + x_{rr} + x_{rr})$$
$$(F_{fr} + F_{fl} - F_{rr} - F_{rl} = K_P(x_{fr} + x_{fl} - x_{rr} - x_{rr})$$
$$(F_{fr} - F_{fl} + F_{rr} - F_{rl} = K_R(x_{fr} - x_{fl} + x_{rr} - x_{rr})$$
$$(F_{fr} - F_{fl} - F_{rr} + F_{rl} = K_W(x_{fr} - x_{fl} - x_{rr} + x_{rr})$$

Where K_H is the heave stiffness, K_P the pitch stiffness, K_R the roll stiffness and K_X the warp stiffness. The system of equations above can be written in the matrix form:

$$\begin{bmatrix} Ffr \\ Ffl \\ Frr \\ Frl \end{bmatrix} = \begin{bmatrix} 1 & 1 & 1 & 1 \\ 1 & 1 & -1 & -1 \\ 1 & -1 & 1 & -1 \\ 1 & -1 & -1 & 1 \end{bmatrix}^{-1} \begin{bmatrix} K_H & 0 & 0 & 0 \\ 0 & K_P & 0 & 0 \\ 0 & 0 & K_R & 0 \\ 0 & 0 & 0 & K_W \end{bmatrix} \begin{bmatrix} 1 & 1 & 1 & 1 \\ 1 & 1 & -1 & -1 \\ 1 & -1 & 1 & -1 \\ 1 & -1 & -1 & 1 \end{bmatrix} \begin{bmatrix} xfr \\ xfl \\ xrr \\ xrl \end{bmatrix} \quad (1.1)$$

Considering a vehicle with the conventional and symmetric front-rear suspension system, the stiffness matrix became:

$$\begin{bmatrix} K_H & 0 & 0 & 0 \\ 0 & K_P & 0 & 0 \\ 0 & 0 & K_R & 0 \\ 0 & 0 & 0 & K_W \end{bmatrix} = \begin{bmatrix} K_s & 0 & 0 & 0 \\ 0 & K_s & 0 & 0 \\ 0 & 0 & K_s + 2K_b & 0 \\ 0 & 0 & 0 & K_s + 2K_b \end{bmatrix} \quad (1.2)$$

With K_s representing the stiffness given by coil springs installed on each wheel corner and K_b the stiffness of the anti-roll bar.

In case of an ideal suspension system that is capable to have a null warp stiffness:

$$\begin{bmatrix} K_H & 0 & 0 & 0 \\ 0 & K_P & 0 & 0 \\ 0 & 0 & K_R & 0 \\ 0 & 0 & 0 & K_W \end{bmatrix} = \begin{bmatrix} K_s & 0 & 0 & 0 \\ 0 & K_s & 0 & 0 \\ 0 & 0 & K_s + 2K_b & 0 \\ 0 & 0 & 0 & 0 \end{bmatrix} \quad (1.3)$$

So, considering K_i the elasticity of each wheel corner, we get:

$$K_i = \frac{1}{4}(K_H + K_P + K_R + K_W) = \frac{3}{4}K_s + \frac{1}{2}K_b \qquad (1.4)$$

That means that with a soft warp mode, other the advantages explained before, *it is also possible to reduce the wheel elasticity from 25% to 50%*, reducing the force transmitted to the sprung mass in case of wheel bump, so increasing the road filtering capability and the related comfort. Same considerations can be done for the damping matrix.

1.3.2 Hydraulic System Modelling

During the years generally two kind of modelling approach have been proposed: the first in time domain to perform simulations that evaluate the effects of the interconnection on vehicle stability and capability to suppress the roll motion; the second, in frequency domain, to evaluate the ride performances through the analysis of frequency response functions. In both approaches non-linear effects can be considered. Generally, the models and the analysis proposed are referred to simplified half-car vehicle model, as illustrated in Fig.20, so the front-rear interconnection is not considered.
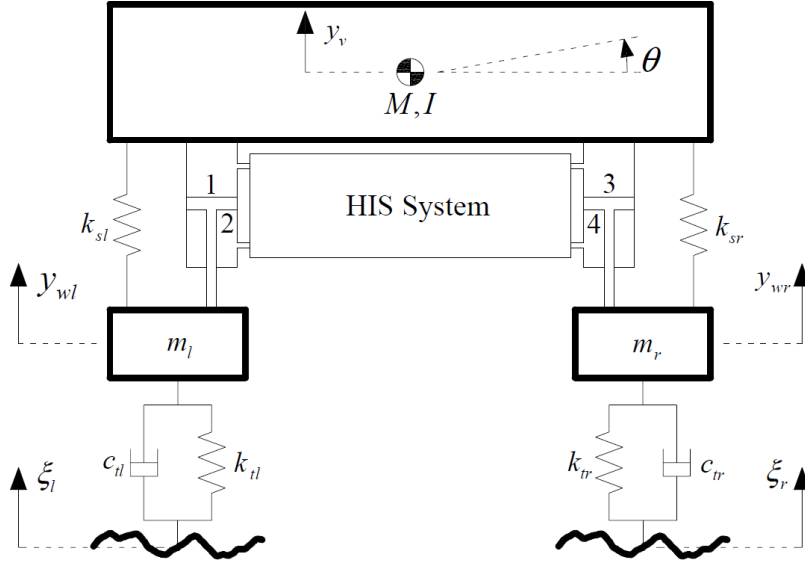
Fig. 20 Half-car schematic with HIS [19]

One of the first analytic analysis in time domain was proposed by P. Liu in [20], where a half-car 4-DOF model provided with a hydro-pneumatic interconnection in the roll plane was considered for study the anti-rollover and ride performance on heavy vehicles. The interconnection scheme is of 'H2' typology with a pneumatic accumulator on each wheel corner (Fig.21).

The analytical model is derived from vertical suspension movement coming from road irregularities and from roll moment acting on the sprung mass. The heave and roll motion equations of the sprung mass are described by:

$$m_s \ddot{x}_s - F_l' - F_r' = 0$$

$$I_s \ddot{\vartheta}_s - F_l' l_r - F_r' l_l = T_\vartheta$$

Where m_s is the sprung mass, I_s the vehicle's roll moment of inertia, l_f and l_r the front and rear half-track and T_ϑ the roll moment generated on the vehicle sprung mass;

F_l F_r are the left and right dynamic strut forces through the suspension, given by the sum of restoring (F_{rs} and F_{ls}) and damping forces (F_{rc} and F_{lc}):

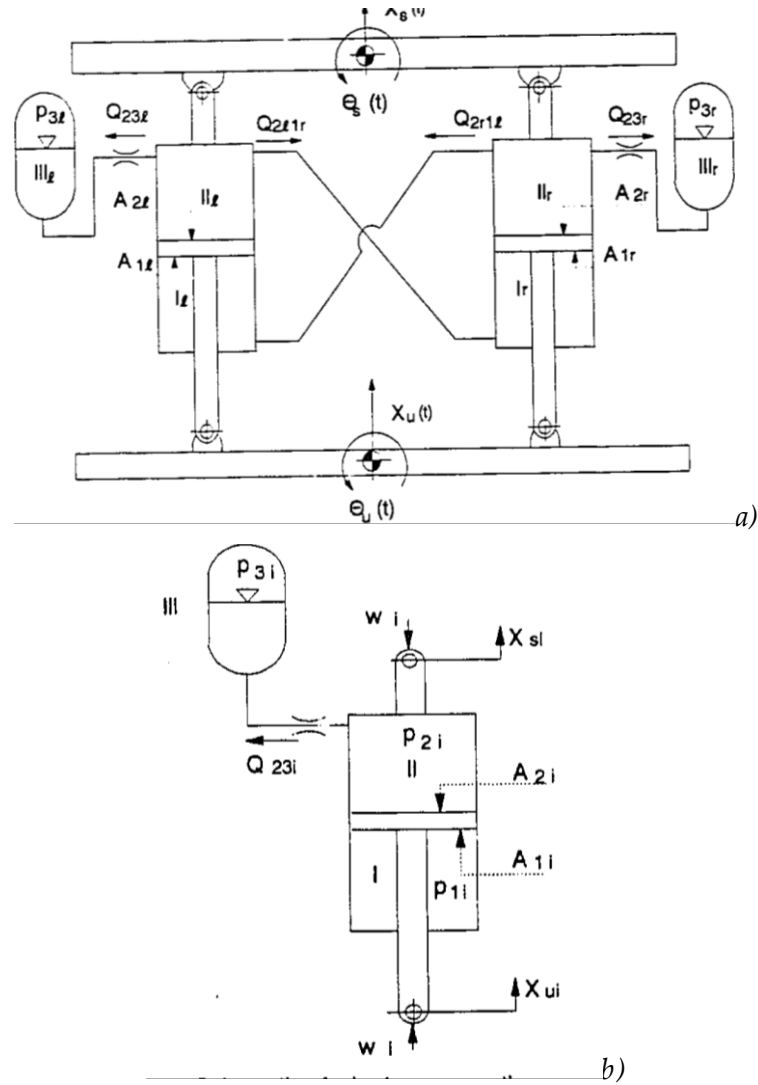$$F_r' = F_{rc}' + F_{rs}' \quad \text{and} \quad F_r' = F_{rc}' + F_{rs}'$$

Fig. 20 a) Schematic half-plane interconnection proposed by Liu   b) suspension strut [20]

The dynamic struct forces are obtained solving the hydro-pneumatic system, using static equilibrium equations, fluid flow equations, mass-conservation equations, pressure equilibrium equations and evaluating the damping forces through the restrictors and the pipes.

In such analysis, the flow through the restrictors is considered as turbulent, that through the pipes as laminar and the processes of gas into accumulator as polytropic; fluid compressibility, fluid inertia and leakages are neglected. Finally, the damping forces are:

$$F'_{cl} = \frac{\rho A_1{}^3 N_u}{2\,C_d{}^2 a^2}[\beta\,(\dot{z}_r - \beta\,\dot{z}_l)^2 sgn(\dot{z}_r - \beta\dot{z}_l) - (\dot{z}_l - \beta\dot{z}_r)^2\,sgn(\dot{z}_l - \beta\dot{z}_r)] - \frac{128\mu L\,A_1{}^2 N_u}{\pi D^4}\dot{z}_l$$

$$F'_{cr} = \frac{\rho A_1{}^3 N_u}{2\, C_d{}^2 a^2}[\beta(\dot{z}_l - \beta\dot{z}_r)^2 sgn(\dot{z}_l - \beta\dot{z}_r) - (\dot{z}_r - \beta\dot{z}_l)^2 sgn(\dot{z}_r - \beta\dot{z}_l)] - \frac{128\mu L\, A_1{}^2 N_u}{\pi D^4}\dot{z}_r$$

With $\beta = A_2/A_1$, A_1 is the lower cylinder's area, A_2 the upper; $\dot{z}_l$ and $\dot{z}_r$ are the vertical rate of suspension struts, D and L the diameter and the length of the hydraulic pipe; N_u is a coefficient that represent the number of strut for each side, C_d and a are respectively orifice's discharge coefficient and flow area.

The restoring forces are:

$$F'_{sl} = p_0 A_2 N_u\left[\left(\frac{v_0}{v_0 - A_1 z_r + A_2 z_l}\right)^n - 1\right] - p_0 A_1 N_u\left[\left(\frac{v_0}{v_0 - A_1 z_l + A_2 z_r}\right)^n - 1\right]$$

$$F'_{sr} = p_0 A_2 N_u\left[\left(\frac{v_0}{v_0 - A_1 z_l + A_2 z_r}\right)^n - 1\right] - p_0 A_1 N_u\left[\left(\frac{v_0}{v_0 - A_1 z_r + A_2 z_l}\right)^n - 1\right]$$

Where p_0 is the pressure due to the static load on the suspension's struts in the, v_0 the static volume, z_l and z_l the vertical displacements of the struts, and n the polytropic coefficient related to the gas inside the accumulators.

Starting from the pressure inside the cylinder chamber, the restoring moment developed by suspension's forces is:

$$M = (p_l - p_r)A_2 l N_u = p_0 v_0{}^n A_2 l N_u\left\{\frac{1}{[v_0 + (x - l\varphi)A_2]^n} - \frac{1}{[v_0 + (x + l\varphi)A_2]^n}\right\}$$

With x and ϕ the vertical movement and the roll angle of the sprung mass and l the half-track.

So, the roll stiffness can be defined as the roll moment change as function of the roll angle:

$$K_\varphi = \frac{dM}{d\varphi} = n p_0 v_0{}^n A_2{}^2 l^2 N_u\left\{\frac{1 - \frac{dx}{d\varphi}/l}{[v_0 + (x - l\varphi)A_2]^{n+1}} + \frac{1 + \frac{dx}{d\varphi}/l}{[v_0 + (x + l\varphi)A_2]^{n+1}}\right\}$$

After Liu, D. Cao et al. in [21] proposed a similar formulation of a full vehicle model, where the axle interconnection is substituted with a front-rear interconnection provided with a 'X' layout

(Fig.21), but also in this case only two struct connections are present. A 14 DOF model is used to study the roll and vertical dynamics of heavy vehicles.
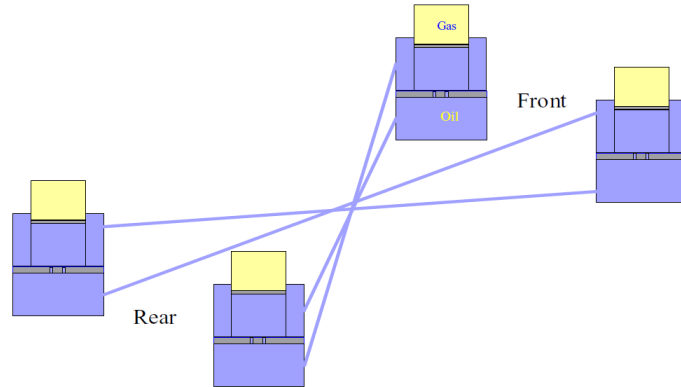

Fig. 20 X-coupled arrangement proposed by Gao [21].

To evaluate the stiffness properties of each mode, a method that consider the sprung mass fixed is used, so the coupling vibration modes effects have been neglected. For example, to evaluate the roll stiffness, it has been assumed that all the wheel displacements are equal:

$$X_{fl} = -X_{fr} = X_{fr} = -X_{rr} = X$$

And then the front and real roll stiffness is evaluated with:

$$K_{\varphi f} = \frac{dM_f}{d\varphi_f} = -\frac{d(F_{fl} - F_{fl})}{dX} l_{sf}^2$$

$$K_{\varphi r} = \frac{dM_r}{d\varphi_r} = -\frac{d(F_{rl} - F_{rr})}{dX} l_{sr}^2$$

Where l_{sf} l_{sr} are the front and rear half-tracks, φ_f and φ_r the front and rear roll axle.

Another formulation in time domain is proposed by W.A. Smith et al. in [22] where a 9 DOF half car vehicle model is presented to evaluate vehicle dynamics in standard manoeuvres, while the fluid dynamic system is modelled considering fluid compressibility and leakages through cylinders. The relation between the pressure and the flowrate is described by a first order nonlinear differential equations solved using a finite-element approach that brings to the determination of the pressure and flowrate values in each point (A, B, C, etc..) of Fig. 21.
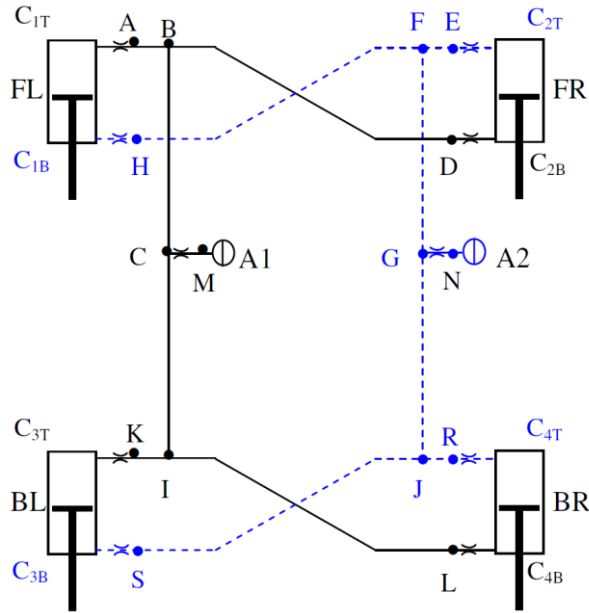
Fig. 21) H2 interconnection scheme [22].

The integrated mechanical-hydraulic system is:

$$M\ddot{Z}(t) + C\dot{Z}(t) + KZ(t) = D_1 AP(t) + F_{ext}(t)$$

Where Z is the vector of the DOF parameters; M, C, K the mass, damping and stiffness matrix respectively; D is a linear transformation matrix; A is the area matrix of cylinder chambers; P is the pressure vector that describe the pressure level in top and bottom cylinder chambers and F which of the external forces applied to the vehicle.

The hydraulic circuit is modelled as:

$$Q(t) = AD_2\dot{Z}(t) + V(t)\dot{P}(t)$$

Where Q is the vector of the flow rate into cylinder chamber, D a linear transformation matrix and V a time-variant matrix as function of cylinder volume and bulk modulus.

For what concern the frequency domain analysis, as said before, it is used to evaluate the ride performance due the fact that when a wheel is subjected to a motion, the pistons inside the chambers drive the fluid into the circuit and a pressure ripple is generated. These vibrations can

propagates from the cylinder mounts to the body, so the frequency response of the hydraulic circuit is studied to individuate the resonance frequency due the fact that the vibrations propagation other than get worse the comfort feeling, can induce a fatigue stress on the hydraulic system mounts.

Also, the frequency domain allows to better study some nonlinear effect that with time domain is difficult to consider.

Zhang et al. in [23] make a free and forced vibration analysis for bounce and pitch mode using the impedance modelling method on the same model described in [22] and illustrated in Fig. 21. This method, that exploit the electromagnetic analogy, allows to use linear equations for the circuit pressure losses, the fluid inertia and the fluid compressibility, describing them respectively as resistance, inductance and capacitance (Fig. 22)
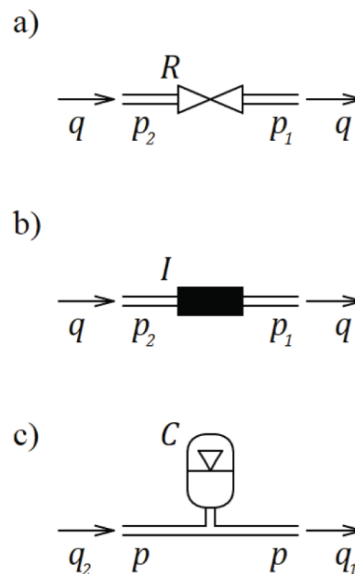
Fig. 22) Analogies representation between hydraulic and electric elements: a) hydraulic resistance; b) hydraulic inertia; c) hydraulic capacitance. [24]

1.4 Experimental results

In this section will described different results coming from experimental test aimed to evaluate potential benefit of interconnected suspension system. It is worth to underline that almost all the tests (the same for the simulations) are performed only on standard steady state manoeuvre.

The first official results, coming from experimental test of Kinetic 'H2' system application, were published by Wilde et al. in collaboration with Tenneco in [25]. A SUV in different configurations (with and without Kinetic system) is tested on a standard Fishhook manoeuvre, used generally to replicate the vehicle behaviour in emergency driving situations, to verify the effect of interconnected suspension on vehicle stability and its anti-rollover capability.

The comparison of the results has showed that the vehicle with the Kinetic system has a lower roll-angle and a more stable behaviour: roll rate, lateral acceleration and yaw rate signals, although comparable in modulus, have lower oscillations. Furthermore, the yaw rate comparison demonstrates a more rapid steering response and the analysis of the radius path have showed that the vehicle with the Kinetic is capable to perform lower path radius, sign of higher obstacle avoidance capability. (Fig. 23)

Fig. 23) Photo taken from the experimental test, illustrating the differences during standard Fishhook manoeuvre between the standard vehicle (on the left) and the Kinetic vehicle (on the right) [25].

The same authors in [26], using a ADAMS model of the vehicle (which include tire modelling) validated with the manoeuvre described above, investigated also the dynamic behaviour on a sinusoidal sweep steering manoeuvre and the ride performance through the analysis of the frequency response functions to pitch and bounce, conducted simulating the transition of the vehicle on a highway at constant speed. The results show that the ride performance of the standard and kinetic vehicle have a very similar ride behaviour despite of a better road holding. The same results were confirmed by Wang et al. in [27], where a standard and a 'kinetic' SUV is tested on a steady-state constant turn manoeuvre. The analysis of lateral acceleration and of the roll angle show that the vehicle with the kinetic system has a more stable behaviour; the analysis of vertical displacement and of the vertical acceleration of the sprung mass, in time domain have the same trend for both vehicles, while, in frequency domain a slightly better performance of the kinetic system is outlined.

J. Fontdecaba in the work presented in the previous section [13], other than illustrate a new kind of wheels interconnection and the theoretical benefits, show the results of three experimental tests done on a SUV vehicle: steady state circular test, pseudo-random steering input and steep steer. The comparison is made between the standard vehicle and other two vehicles, both provided with hydro-pneumatic interconnection but one in low stiffness configuration and the other with high stiffness. The author's attention is focused in two parameters: the roll gradient and the understeer gradient, both defined as deg/(m/s^2), where the acceleration considered is the lateral. The results demonstrate that the vehicle with the high stiffness configuration is able to reduce of 70% the roll gradient and of 30% the understeer gradient, while in case of low stiffness configuration, the roll gradient is reduced of 40% and the understeer gradient of 22%.

As said before, also Mouton conducted some experimental test to evaluate the effect on ride performances of its hydro-pneumatic front-rear interconnection [11]. The test carried out on different vehicle segment show the proposed interconnection can increase road irregularities filtering below 15 Hz, while above not a precise behaviour is evaluated.

The low warp stiffness effect on vehicle handling is presented by the AMZ Formula Student team's members in [28]. Fig. 24 shows the warp forces as function of lateral acceleration, calculated as the difference between the vertical load on wheels (measured with pressure sensors) of one car diagonal and which of the other diagonal. The graph below shows that with modes decoupling and soft warp mode (on the right) the wheel load variations on the diagonals due to road irregular surface are eliminated, so an important amount of grip is gained, making the vehicle behaviour more predictable and neutral in all surfaces condition. Also, the fact that the warp forces are almost 0, means that a quasi-zero warp stiffness can be reached with all the benefits described in the previous section.
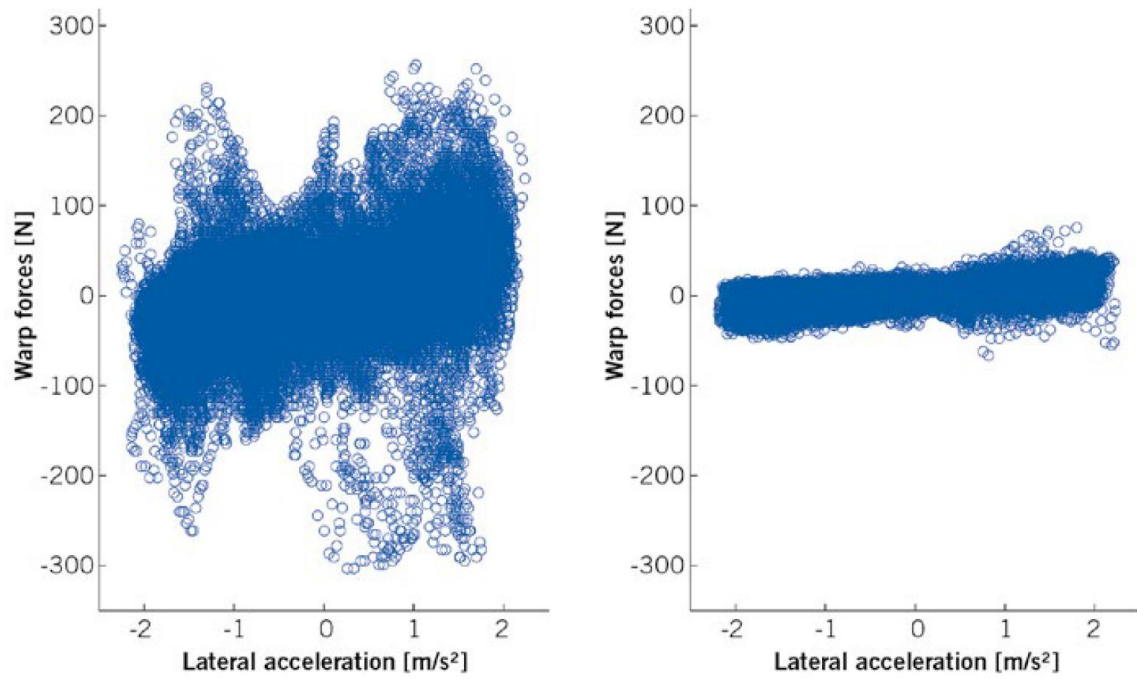
Fig. 24) Warp forces comparison between a standard prototype (on the left) and a prototype provided with hydraulic interconnected suspension and soft warp mode during a test in a track lap. (©AMZ [28])

1.5   Objectives of the Thesis project

The main task of this work is to analyse if a front-rear interconnected system can bring an advantage to the vehicle dynamics performances and quantize it. For this reason, it is proposed an interconnection scheme, realized with mechanical and hydraulic components, capable to realize an interconnection in the roll plane and a soft warp mode. The main aspects that want to be evaluated are the capability to decouple pitch and heave modes from roll and warp, so the capability to absorb oscillations coming from the road's obstacles demanded only to the heave springs: in this way it could be possible that increasing only roll stiffness the ride level remains almost the same while the handling performances became better in the cornering and in the transient manoeuvres. The second aspect to evaluate is how much a soft warp mode influences the load transfer due to road's irregularities and consequently the available grip of the tires.

Initially, it is necessary to verify if the proposed system it is feasible and if it can behave as desired, so a physical modelling in Simscape environment has been carried out. Then, a simplified model it is introduced in the appendix, with the aim to propose a solution to eventually test the model in a DIL simulator and speed up the simulation time.

The effects on vehicle dynamics are evaluated in co-simulation environment between Simscape-Vi CarRealTime; it is choose to evaluate the effect of the system on a high performance vehicle model because the vehicle's architecture, the suspension system's complexity and the eventually costs involved are more compatible with an high level car's segment.

Another important aspect to highline is the road surface: to see the effect of the soft warp mode it is necessary to model it in a realistic way, including elevation profile, banking angles in the corners, kerbs and bumps. For this task is used Vi-Road, a toll coming from Vi-Grade suite that gives a high freedom in the design of the desired road's characteristics.

2 Suspension modelling

2.1 Interconnection Layout

The suspension layout proposed abandon the classical scheme with a spring-damper for each wheel corner in favour of one spring-damper to control the pitch at each axle and another to control the roll of the whole car. The conceptual scheme is shown in Fig. 2.1.
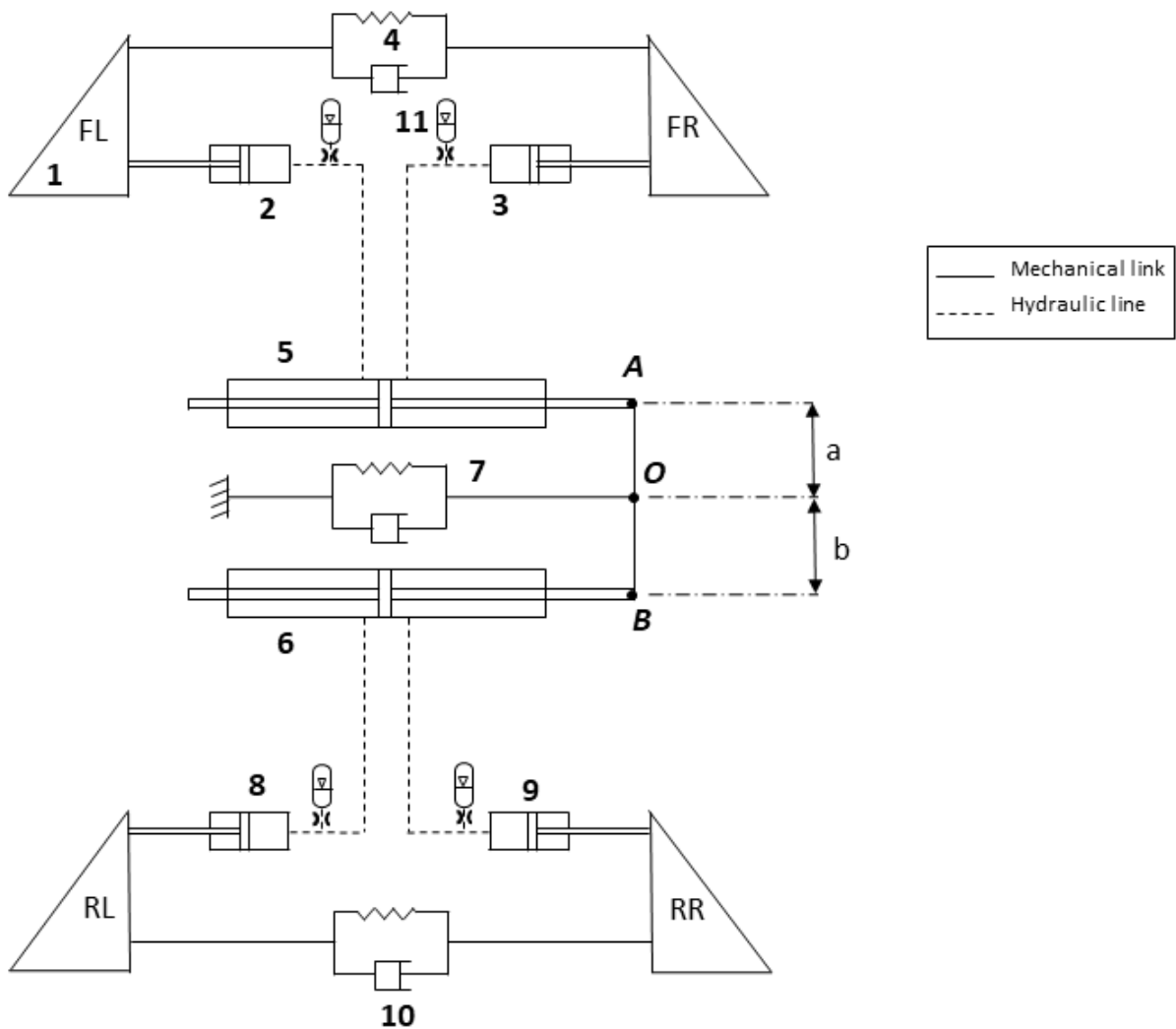

Fig. 2.1 Overall suspension architecture with interconnection mechanism: **1** *Rockers* – **2** - **3** - **8** - **9** *hydraulic actuators* – **4** *front heave spring-damper* – **5** *front double hydraulic cylinder actuator* – **6** *rear double hydraulic actuator* – **7** *roll spring-damper* – **10** *rear heave spring-damper* – **11** *gas-charged accumulator and orifice group*

The elements 1 are simple mechanical rocker arms to transfer the vertical motion of the wheels to the suspension components; the elements 2-3-8-9 are hydraulic actuators that allow to send oil to the central hydraulic double acting cylinders 5 and 6 (the two chamber of each cylinder have the same area): them in turn are able to activate the roll spring-damper 7 by a lever arm. The elements 4 and 10 are simple spring-dampers that work as 'third spring' or Z-bar to control the pitch and the heave of the axle where they are installed. The segment AB represent a lever arm with a fulcrum in the point O that can be subjected to a roto-translational motion.

The accumulators 11 serve as compensation volume, to allow the flow coming from actuators 2-3-8-9 to be stored during pitch motion of the suspension; at the inlet of the accumulators is installed an orifice to improve the dynamics of the hydraulic system.

Depending the suspension mode, the system has a different behaviour:

- *In pure pitch mode*, the elements that work are 4 and 10; in fact, assuming a pure braking motion, at front axle the symmetric wheel displacements cause that the oil in the actuators 2 and 3 is moved in appropriate accumulators (collocated before the 5 element, not represented in the Figure) so that the piston inside the hydraulic cylinder not undergo any significant displacement because only a very low quantity of oil slows in it in such a way that the 7 element is not activated. At rear, the oil inside the accumulators flows into the actuators 8 and 9 to compensate the drop travel of the rear wheels;

- *In heave mode,* it is possible to see the same behaviour as pitch mode with the only difference that front and rear axle are in phase;

- *In pure roll mode,* the rocker arm on the same axle rotate in the opposite direction so that the spring and the damper in 4 and 10 are not compressed or extended; meanwhile, assuming a roll of the sprung mass towards left, the opposite motion of the wheel on the same axle comports that the left chamber of the elements 5 and 6 receive oil from 2-8 while the right chamber discharge oil into 3 and 9: in this way the pistons of the elements 5 and 6 move axially dragging the point O of the central lever arm that as consequence extends the roll-spring damper 7. In case of roll toward right, the element 7 is compressed instead of being extended.

- *In pure warp mode,* the roll direction is opposed between front and rear axle such as the cylinders' 5 and 6 pistons moves axially in opposite direction causing the rotation of the arm AB: the point O is still and the element 7 is not compressed or extend: in this way is realized a soft warp mode. Generally, to have a pure rotation of the AB lever arm and not a roto-translation motion it is required that the roll stiffness distribution at wheels is the same between front and rear axle.

- *In single-wheel bump,* it is possible to note a combination between the roll and the pitch mode; in case of a conventional vehicle provided with anti-roll bars, both the coil springs that the anti-roll bar are actuated. Instead, with this solution it is possible to reduce the contribution of the roll element reducing the wheel's elasticity and consequently increasing the capability of road irregularities absorption.

2.1 Simscape Model

To model the whole suspension system, it is chosen to use Simscape model because it can easily interact with Vi-CarRealTime by means of Simulink environment. Also, Simscape is a very intuitive and it is provided of considerable libraries capable to describe the physical laws of most of basic component regarding mechanics, hydraulic, multibody, electrics and electronics system and so on.

For this work have been used three libraries: the 'Mechanical' and 'Hydraulic' belonging to the 'Foundation library' and the 'Hydraulic Isothermal' belonging to the 'Fluid Library' that is one of the Add-on of MATLAB and general not available for the basic version of the software.

The physical model can be divided in three parts:

- Hydraulic circuit (front and rear);
- Spring-damper system for the control of pitch and heave (front and rear)
- Central lever arm.

2.1.1 Hydraulic Circuit
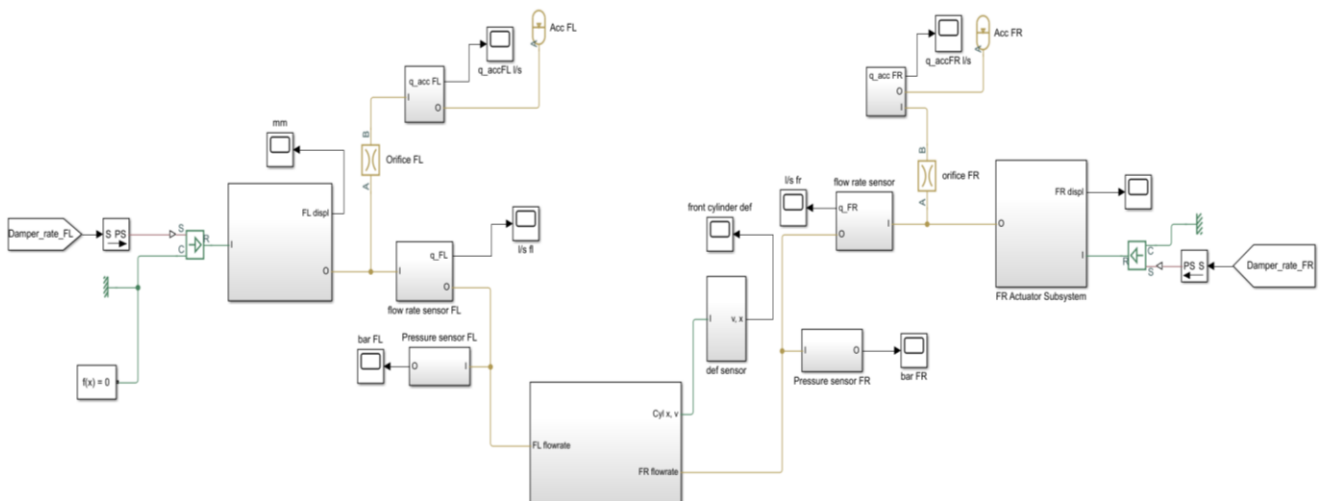
Fig. 2.2 Front hydraulic scheme on Simscape.

The figures above represent the hydraulic scheme for the front axle, and it is composed by:

- Ideal translational velocity sources, where are connected the rockers' rates coming from Vi-CarRealTime that represent the input signal of the system;

- Hydraulic actuators (Actuator FL and Actuator FR subsystems in Fig. 2.2, whose detail is shown in Fig. 2.3 a) connected mechanically to the rockers and hydraulically at front
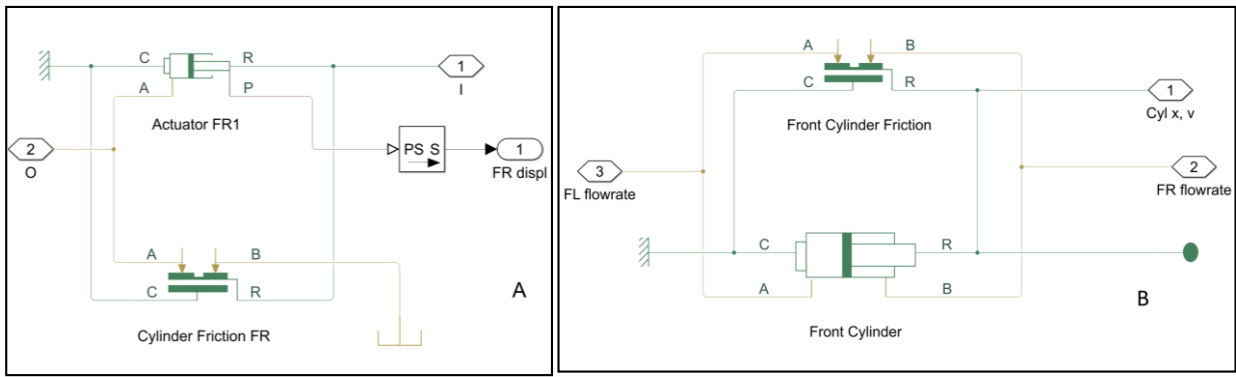
Fig. 2.3 a) FR actuator subsystem detail; b) Front-cylinder subsystem detail.

cylinder. For this analysis it is chosen the simpler version that neglect the fluid compressibility and the leakages, while the hard stops are assumed to be inelastic to eliminate oscillations at end of the stoke; this solution permits to increase the numerical computation and make available the model for real time or HIL simulations.

- Cylinder friction block, linked in parallel with the actuators to represent the friction in the contact between the moving bodies in the cylinders; in particular, it allow to describe the friction as function of the pressure and of the relative velocity: the friction force is calculated as the sum of a viscous component, the Stribeck component and the Coulomb one that consists in the pre load force generated due to the contact with seals. The presence of this friction is useful to reduce the flowrate's oscillations.

- A double acting hydraulic cylinder (Fig. 2.3) provided with two chambers of the same area and same volume. The chamber A is connected to the actuator FL while the chamber B with actuator FR. The body of the cylinder is fixed to the vehicle's chassis,

    while the one ends of the piston is connected to the central system that is shown the next paragraph. For this cylinder is also valid the simplifications done for the single actuators above.

- Two gas-charged hydraulic accumulators that work as compensation volume to store the flow coming from actuators during the pitch motion: without them the suspension would be locked. The accumulators also fix the pre-charge pressure level in the circuit. The amount of flow entering inside the accumulators, depends on the pressure level of the flow acting against the pre-charge pressure of the accumulators. The process in the

gas chamber is assumed as polytropic and the fluid compressibility and the separators properties are not evaluated.

- Fixed-area orifices, that act as dynamic orifices to improve, together with the accumulator, the dynamic of the hydraulic system reducing the amplitude of the flowrate ripple.

- Flowrate, pressure and force sensors to control the system expressed respectively in l/s, bar and N.

- A mechanical reference and the solver configurator block that are necessary for Simscape coding.

The piston of the front hydraulic cylinder is subjected to a displacement toward left or right only in roll condition of the axle, otherwise the oil flows into the accumulators.

The aim of this project is not to size each component rigorously, because this operation depends on different practical issues, such as the architecture of the vehicle involved, the available space, the desired weight or the material employed for different components. For these reasons, the Table 2.1 at end of the chapter gives the values used for this modelling operation but they are not so important for the results. What it is important it is the behaviour of the system, that can be achieved with different parameter's size, evaluated as function of the different practical requirements to satisfy.

On the other side, there are some constraints to consider into the design phase: the stroke of the wheel's hydraulic actuator has to take into account the maximum travel of the wheel; also, the maximum volume of the accumulator should be equal to the maximum volume that each actuators can displace. Furthermore, the ratio between the area of the wheel's actuators and the area of the central cylinder define the transmission ratio between the wheel displacement and the which of the roll spring, so the evaluation of the spring stiffness has be done considering this parameter; in this work it is chosen a transmission ratio equal to 1 in pure roll motion, so the area of the central cylinder is slightly lower than which of the actuators to take in considering the flow that goes into the accumulators.

2.1.2 Spring-damper system for controlling pitch and heave motion
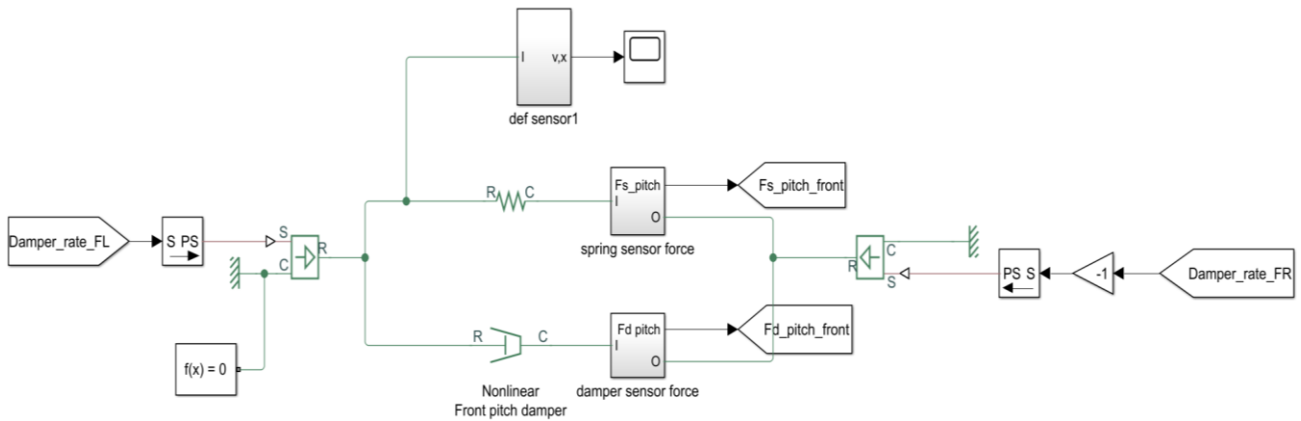
Fig. 2.4 Mechanical system for heave and pitch on the front axle.

The model woks in parallel with one described in the previous paragraph and it is constituted by the following components:

- Ideal translational source generations, where it is connected the rocker rate signal that is the input of the system;

- Spring-damper system to control heave and pitch mode at front axle: this substitute the conventional configuration with a spring-damper for each wheel of the axle. The damper model is the non-linear type to emulate the same damper characteristics of the standard vehicle model chosen as reference in Vi-CarRealTime; the nonlinear curve it is parametrized with a lookup table.

- Force and motion sensors.

2.1.3 Central lever arm
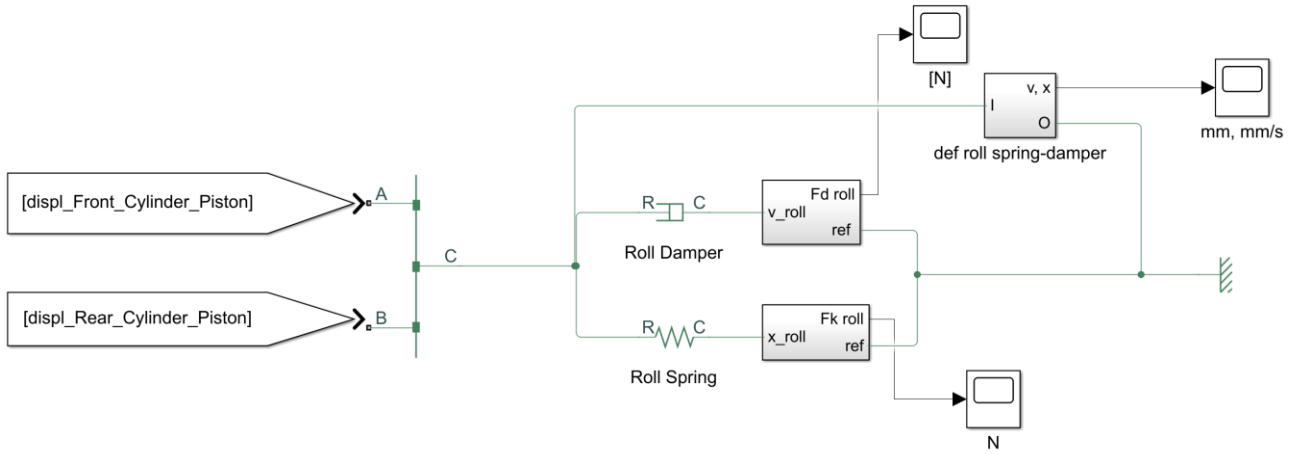
Fig. 2.4 Central lever arm

The system has been modelled with the 'free lever' block present in the Mechanical library: it allows to describe the roto-translational dynamics of the lever AB with the C point as a fulcrum. The point A is mechanically connected with the front central cylinder while the point B with the rear. The point C is also part of an arm that activate the roll spring-damper.
The system it is described by the following equations:

$$x_C = \frac{x_A\, l_{BC} + x_B\, l_{AC}}{l_{AC} + l_{BC}} \qquad (2.1)$$

$$F_A = \frac{l_{BC}}{l_{AC} + l_{BC}}\, F_C \qquad (2.2)$$

$$F_B = \frac{l_{AC}}{l_{AC} + l_{BC}}\, F_C \qquad (2.3)$$

$$\vartheta = \arctan\left(\frac{x_B - x_A}{l_{AC} + l_{BC}}\right) \qquad (2.4)$$

Where x_A, x_B, x_C are the lever joints displacements in points A, B, C; l_{AC}, l_{BC} the length of the arms AB and BC; F_A, F_B, F_C the lever joints forces and ϑ the angle that represent the rotational motion of the AB lever arm.

The length of the arm AB and BC allows to set the front-rear roll stiffness distribution:

$$\%F \ = \ \frac{l_{BC}}{l_{AC} + l_{BC}} \qquad (2.5)$$

$$\%R \ = \ \frac{l_{AC}}{l_{AC} + l_{BC}} \qquad (2.6)$$

For the present work, as said in 2.2.2 paragraph, is not important the absolute values of l_{AC} and l_{BC} but only their ratio: their values have been selected in order to have the same front-rear roll distribution as the model selected in Vi-CarRealTime, corresponding at 43.64% at front and 56.36% at rear axle.

2.1.4 Complete model
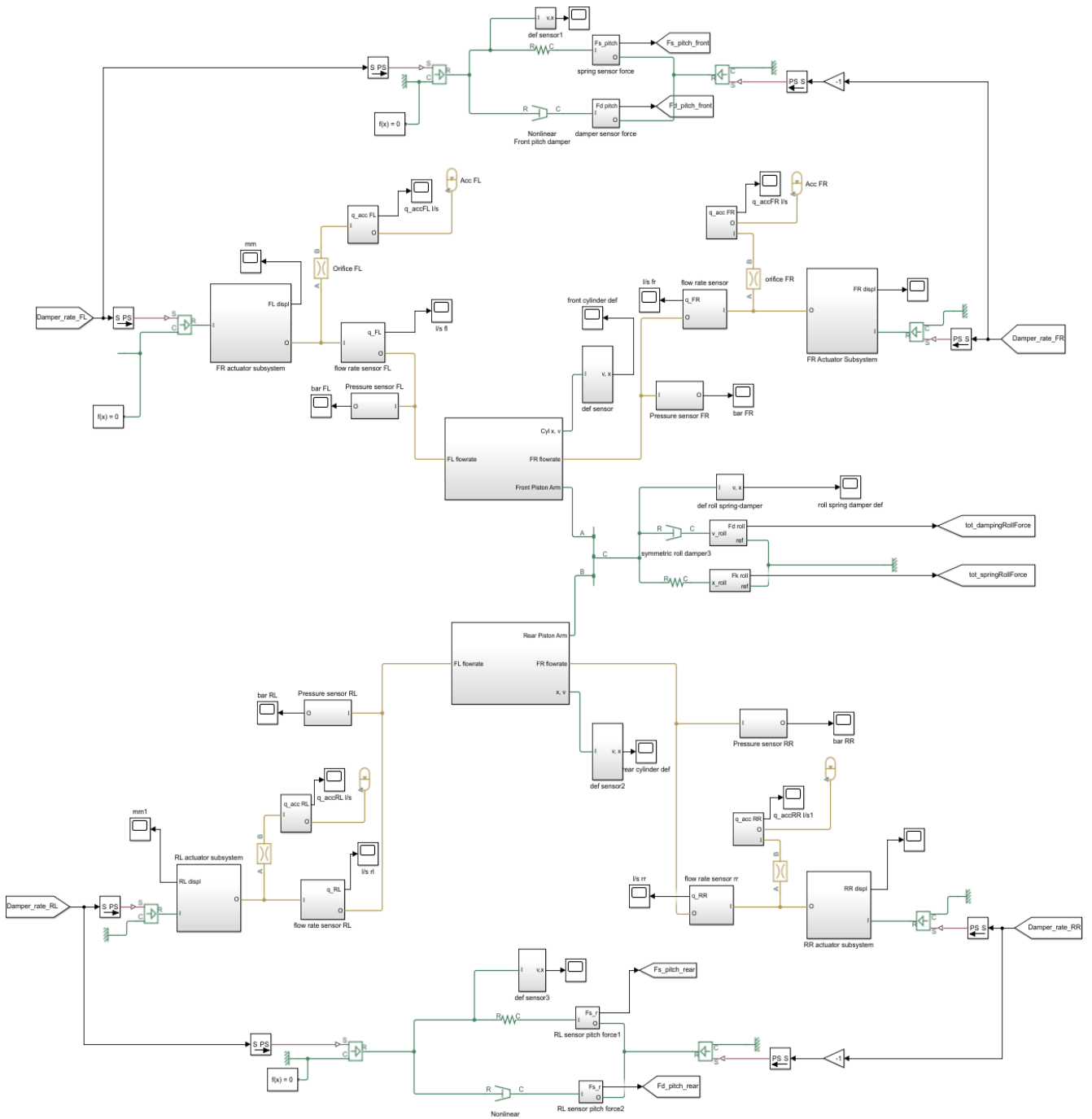
Fig. 2.5 Complete suspension system model in Simscape environment.

Before to integrate this system with Vi-CarRealTime environment, it is tested with constant and sinusoidal input to set all the parameters with the aim to obtain the desired behaviour described in the first paragraph.

The design parameters attributed to the components are described in Table 2.1: the value of the spring stiffnesses, damping coefficient will be explained in the fourth chapter.

Parameter	Component	Value	Unit
piston area	actuators FL, FR, RL, RR	133	[cm²]
piston stroke	actuators FL, FR, RL, RR	150	[mm]
initial piston distance from cap	actuators FL, FR, RL, RR	75	[mm]
pre-load force	cylinder friction FL, FR, RL, RR		
orifice area	orifice FL, FR, RL, RR	0.5	[cm²]
discharge coefficient	orifice FL, FR, RL, RR	0.9	-
piston area A	front, rear double acting cylinder	130	[cm²]
piston area B	front, rear double acting cylinder	130	[cm²]
piston stroke	front, rear double acting cylinder	150	[mm]
piston initial distance from cap	front, rear double acting cylinder	75	[mm]
accumulator volume	accumulator FL, FR, RL, RR	1	[l]
minimum gas volume	accumulator FL, FR, RL, RR	5.00E-05	[l]
pre-charge pressure	accumulator FL, FR, RL, RR	8	[bar]
spring stiffness	front pitch spring	47.5	[N/mm]
spring stiffness	rear pitch spring	52.5	[N/mm]
spring stiffness	roll spring	282.3	[N/mm]

Table 2.1 Description of the parameters' values. Parameters not mentioned in this table are left as the default value of each block.

3. Simulation Environment

3.1 Introduction to Vi-CarRealTime

The analysis of the interconnected suspension system is carried out on VI-CarRealTime, a virtual simulation software developed by Vi-Grade GmbH, a leader company for software products and services for applications in the field of advanced system simulations and dynamic driving simulators, that is partner of this work.

Nowadays, the simulation software hold a fundamental role in the design process for each kind of applications, making possible to reducing costs and time in the development phase: in this scenario it is collocated Vi-CarRealTime, that allows to create vehicle models with an high level of flexibility, and perform off-line and real time SIL/HIL/DIL simulations, to aid the engineers in the design and testing of each kind of vehicle's parameter and evaluate its contribution on the vehicle performances.

Vi-CarRealTime is a virtual simulation environment where the vehicle models are described by a 14 DOF equations of motion, six of which related to the sprung mass translations and rotations in the space, four to describe the vertical motion of the wheels and the remaining four for the longitudinal slip of the tires.

The modelling approach is simplified, in the sense that the components are described by lookup tables, as the suspension and the steering system, or by algebraic or differential equations, as for the powertrain and the inertia properties, so not linkages or physical components are included. It also includes a sophisticated virtual driver model, able to perform a large quantity of user defined manoeuvres.

Furthermore, it has the great advantage to interact with other simulation environments, such as Adams Car or Simulink: in this way it is possible to design and testing not standard components or control system codes.

In the complete package, other Vi-CarRealTime are present also other tools that allows to increase the description capability of the vehicle model:

- Vi-SuspensionGen, that allows to analyse the elastokinematic of the suspensions and to create the suspension's lookup tables for Vi-CarRealTime;
- Vi-TireLimits, that allows to evaluate the tires' characteristics using the *.tir* property files;
- Vi-Animator, the post-processing toll for plots and vehicle's animations;
- Vi-Road, a toll that generate driver paths and road profiles.

In this chapter will be explained how the suspension models described in the previous sections are integrated with Vi-CarRealTime environment.
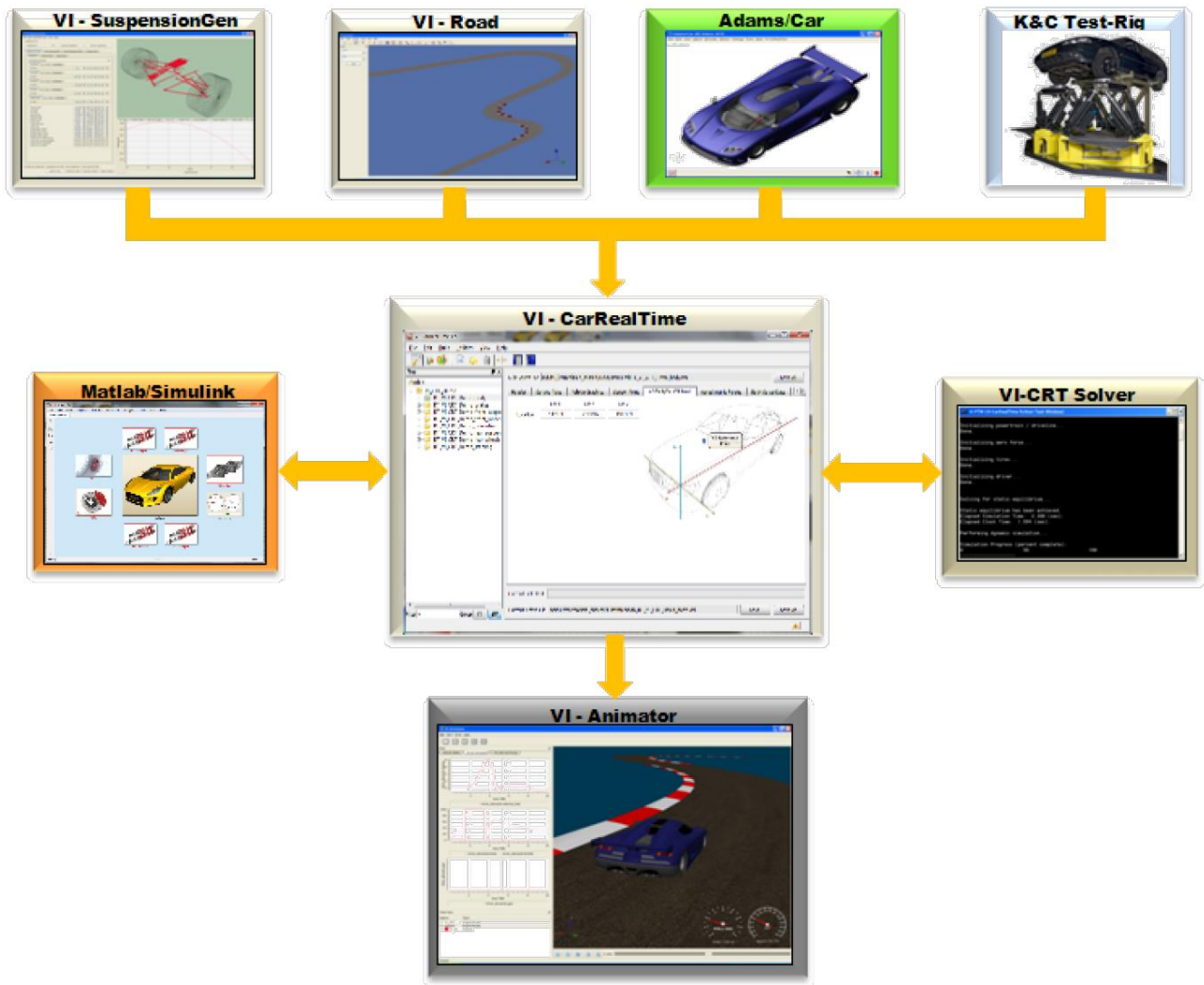
Fig. 3.1 Vi-Grade utilities and process flow [30].

3.2 Vehicle model

3.2.1 General vehicle data

The vehicle model selected for this work is a high-performance vehicle, because for architecture and costs involved, it is the most suited for the interconnected suspension system proposed. Indeed, the front pitch/heave spring-damper is compatible only with a vehicle with the combustion engine installed at rear, in a central position or with an electric powertrain configuration, because the space required by the front spring damper cannot coexists with the a combustion engine installed at front. Also the costs, despite the interconnected suspension system proposed is fully passive and do not require any hydraulic pumps or electronic controlled components, it increase the number of component of the suspension system and raise the complexity level, that has an effect in the vehicle installation phase and in which of the maintenance: for this reason it is suitable only for premium cars.

The high-performance car model available in the Vi-CarRealTime library do not correspond to any real vehicle produced, but it is a model with realistic characteristics and performances. Even the tire models, described in .tir format, replicates realistic data. The name of the model's database is 'SportCar' and it is updated at 19.2 release.

Most of vehicle data are described in the Table 3.1. The dampers' characteristics are shown in 3.2.2 paragraph.

In order to better describe the vehicle model used, starting from the parameters in the Table 3.1, it is possible to evaluate the front and rear wheel rates, the roll stiffnesses and the ride frequencies.

The wheel rates, that represent the stiffness at wheels given by the coil springs, are evaluated from the spring stiffness and the motion ratios:

$$WR_{sf} = \frac{k_{sf}}{MR_{sf}} = 35.32 \; \frac{N}{mm} \qquad (3.1)$$

$$WR_{sr} = \frac{k_{sr}}{MR_{sr}} = 62.13 \; \frac{N}{mm} \qquad (3.2)$$

Table 3.1

Parameter	Symbol	Value	Unit
Overall vehicle mass	m	1554.2	[kg]
Sprung mass	m_s	1360	[kg]
Front unsprung mass	m_{uf}	91.72	[kg]
Rear unsprung mass	m_{uf}	102.6	[kg]
Rear weight distribution	-	55.50%	-
Rear axle to CG	b	1220	[mm]
Wheelbase	W_b	2740	[mm]
Height of vehicle CG	h_{CG}	456	[mm]
Height of sprung mass CG	h_{smCG}	486	[mm]
Front track	t_f	1678	[mm]
Rear track	t_r	1691	[mm]
Rear/Front wheel radius	r_r, r_f	326	[mm]
Motion ratio front spring*	MR_{sf}	1.64	-
Motion ratio rear spring*	MR_{sr}	1.30	-
Spring rate front	k_{sf}	95	N/mm
Spring rate rear	k_{sr}	105	N/mm
ARB rate at front wheel	W_{ARBf}	5	N/mm
ARB rate at rear wheel	W_{ARBr}	15	N/mm
Front tire vertical rate	k_{tf}	200	N/mm
Rear tire vertical rate	k_{tr}	300	N/mm
Motion ratio front ARB*/**	MR_{ARBf}	3	-
Motion ratio front ARB*/**	MR_{ARBr}	1.81	-
Roll gradient**	RG	2.55	deg/g$_{lat}$
Engine power	-	554	CV
0-100 km/h	-	3.4	s
Max speed	-	340	km/h

*wheel displ/spring dispacement   **calculated or evaluated from simulations*

The front and the rear ride frequencies are (from [32]):

$$f_f = \frac{1}{2\,\pi\,MR_{sf}} \cdot \sqrt{\frac{k_{sf}}{m_{sf}}} = 1.72\ Hz \qquad (3.3)$$

$$f_r = \frac{1}{2\,\pi\,MR_{sr}} \cdot \sqrt{\frac{k_{sr}}{m_{sr}}} = 2.04\ Hz \qquad (3.4)$$

Where m_{sf}, m_{sr} are the front and the rear sprung mass of a single wheel.

To calculate the roll stiffness at wheels (that we will call 'WRS'), we must consider both the coil springs contribution and the antiroll bar contribution [31]:

$$WRS_{roll} = WRS_{roll\_spring} + WRS_{roll\_ARB} \qquad (3.5)$$

$$WRS_{roll\_spring\_f} = \frac{WR_{sf} \cdot t_f{}^2}{2} \cdot \frac{\pi}{180} = 867.86\ \frac{Nm}{deg} \qquad (3.6)$$

$$WRS_{roll\_spring\_r} = \frac{WR_{sr} \cdot t_r{}^2}{2} \cdot \frac{\pi}{180} = 1550.4\ \frac{Nm}{deg} \qquad (3.7)$$

$$WRS_{roll\_ARB\_f} = \frac{WR_{ARBf} \cdot t_f{}^2}{2} \cdot \frac{\pi}{180} = 122.86\ \frac{Nm}{deg} \qquad (3.8)$$

$$WRS_{roll\_ARB\_r} = \frac{WR_{ARBr} \cdot t_r{}^2}{2} \cdot \frac{\pi}{180} = 374.4\ \frac{Nm}{deg} \qquad (3.9)$$

Where deg indicate the roll angle of the vehicle body. So, the front and the rear roll stiffness are:

$$WRS_{roll\_f} = K_{roll\_spring\_f} + K_{roll_{ARB\_f}} = 990.72\ \frac{Nm}{deg} \qquad (3.10)$$

$$WRS_{roll\_r} = K_{roll\_spring\_r} + K_{roll_{ARB\_r}} = 1924.70\ \frac{Nm}{deg} \qquad (3.11)$$

The total roll stiffness is:

$$WRS_{roll\_TOT} = K_{roll\_f} + K_{roll_r} = 2915.4 \ \frac{Nm}{deg} \qquad (3.12)$$

From equations 3.10, 3.11 and 3.12 it is possible to evaluate the front-rear roll distribution at wheels:

$$\%k_{roll\_f} = \frac{WRS_{roll\_f}}{WRS_{roll\_TOT}} \cong 34 \ \% \qquad (3.13)$$

$$\%k_{roll\_r} = \frac{WRS_{roll\_r}}{WRS_{roll\_TOT}} \cong 66 \ \% \qquad (3.13)$$

3.2.2 Damper characteristics

The conventional damper characteristics for automotive application are not linear, this because it is required an high damping coefficient at low dampers rate to absorb the elastic energy involved in roll or pitch motion, while at higher dampers rate, where the wheels are generally subjected to a road obstacles or irregularities, it is preferred a lower damping coefficient to increase the filtering action.

Furthermore, the curves are not symmetric in the bounce and rebound working area, because it is generally preferred a higher damping in the rebound phase to avoid pumping phenomena.

All the above considerations are present in the characteristic damping curve for the vehicle model in Vi-CarRealTime. Them are described in the software by mean of tables.

The front and rear damper forces as function of damper rates are illustrated in Fig. 3.2 and Fig. 3.4, while the damping coefficients as function of the damper rate in Fig. 3.3 and 3.5: them are needed for the evaluation of the damping force according to the formulation that will be explained in the appendix A.3.1 and A.3.2 section.
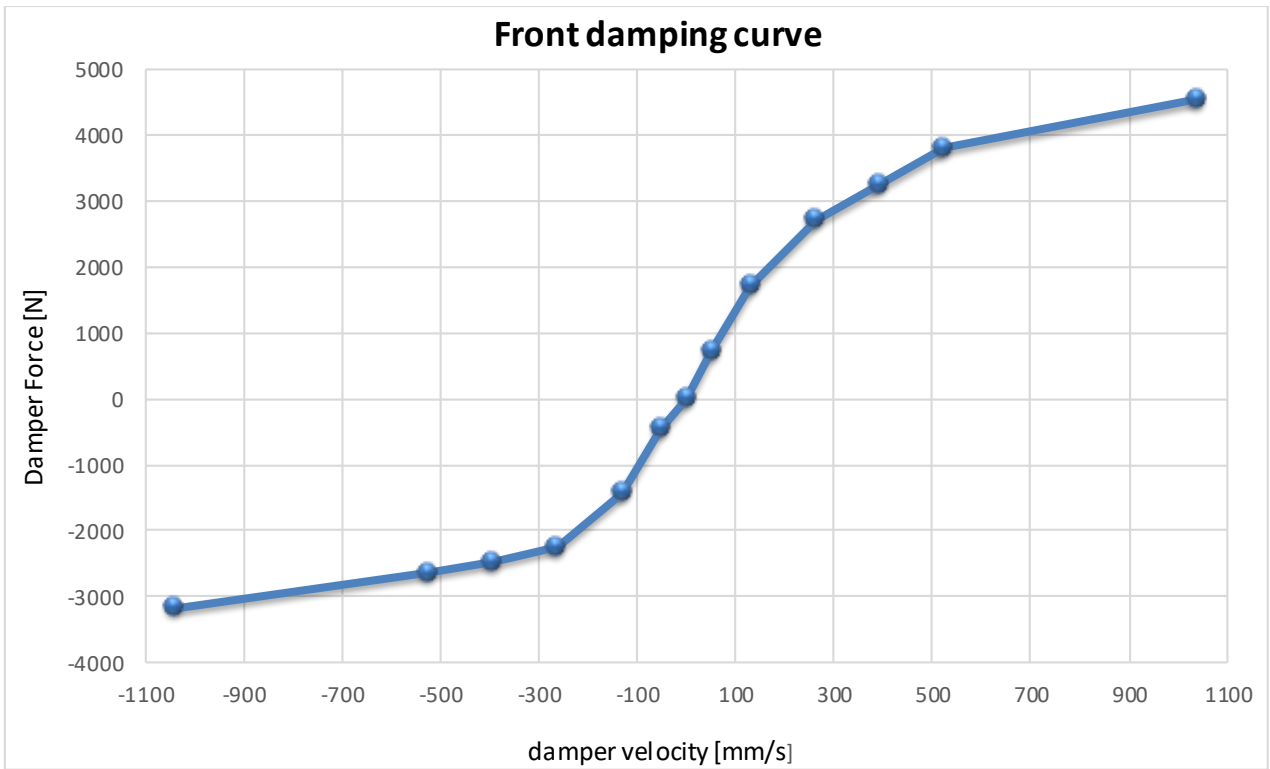
Fig. 3.2 Damping curve for front dampers of base model in Vi-CarRealTime (positive velocity in rebound).
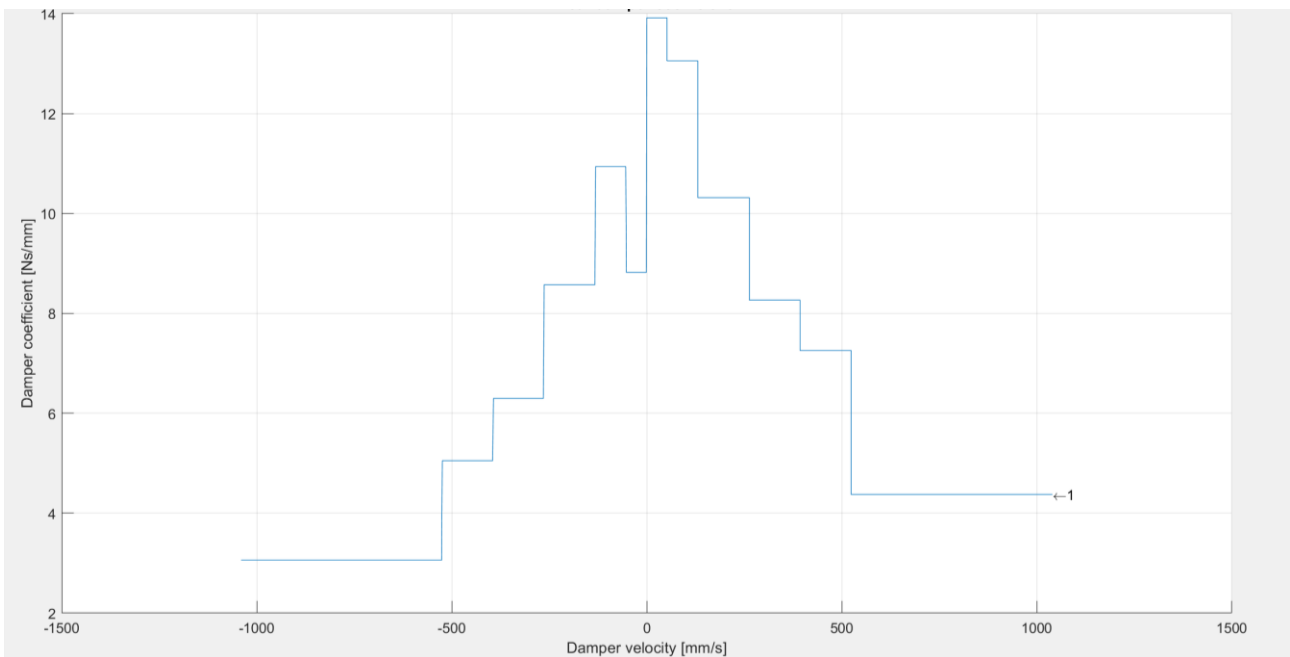
Fig. 3.3 Front damping coefficient as function of the damper rate (positive velocity in rebound).
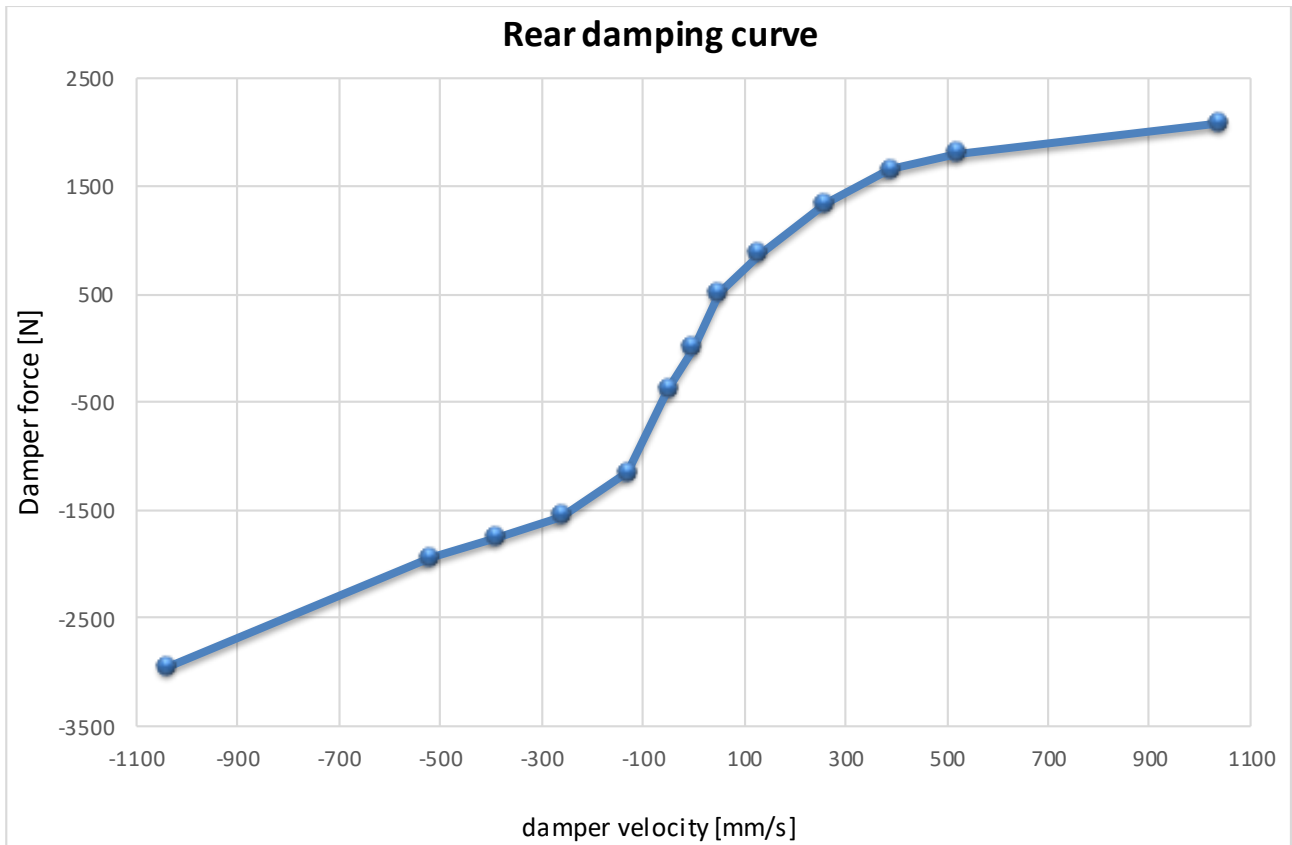
Fig. 3.4 Damping curve for rear dampers of base model in Vi-CarRealTime (positive velocity in rebound).
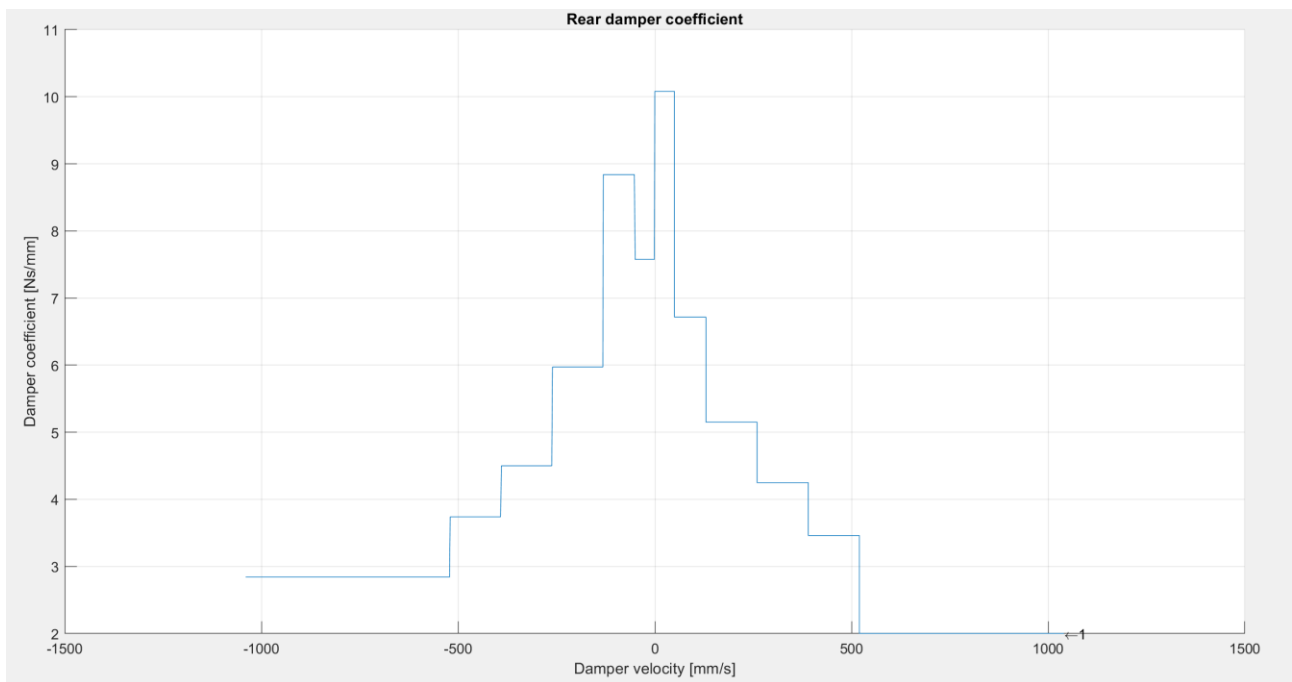
Fig. 3.5 Rear damping coefficient as function of the damper rate (positive velocity in rebound).

3.3 Definition of roll and damping properties for interconnected vehicle

The aim of this work is to propose a comparison between the standard vehicle and the same that it is provided with interconnected suspension, but this require to revise some parameters such as the roll spring and damping system, that in the case of the base model are integrated in the conventional suspension system, while now, we have to decouple the different contributions and define a roll spring stiffness and a dedicated roll damping characteristics. Indeed, for simplicity, for the pitch/heave suspension's part it is decided to maintain the same properties of the standard model in Vi-CarRealTime, that means the same values of spring stiffness and same damping curve: this because the aim is to evaluate the effect of the interconnection without optimize the single parameter introducing other variables.

The idea to integrate the interconnection into Vi-CarRealTime environment is to disable the internal suspension model into the software and add them externally by means of interaction with Simulink environment; this choice is due the fact that the proposed suspension system is not conventional and there aren't in Vi-CarRealTime any similar templates to describe it. Furthermore, also the interconnected model will be seen by Vi-CarRealTime as a vehicle provided with four spring-dampers system for each wheel, so our aim will be to define *four equivalent stiffnesses and four equivalent damping coefficients* that allows to describe the behaviour of the interconnection as a conventional suspension system. All the stiffness and damping are defined at spring and at damper level and not at wheels, so it means that the following calculations do not take into account the motion ratios between the spring and the wheels, that are still evaluated by Vi-CarRealTime environment.

3.3.1 Roll spring definition

One of the main aspects to evaluate is to define the stiffness of the roll spring, in the way that gives the same roll stiffness contribution as the standard vehicle. In order to do that it is not adequate to use the equation 3.12 because it is defined at wheel level (it includes the contributions of motion ratios and of front and rear tracks), while it is necessary to define a stiffness expressed in N/mm.

The equations that allow to get the spring stiffness are:

$$K_{roll\_f} = K_{sf} + 2 \cdot K_{ARBf} = K_{sf} + MR_{ARBf} \cdot W_{ARBf} = 124 \ \frac{N}{mm} \quad (3.14)$$

$$K_{roll\_r} = \ K_{sr} + 2 \cdot \ K_{ARBr} = K_{sr} + MR_{ARBr} \cdot W_{ARBr} = 156.9 \ \frac{N}{mm} \qquad (3.15)$$

Where K_{sf} and K_{sr} are the spring rate of coils springs for the standard vehicle; K_{ARBf} and K_{ARBr} the stiffness of the anti-roll bars expressed in N/mm assuming as them act at coils spring level: this choice is related to the assumption that we are interested to define four equivalent stiffness to interact with Vi-CarRealTime. W_{ARBf} and W_{ARBr} are the anti-roll bar wheels rate, expressed in Vi-CRT software; the motion ratios MR_{ARBf} and MR_{ARBr} of the Table 3.1 are obtained from iterative simulation tests, to bring the anti-roll forces at main spring level.

So, the roll spring stiffness is:

$$K_{roll\_TOT} = K_{roll\_f} + K_{roll\_r} = 282.9 \ \frac{N}{mm} \qquad (3.16)$$

Therefore, the front and rear roll stiffness distribution are 43.94% at front and 56.06 at rear axle.

3.3.2 Roll damper characteristic

For the roll damper characteristics it is used the same approach seen before for the spring, but with two differences: first, the conventional vehicle has not a roll dampers, so to evaluate the damping coefficients we have only the contribution of the traditional dampers; then, we need a symmetric characteristics because if the roll of the car is in a direction, the damper speed is in a direction, while if the car roll is in the other direction the damper speed is opposite; in this way the different behaviour in bounce and rebound disappears for the roll motion and for this reason, to evaluate a unique damper characteristics, for each axle, has been taken the mean of damping coefficient between the bounce and the rebound evaluated in the same range of damper rate, and then summed with which of the other axle in the same damper rate range (the damping curves of the original dampers are divided in 12 ranges to define the parametrization of the curves, as it possible to see looking at Fig. 3.3 and 3.5, at which correspond 12 damping coefficients for each dampers). So, for each damper rate range, the damper coefficient for the roll damper is obtained as:

$$c_{roll} = c_F{}' + c_R{}' \qquad (3.17)$$

Where $c_F{}'$ and $c_R{}'$ are the mean of damper coefficient in bounce and rebound for the front and the rear axle.
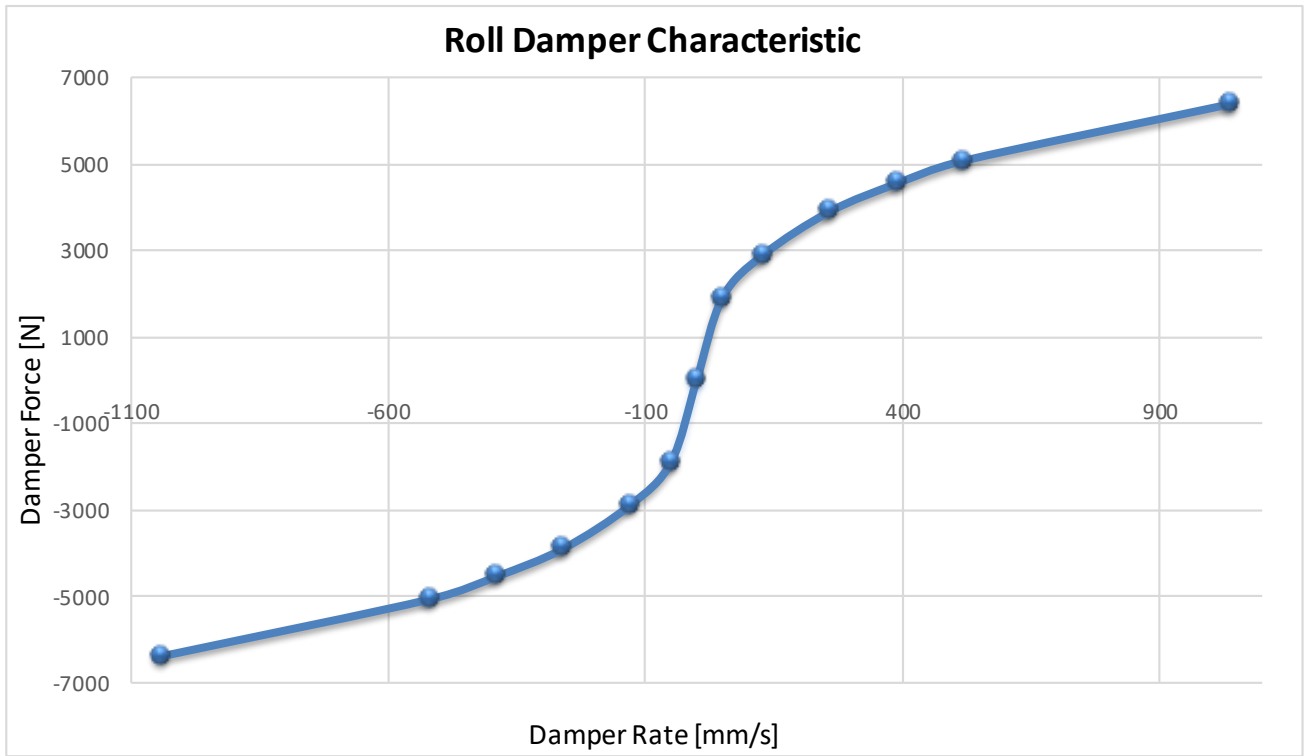
Fig. 3.6 Roll damper curve for the interconnected vehicle model.
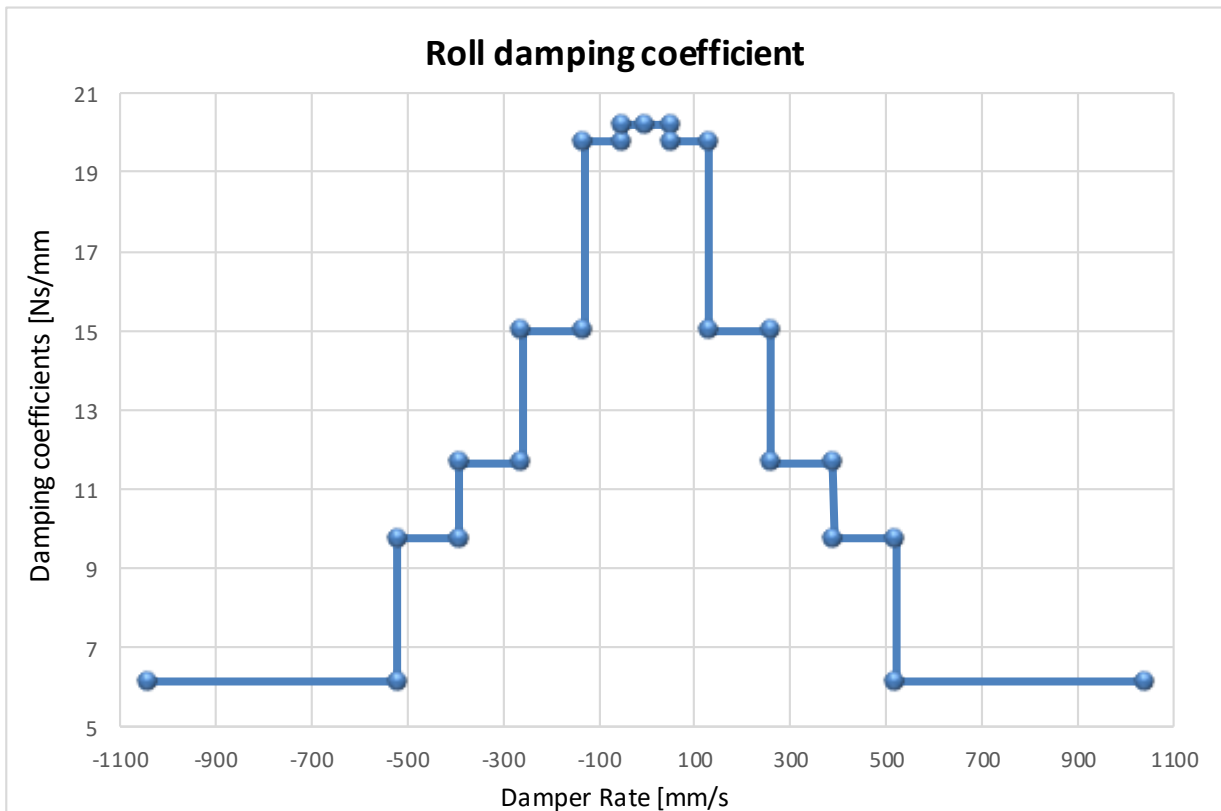
Fig. 3.7 Roll damping coefficients for the roll damper curve evaluation.

3.4 Integration of Simscape model with Vi-CarRealTime

3.4.1 Models integration

The integration of Simscape model and Vi-CarRealTime is done by means of Simulink environment, where it is possible to connect the vehicle model with controls systems or external components by means of a s-function where the car and manoeuvre data of Vi-CarRealTime are transferred as parameters to Simulink.

The inputs and the output of the s-function can be selected by two lists and then connected to other blocks in Simulink.

The s-function graphical interface connected with the Simscape model is illustrated in the Fig. 3.8.
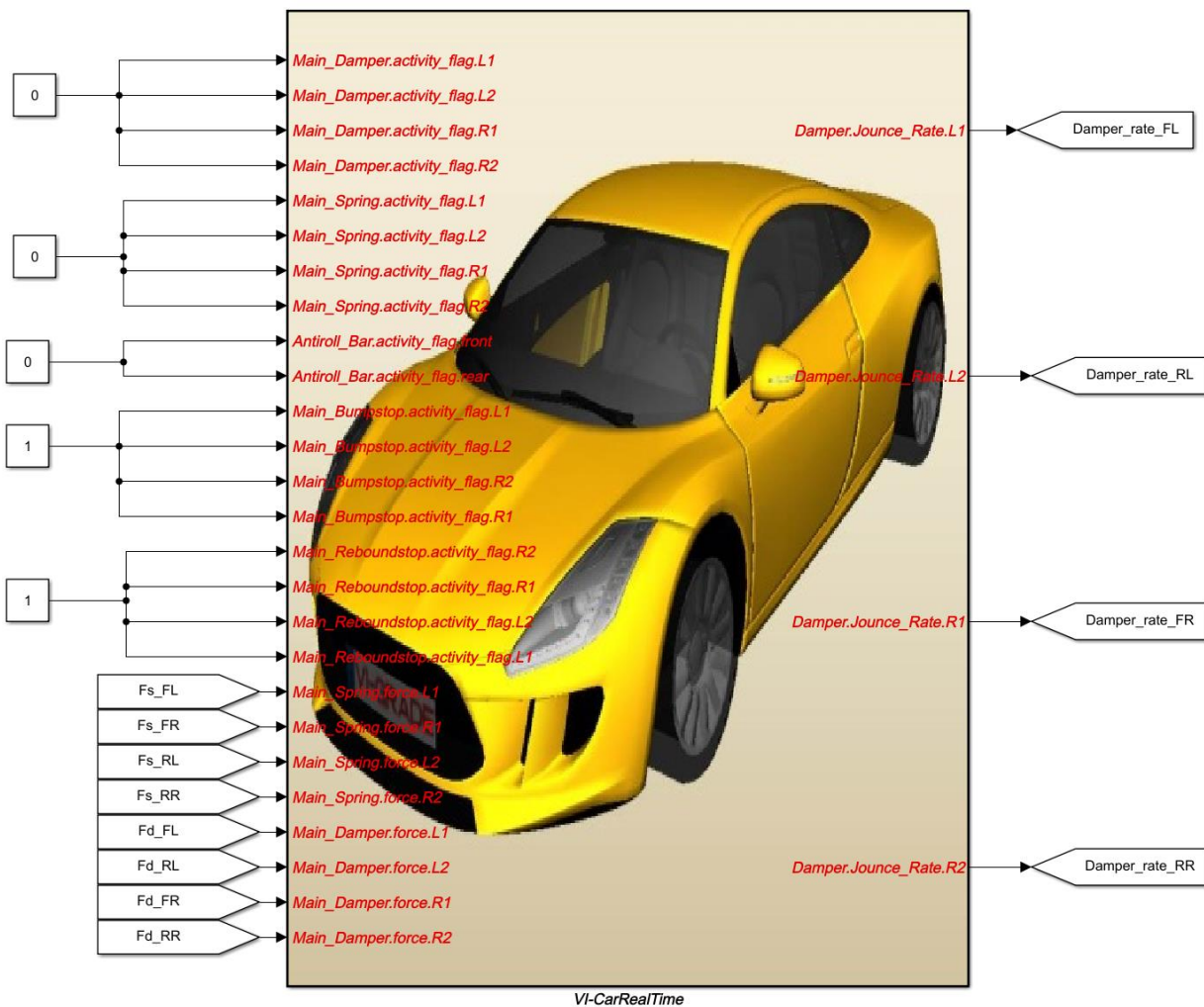
Fig. 3.8 S-function graphical interface for the physical suspension system model.

As it is possible to see in the figure, there are some input signals marked as 'flag' to which are associated 0 or 1 constant: they represent the signal that allow to activate or disactivate the components internal to Vi-CarRealTime. In this case have been disactivated the spring forces, the damper forces and the antiroll bar elastic force because their evaluation comes from the Simscape model. The output signals of the s-function are only the damper rates, that are the input of the physical model, where are linked to the ideal source generator blocks.

The input signal to the s-function, representing the elastic and the damper forces are equivalent forces because Vi-CarRealTime seem them as coming from a conventional suspension system, as said at beginning of the paragraph; as a matter of the fact them contain both the pitch/heave forces and the roll/warp forces, evaluated in different suspension points (see Fig. 2.5). The equivalent forces are evaluated in a dedicated subsystem and shown in the Fig. 3.8.
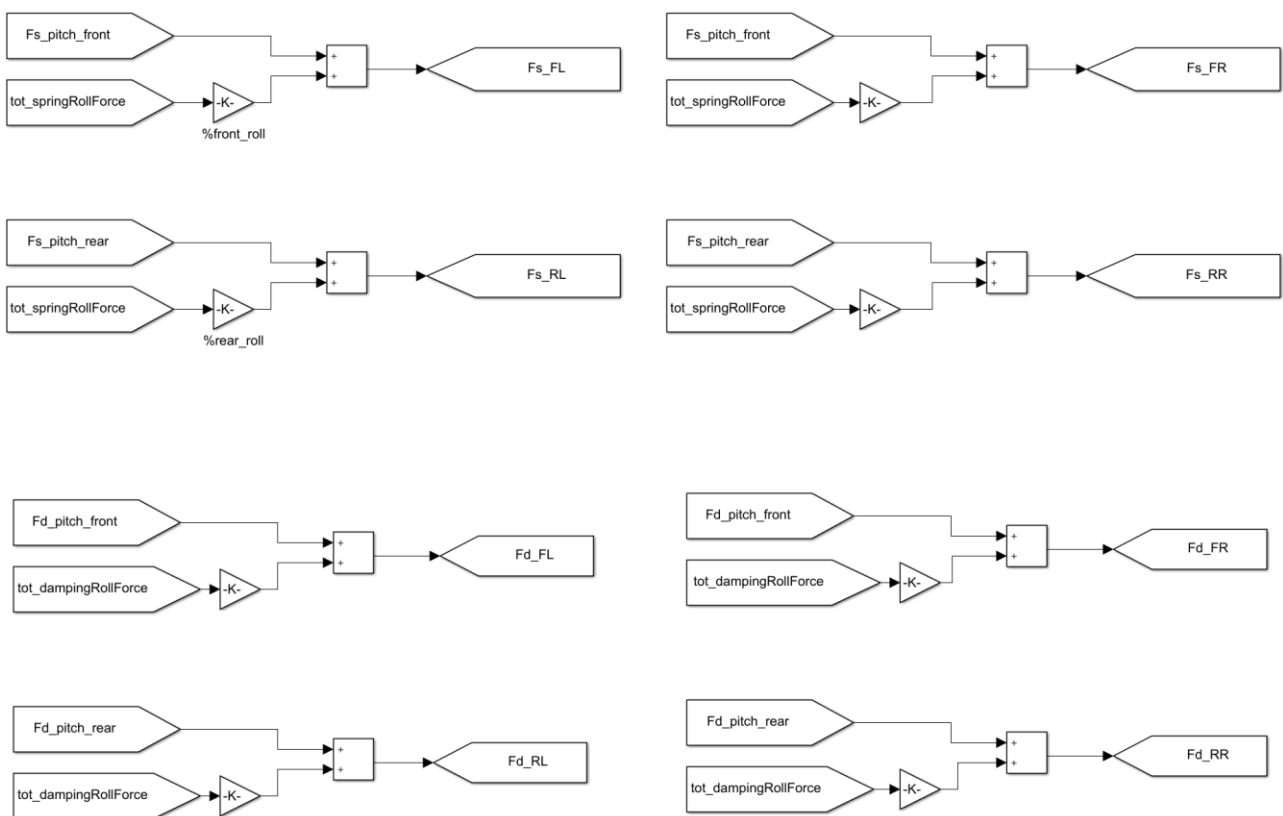
Fig. 3.8 Force evaluation subsystem. The gain linked to the total roll force and total damping force refer to the front-rear roll stiffness distribution (not at wheels level).

Before to run co-simulations, there are some other parameters that need to be modified for the integration of the physical model with Vi-CarRealTime environment. One of them is the beginning values of the deformation of the front and rear pitch springs that allow to define the ride heights of the vehicle. The model of the vehicle in Vi-CarRealTime define this parameter with a pre-load force applied at front and rear springs of the values of 5500 N for the front springs and 6500 N for the rear springs. The final spring preloads are set to 104.5 mm at front axle and 93.2 mm at rear axle, and put in front and rear pitch spring blocks, in the 'beginning value' section (Fig. 3.9) These values are calculated starting from the preload force and the springs stiffness, and then through iterative co-simulation to find the rights values.

Concerning the front-rear roll stiffness distributions, them are set to the value obtained in the 3.3.1 section (43.94% at front and 56.06% at rear), obtained setting up the *a* and *b* lever arms of the central mechanism to 80 mm and 62.70mm.

Other than the spring preloads, it is required to apply a transformation to the front and the rear pitch-damper curve implementation, because the standard vehicle model has single acting dampers while the interconnection scheme introduce double acting dampers, which means that the relative speed sensed by the dampers change. Generally, in pure pitch condition the relative speed became double, so for this reason, starting from the characteristic curves seen above, the speed point for which is defined a point is doubled.

In the following pages are illustrated the results coming from two simple manoeuvre, where no effects are expected by the interconnection scheme, to verify if the standard vehicle and the interconnected one have the same ride heights, front/rear forces distribution, roll gradients, damper forces etc. This represent the first step before to proceed with comparisons and analysis process.
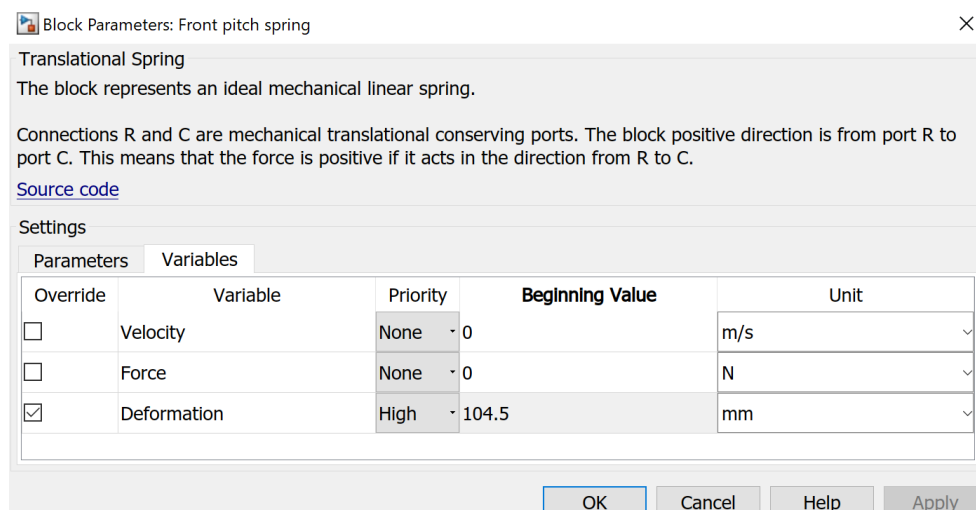
Fig. 3.9 Implementation of front pitch spring preload in Simscape block.

3.4.2 Acceleration manoeuvre

In order to verify the behaviour of the integration described above, one of the first manoeuvre conducted is an acceleration on a straight line path on an ideally flat road. This kind of simulation has been useful to set the springs preload and consequently the ride heights.

In the following graphs, are compared the standard vehicle (red) with the interconnected one (blue), in order to show the fact that on these basic manoeuvres, where the interconnection has not effects, the two models have almost overlapped behaviours. The Fig. 3.10 describe the virtual driver's input during the manoeuvre.
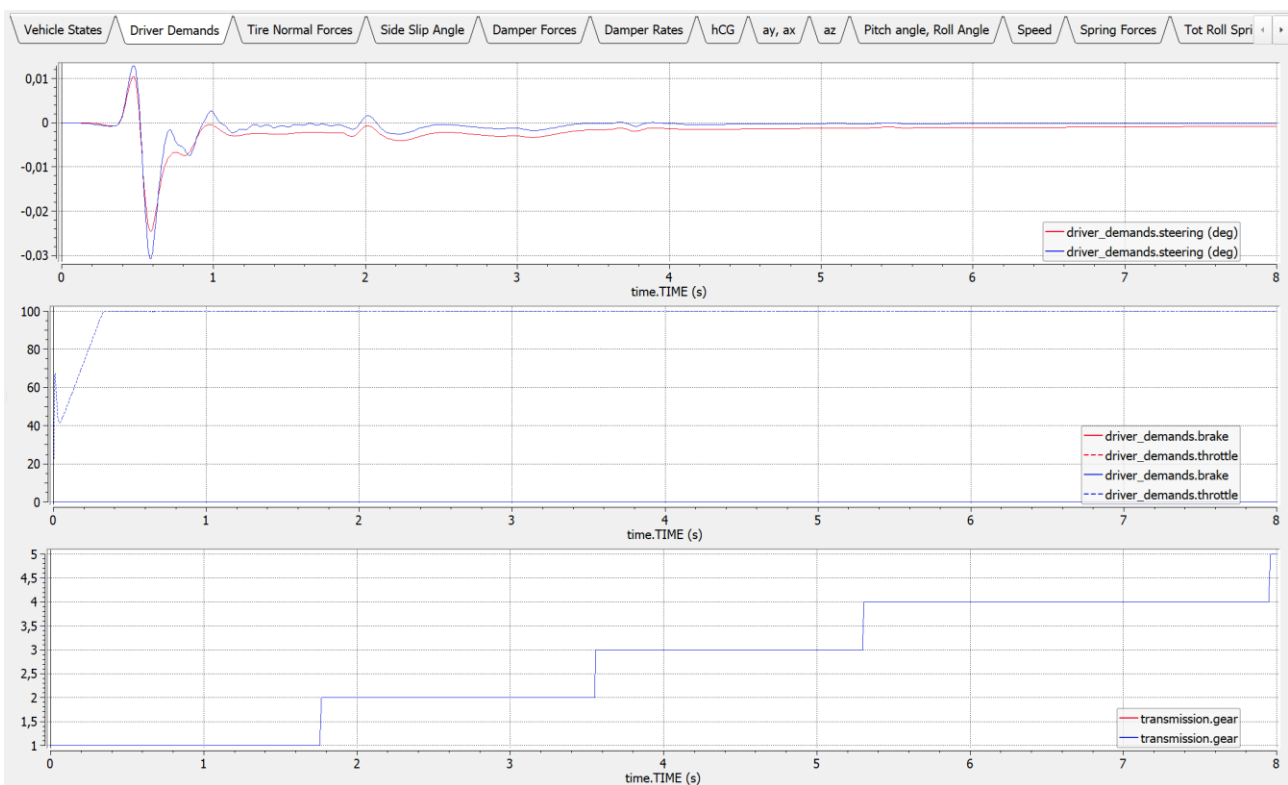
Fig. 3.10 base – interconnected Driver inputs, from top to bottom respectively the steering angle, the accelerator/brake pedal position and the gear engaged.
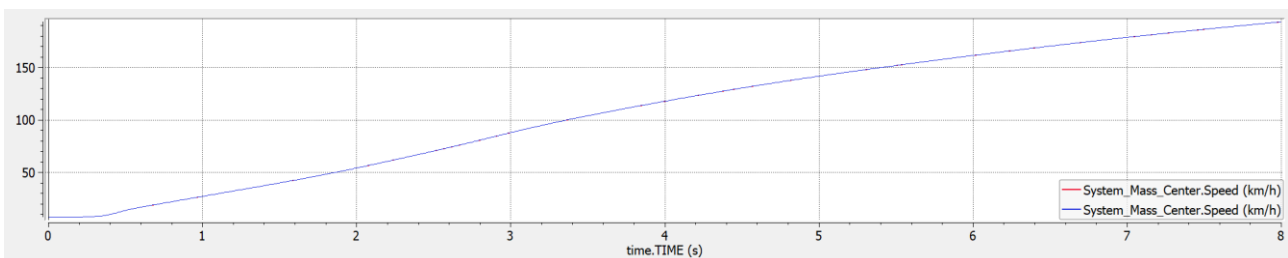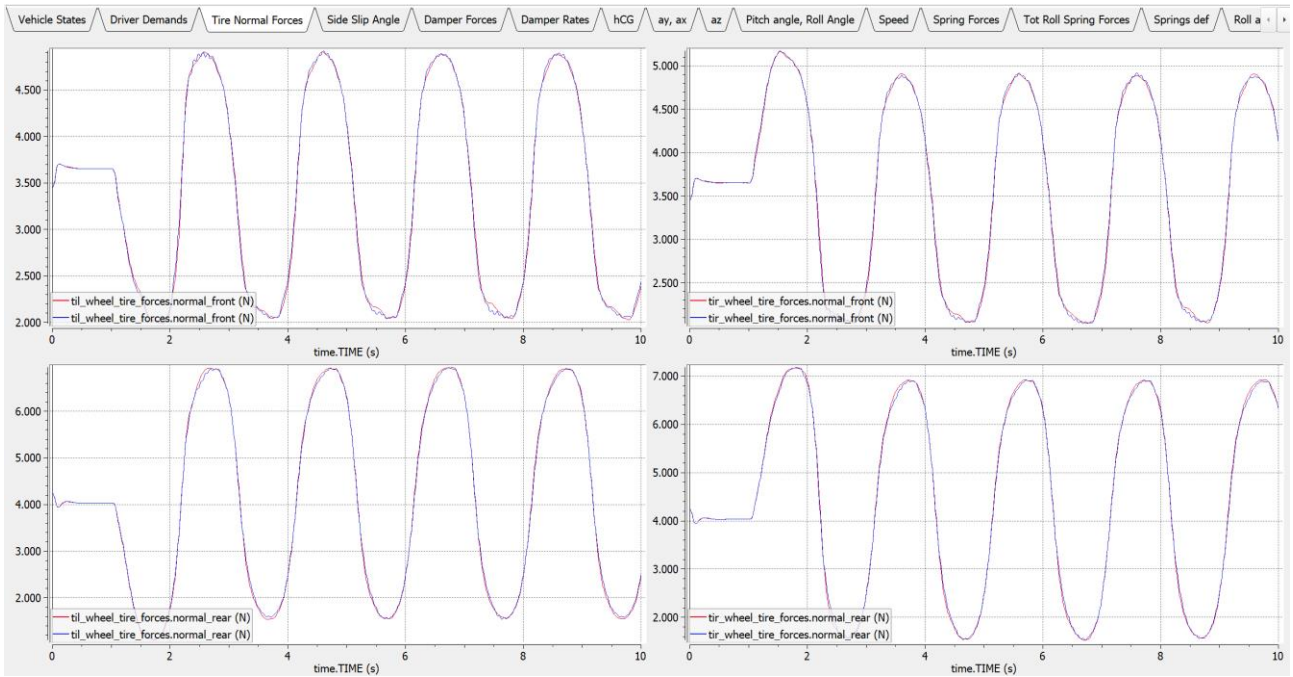

Fig. 3.11 base – interconnected Vehicle speed.
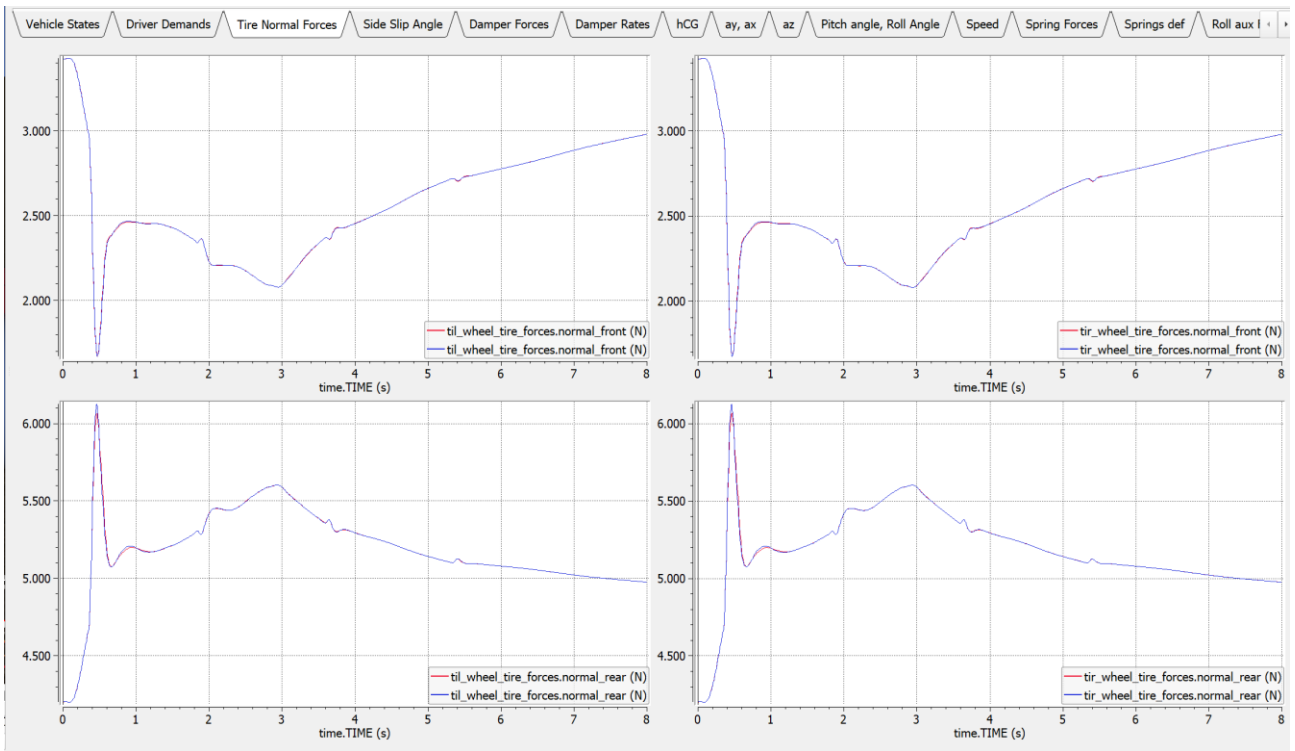
Fig. 3.12 base – interconnected Tire normal forces (above front axle).
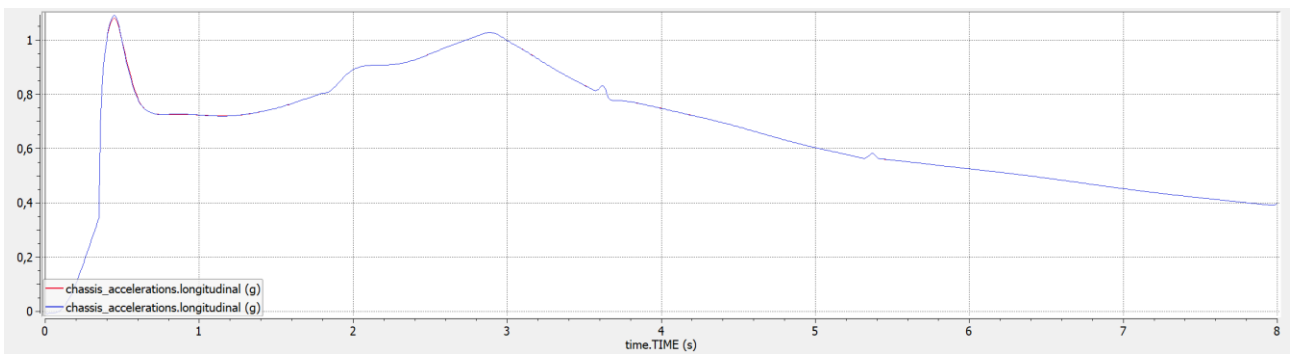
*Fig. 3.13 base – interconnected Longitudinal acceleration.*
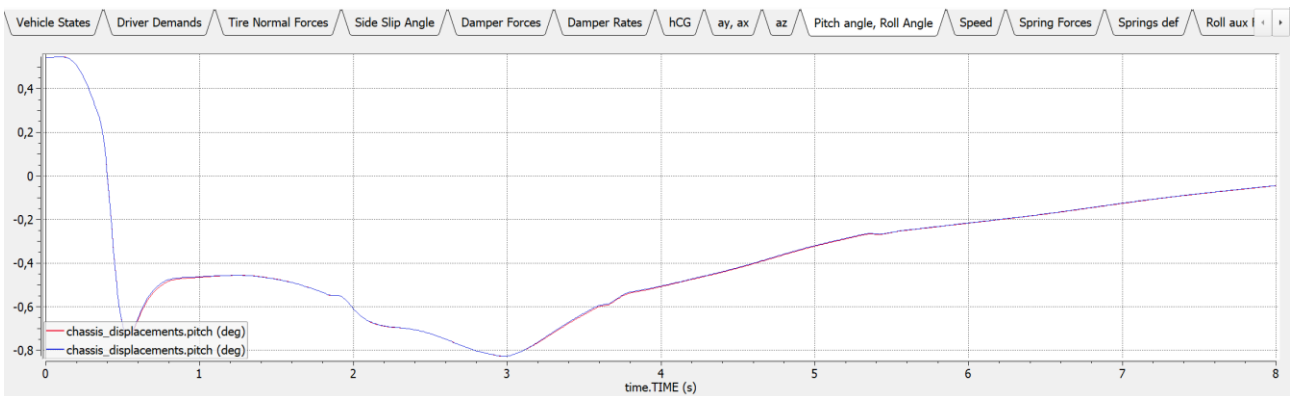
Fig. 3.14 base – interconnected Pitch angle.
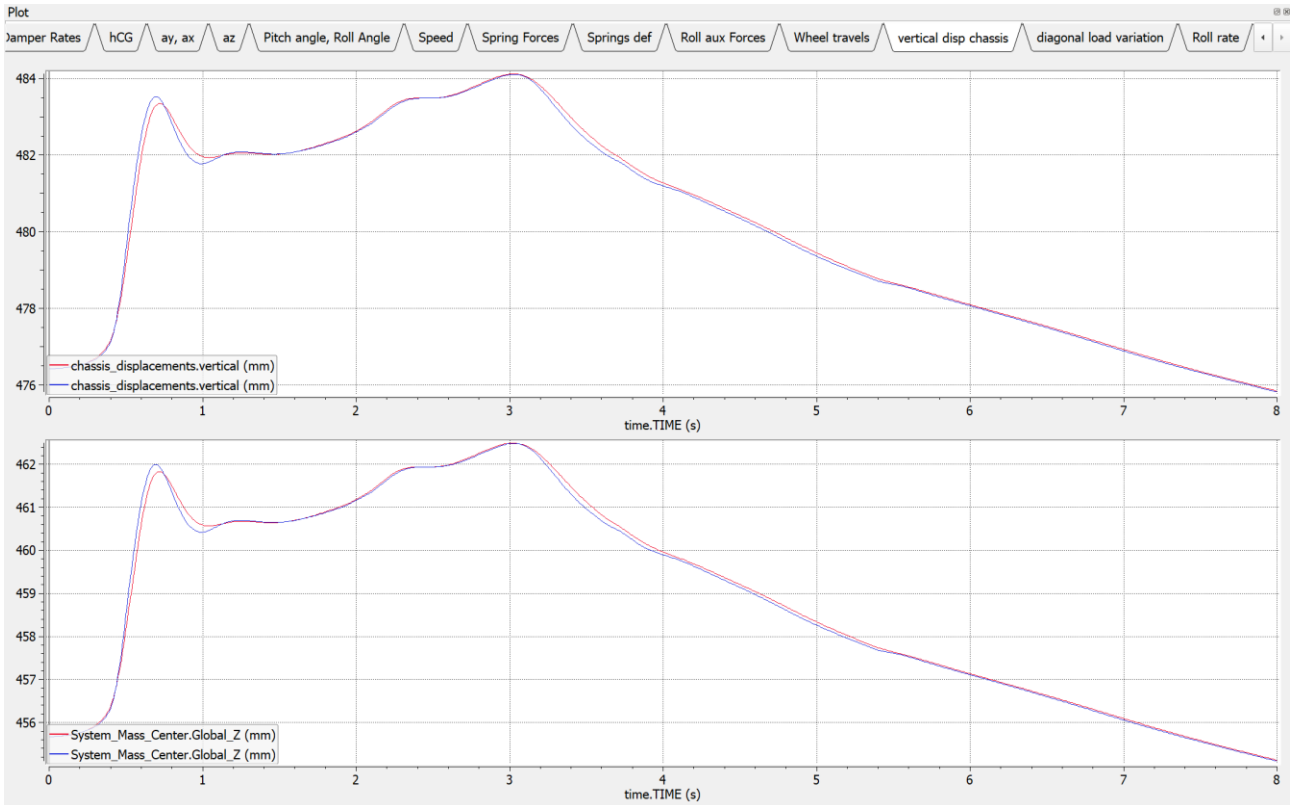
Fig. 3.15 base – interconnected Vertical displacement of the total CG of the body (top) and of the total vehicle (bottom).
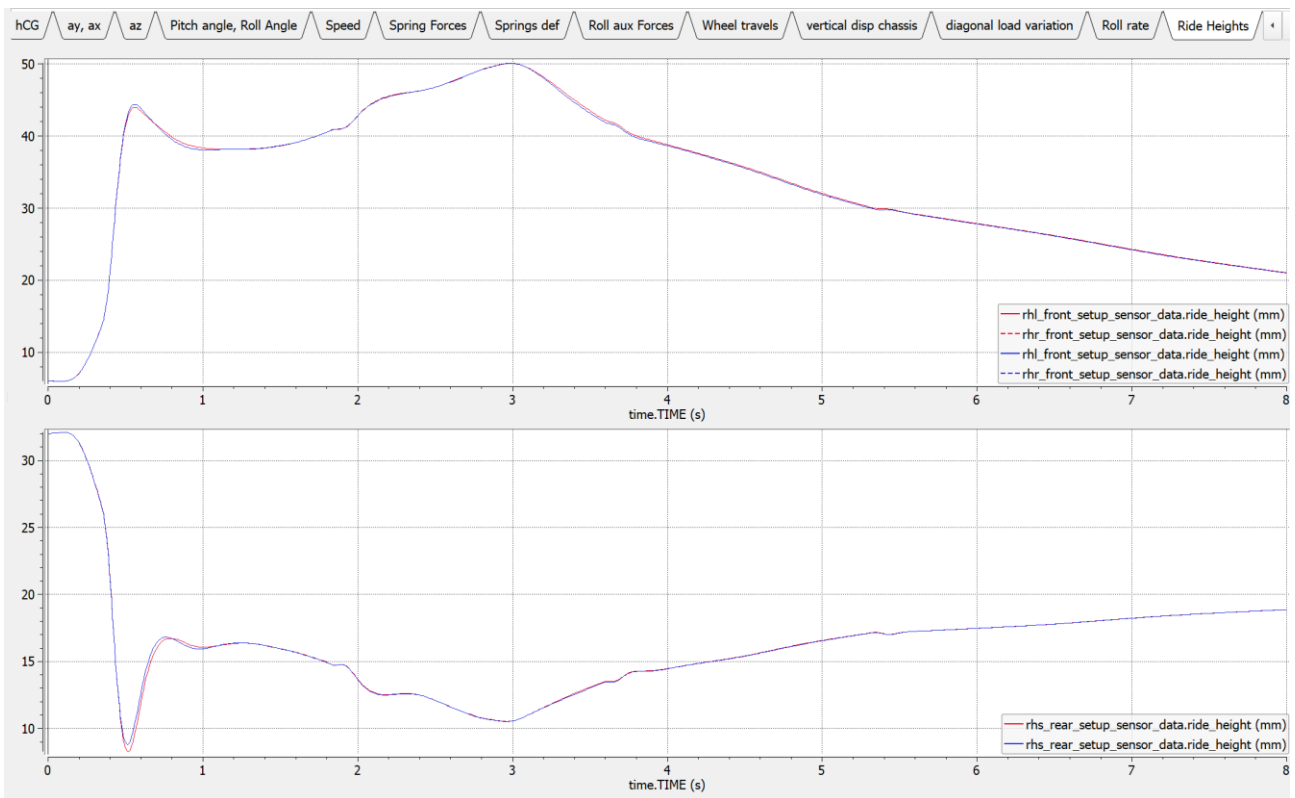
Fig. 3.16 base – interconnected Above the left and ride front ride heights and bottom the rear ride height.
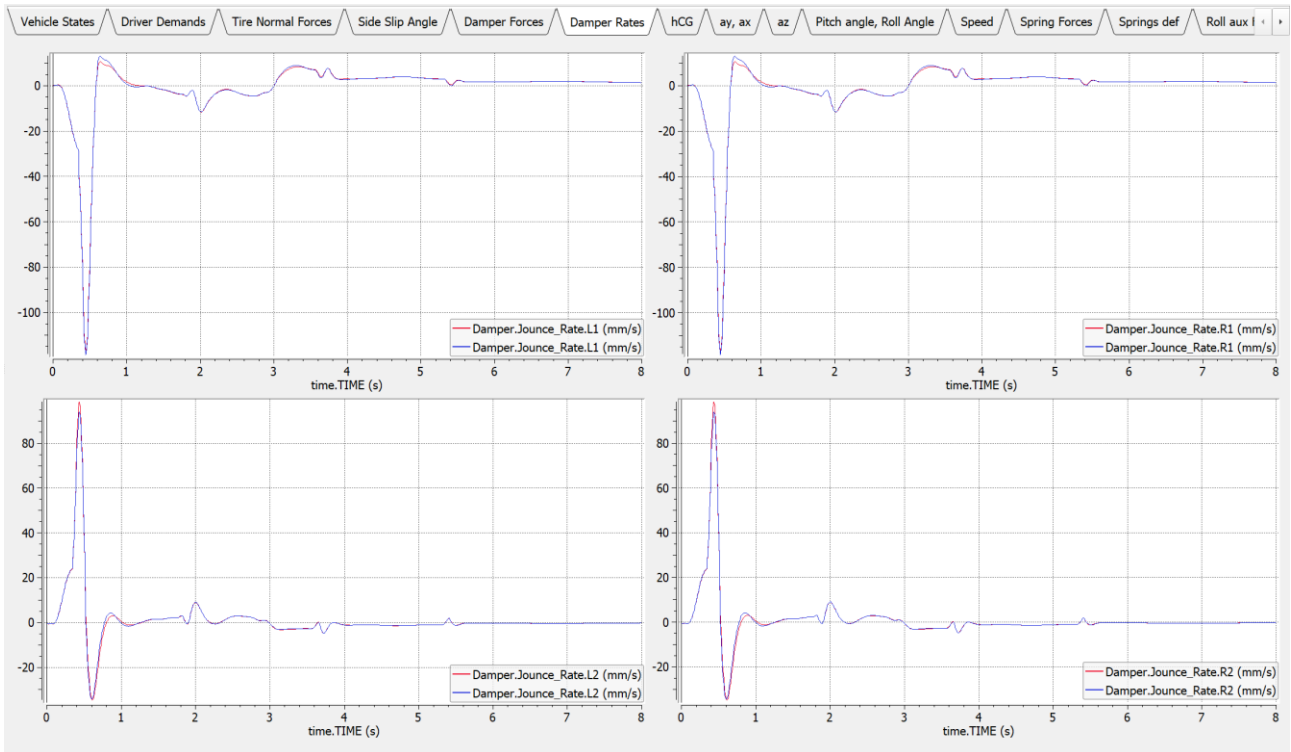
Fig. 3.17 *base* – *interconnected* *Damper rates (above the front axle). These data are important because they represent the input data at physical model.*
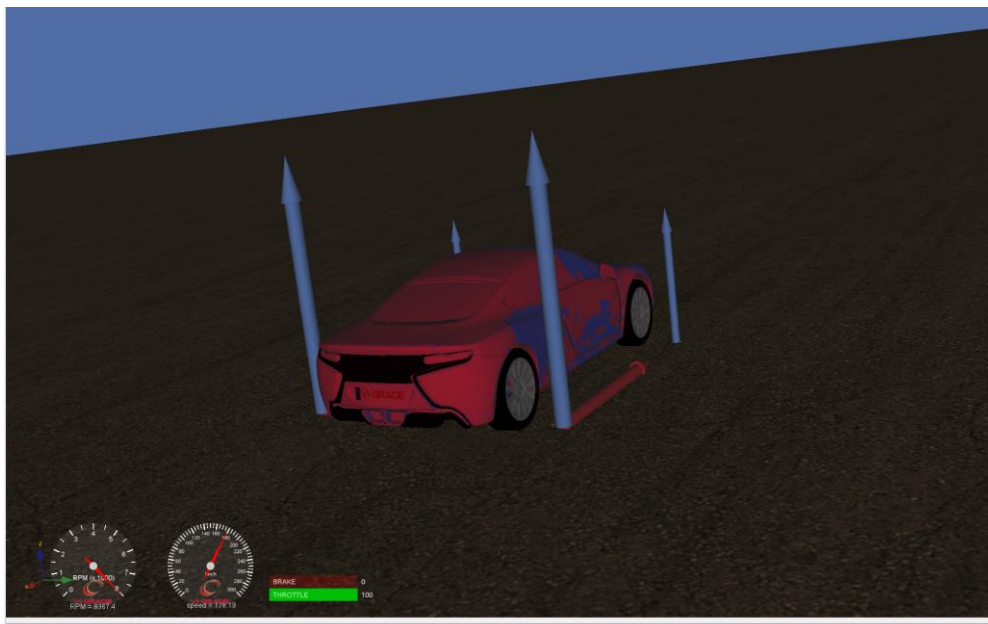
Fig. 3.18 *base* – *interconnected* *Animation of the manoeuvre in Vi-Animator.*

3.4.3 Constant radius cornering manoeuvre

A manoeuvre done to verify the behaviour of the interconnected model is a cornering phase, is the constant radius cornering where the vehicle, starting on a straight line turn toward left and maintains a constant radius. Also in this case, there are not effects expected from the interconnection and it is possible to see from the following graphs that the two models have almost the same trends.
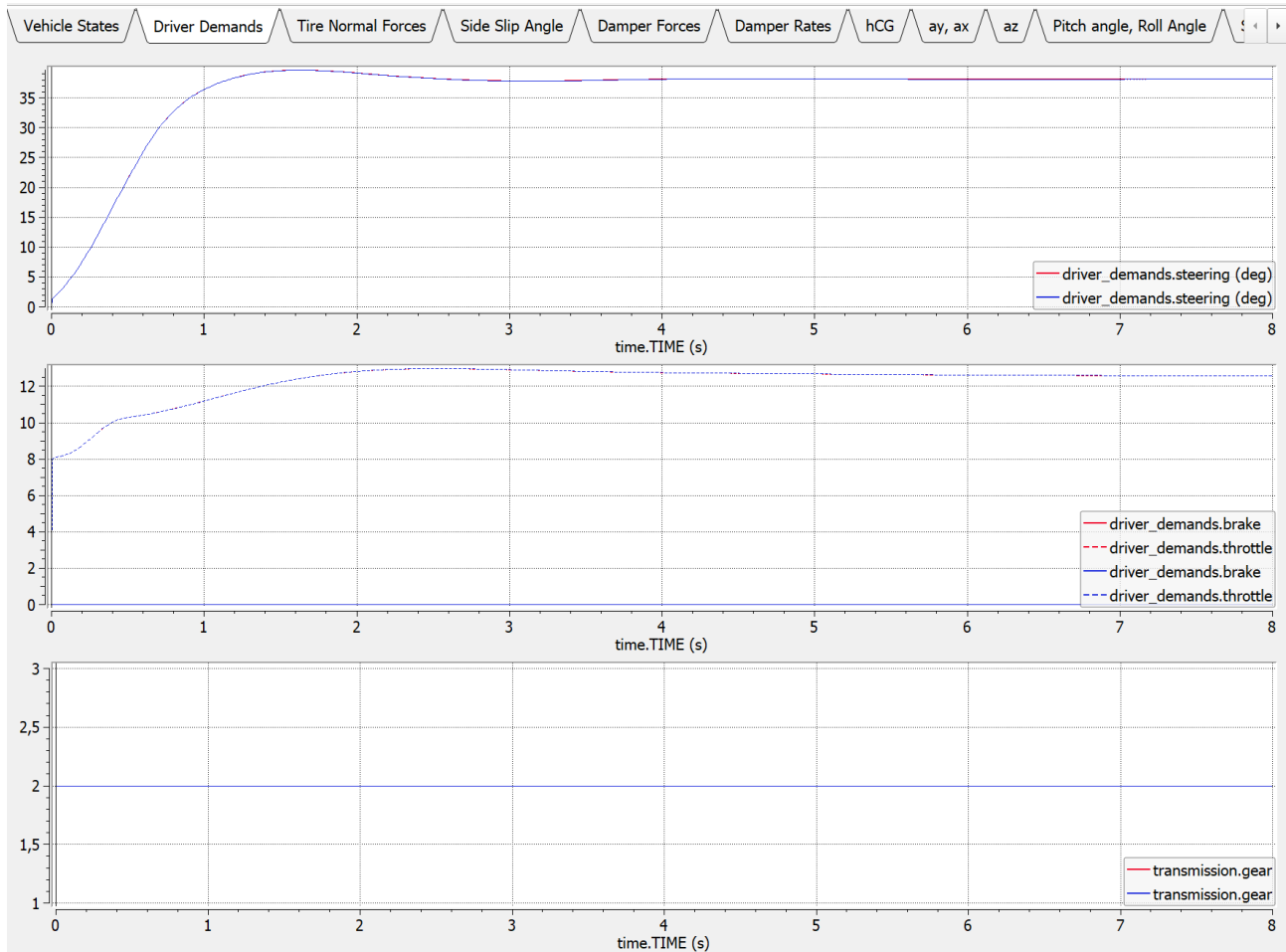
Fig. 3.19 base − interconnected Driver inpust, from top to bottom respectively the steering angle, the accelerator/brake pedal position and the gear engaged.

Fig. 3.20 base − interconnected Vehicle speed.
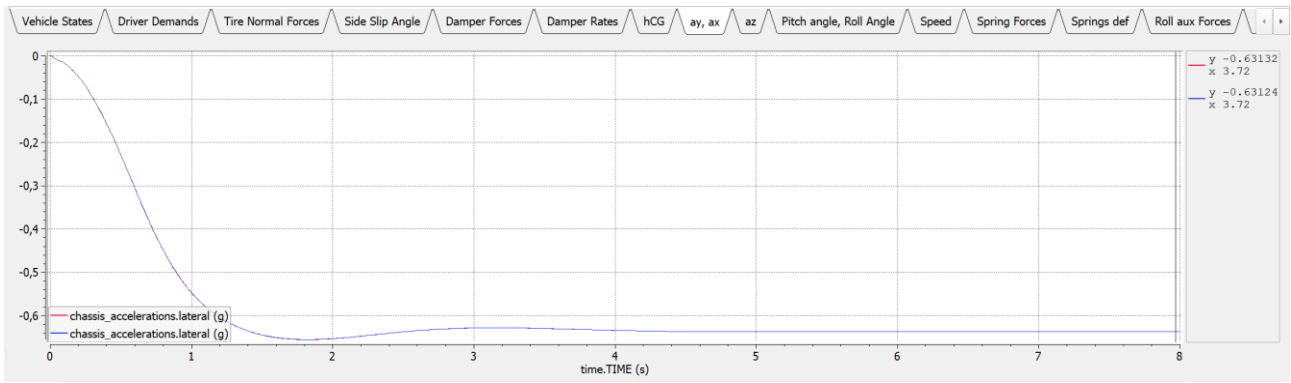
Fig. 3.21 base – interconnected *Lateral acceleration.*
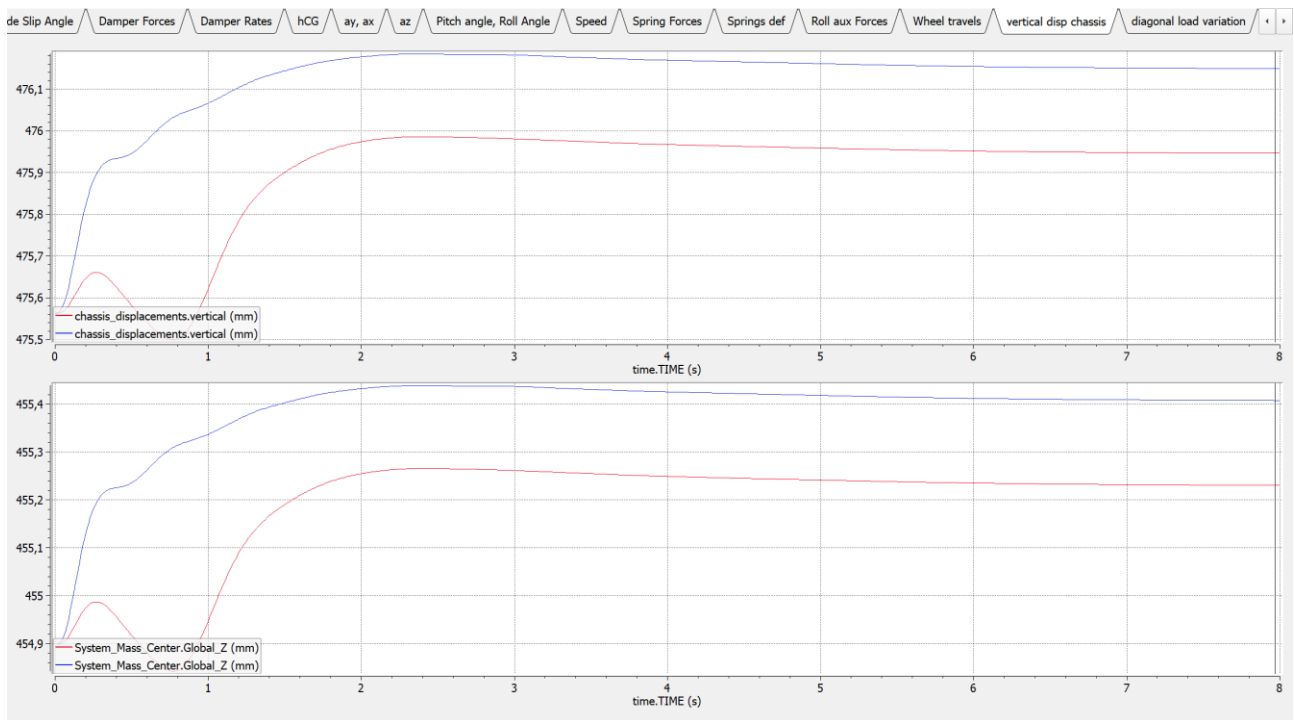
Fig. 3.22 base – interconnected *Vertical displacement of the total CG of the body (top) and of the total vehicle (bottom).*
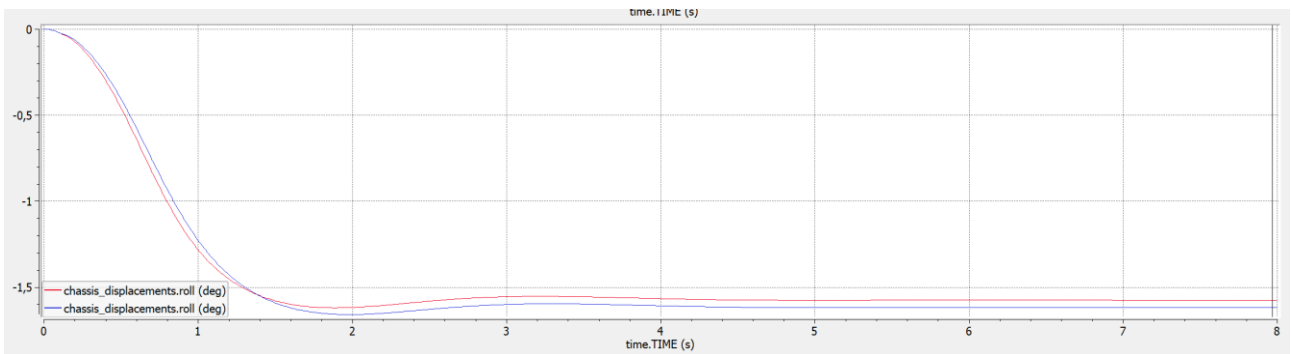
Fig. 3.23 base – interconnected *Roll angle: the difference is in the order of tenth of a degree.*
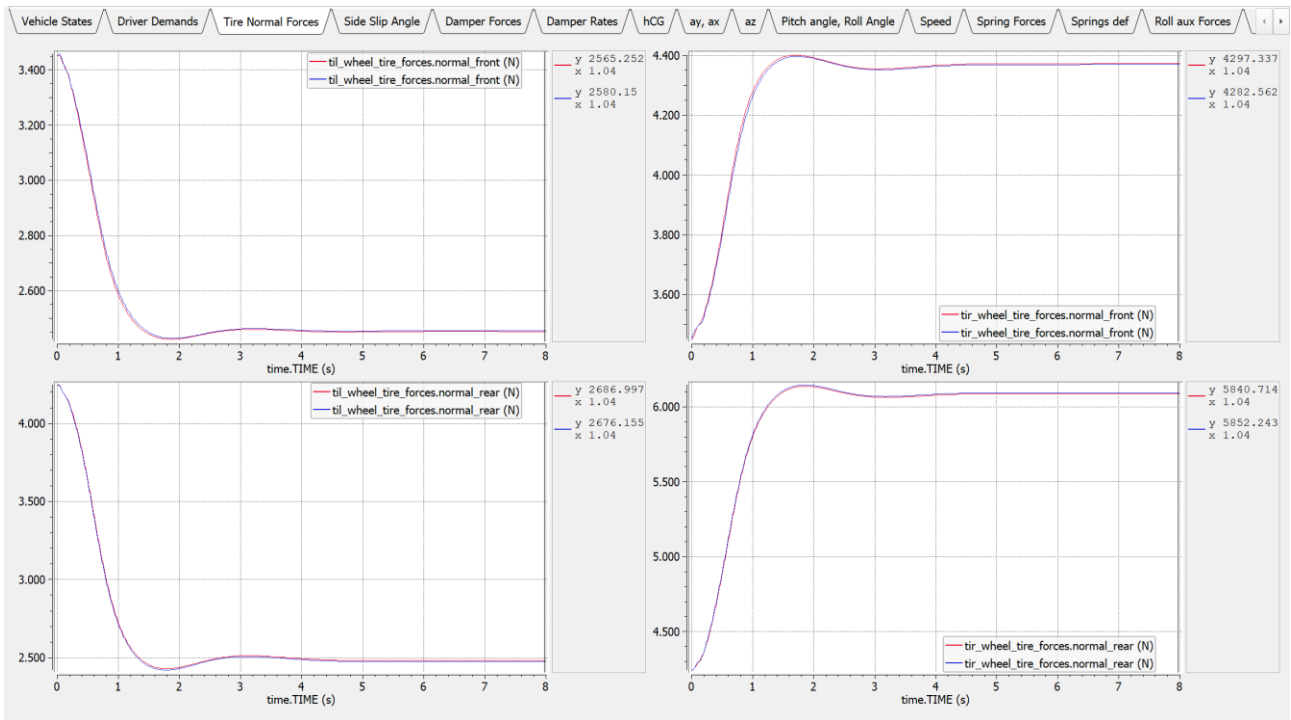
Fig. 3.24 base – interconnected Tire normal forces (above front axle).

Fig. 3.25 base – interconnected Animation of the cornering manoeuvre in Vi-Animator.

3.4.4 Sine-steer manoeuvre

It is chosen to illustrate a comparison during the sine-steer for two reason: the first because it is constituted by an alternance of transients and steady states that allows to highline the behaviour in roll steady state (as done before for the physical modelling test in a constant radius cornering) and in a transient warp condition that it is realized when the vehicle change direction, in fact in this condition the front axle tends to roll into the new direction while the rear axle is still rolling in the other. The second aspect that this kind of manoeuvre allow to underline is the increase of damping force: the conventional vehicle is not provided of roll dampers that works in parallel with the anti-roll bars, while into the interconnected vehicle the roll-damper allow to increase the damping contribution for the whole roll motion and as a consequence the vertical variation of the body centre of mass is reduced (Fig. 3.29); it is possible to appreciate a slightly reduction also for the roll and pitch angles (Fig. 3.30)
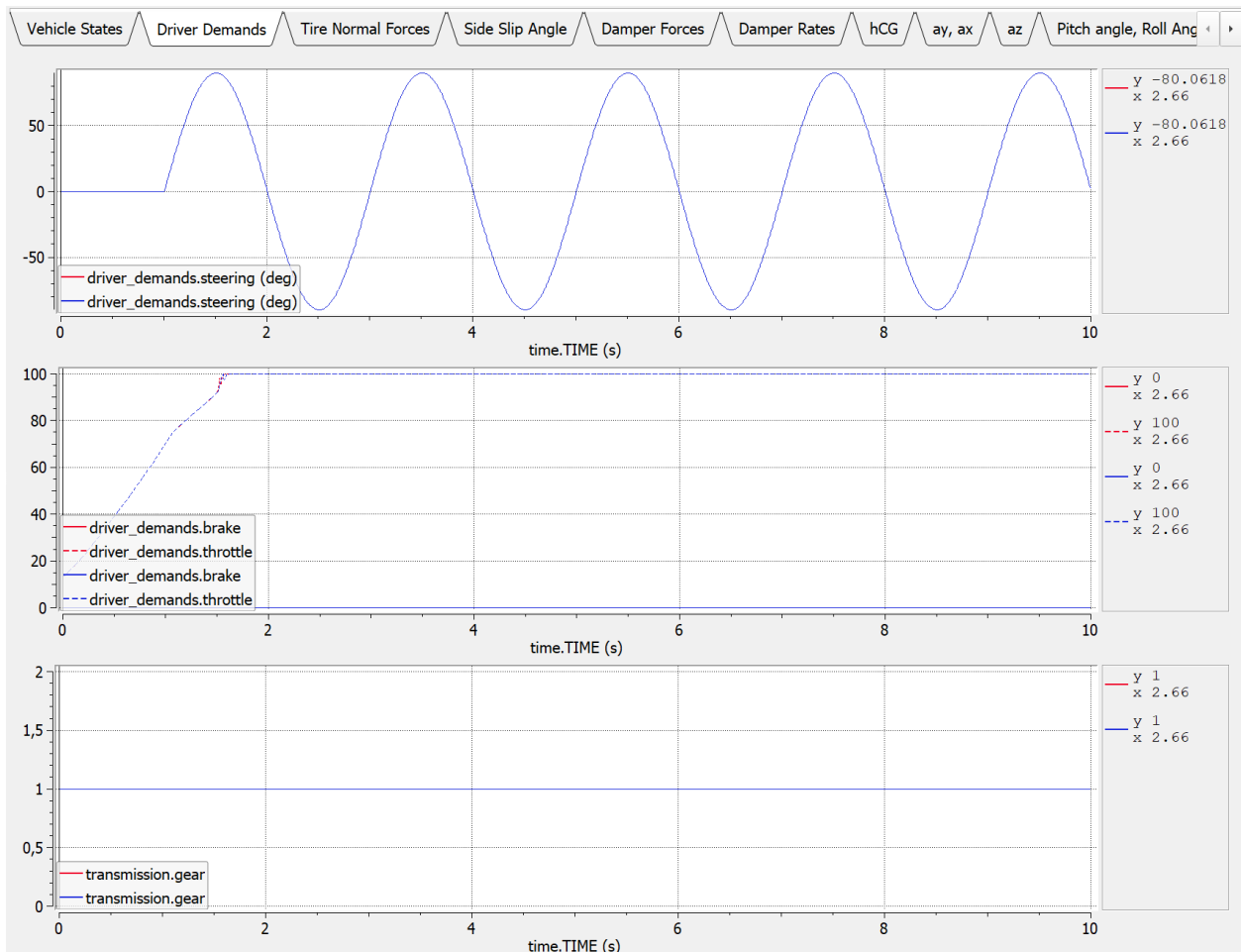
Fig. 3.26 base – interconnected Driver input, from top to bottom respectively the steering angle, the accelerator/brake pedal position and the gear engaged.

Fig 3.27 base – interconnected Tire normal forces (above front axle).
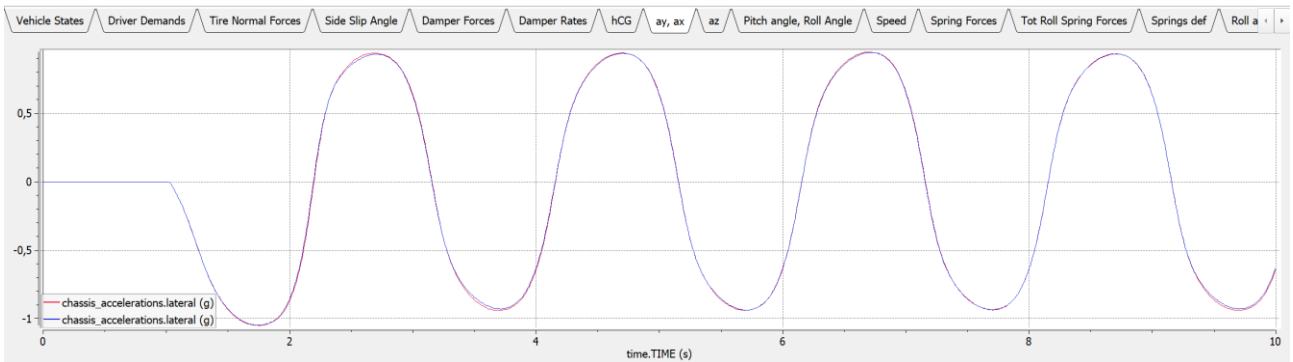
Fig. 3.28 base – interconnected Lateral acceleration.
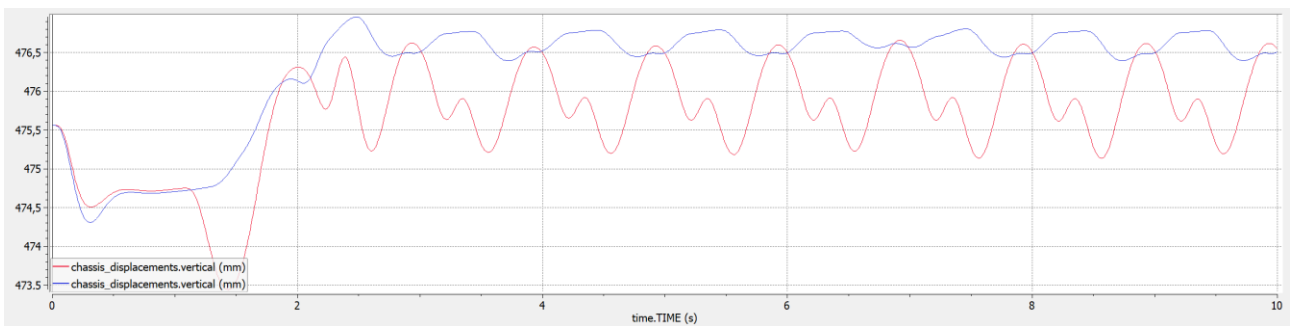
Fig. 3.29 base – interconnected Vertical displacement of the vehicle body.
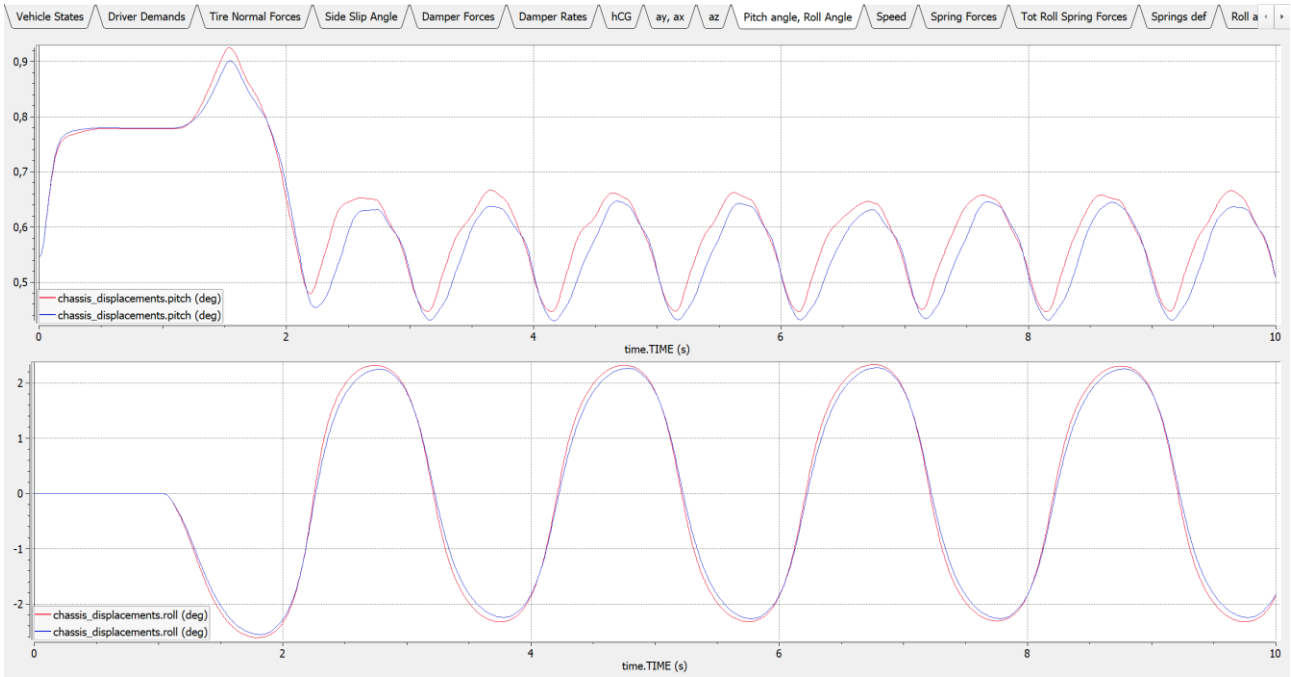
Fig. 3.30 base – interconnected Pitch angle (above) and roll angle.
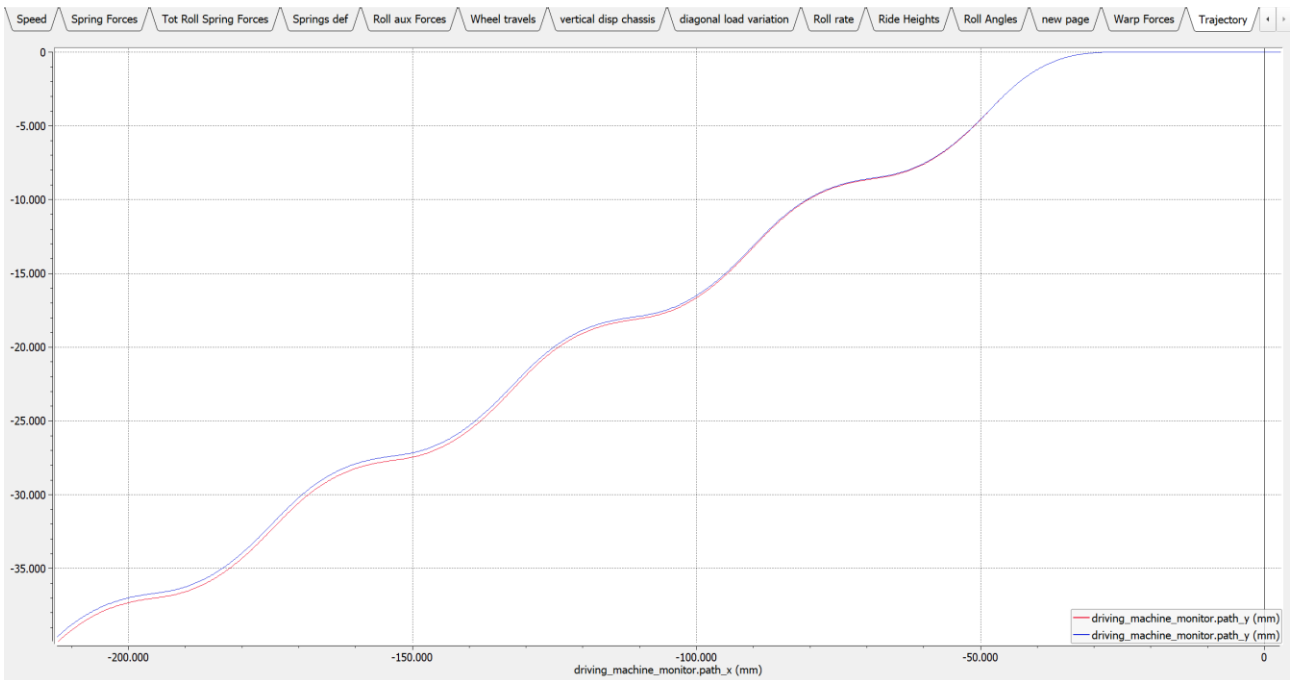
Fig. 3.31 base – interconnected Vehicle path.
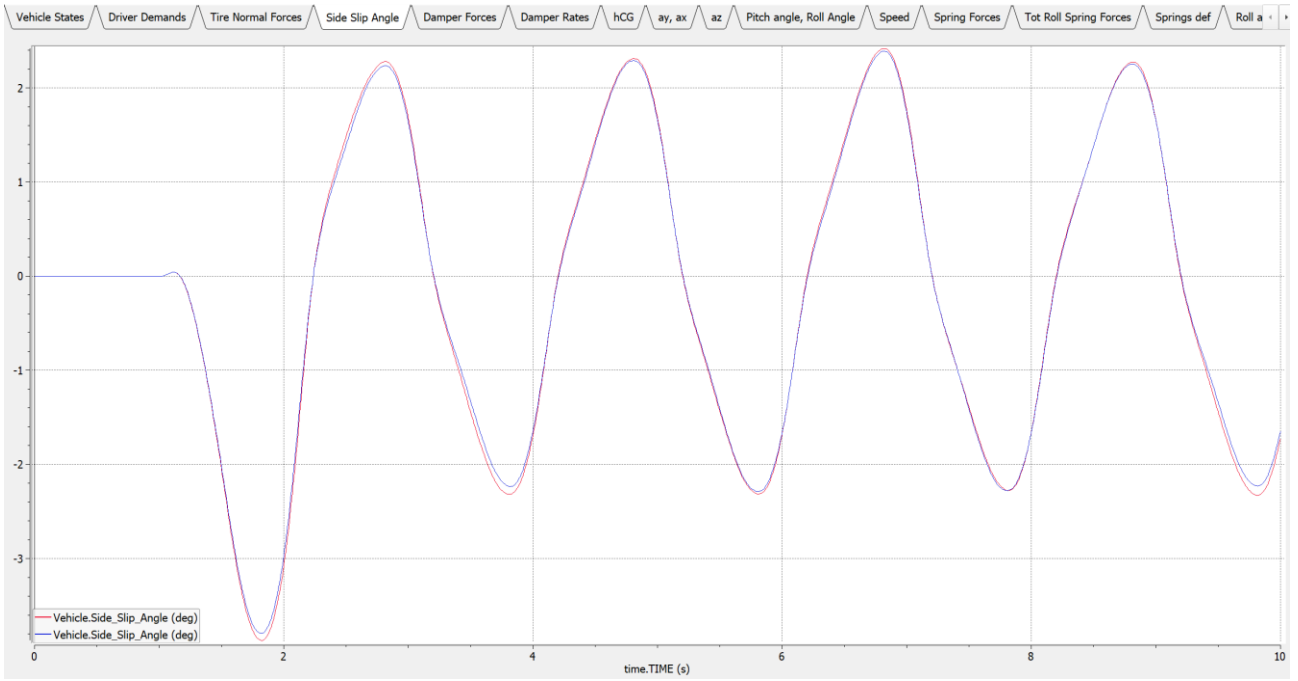
Fig. 3.32 base − interconnected Vehicle side slip angle.

4 Results

4.1 Introduction to results

In the next pages will be illustrated the results coming from the comparison between the standard vehicle and the same provided with the interconnected suspension system. It is decided to adopt the physical model to describe the suspension system, because the simplified model has shown to not represent with enough accuracy the behaviour of the physical system, highlighting that it requires more investigation and a dedicated tuning action.

The first manoeuvre chosen is a step steer manoeuvre, that is a standard manoeuvre done to characterize the lateral dynamics of the vehicle, analysing the response of the two models due to an impulsive steering input. The second one is a Fishhook manoeuvre, a test generally done to evaluate the stability properties and the obstacle avoidance capabilities of a vehicle. Then, to analyse the ride performances, have been chosen two type of tests: the first, an acceleration manoeuvre on a sinusoidal road profile and then a passage over a bump situated on the right side of the roadway. Finally, a comparison in a lap-time simulation is proposed.

In order to evaluate the effectiveness and the mode decoupling between the pitch and the roll modes for the interconnected suspension system, **the interconnected vehicle model has higher roll stiffness with respect the standard one**: the standard vehicle has a roll gradient (a coefficient that indicates the roll angle of the sprung mass for 1 g of lateral acceleration) of 2.60 deg/g_{lat}, while the interconnected one a roll gradient of 1.80 deg/g_{lat}. The effect of this choice on the ride performance will be analysed in the test on a sinusoidal road profile.
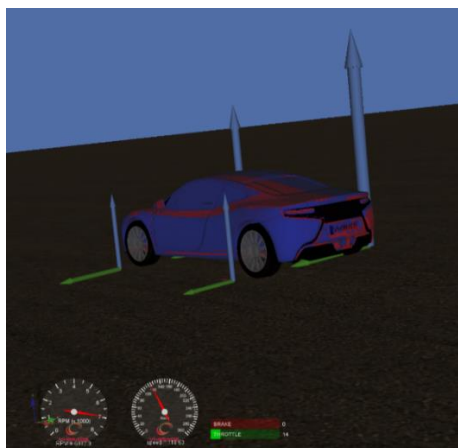
Figure 4.1 Vehicle animations in Vi-Animator.

4.2 Step-steer manoeuvre

As said before, the step-steer manoeuvre is a standard test done on a vehicle to characterize its lateral response due to an impulsive steering input. This is one of the standard manoeuvres already present in Vi-CarRealTime library in 'Test Mode', that requires to select the initial vehicle speed, the steering inputs and the duration of the step input. For this analysis, it is chosen a speed of 120 km/h and a steering input of 90 deg of the step duration of 1s (Fig. 4.2).
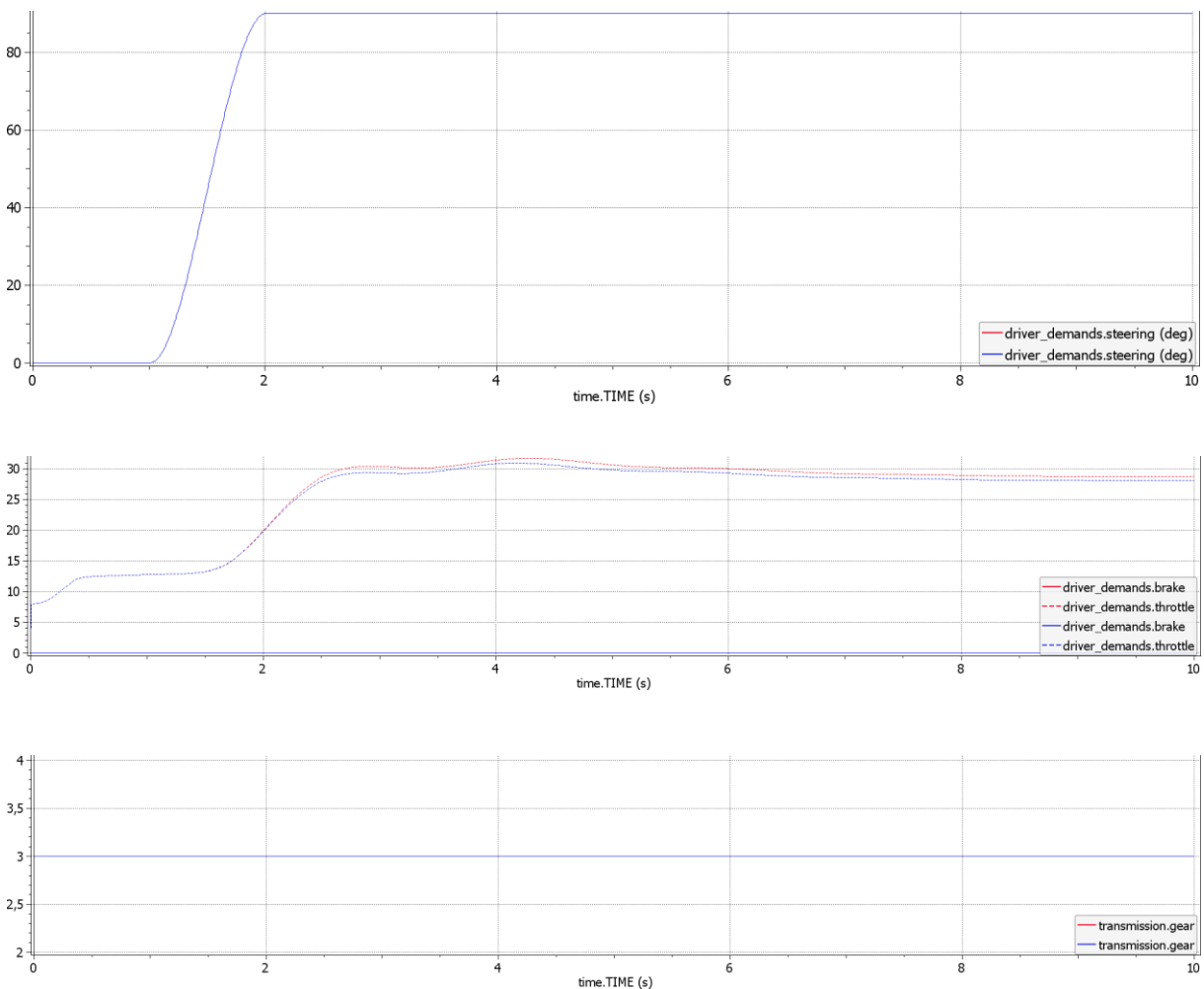
Figure 4.2 Driver inputs, from above the steering wheel angle, the accelerator position and the gear engaged (interc − base).
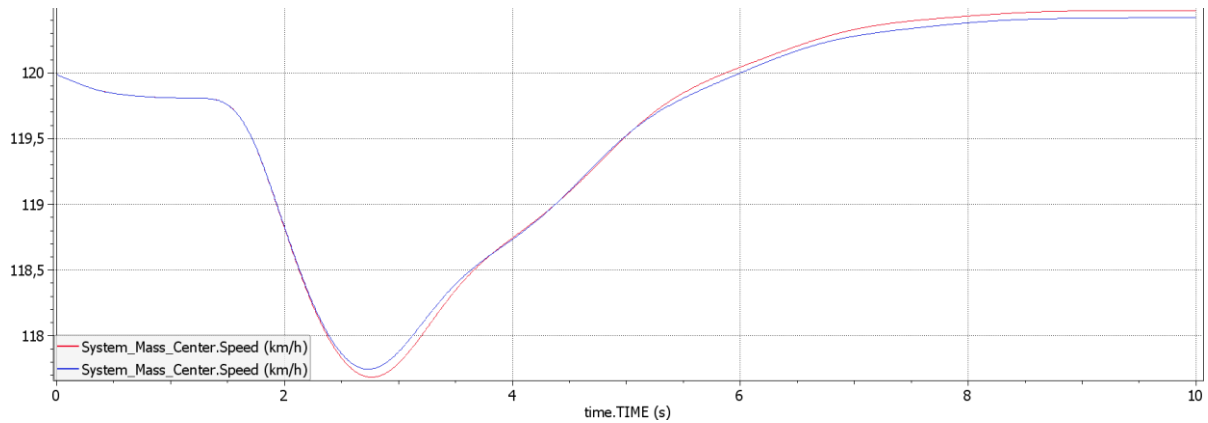
Figure 4.3 Vehicle speed (interc − base).
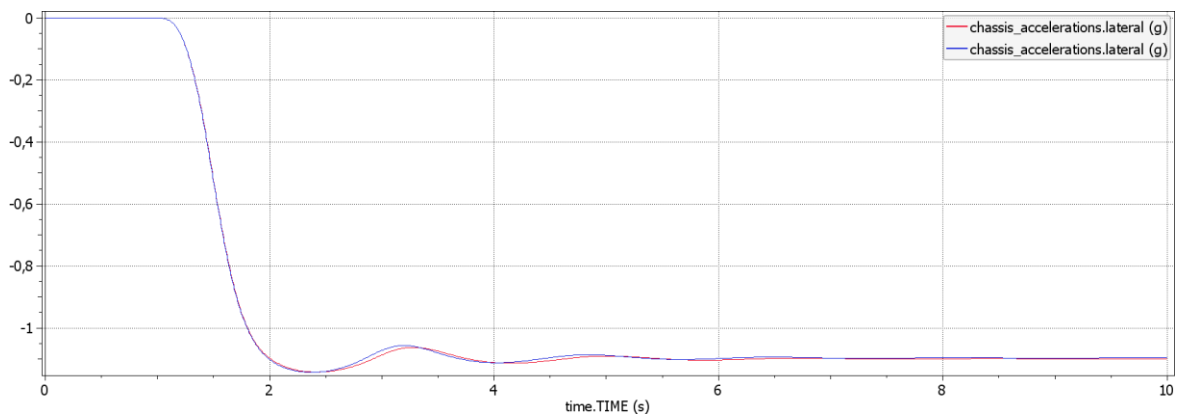
Figure 4.4 Lateral acceleration (interc − base).

The next graphs show four of the main important outputs of this kind of manoeuvre:

- the *curvature gain*, called also understeer gradient, given by the ratio between the path curvature of the vehicle and the steering angle of the front wheels with respect the road; it defines the understeer or oversteer tendency of the vehicle. In this case, there are no difference between the two models (Fig. 4.5).

- the *acceleration gain*, that is the ratio between the lateral acceleration and the steering angle; it allows to indicate the capability of the vehicle to make grow lateral acceleration as effect of a steering input: also in this case there are no differences (Fig. 4.6).

- the *sideslip gain*, given by the ratio between the side slip angle of the vehicle and the steering angle. In Fig. 4.7 is it possible to see that the mean values for the interconnected vehicle is lower of the 7%, sign of a better stability and road holding.

- The *roll angle gain*, representing the ratio between the roll angle of the vehicle and the steering angle; in this case (Fig. 4.8) the interconnected vehicle has a significative reduction of 30% with respected of the standard vehicle, as effect of the higher roll stiffness.
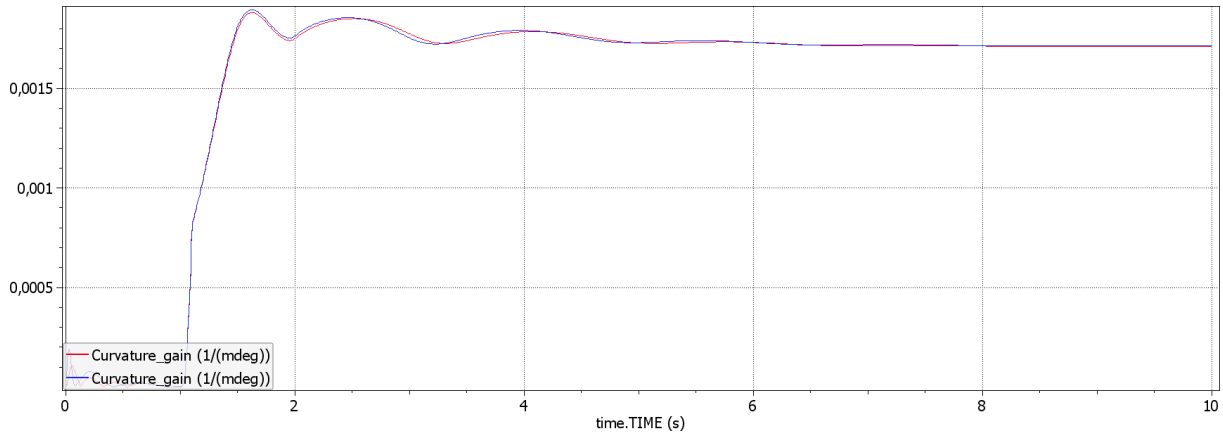
Figure 4.5 Curvature gain or understeer coefficient (interc − base).
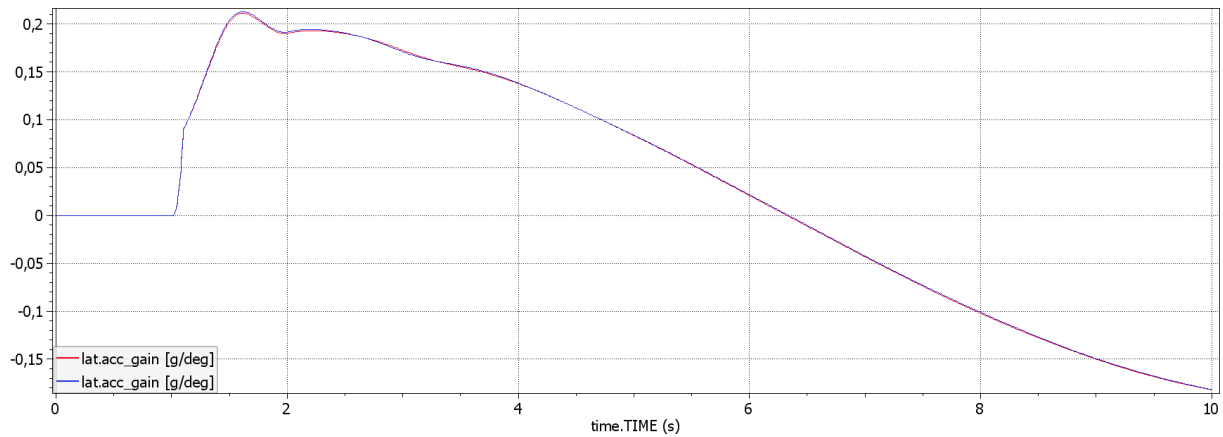
Figure 4.6 Lateral acceleration gain (interc − base).
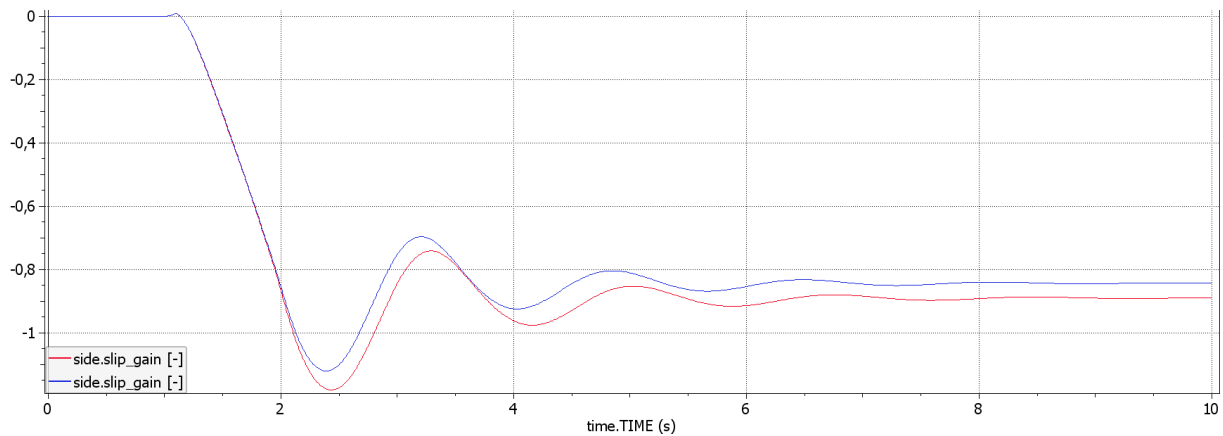
Figure 4.7 Sideslip gain (interc − base).

79
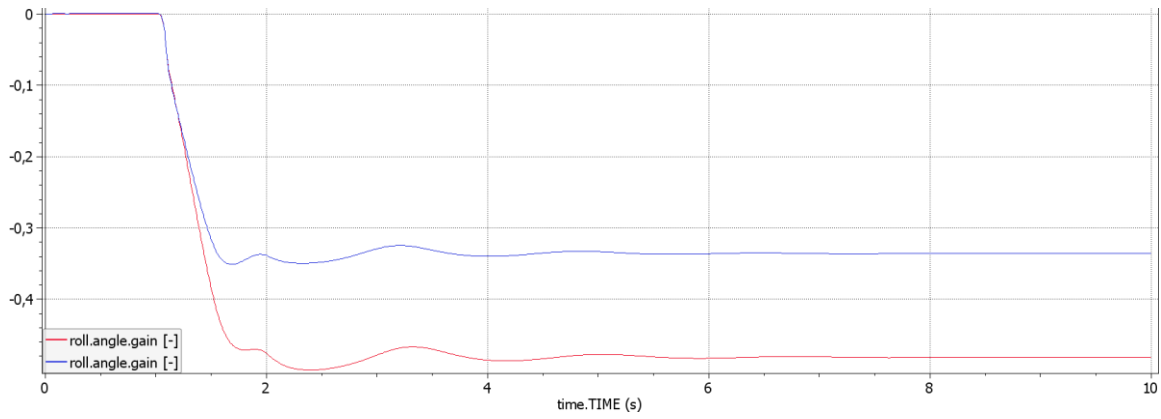
Figure 4.8 Roll angle gain (interc − base).

As showed by the sideslip gain, the sideslip angle for the interconnected vehicle is lower; this is an important parameter for the lateral vehicle dynamics because it is related with the slip angles of the front and rear tires: small tire slip angles indicate that the tire is working in the linear area of the tire lateral characteristic (F_y vs slip angle), sign of a better tire employment and grip capabilities (Fig. 4.9). Therefore, also the yaw rate trend is slightly better for the interconnected vehicle (Fig. 4.10), while the curves of the lateral accelerations are practically overlapped.
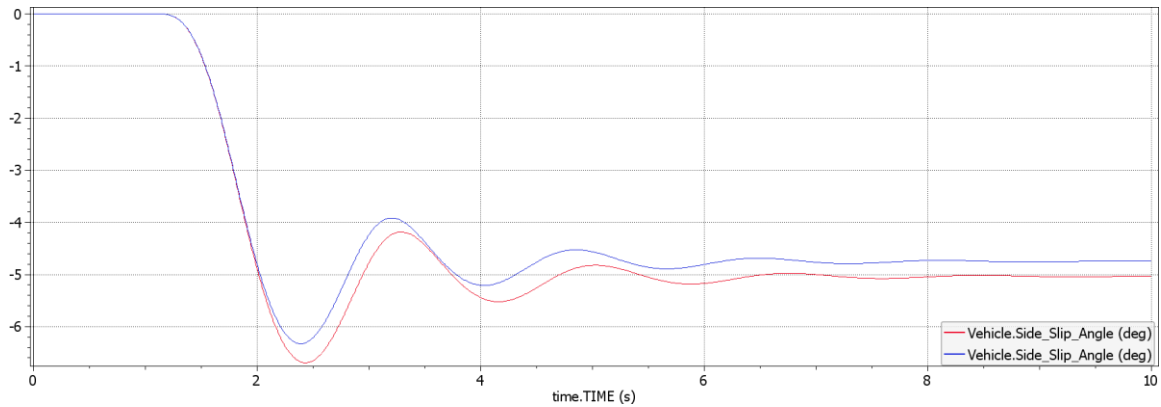
Figure 4.9 Vehicle side slip (interc − base).
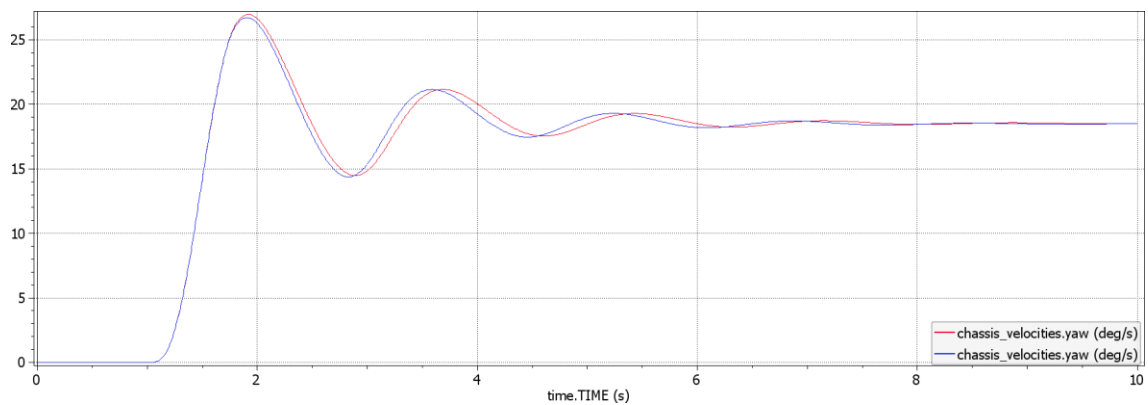
Figure 4.10 Vehicle yaw rate (interc − base).

As it is possible to see in the Fig. 4.11 the roll angle for the interconnected vehicle is reduced of 38.2%, thanks to the increasing in roll stiffness. It is important to highline that this fact has significative benefits because it allows to better exploit the suspension kinematics, in fact when the car is subjected to a roll motion, there are two effect on the wheel's angles:

- The external wheels, that are the more loaded and the more influents for the dynamics, moves upward but not in a vertical direction but in a circular one (defined by the kinematics of the suspension analysed) so that their *camber angles* tend to became positive reducing the contact area with the road and as a consequence the grip capabilities of the car;
- The wheels are subjected at the 'bump steer' that means an undesired and uncontrolled variation of the wheels' *toe angles* that influences negatively the directional stability of the vehicle.

For this reason, reducing the roll angle allows to reduce these undesirable effects and improve the handling of the car. In this analysis has been observed a reduction of the 6% of bump steer at right rear wheel that is the external one and a decrease of 15.3% for the left rear wheel (Fig. 4.12). In the Fig. 4.13 it is possible to observe the effects on the wheel's camber angle: with the interconnected configuration the external wheels' angle (right) are always negative, allowing to exploit the so called 'camber trust' that generate an additional contribution in lateral force generation.
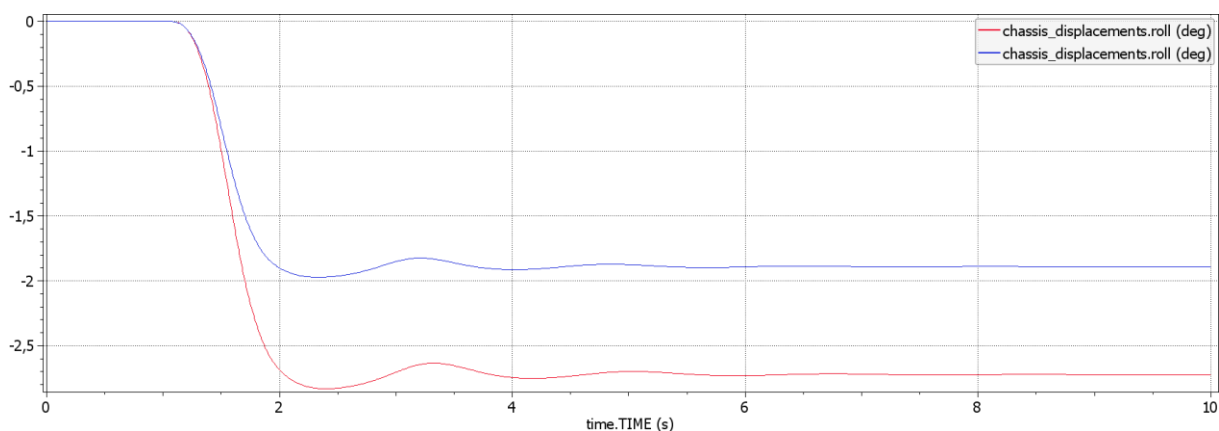
Figure 4.11 Roll angle (interc − base).
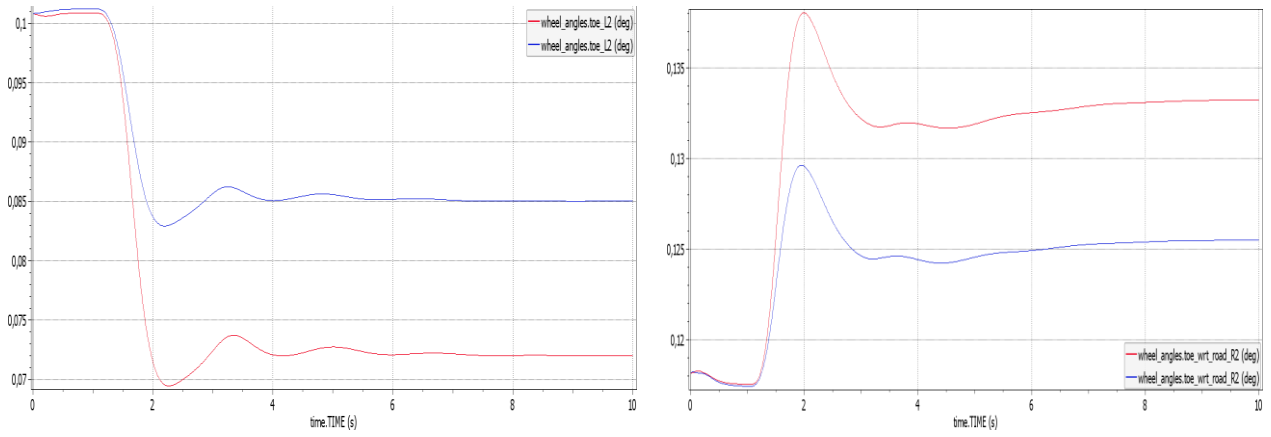
Figure 4.12 Toe angle variation at left rear tire (on the left) and at right rear (on the right) interc − base.
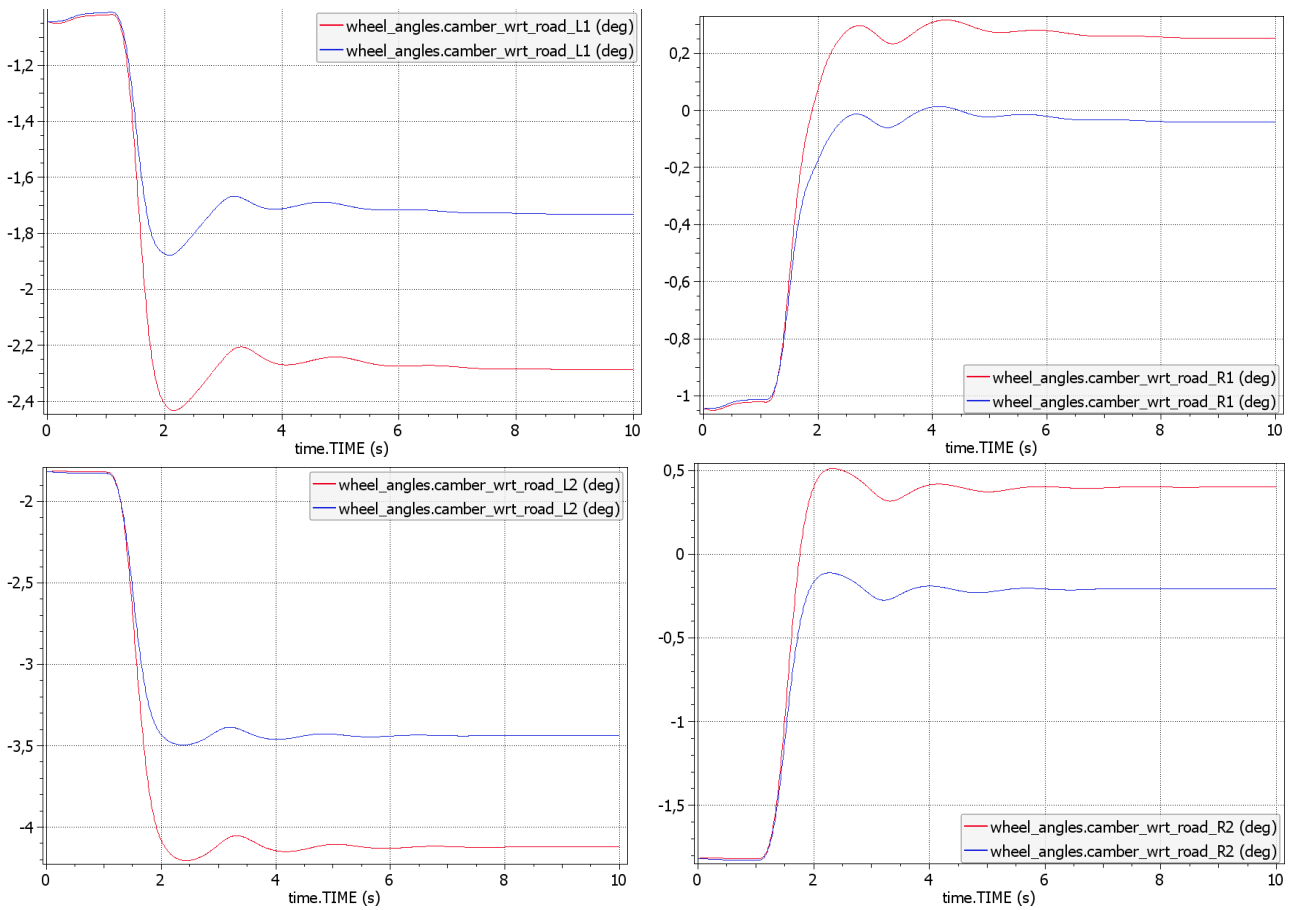
*Figure 4.13 Camber angle; above the front axle (*interc − base*).*

The graphs seen up to now describes the improvement of this type of suspension system on the vehicle handling, while the next ones are two parameters involved with the vehicle comfort: the roll rate and the roll acceleration, respectively Fig. 4.14 and 4.15. As before, it is possible to observe an improvement for the interconnected configuration, that allows to reduce significantly both the roll rate (-30%) and the roll acceleration.
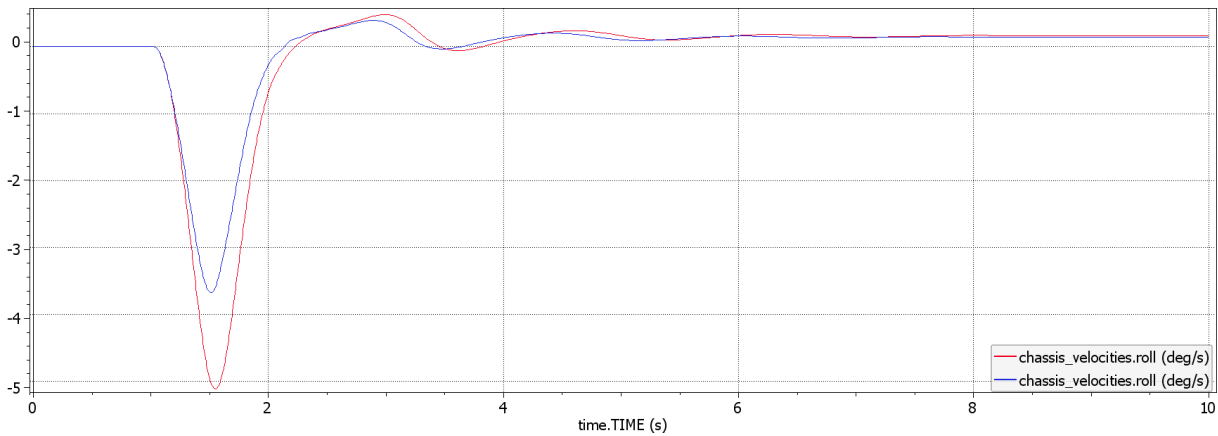
Figure 4.14 Roll-rate (interc − base).
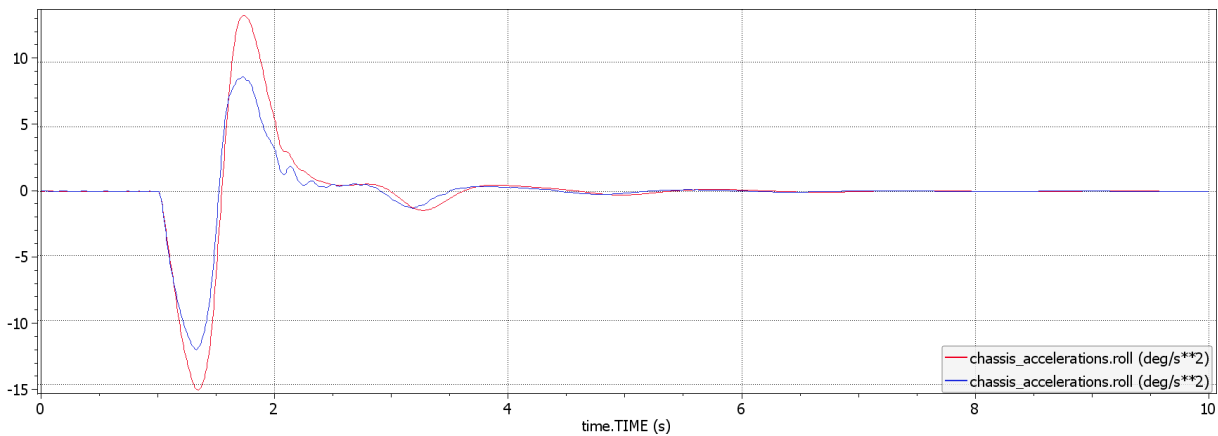
Figure 4.15 Roll acceleration (interc − base).

For completeness of information, the next graphs show the evolution of the parameters involved with the modelling of the suspension system: the Fig. 4.16 illustrate the displacements of the piston inside the wheels' actuator; in the Fig. 4.17 are shown the oil pressure in the hydraulic lines between the wheels' actuators and the double acting central cylinders; in Fig. 4.20 are described the deformation of the roll spring and the displacements of the pistons inside the front and the rear double acting central cylinders.
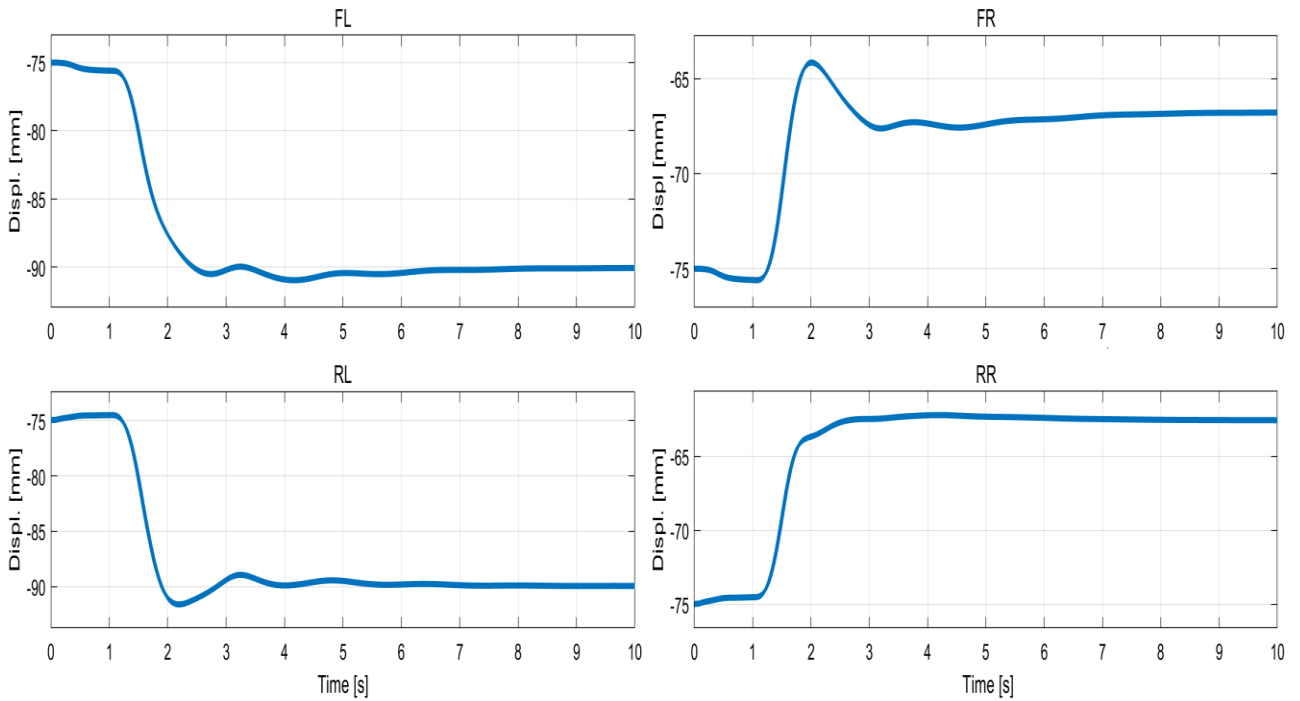
Figure 4.16 Displacements of wheel's actuators [mm]. The starting point is -75 mm because of the compression and the drop travel of the wheels; in this case the right wheels are subjected to compression travel, while the left to drop.
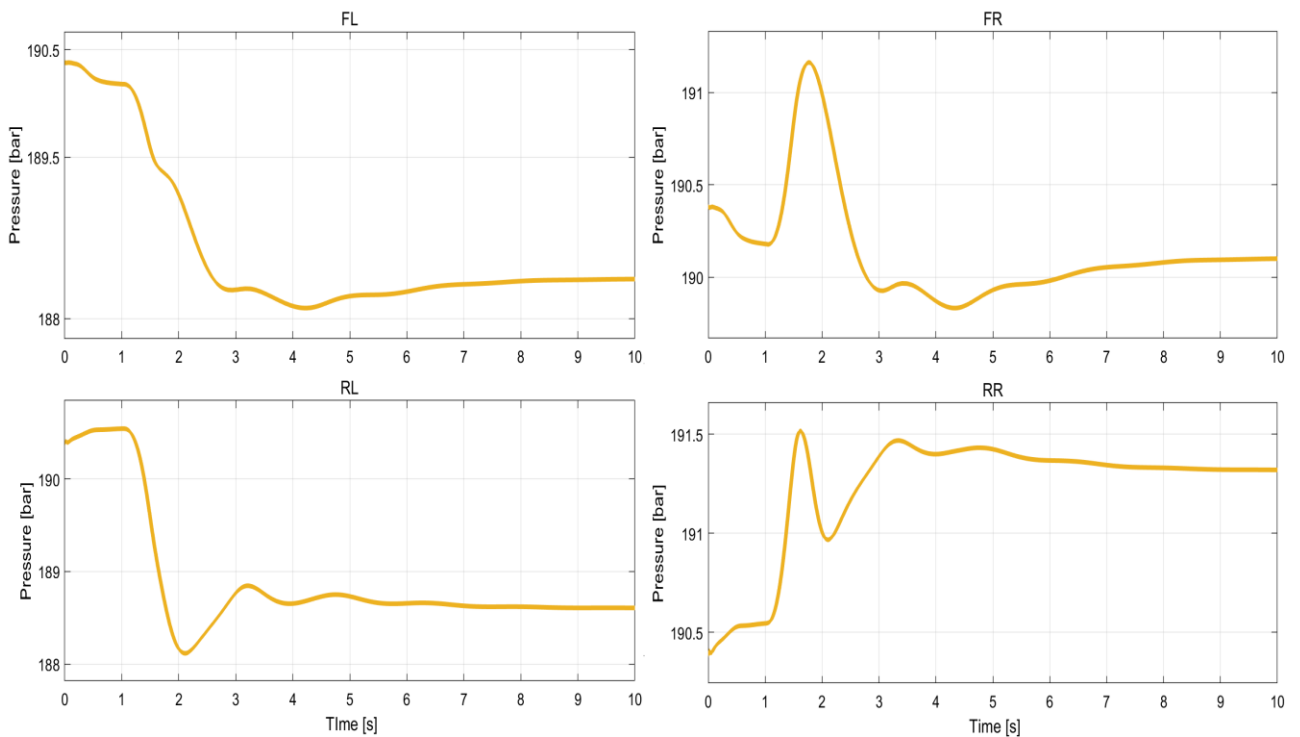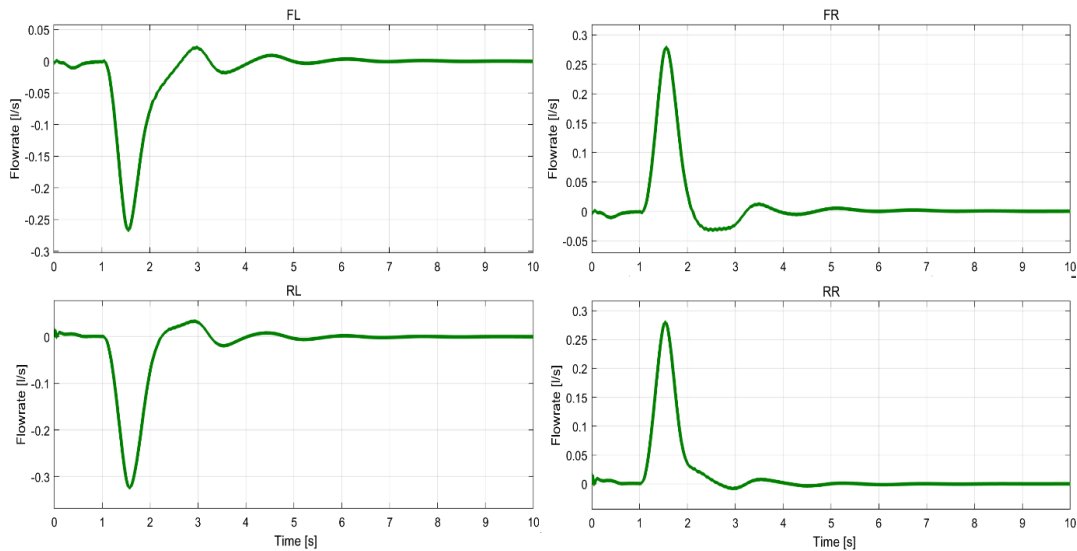

Figure 4.17 Pressure in the hydraulic line between the wheels' actuators and the double acting central cylinders [bar]. For the right wheels is possible to see an increase of pressure at time 1.5s due to the beginning of the roll motion.

It is interesting to evaluate the difference between the flowrate of oil that enters in the double acting central cylinders (Fig. 4.18) and the oils that from the wheels' actuators flow inside or outside the accumulators (4.19). In this case, due the flat surface of the road, only a small portion of oil enters/exit from the accumulators to compensate the volume variation of the wheels' actuators cylinders due to the wheel travels, while the main part of the oil is displaced in the central cylinders.

Figure 4.18 Flowrates in the hydraulic line between the wheels' actuators and the double acting central cylinders [l/s]. For the right wheels, subjected to compression travel the oil is outgoing.
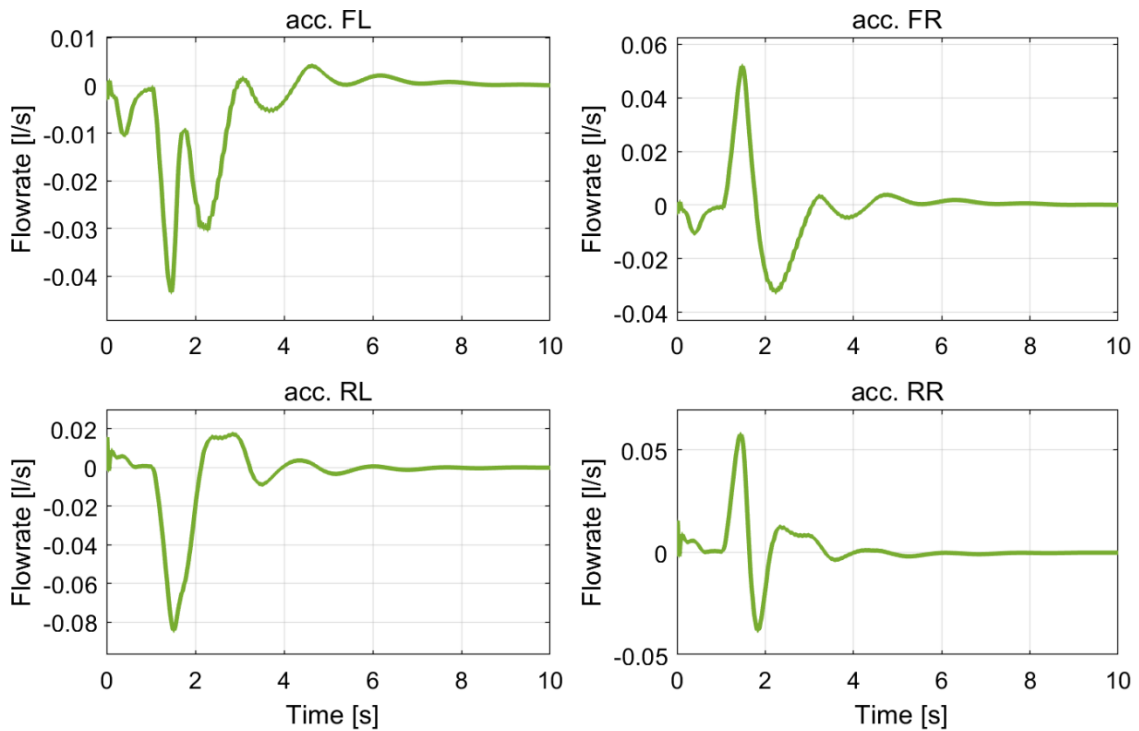
Figure 4.19 Flowrate entering/exiting in the hydraulic accumulators.

85
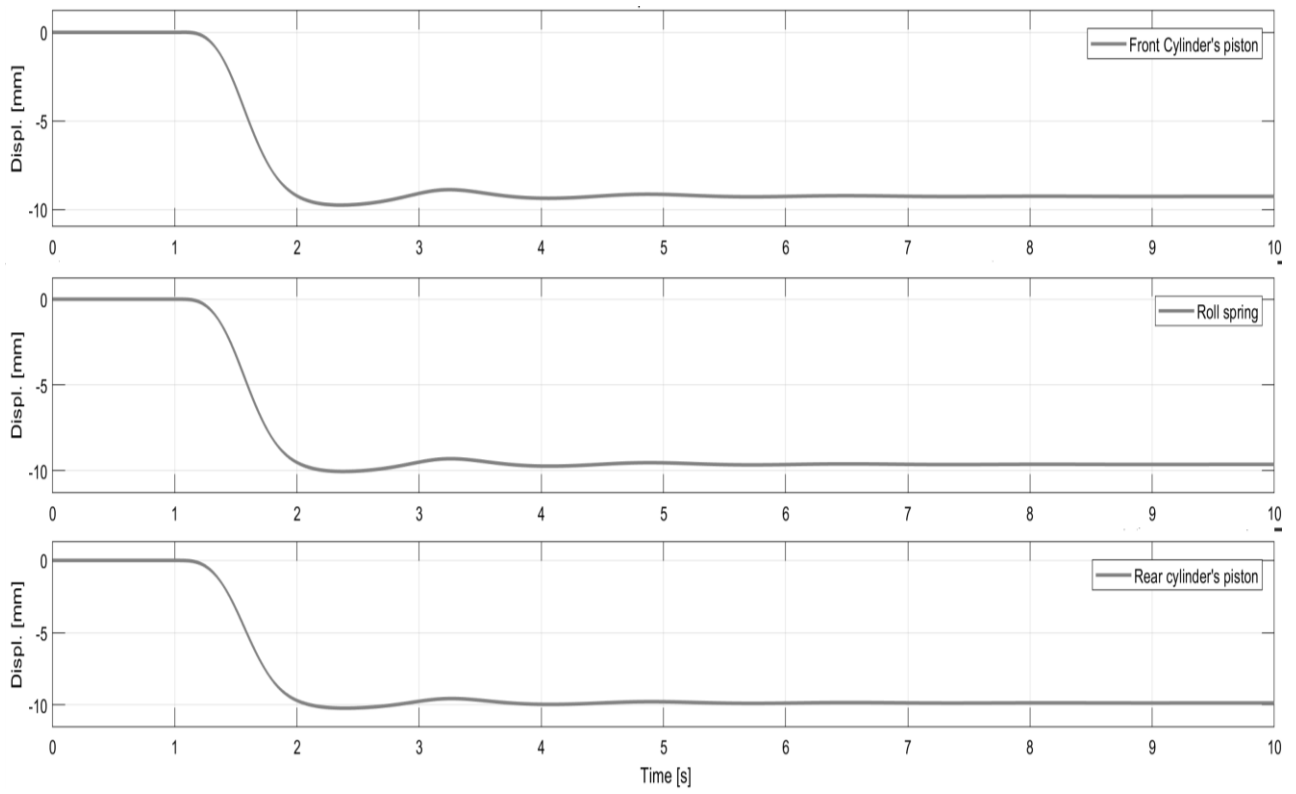
Figure 4.20 Displacements [mm].

4.2 Fishhook manoeuvre

This is a manoeuvre standardized by the NHTSA (National Highway Traffic Safety Administration's) NCAP (New Car Assessment Program) that has the scope to evaluate the stability and the rollover tendency of a vehicle in case of an avoidance manoeuvre; indeed, it replicate the behaviour of the vehicle when it is trying to avoid an obstacle on its lane, so at first it steer toward the other lane and then counter-steer to return in its lane. The name of the manoeuvre comes from the shape that the trajectory of the vehicle assumes during the test. Generally, the vehicle speed assumed at the beginning of the manoeuvre before to start the steering action is between 50 km/h and 80km/h, then the test consists in the following steps [30]:

- Initial steering input, the peak value is the steady-state steering angle which gives a lateral acceleration of 0.3g multiplied by a factor of 8;
- The peak of steering wheel is maintained until the roll rate falls below 1.5 deg/sec;
- Steering in the opposite direction until the opposite peak value of steering angle is reached;
- Maintain for 3 seconds the latter peak value of steering angle;
- Steering back until the steering angle comes back to 0 degrees.

For our analysis, this test gives us information about the stability and the handling capabilities of the vehicle provided with the interconnected suspension system and higher roll stiffness. The analysis result will be presented in the next graphs. The first thing to highline is the fact that the interconnected model reach before the steady roll condition (Fig. 4.24) and the threshold of 1.5 deg/s, in fact the interconnected vehicle starts to counter-steer 0.13s before the standard model (Fig. 4.21). This allow a better dynamic response and a closer trajectory (Fig. 4.25) that are indication of a better road holding capabilities and obstacle avoidance.
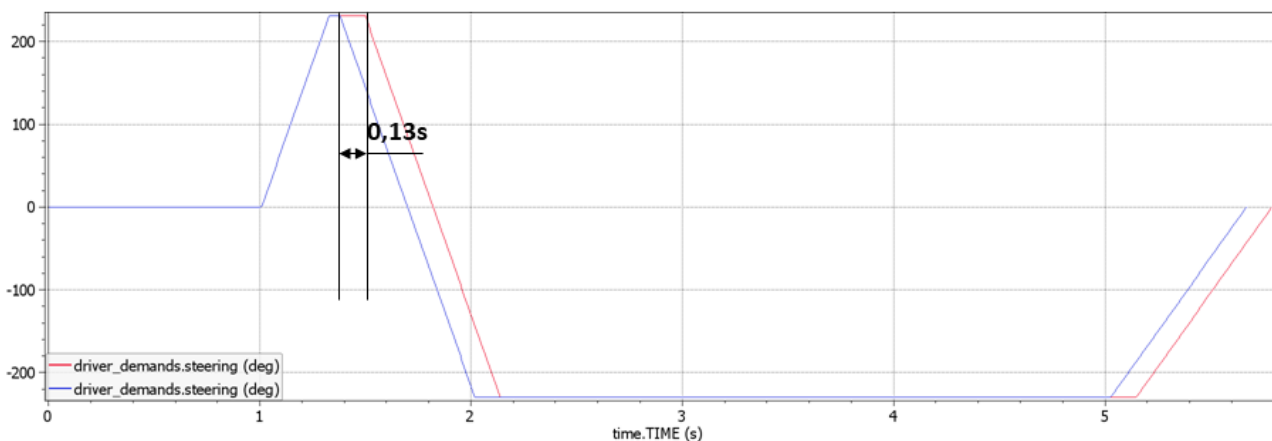

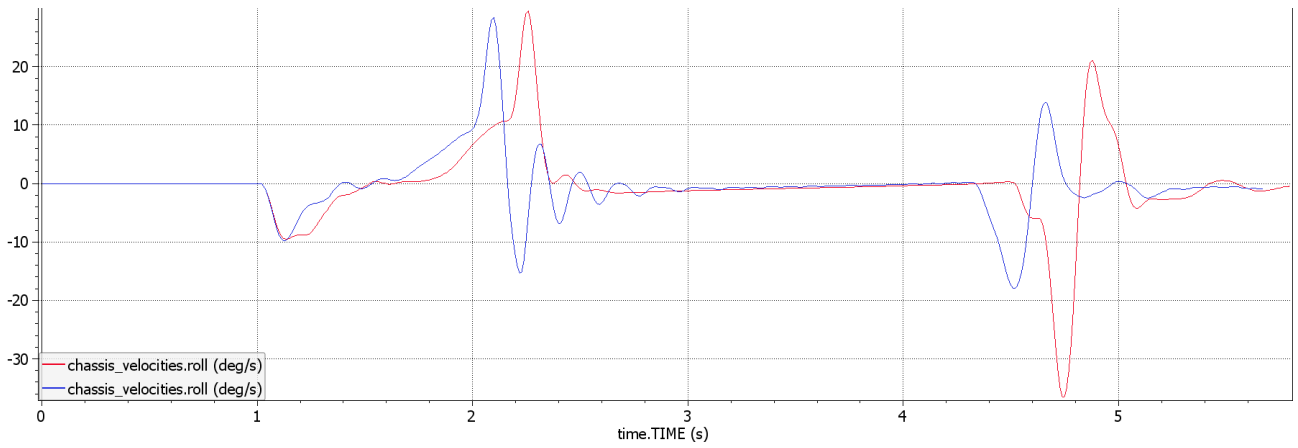*Figure 4.21 Steering inputs. The max value is ±231 degrees (interc − base).*
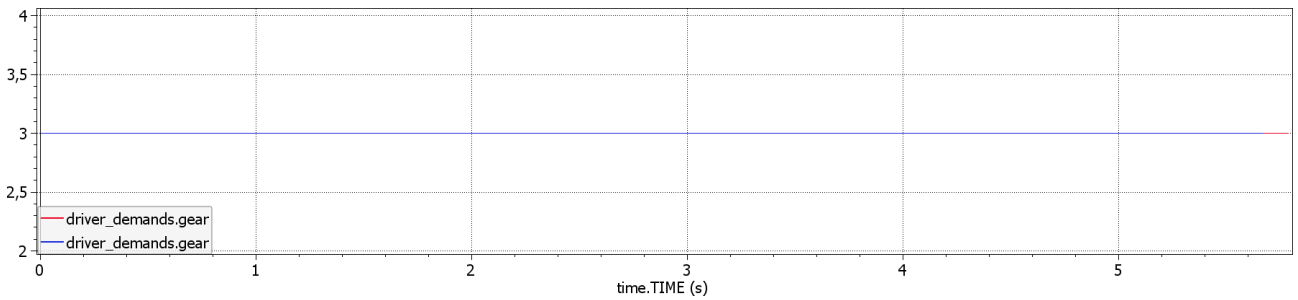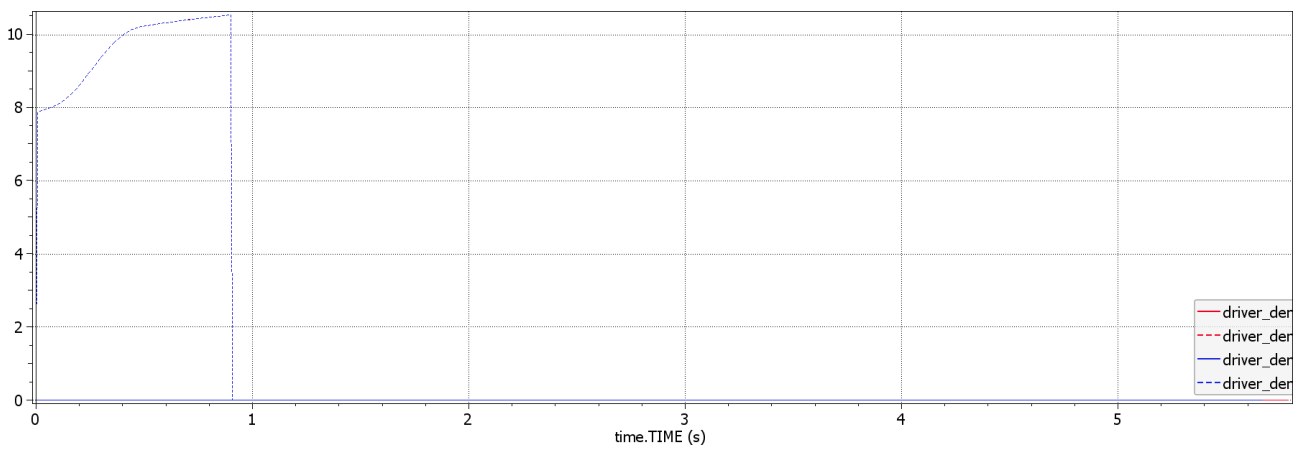
Figure 4.22 Roll rates (interc − base).

Figure 4.23 Driver inputs: above the position of the accelerator pedal and below the gear engaged (interc −
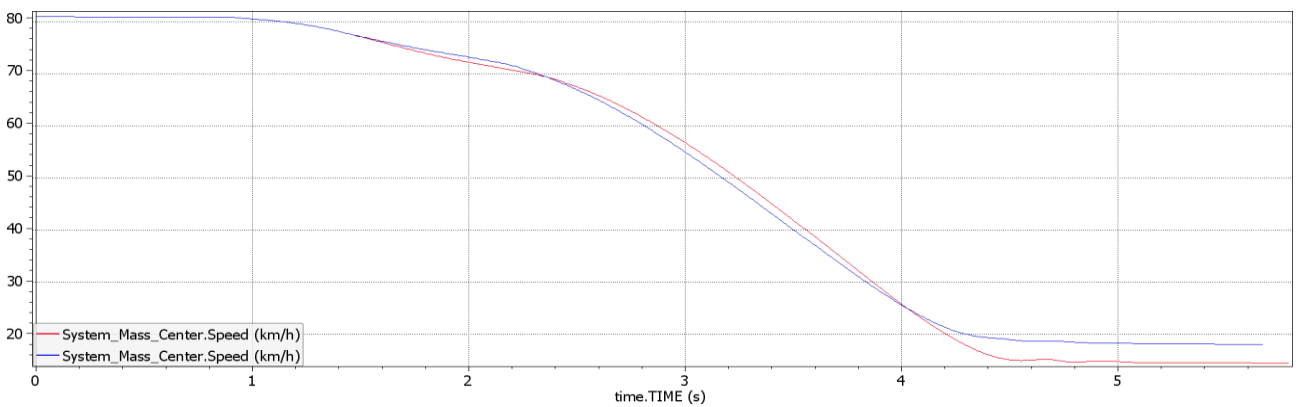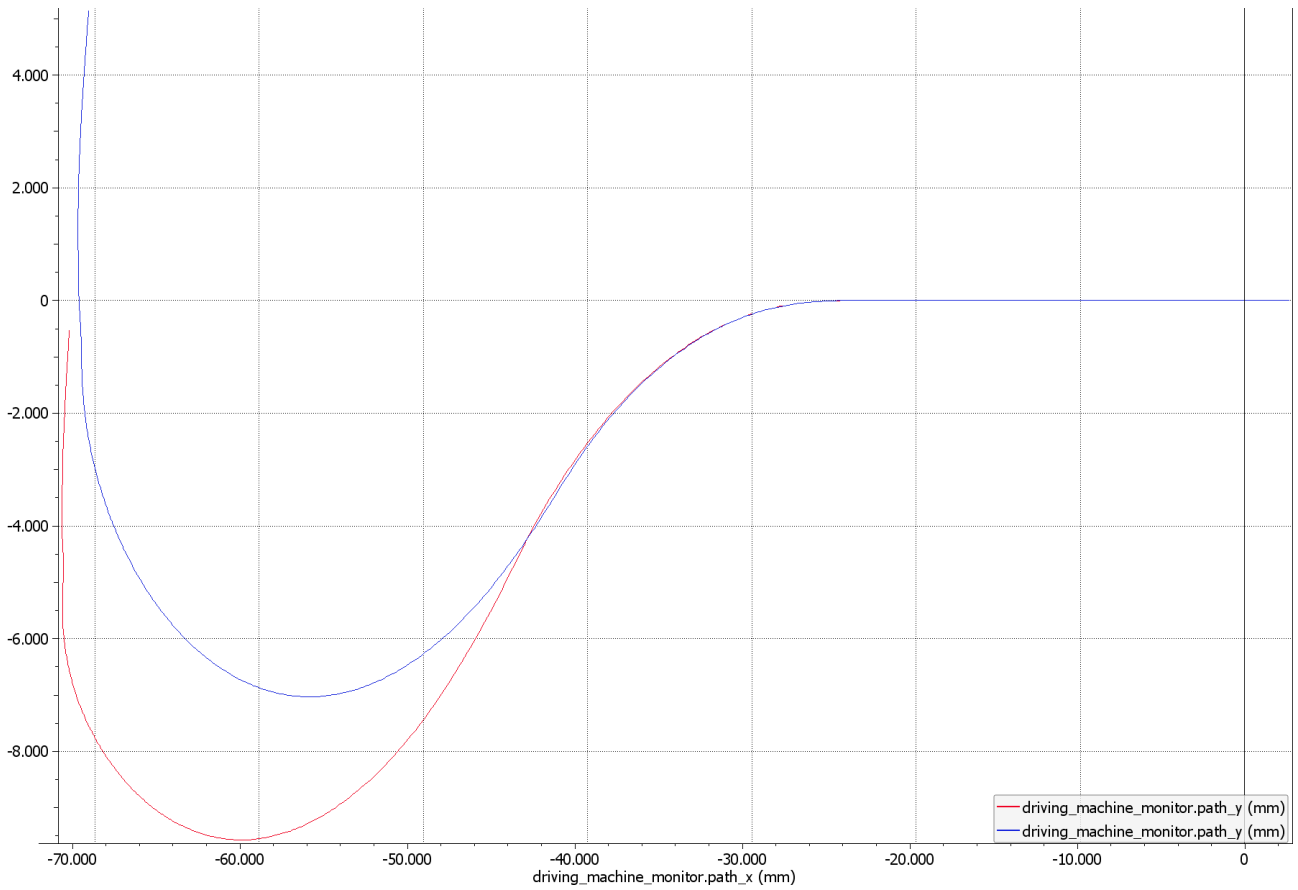
base).

Figure 4.24 Vehicle speed (interc − base).

Figure 4.25 Vehicle trajectory (interc − base).

It is possible to note the improvement on the dynamic response of the interconnected vehicle also in the lateral acceleration trend and especially at 4.77s during the second counter steering manoeuvre (Fig. 4.26). The better stability capabilities are also shown by the sideslip angle (Fig. 4.27), that is significantly reduced, and by the yaw rate (Fig. 4.28).
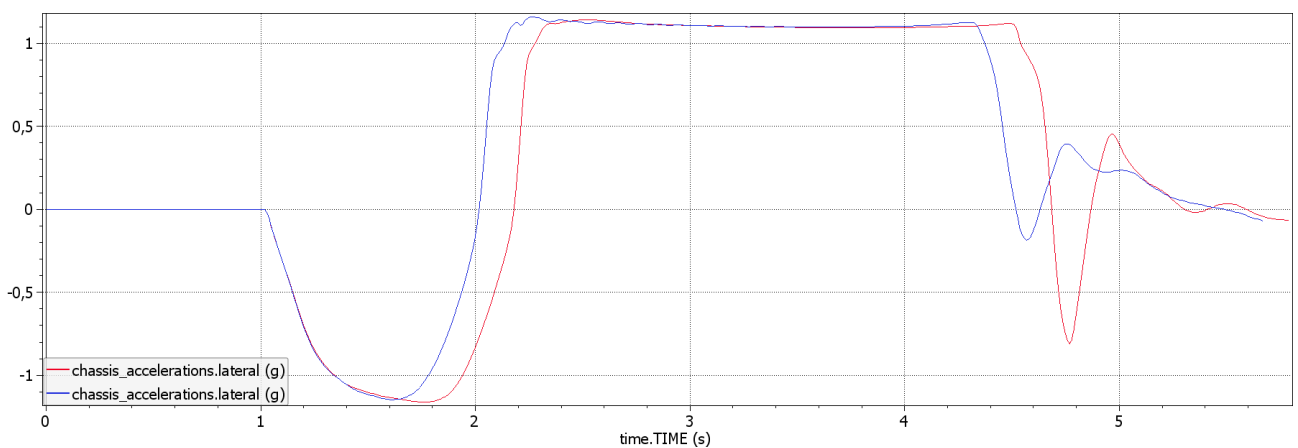
Figure 4.26 Lateral acceleration (interc − base).
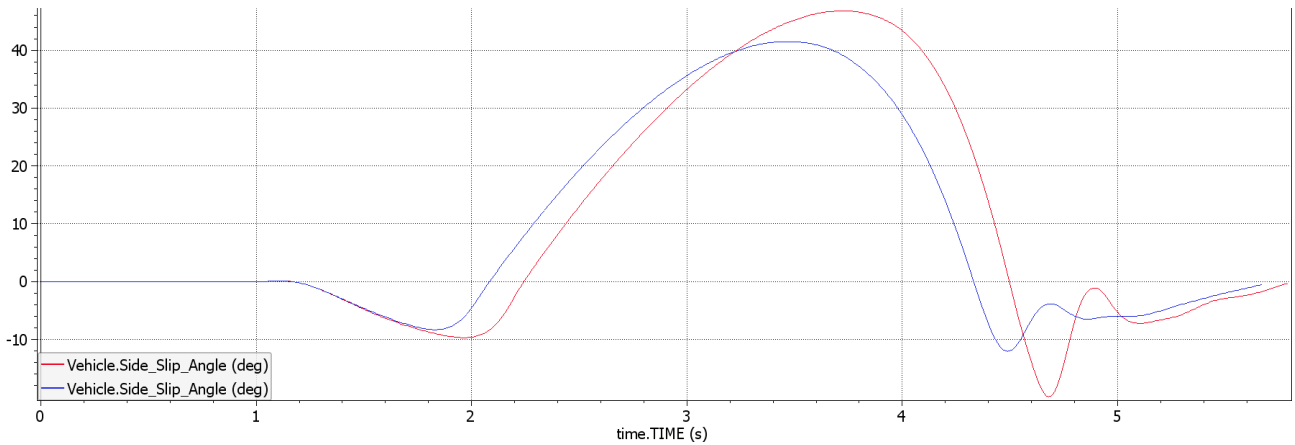
Figure 4.27 Vehicle side slip angle (interc − base).
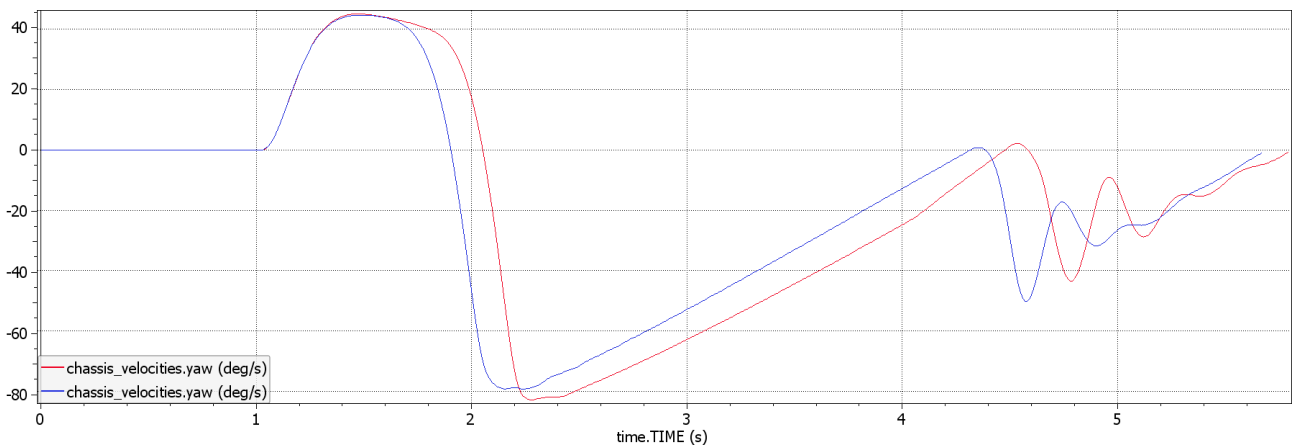
Figure 4.28 Yaw-rate (interc − base).

As expected, the roll angle is reduced by the 30% and a reduction is observed also in the pitch angle, Fig. 4.29 and 4.30 respectively. For what concern the comfort evaluation, the Fig. 4.31 shows the trends of the roll acceleration: it is possible to note that the interconnected vehicle allow to clearly reduce the main peak present at 4.77 s of the standard vehicle due to the counter-steer action, but at beginning and at end of the steady-state roll phase it is slightly higher with respect the standard vehicle.
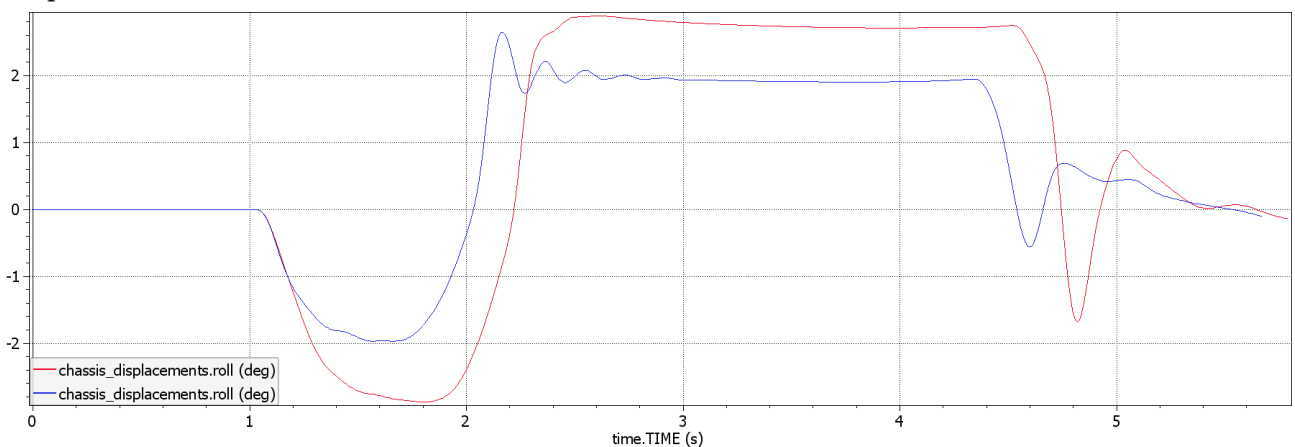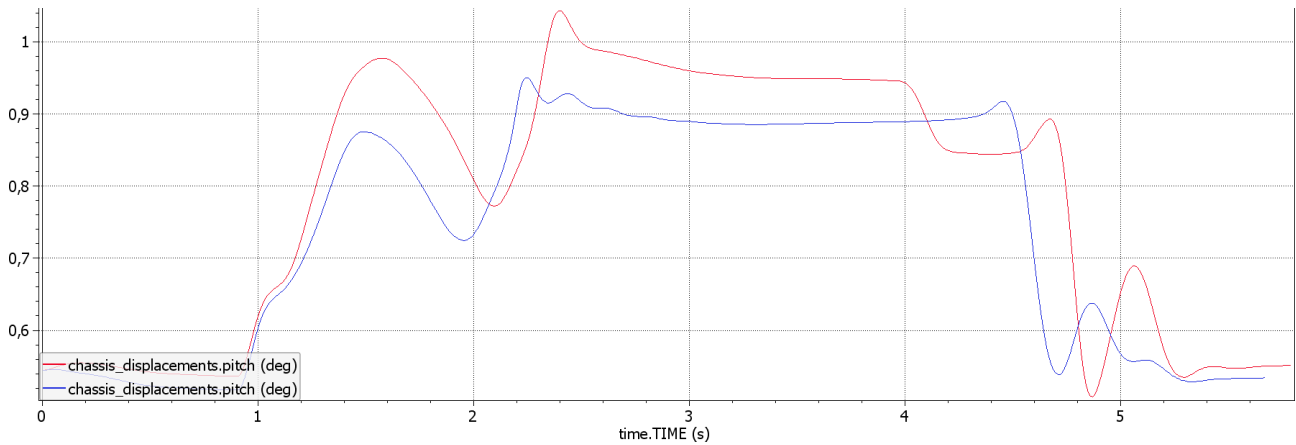

Figure 4.29 Roll angle (interc − base).

90

Figure 4.30 Pitch angle (interc − base).

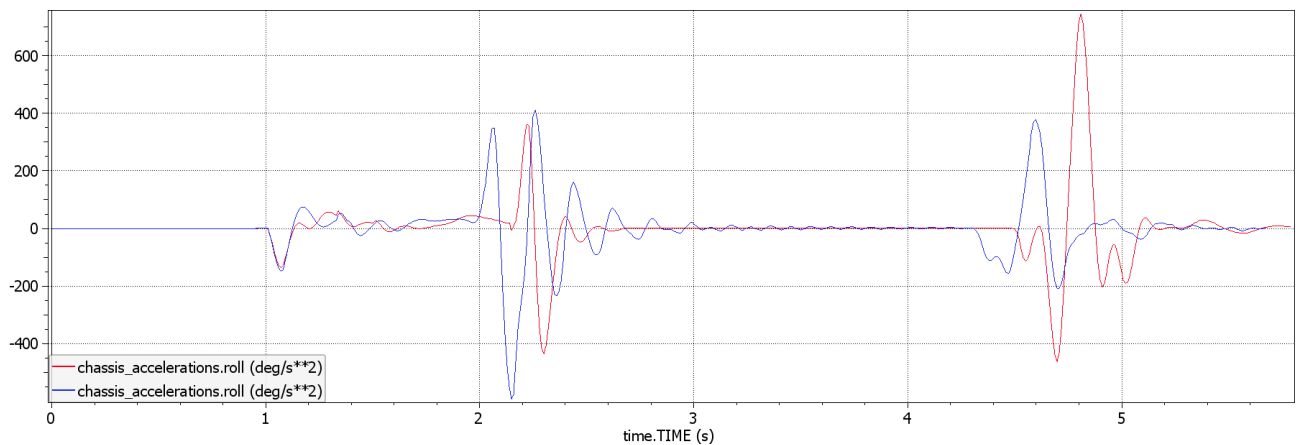*Figure 4.31 Roll acceleration (interc − base).*

In the next pages are shown the trend of the suspension system component, coming from the Simscape environment. How it is possible to see, there are some oscillations in the flowrate entering in the central cylinders (Fig. 4.32) that have not influences on the displacement of the pistons inside the wheels' cylinders (Fig. 4.34) and on the piston's displacements inside the front and the rear double acting central cylinder that are damped enough (Fig.4.36). It is possible to from Fig. 4.33 that part of the oils comes into/from the hydraulic accumulators, contributing to reduce the peaks of flow rate oscillations that would go into the central hydraulic cylinders.
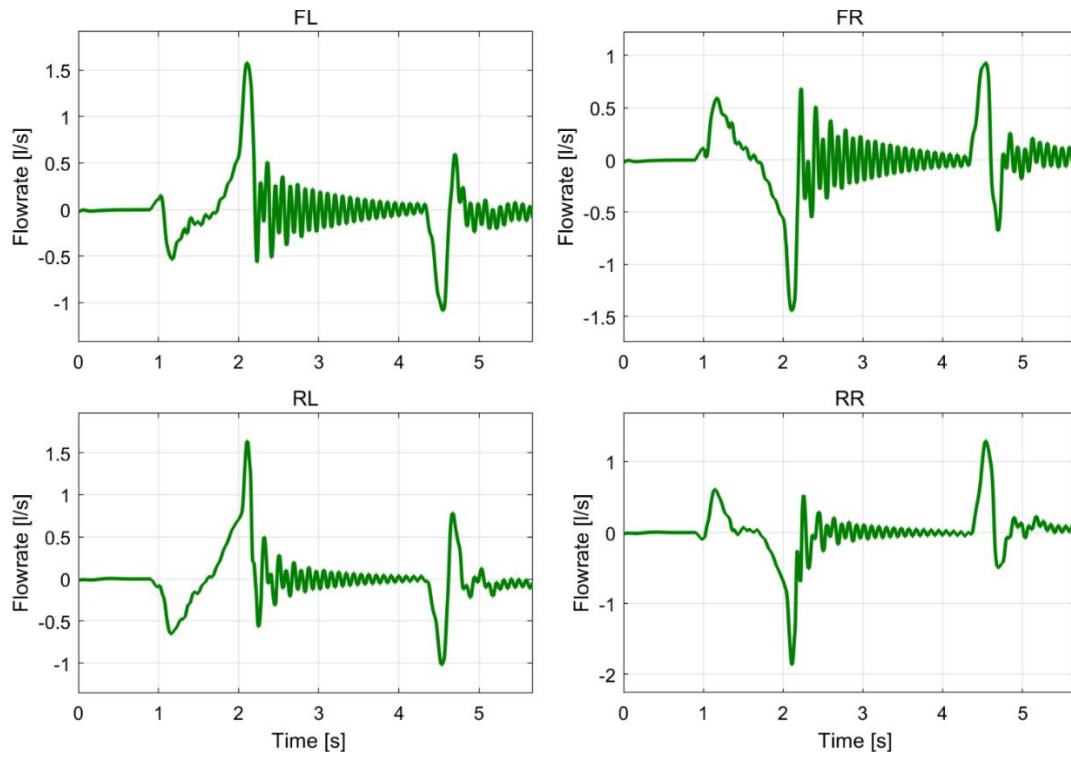
91

Figure 4.32 Flowrates in the hydraulic line between the wheels' actuators and the central cylinders [l/s].
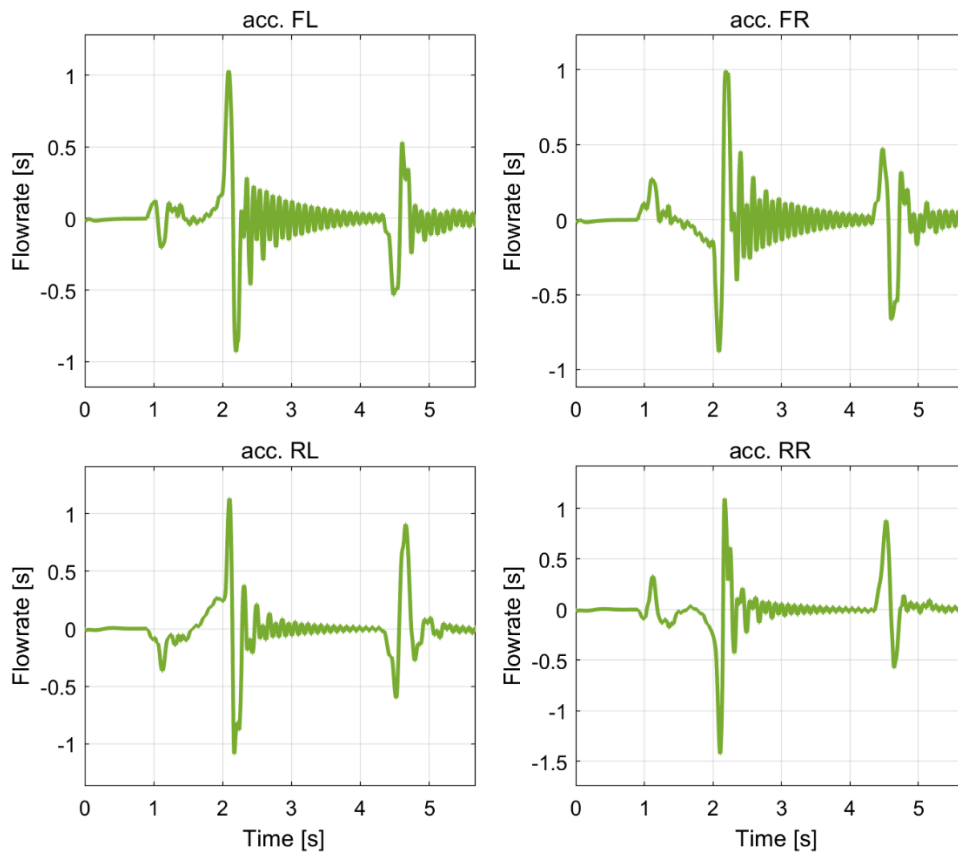

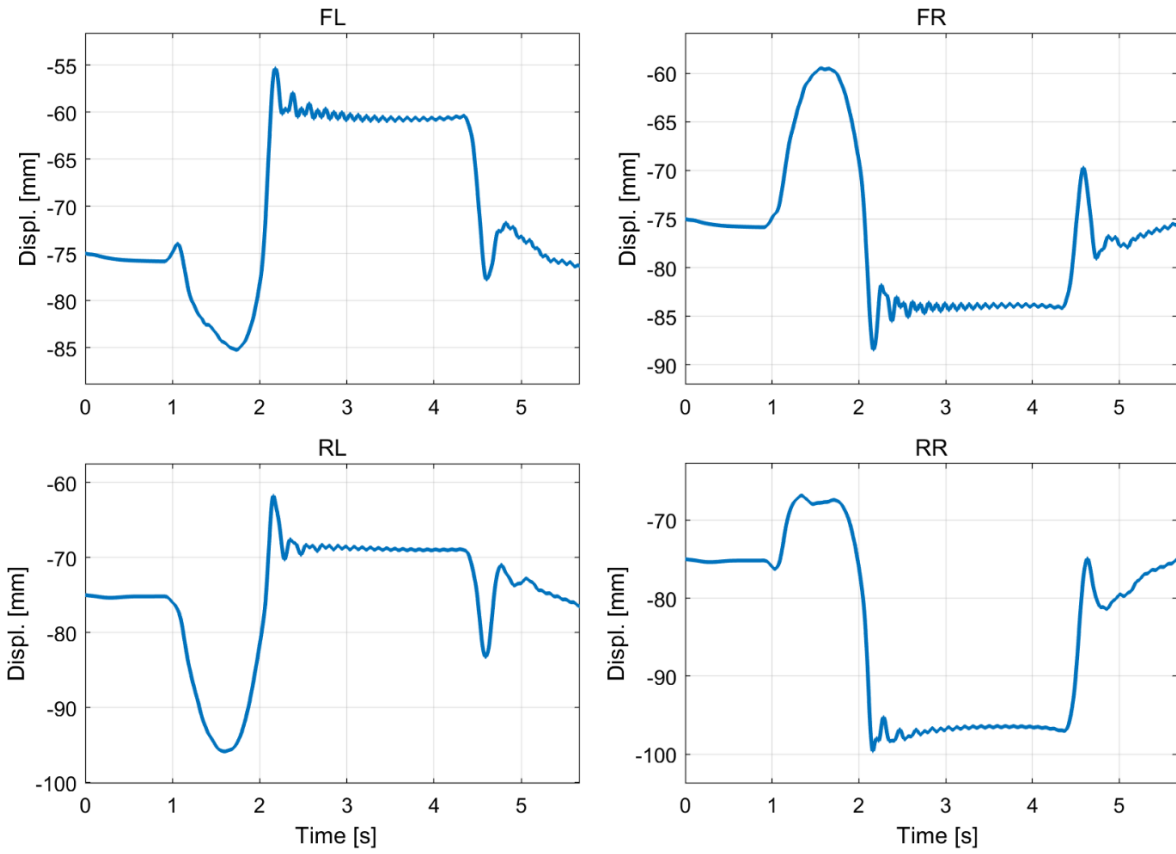*Figure 4.33 Flowrate entering/exiting to/from the hydraulic accumulators.*
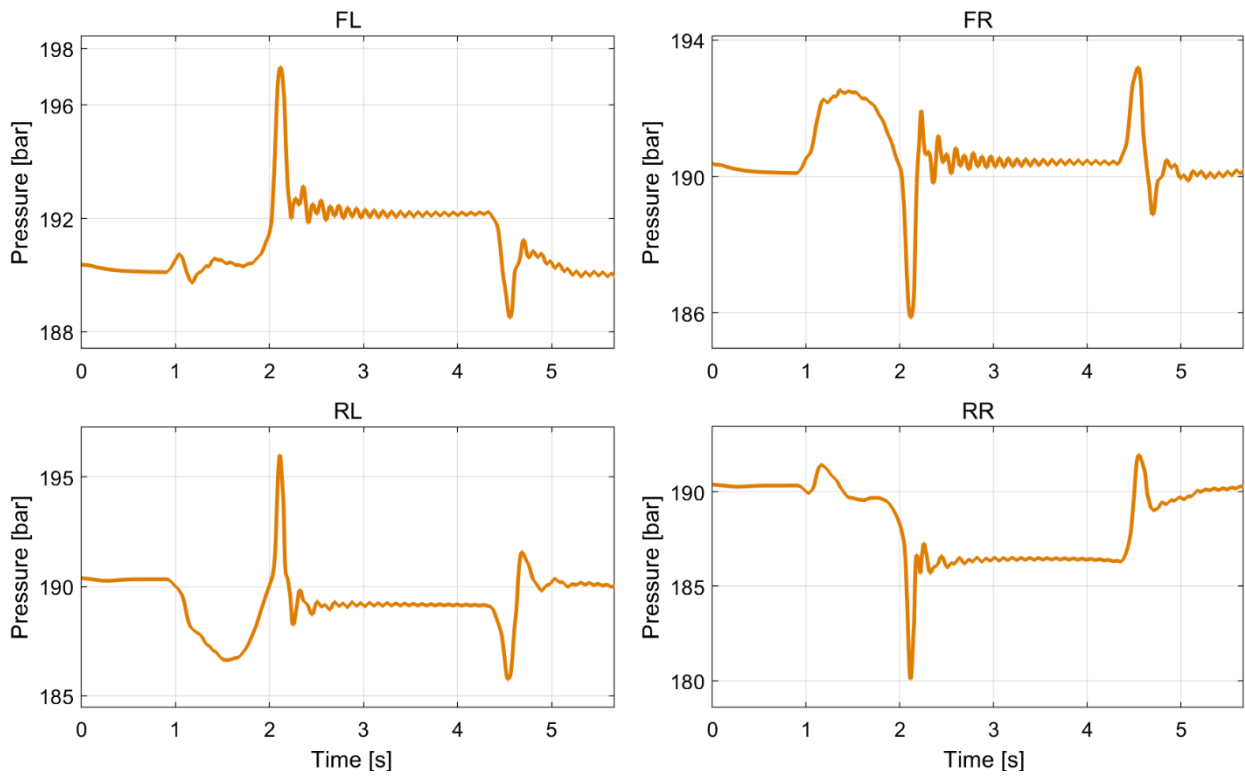
Figure 4.34 Wheel actuators displacements [mm].

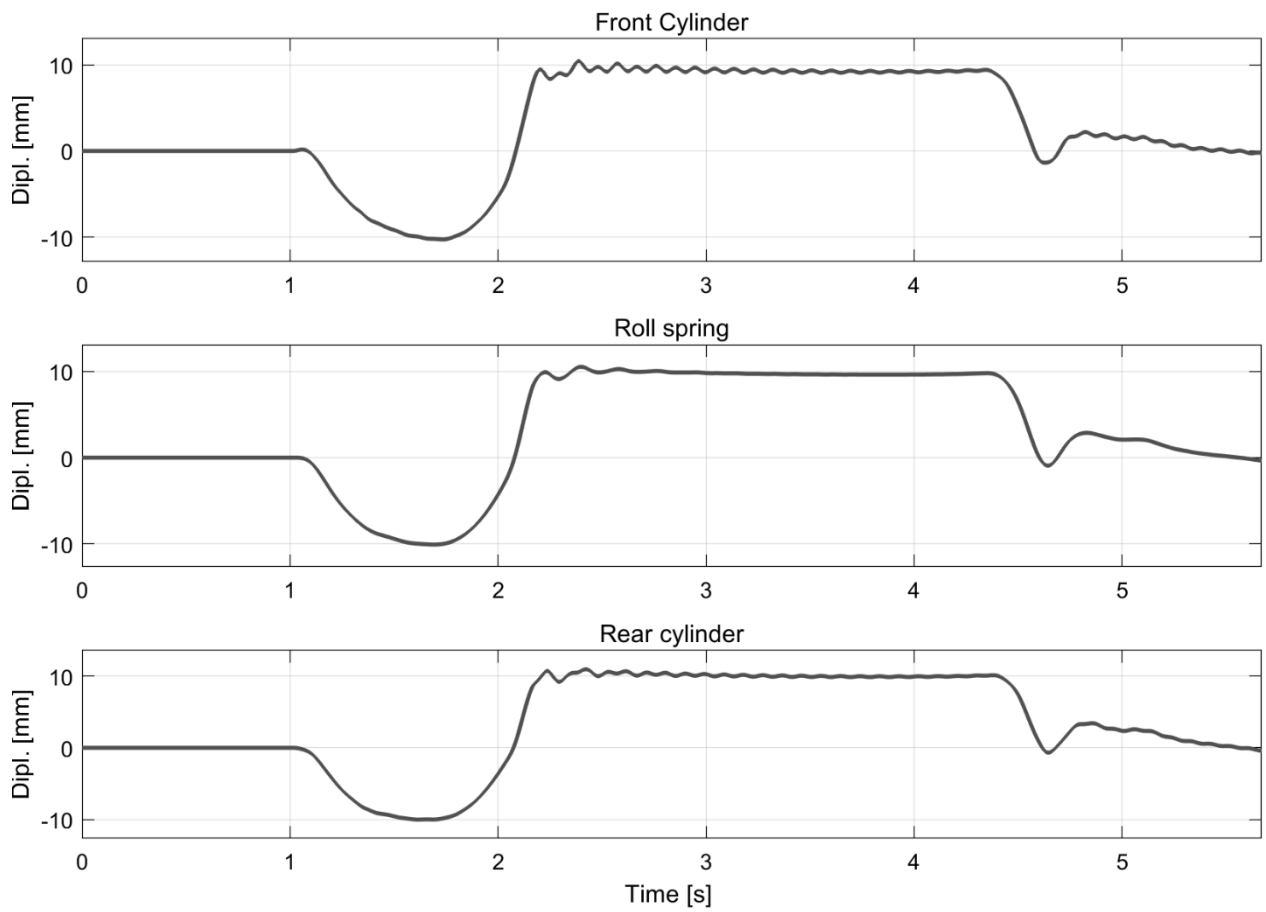*Figure 4.25 Pressure in the hydraulic line between the wheels' actuators and the central cylinders [bar].*

Figure 4.36 Displacements [mm].

4.3 Sine road excitation

The next test is done to analyse the ride performance of the vehicle on an acceleration test carried out on a road that on the left side is flat while on the right side presents a sine profile with a period equal to two time the wheelbase of the car. This manoeuvre is done to verify if the interconnection configuration proposed can free the articulation mode, so to not propagate the road oscillations to the body and to reduce the tire vertical oscillation increasing the grip available for the tires. The interconnected vehicle, also in this case, have the same roll stiffness of the previous case that is higher of the 70% with respect the roll stiffness of the standard vehicle.

The road profile is illustrated in the Fig. 4.37; the maximum height of the sine profile is 15 mm, that considering the typology of the vehicle is quite severe.
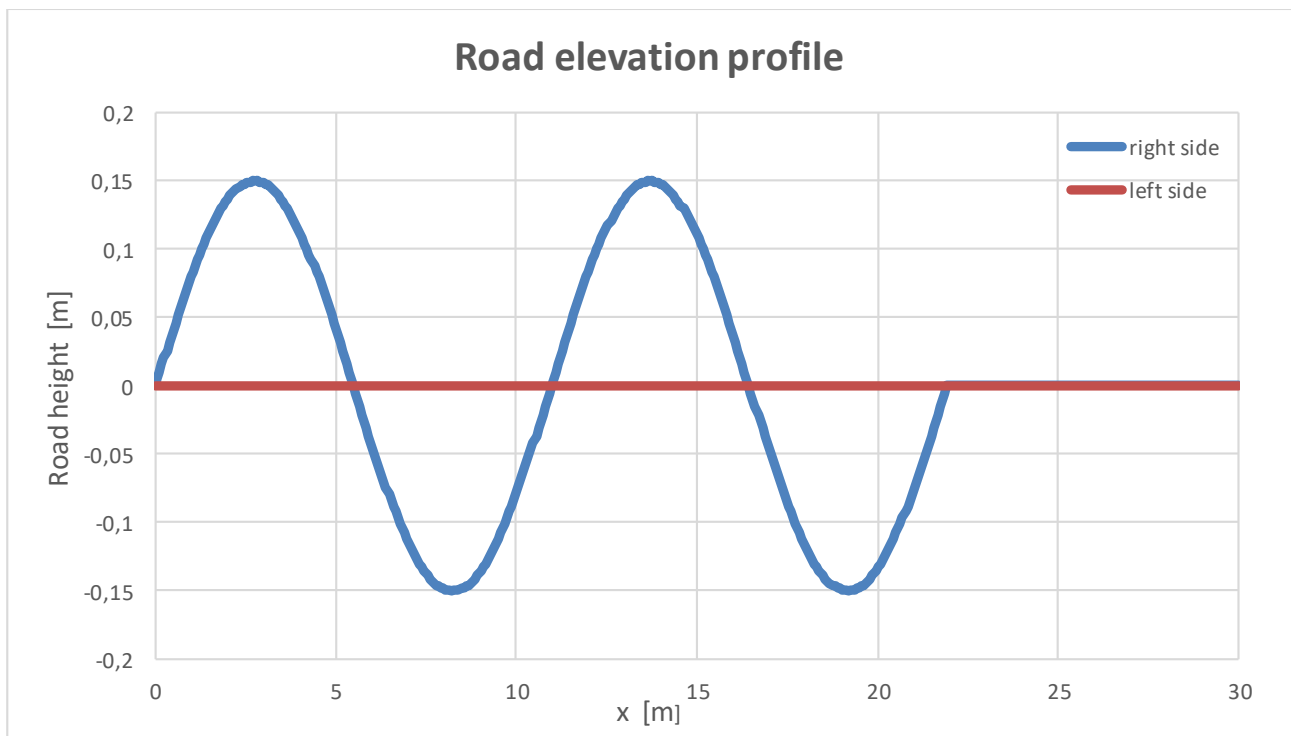

Figure 4.37 Road elevation profile.

The sinusoidal road profile has been created with the Vi-Road tool: the mathematical profile has been calculated in an Excel spreadsheet and then it has been imported in Vi-Road copying the profile in a .rdf file; then the tool automatically has generated the graphic files of the sinusoidal road profile.

The different choice of front and left road profile has been done in Vi-CarRealTime environment, selecting the desiderated road profile for each wheel.
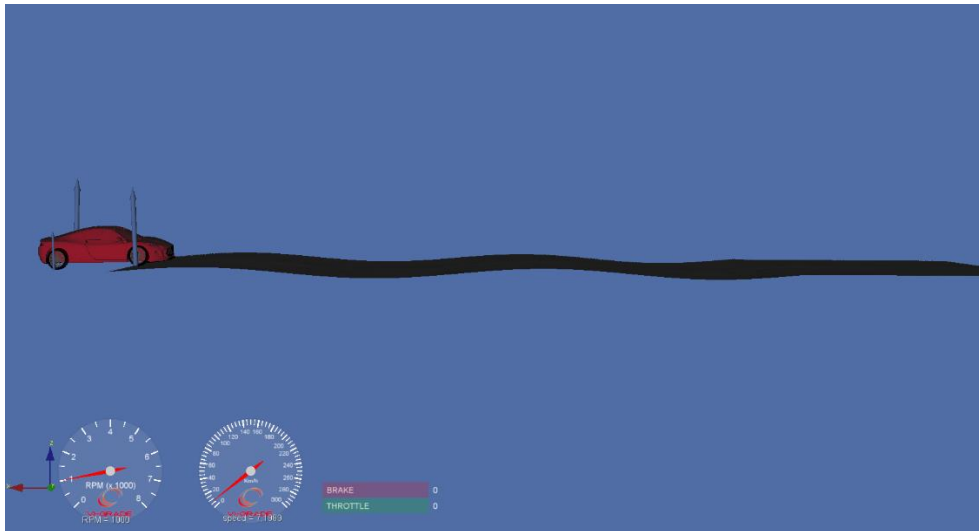
Figure 4.38 Graphic animation of the simulation in Vi-Animator.

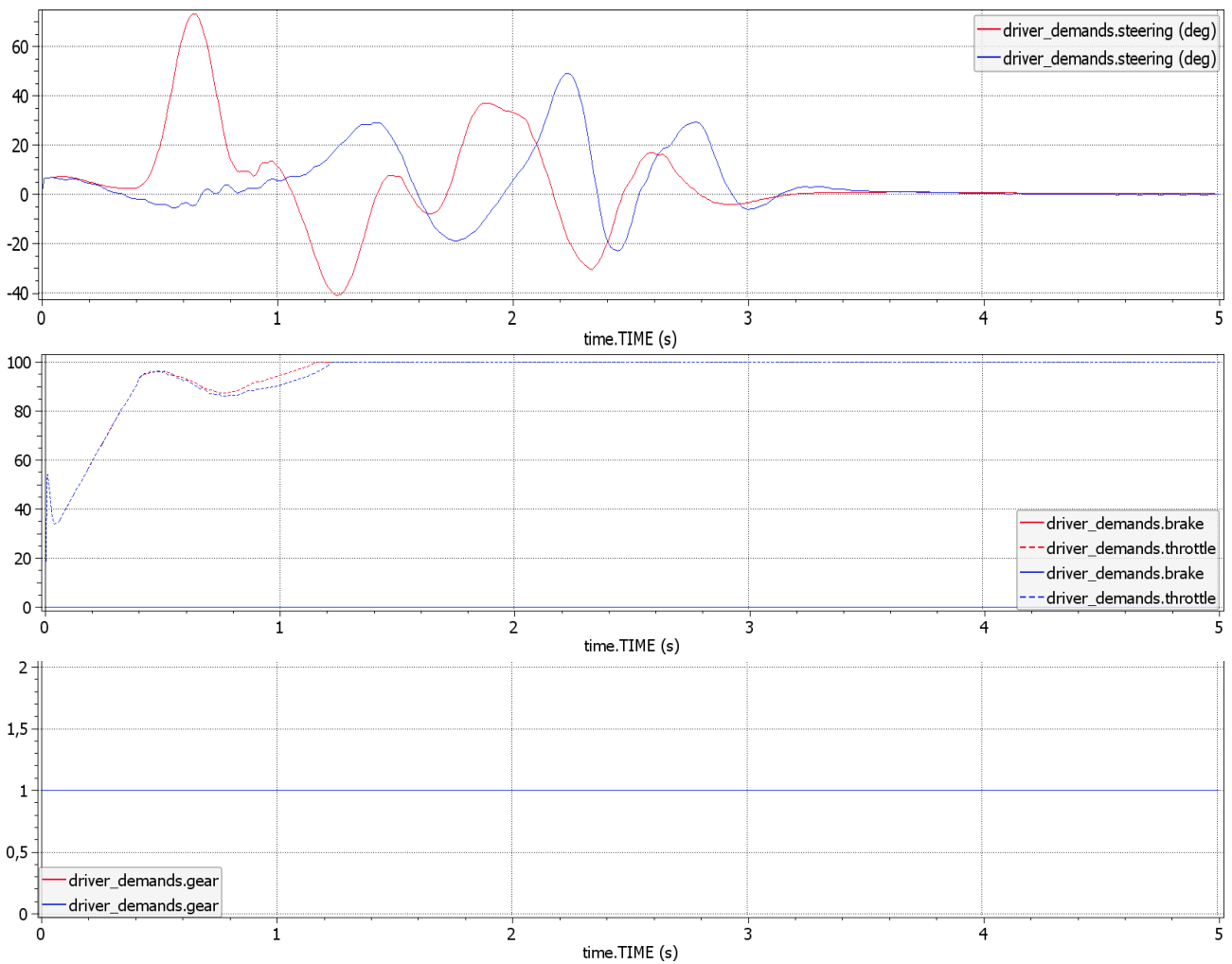The inputs of the virtual drivers are illustrated in Fig. 4.39.

Figure 4.39 Driver inputs (interc − base).

This analysis shows two important aspects, the first is that the interconnection proposed is able to realize a soft warp mode as assumed at beginning of the work, in fact, as it is possible to see from the following graphs, the interconnected vehicle can follow better the road profile because the wheels have a bigger vertical travel (Fig. 4.40) that allow to the tires to maintain the contact with the road increasing the capabilities to generate forces : this is the effect of a reduced wheel elasticities. Then, are significantly reduced the tire vertical forces variation (Fig.4.44) due to the road irregularities; this effect can be seen introducing the 'Warp Forces':

$$WF = \left(\left(F_{Zfl} + F_{Zrr} \right) - \left(F_{Zfr} + F_{Zrl} \right) \right)$$

Where F_Z indicate the tire vertical forces, and the subscript the wheel of reference.

Intuitively, the Warp forces indicate the amount of lateral load transferred between the two diagonals of the car; in all conditions a load transfer is an undesired effects, because of the tire sensitivity, that is the relation between the vertical forces and the lateral one: in synthesis this relation is linear up to a value of the vertical load, but increasing the vertical load it tends to saturate up to a value and then decreases, so it means that if the vertical load is transferred from a wheel of an axle to another of the other axle is very likely that the latter saturates and is not able to generate the same amount of lateral force that it would generate if it works in the linear region. So, generally the load transfer is a negative effect, because unload an axle to 'overload' the other. On a flat road the lateral load transfer is due to the lateral acceleration, while on an irregular road profile it is also generated by the presence of a different heights at the vehicle corners, so in this case a suspension that it is able to generate a soft warp mode is able to reduce the load variation (Fig. 4.45) and increase the available grip, as demonstrate by the longitudinal acceleration in the Fig. 4.41 and the speed profile in Fig. 4.42 that for the interconnected vehicle are clearly higher with respect the standard vehicle. The fact that the interconnected system work as desired is confirmed also by the Fig. 4.51, where it is represented the roll spring deformation that is practically null, sign of a not activation of the roll spring and of the reduced stiffness contribution.

Furthermore, despite the interconnected vehicle has a roll stiffness bigger of the 70% with respect the standard model, the values of the vertical acceleration are lower than the standard vehicle such as the vertical movement of the sprung mass (Fig. 4.46) and the roll angle (Fig. 4.43). Finally, the virtual driver does lower steering corrections with the interconnected vehicle (Fig. 4.39).

The second aspect to consider is that this test has brought out is the presence of oscillations in the tire vertical forces and in the vertical wheel displacements in the frequency range of the unsprung mass resonance peak (10 Hz); so it is necessary to further investigate this phenomena and eventually add some dampers at each wheel corner to damp this oscillation due to the road irregularities.
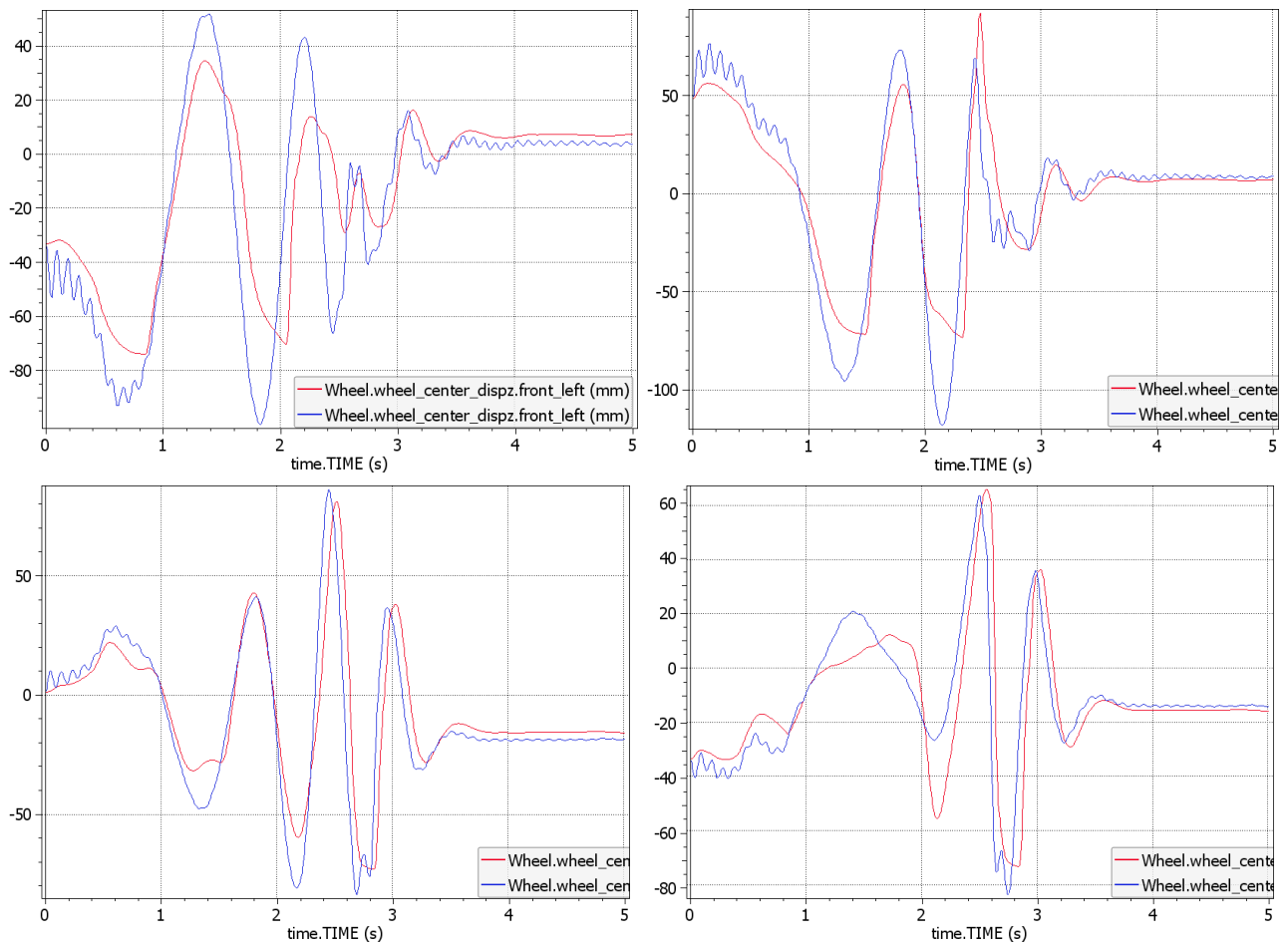

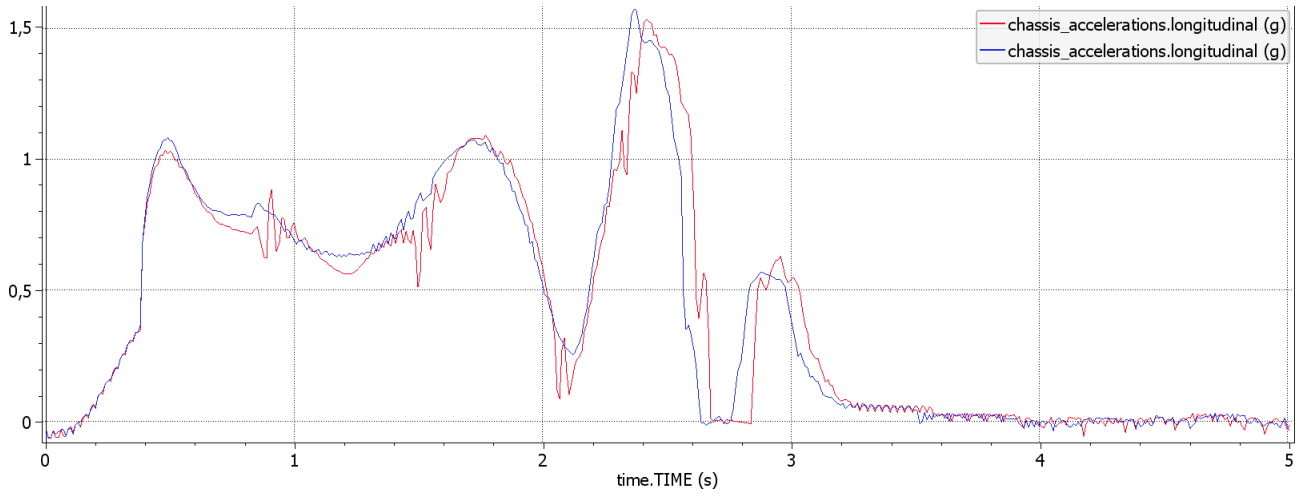*Figure 4.40 Vertical wheels' travel, above the front axle (interc – base).*

Figure 4.41 Longitudinal acceleration (interc − base).
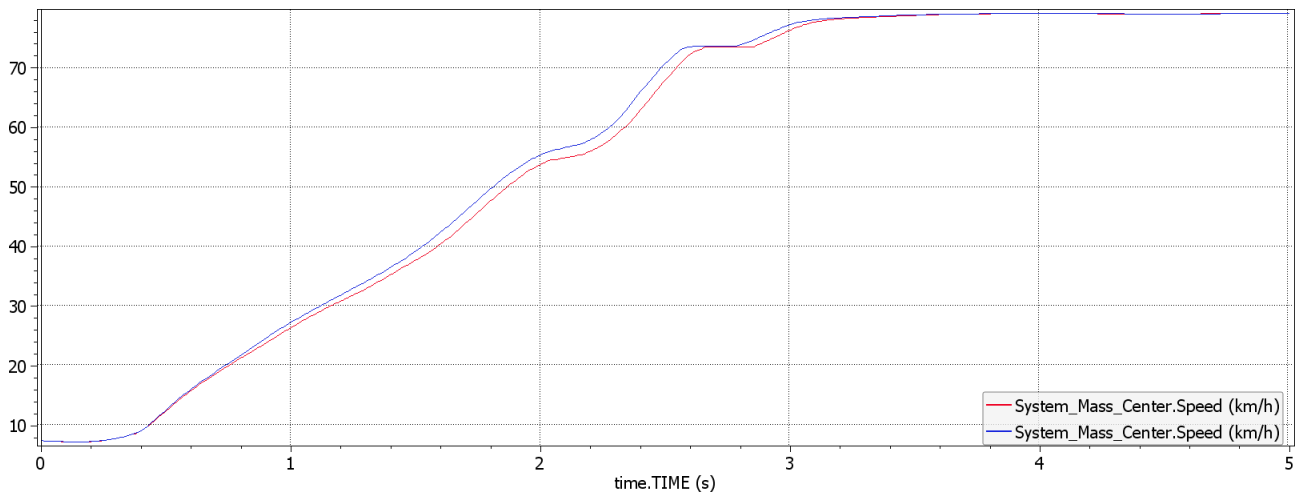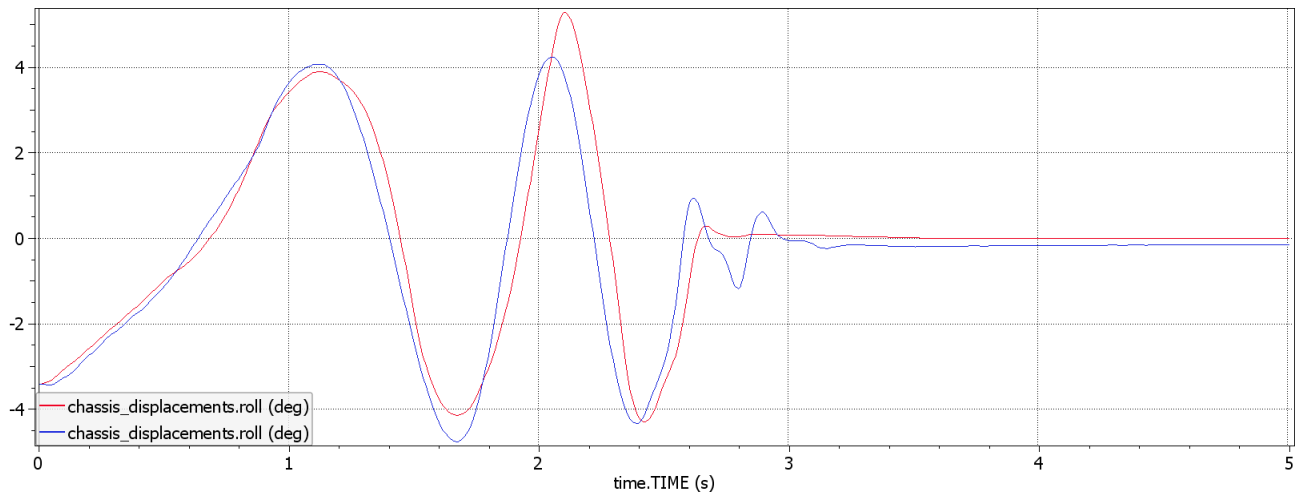

Figure 4.42 Speed profile (interc − base).

Figure 4.43 Roll angle (interc − base).

99

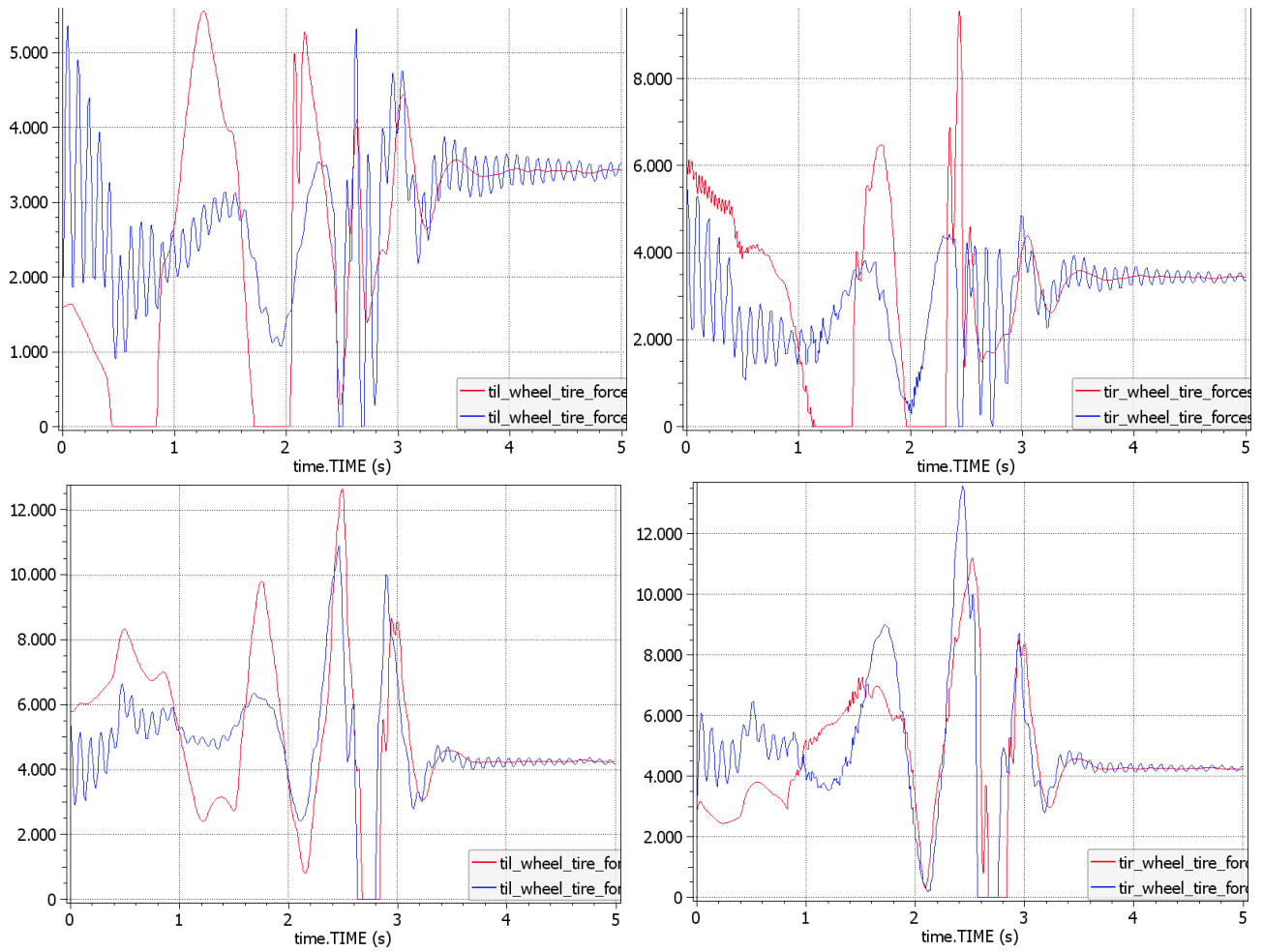*Figure 4.44 Tire normal forces (interc – base).*
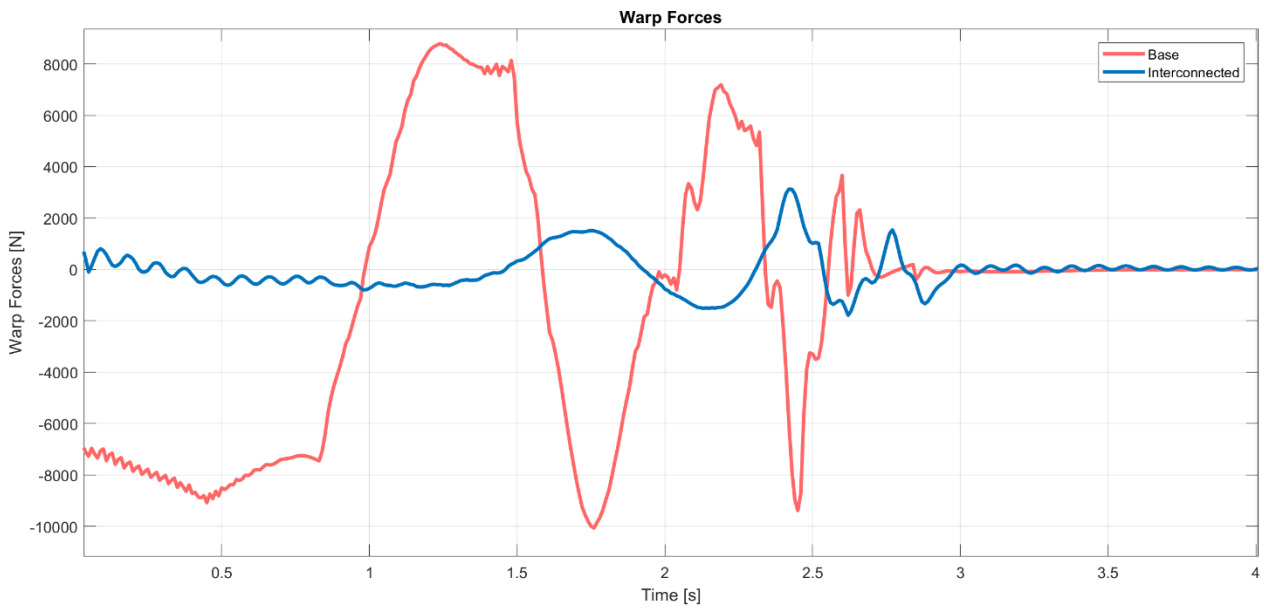
Figure 4.45 Warp forces, alias diagonal forces variations (interc – base).
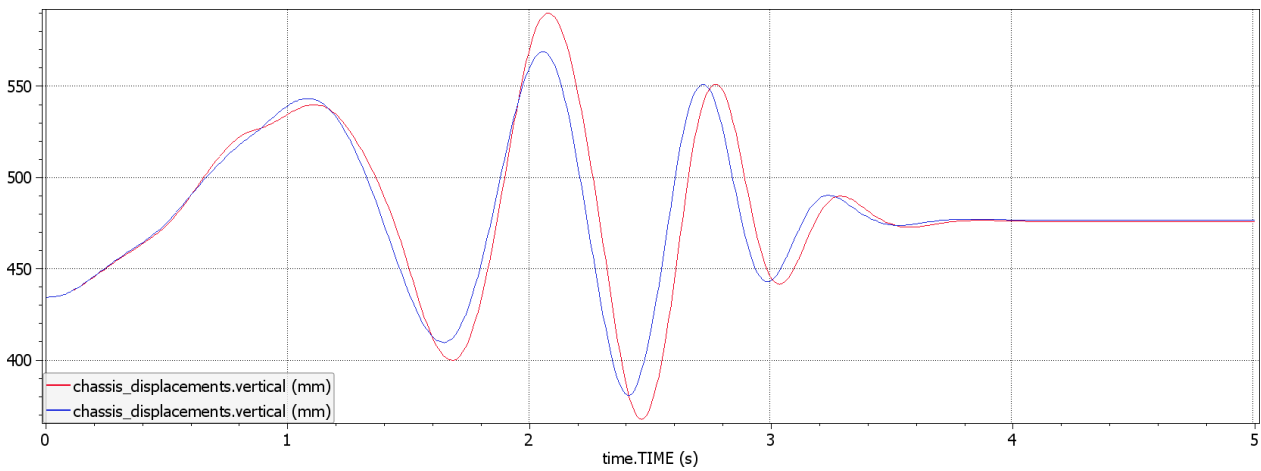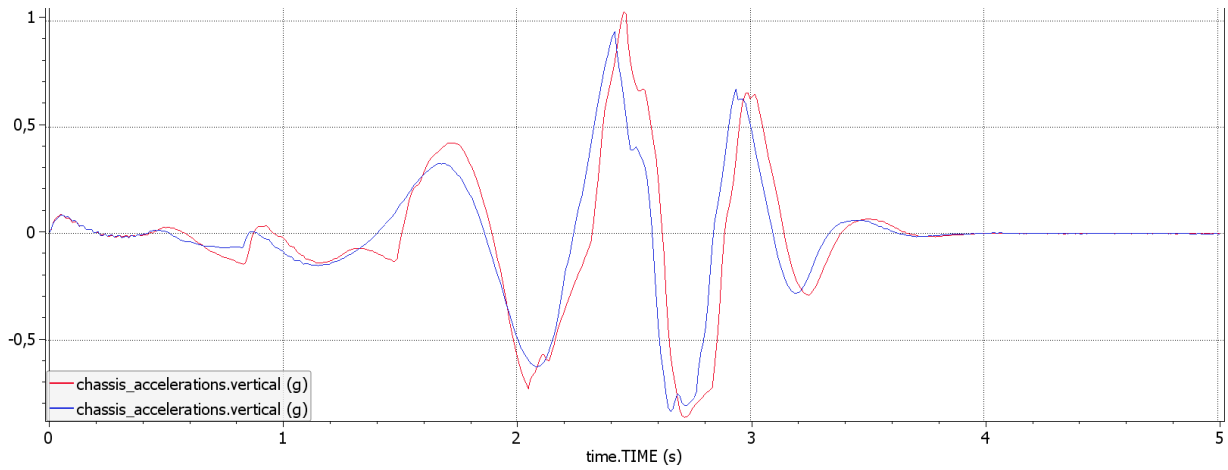
Figure 4.46 Vertical acceleration (above) and vertical movement of the vehicle body (below) (interc − base).

The graphs that follow show the dynamics of the components of the hydraulic system are shown below. In the Fig. 4.51 it is possible to appreciate the effect of the fact that the two axles, working in counter phase (piston of the front central cylinder and the piston of the rear central cylinder) allow to the central lever arm of the interconnection to rotate and not compress the roll spring, reducing the equivalent stiffness to the wheels.
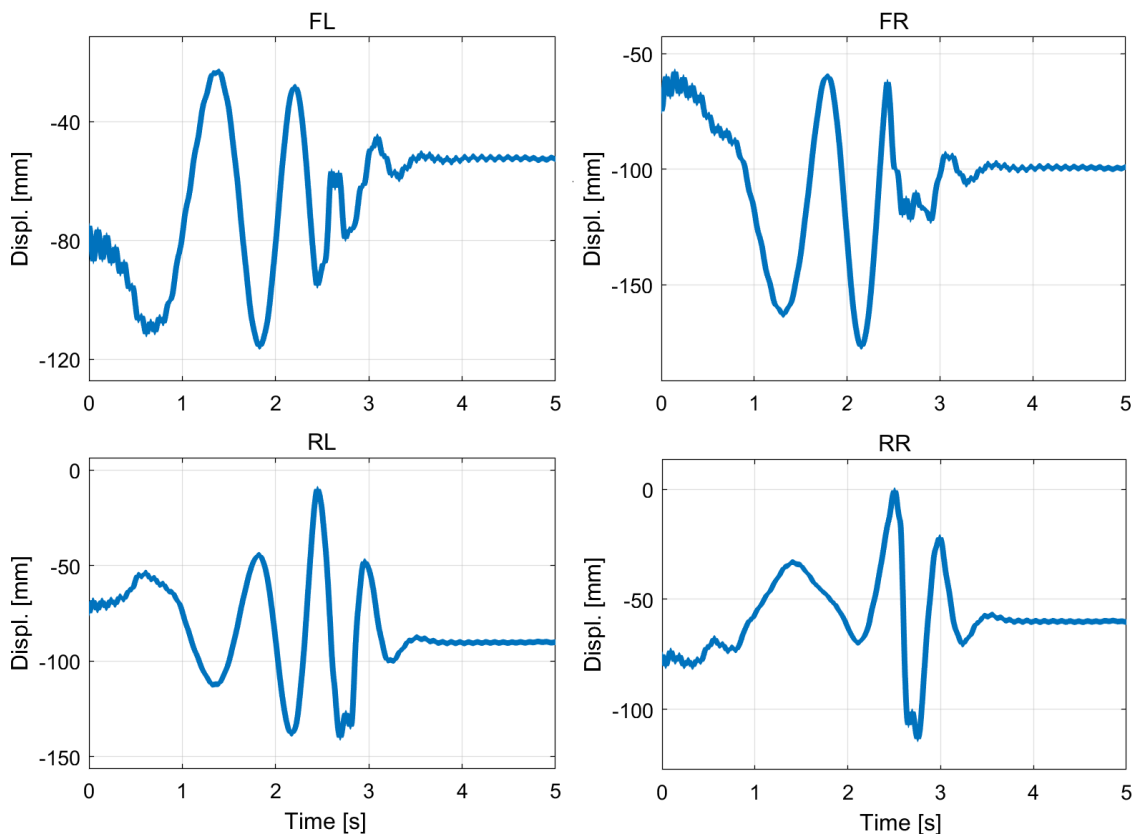
Figure 4.47 Displacements of wheel's actuators [mm].
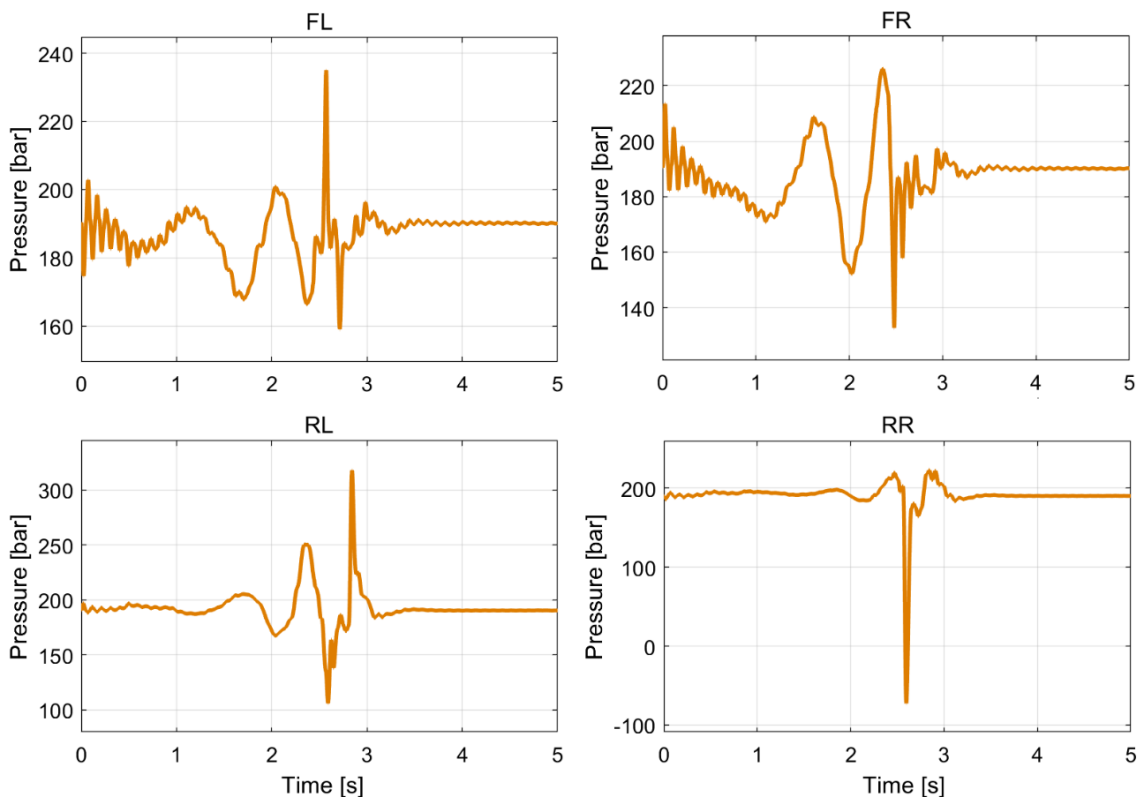
Figure 4.48 Pressure in the hydraulic line between the wheels' actuators and the double acting central cylinders [bar].
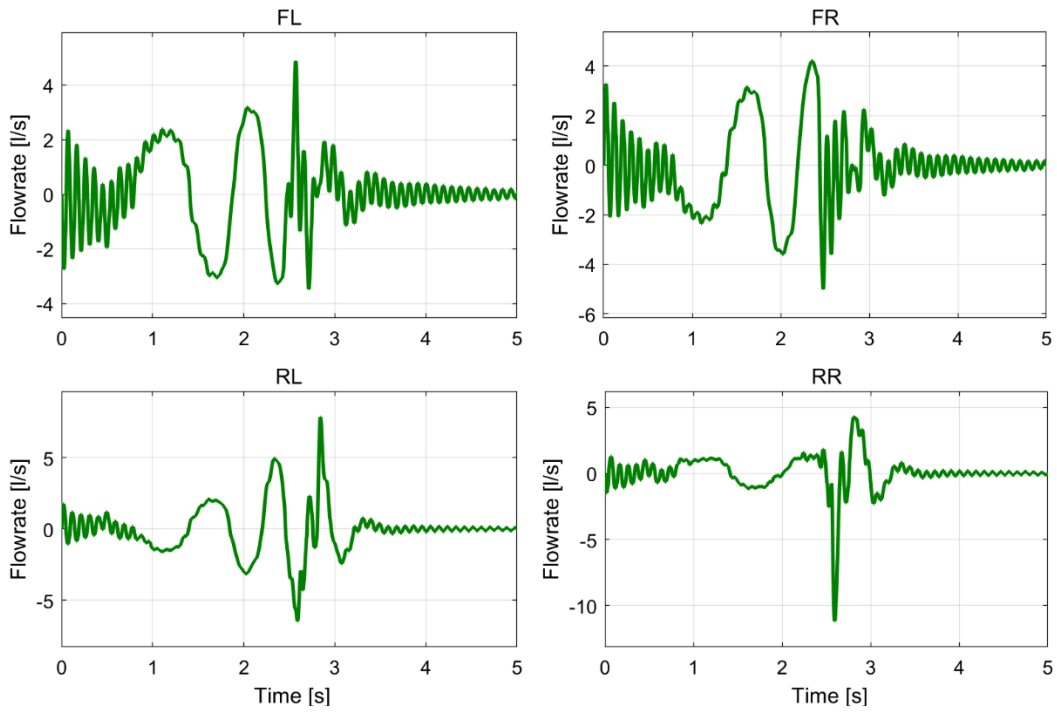
Figure 4.49 Flowrates in the hydraulic line between the wheels' actuators and the double acting central cylinders [l/s].
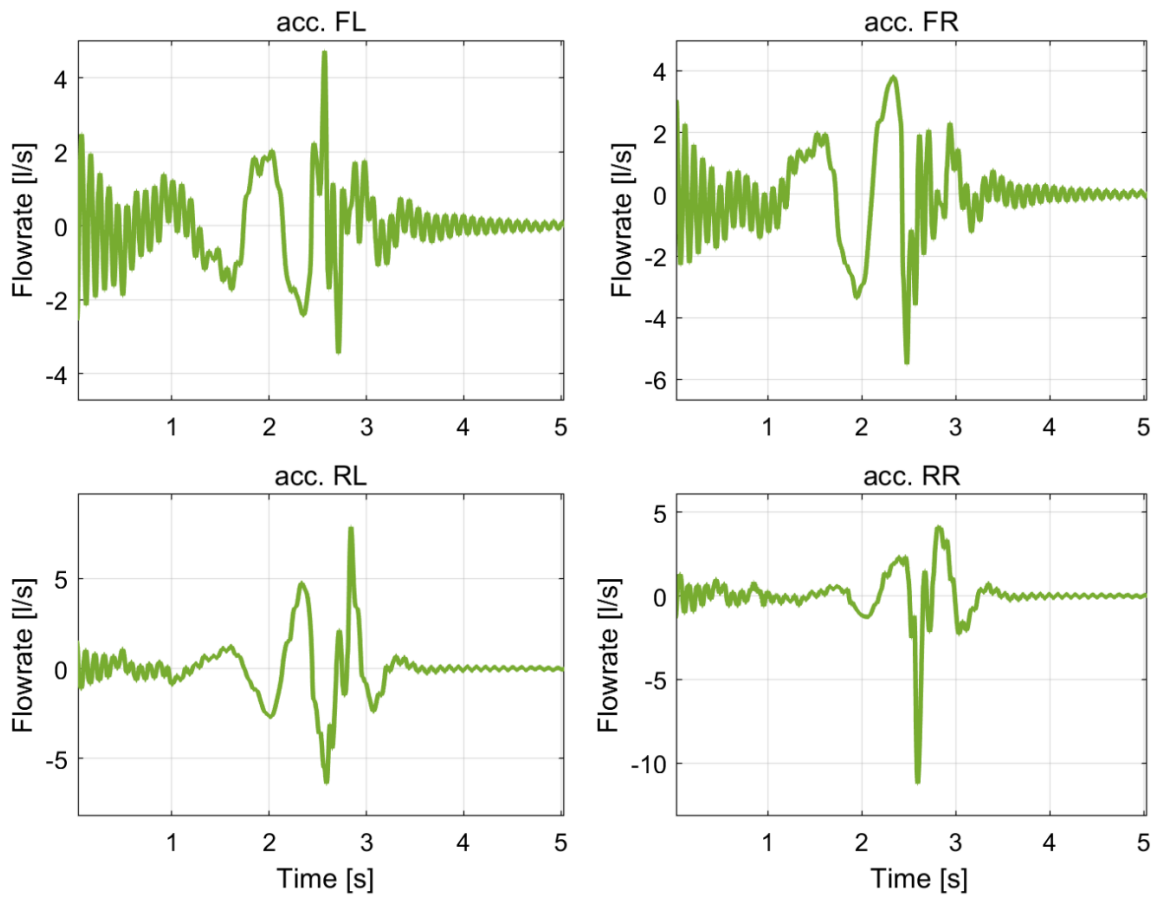
Figure 4.50 Figure 4.33 Flowrate entering/exiting to/from the hydraulic accumulators.

The Fig. 4.50 shows the oil flow rate that flows through the hydraulic accumulators: comparing this Figure with the wheel's actuator displacements, it is possible to appreciate the volume compensating effect of the accumulators.
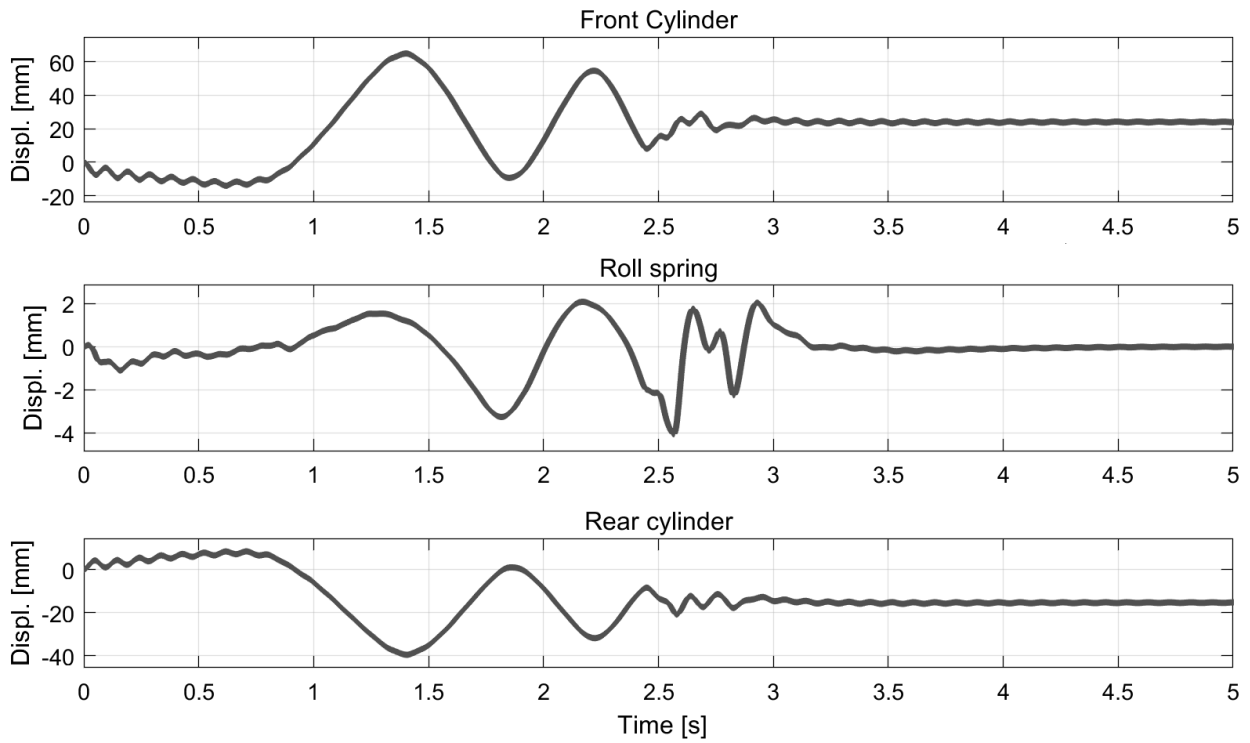
Figure 4.51 Displacements [mm].

4.4 Passage over a right bump

The aim of this test is to evaluate the ride comfort in case of crossing over a bump collocated only on one side of the track to see how the system behaves in case of 'single wheel bump', and if the increase of the roll stiffness causes a degradation of the ride performances. The test is constituted by a mild acceleration on a straight-line path, where at 20 m from the starting point, it is collocated an obstacle 4 cm high and 75 cm wide that the vehicles impact at 65 km/h (Fig. 4.52); considering that the Italian traffic laws states that the artificial bumps, for speeds equal or lower than 50 km/h, must be at maximum 3 cm high and minimum 60 cm wide [33], it is possible to affirm that the obstacle selected is quite severe, also taking into consideration the type of vehicle model adopted.
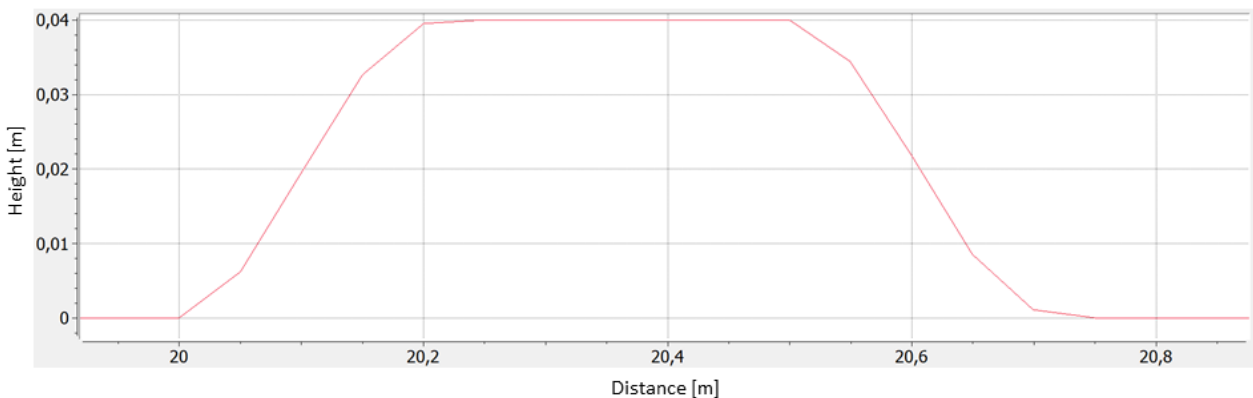

Figure 4.52 Obstacle's characteristics.

Looking at the figures, it is possible to see that, during the crossing over the bump, the virtual driver of the interconnected vehicle has to apply a higher steer wheel angle to correct the path (Fig. 4.53). One of the main things that this test has revealed it is the presence of heavy oscillations in the vertical displacements of the wheels that have repercussions in the tire normal forces (Fig. 4.55). We have already seen them in the previous test, but in this case, they are more pronounced. As said before, it is reasonably to think that the road's irregularities cause the resonance of the unsprung masses that the interconnected suspension system is not able to damp; for this are required further investigations that lie outside the aim of this work. On the other side, looking at other signals reported, as which of the longitudinal acceleration (Fig. 4.56), or the vehicle speed (Fig. 4.54), it is easy to see that these oscillations have not a significant influence on the vehicle dynamics, in fact the two trends are almost overlapped, meaning that the handling capabilities are not wasted (both vehicles observe the lift of the right wheels in the same way).

105
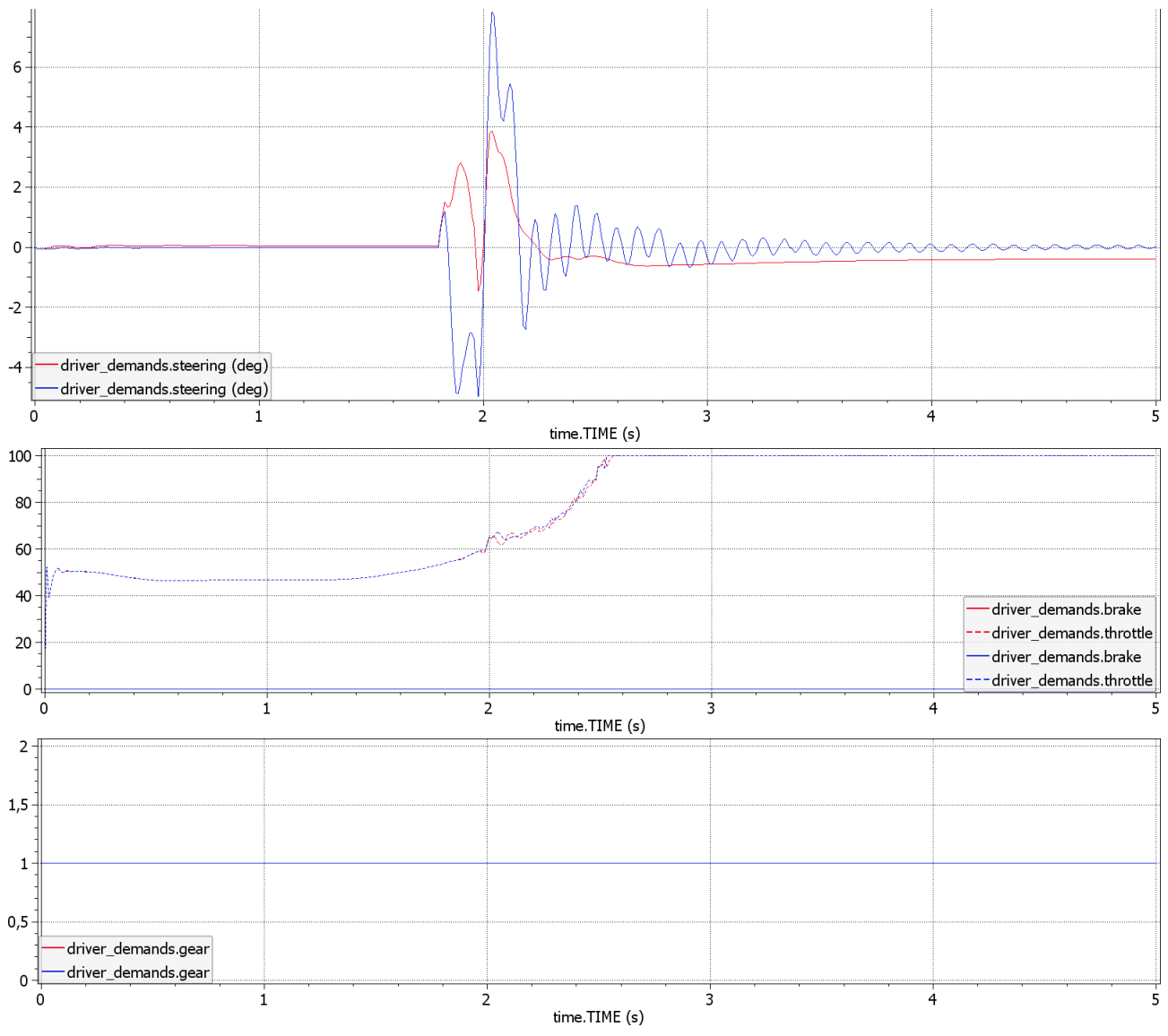
Figure 3.53 Driver input, from above the steering wheel, the accelerator position pedal and the gear engaged (interc − base).
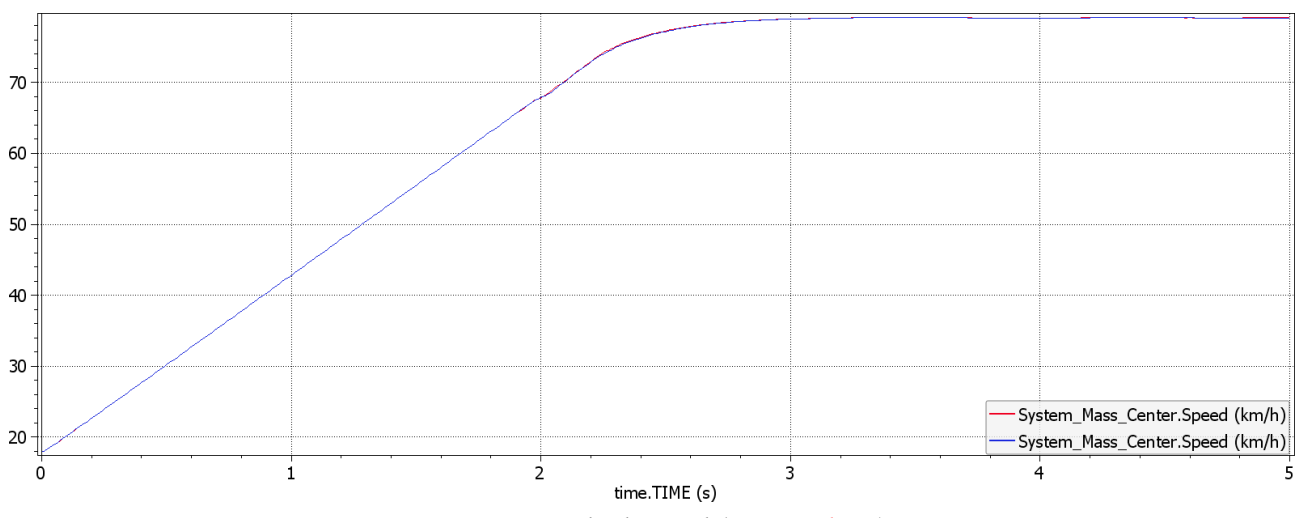
Figure 4.54 Vehicle speed (interc − base).
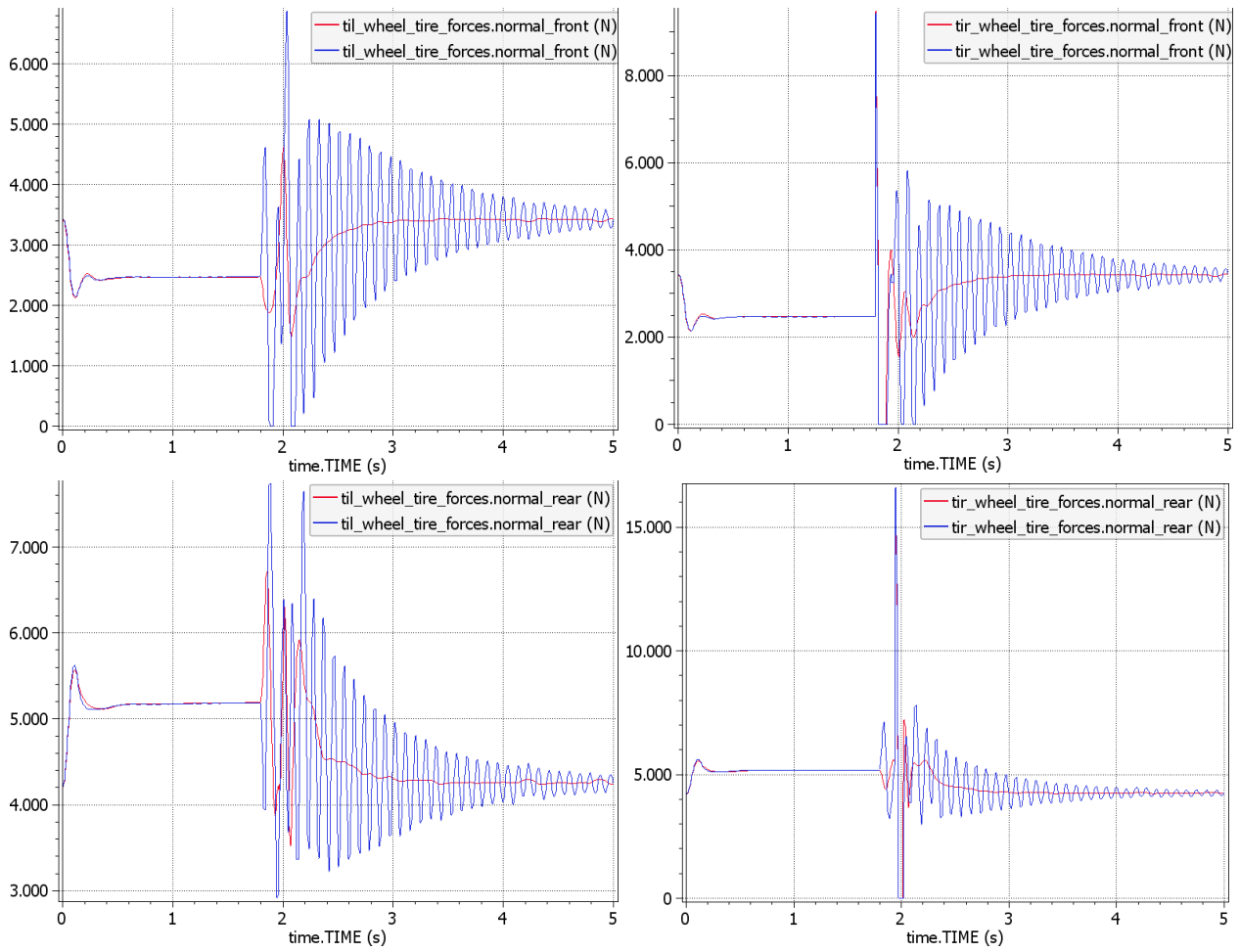
Figure 4.55 Tire's normal load (above the front axle) - (interc – base).
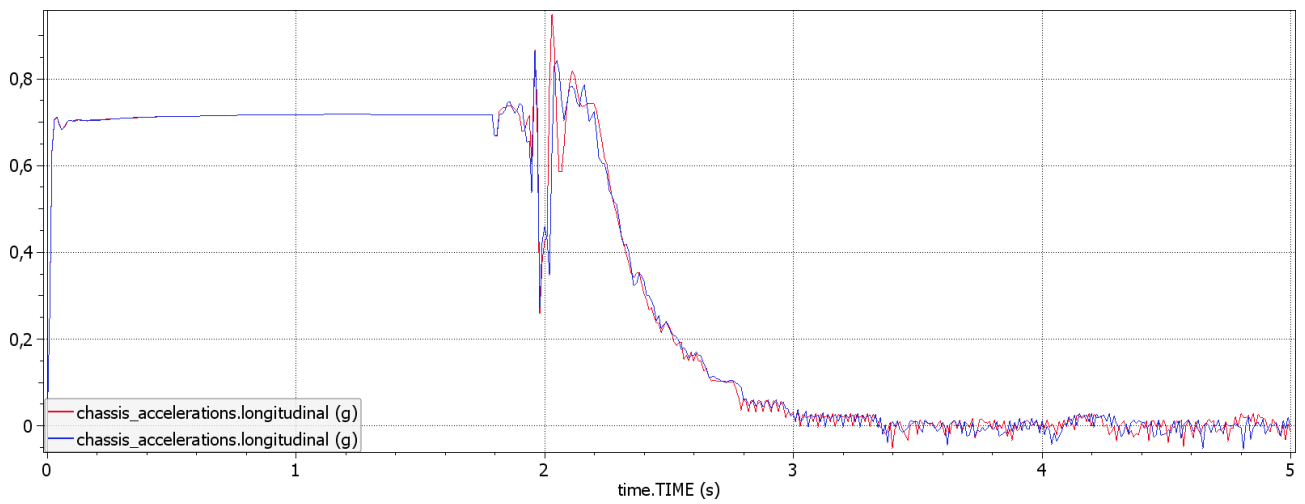
Figure 4.56 Longitudinal acceleration (interc – base).
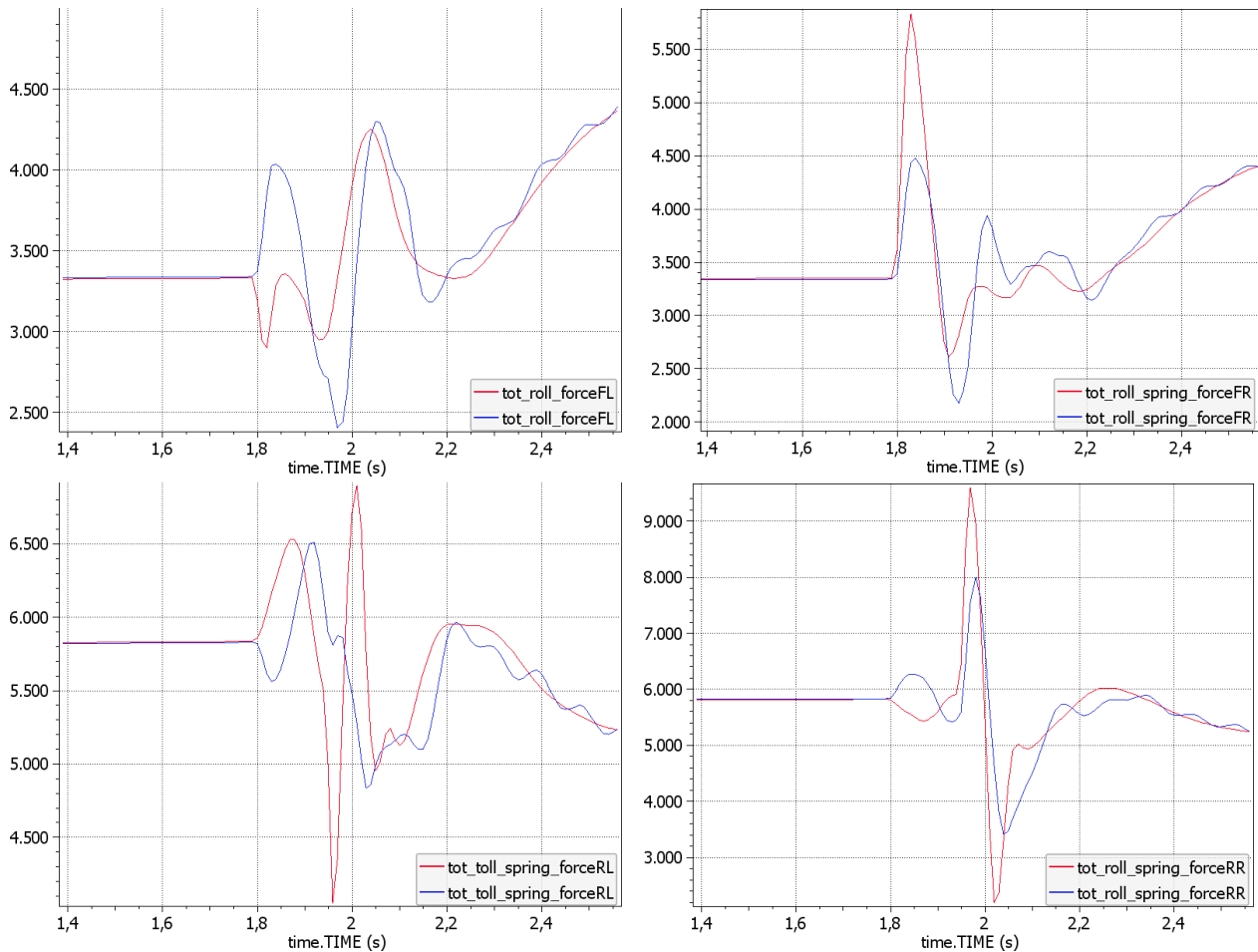
Figure 4.57 Force at springs in the time instants near the passage over the bump (interc – base).

The Figure above (4.57) describe the elastic forces at spring level: it is possible to see that, thanks to the interconnection, the wheel elasticities are reduced and as consequence the peaks of the spring's forces; this allows to reduce the forces propagation due to the impact and enable the wheels to better follow the profile of the obstacle. This phenomenon is due to the hydraulic system, where the flowrate, exiting from the right wheels' actuators as consequence of the impact, flows inside the accumulators instead to activate the roll spring that is practically not deformed (Fig. 4.58) : the central lever am of the interconnection is subjected at a rotation that avoid to activate the roll spring making possible to null the warp stiffness and reduce the wheel elasticities as seen into the 1.3.1 paragraph. The rotation of the centre lever arm it is also helped by the counter-phase motion of the piston inside the front and the rear double cylinder, as shown in Fig.4.58.
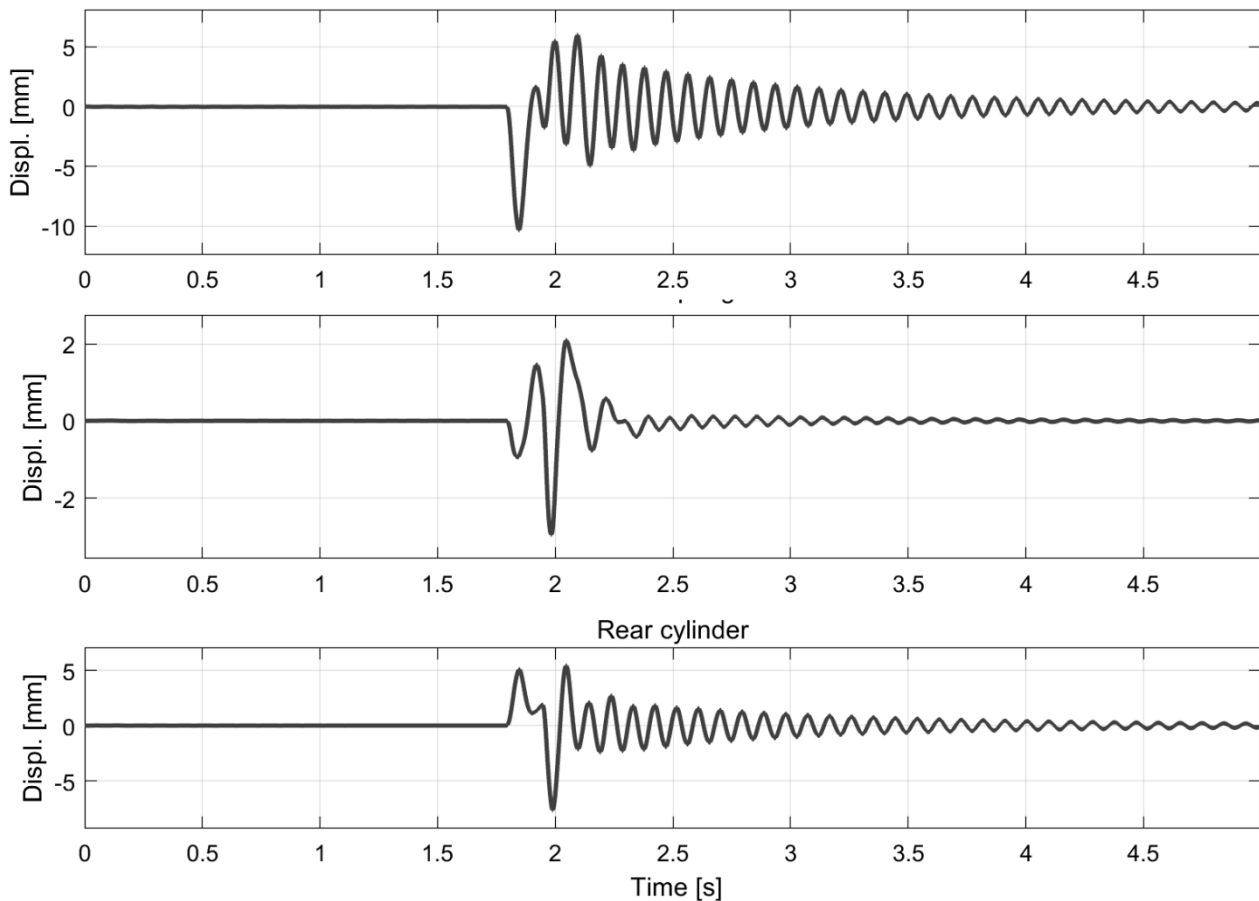
Figure 4.58 Are represented, respectively, the piston's displacement of the front double acting cylinder, the roll spring deformation and the piston's displacement of the rear double acting cylinder.

Finally, looking at the vertical acceleration comparison (Fig. 4.59), **it is possible to affirm that the ride performances of the two vehicles are practically the same**, so, also in this case the effect of the higher roll stiffness has not significative negative effects on the comfort.

In the Fig. 4.60 are shown the roll and the pitch angle of the vehicle: both movement are more pronounced and the roll angle presents higher oscillations for the interconnected vehicle at time instant 2.13 s that correspond with the instant in which the right rear tire has just passed the bump.

In Fig. 4.61 are illustrated the pressure trends in the hydraulic lines between the wheels' actuators and the central double cylinders; also in this case, it is possible to see the effect of the oscillations that the orifice-accumulator groups are not able to damp. In this simulation has been observed the peaks values for the pressure levels, corresponding to 283 bar for the right front hydraulic line and 368 bar for the rear.
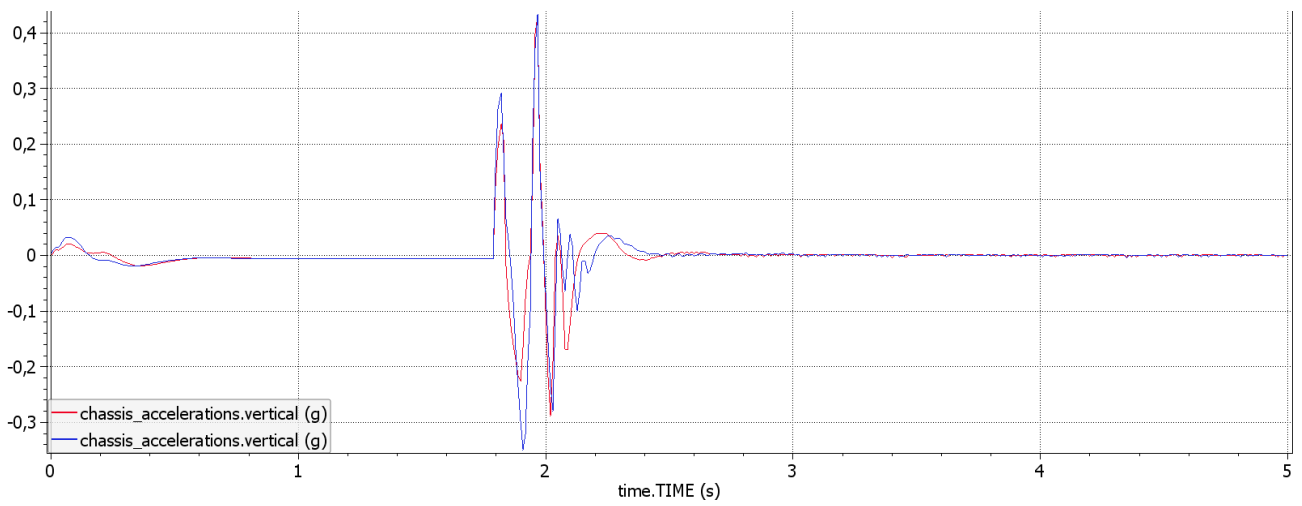
Figure 4.59 *Vertical acceleration (interc − base).*
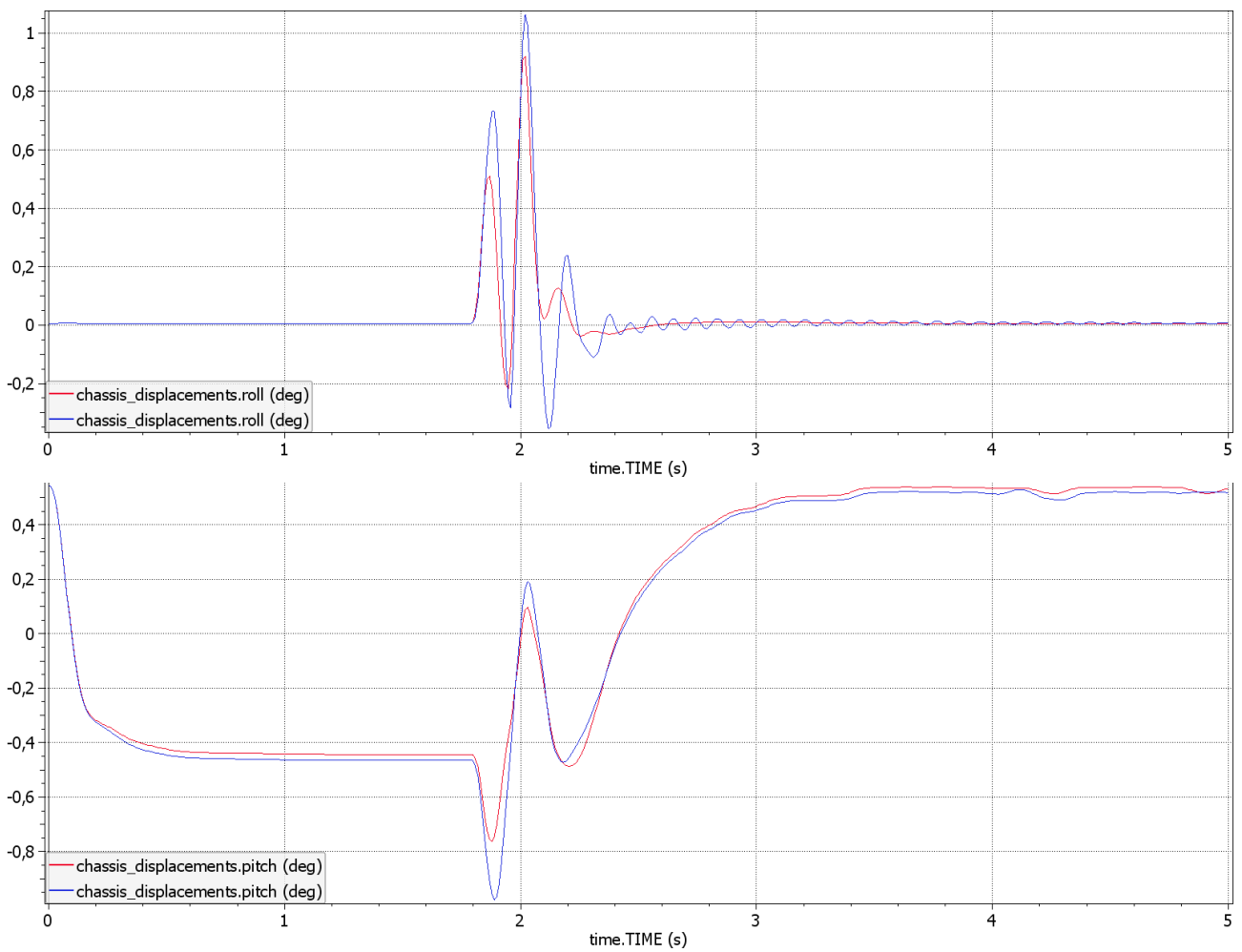
Figure 4.60 *Roll angle (above) and pitch angle (interc − base).*
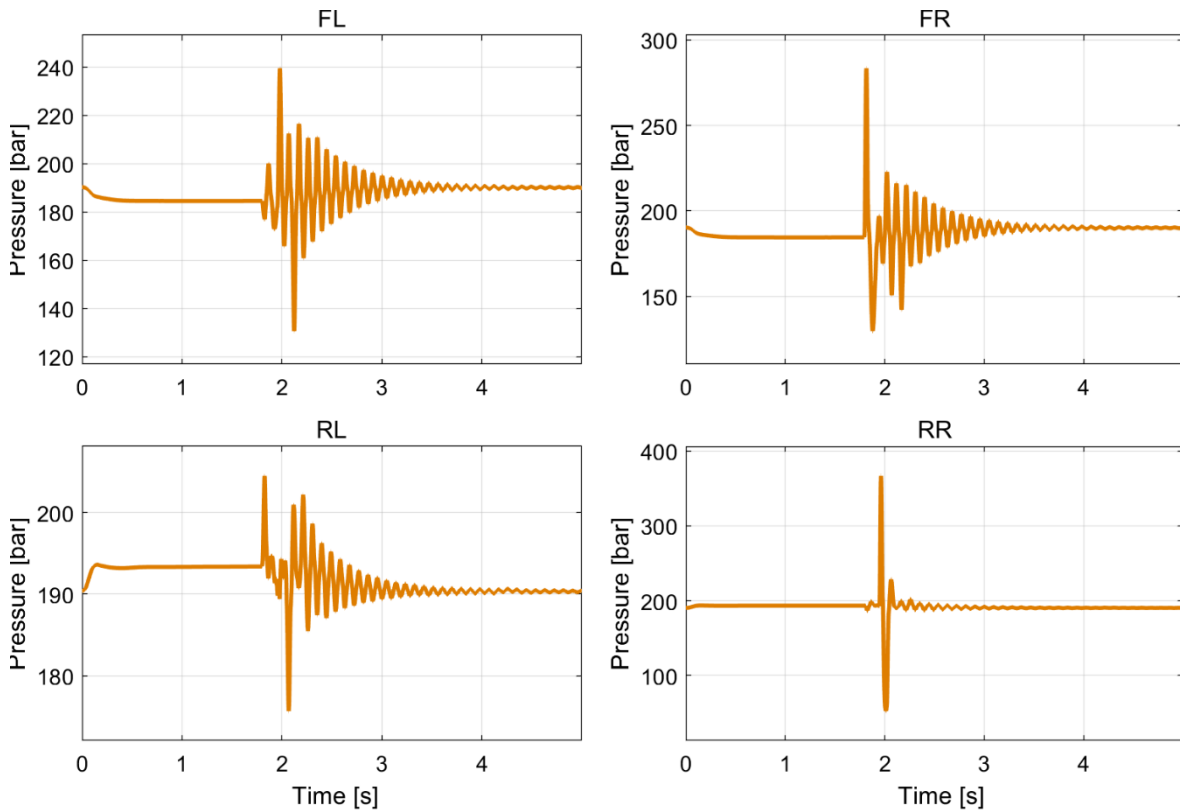
Figure 4.61 Pressure in the hydraulic lines between the wheels' actuators and the central double cylinders.

In the next page are shown two graphs that represent the flowrate that goes into to the central double acting cylinders (Fig. 4.62) and the flowrate that goes throught the hydraulic accumulators (Fig.4.63). It is interesting to note the comparison between the two figures and the fact that the flowrate into the right wheels is higher with respect the flow rate in the left wheel (more accentuated at rear): this, as said before, represent the hydraulic contribution in the realization of the soft warp mode, because reduce the motion of the pistons inside the central double acting cylinders that acts on the roll spring.
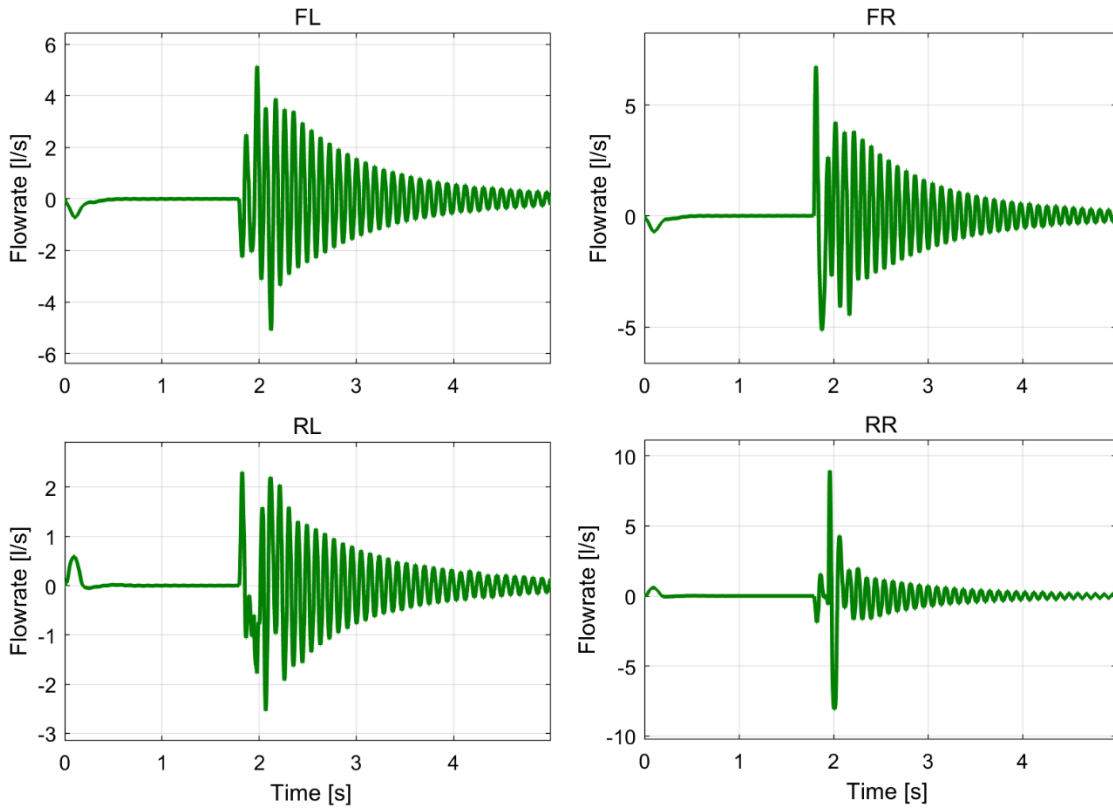
Figure 4.62 Flowrate in the hydraulic lines between the wheels 'actuators and the central double cylinders.
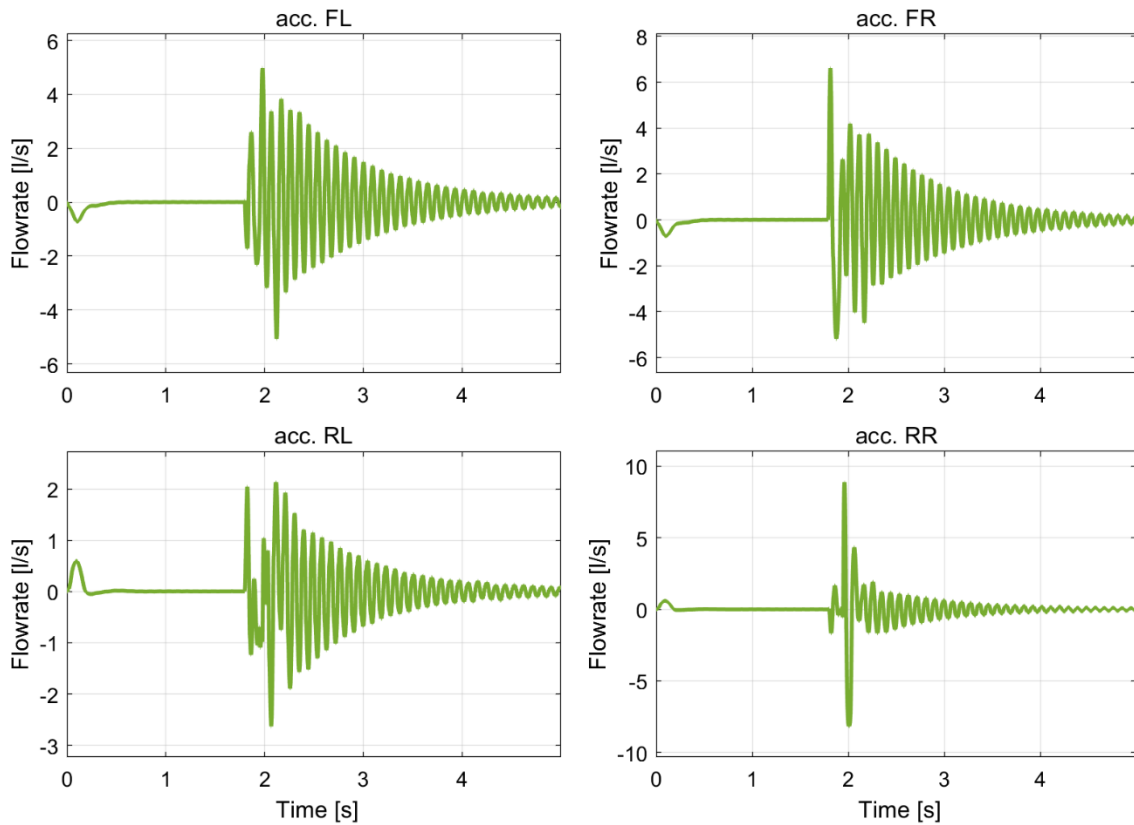
Figure 4.63 Flowrate into the hydraulic accumulators collocated between the wheels' actuators and the double acting cylinders.

112

4.5 Lap-time simulation

In this paragraph will be shown the results obtained from the comparison between the two models in a lap-time simulation. For this simulation has been important the modelling of the road: to see the effect of the soft warp mode, it is not enough to use an ideal flat road, and for this reason the idea was to start with a defined track path already defined in the Vi-CarRealTime library and then add, through the Vi-Road toll kerbs, bank angles and an elevation profile. The selected track is 'Vi-Track' and in order to have a reference for the elevation profile, has been chosen the initial portion of the 'Circuit de Barcelona-Catalunya', characterized by high variations in the elevation profile. The elevation profile has been acquired by Google Earth application and then implemented in the selected track, copying the height vector in the .rdf road file. Then, in each corner is added a bank angle of 2.5 deg in the corner apex and finally, have been added the kerbs, of triangular shape wide 1 m and characterized by a slope ok 15%. Then, by means of Vi-Road it has been generated a path to optimize the driving line and make sure that the trajectory pass over the kerbs. With this implementation, it was possible to include in the analysis of the lap-time the combined effect of longitudinal slope, bank angle and road irregularities as the kerbs.
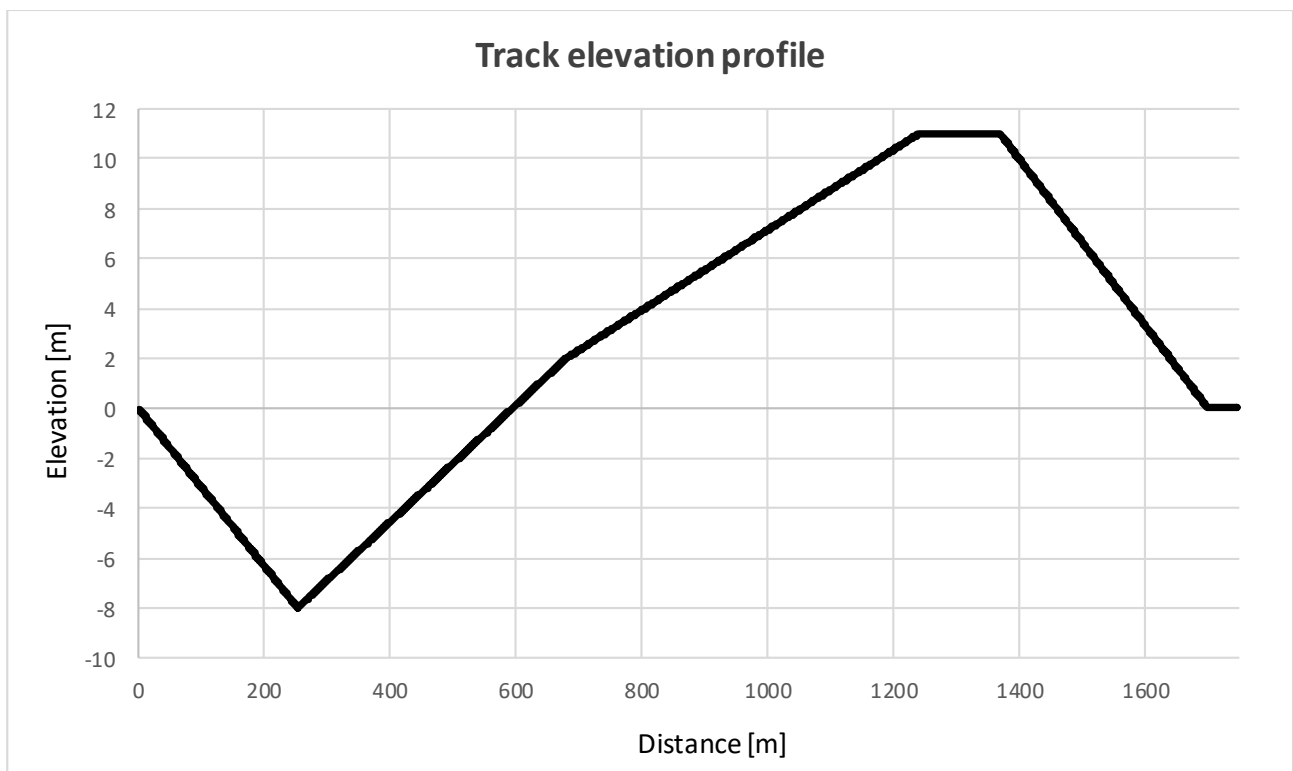
Figure 4.64 Elevation of the track [m].

113

Figure 4.65 'Vi-Track' in Vi-Road with elevation profile, kerbs and bank angle in the corners. The blue path represents the driving line generated by the tool to optimize the vehicle performances, while the red path is the track centreline.

The lap-time simulation comparison is performed with the 'Max Performance Event', an event integrated in the Vi-CarRealTime software that, given in input the blue path generated in Vi-Road, through iterative calculation, evaluates the maximum speed profile for each part of the track for the vehicle model selected; in case in which the initial speed for a certain corner is too high and the vehicle is not able to follow the predefined path, it recalculate a lower speed profile reducing the lateral performance of a scalar factor that became lower and lower up to the right speed values that allow to the vehicle to follow the defined path.

The lap-time results are illustrated in the 5.1 Tab.

Table 5.1

model	Lap-time [s]	delta [s]
standard	57.83	- 0.19
interconnected	58.02	0.19

114

How it is possible to see from the above table the lap time simulation has revealed that the interconnected vehicle in the selected track is slower of 0.19 s with respect the standard vehicle. Analysing the speed profiles in Fig. 4.66 it is possible to observe that the standard vehicle is faster in the third and in the fifth corner (Fig. 4.67), that are quite long corners that the vehicles cross in steady state manoeuvre. The reason of the slower speed profile is main due to an enhanced understeer behaviour due to the soft warp mode that in this corners, characterized by kerbs and a combination of vertical and lateral slope, try to even the vertical load between the front and the rear axle. Indeed, the understeering behaviour is easy to see from the signal of the steering angle (Fig. 4.68) and from the evaluation of two variables: the difference between the front and the rear tire vertical load (Fig. 4.69) and the understeer angle (Fig. 4.70), evaluated as:

$$und_{angle} = \delta - \beta \quad [31]$$

Where, δ is the steering angle at wheels and β the vehicle side slip angle.

The Fig. 4.70 shows that both the vehicles have an understeer behaviour (because the understeer coefficient is always positive) that for the interconnected model is more accentuated. In fact, also looking at the Warp Forces as function of the time and as function of the lateral acceleration (Fig. 4.71), it is possible to affirm that the soft warp mode contribute to even the vertical loads and to modify the front-rear roll stiffness distribution with respect the standard vehicle in case of a not perfect flat surface.
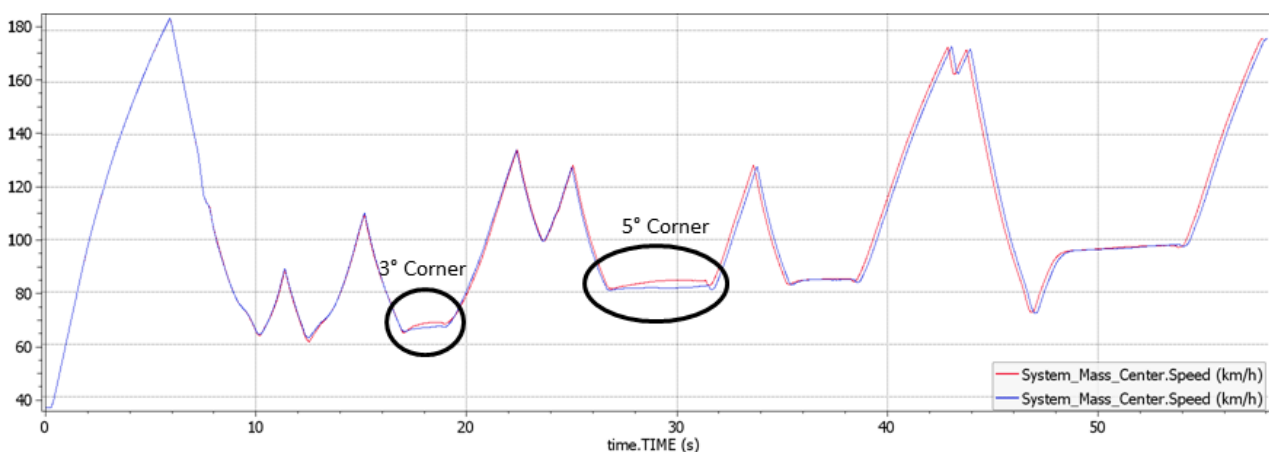
Figure 4.66 Speed profile; in the circles are highlighted the third and the fifth corner where the standard vehicle is faster than the interconnected (interc – base).
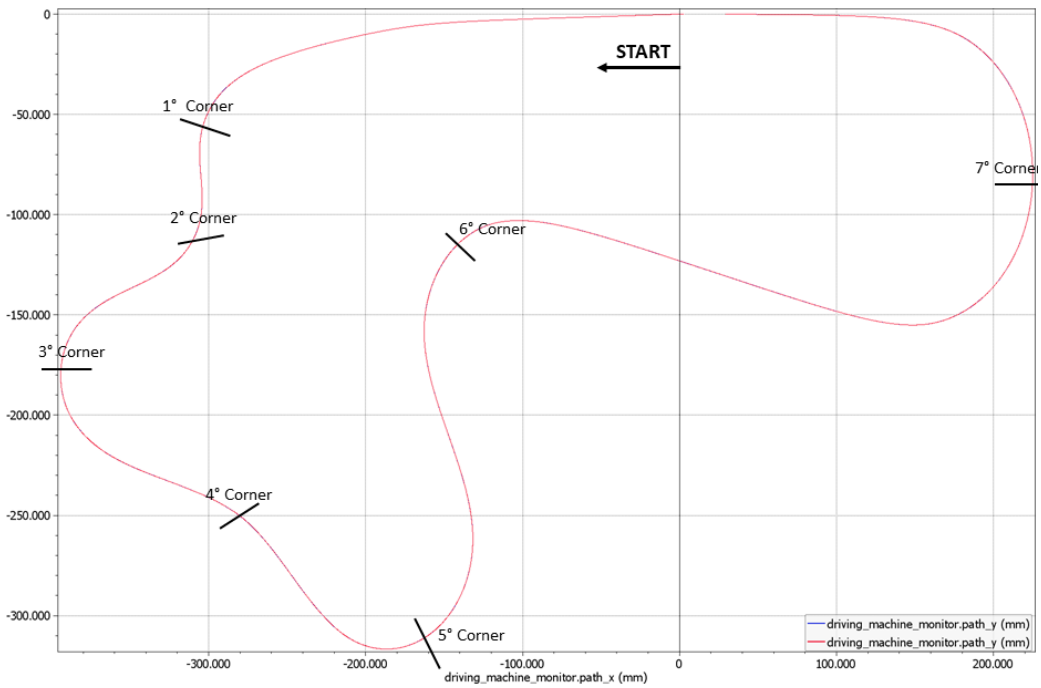
Figure 4.67 Vehicle path: the vehicles follow the same trajectory due to the Event selected.
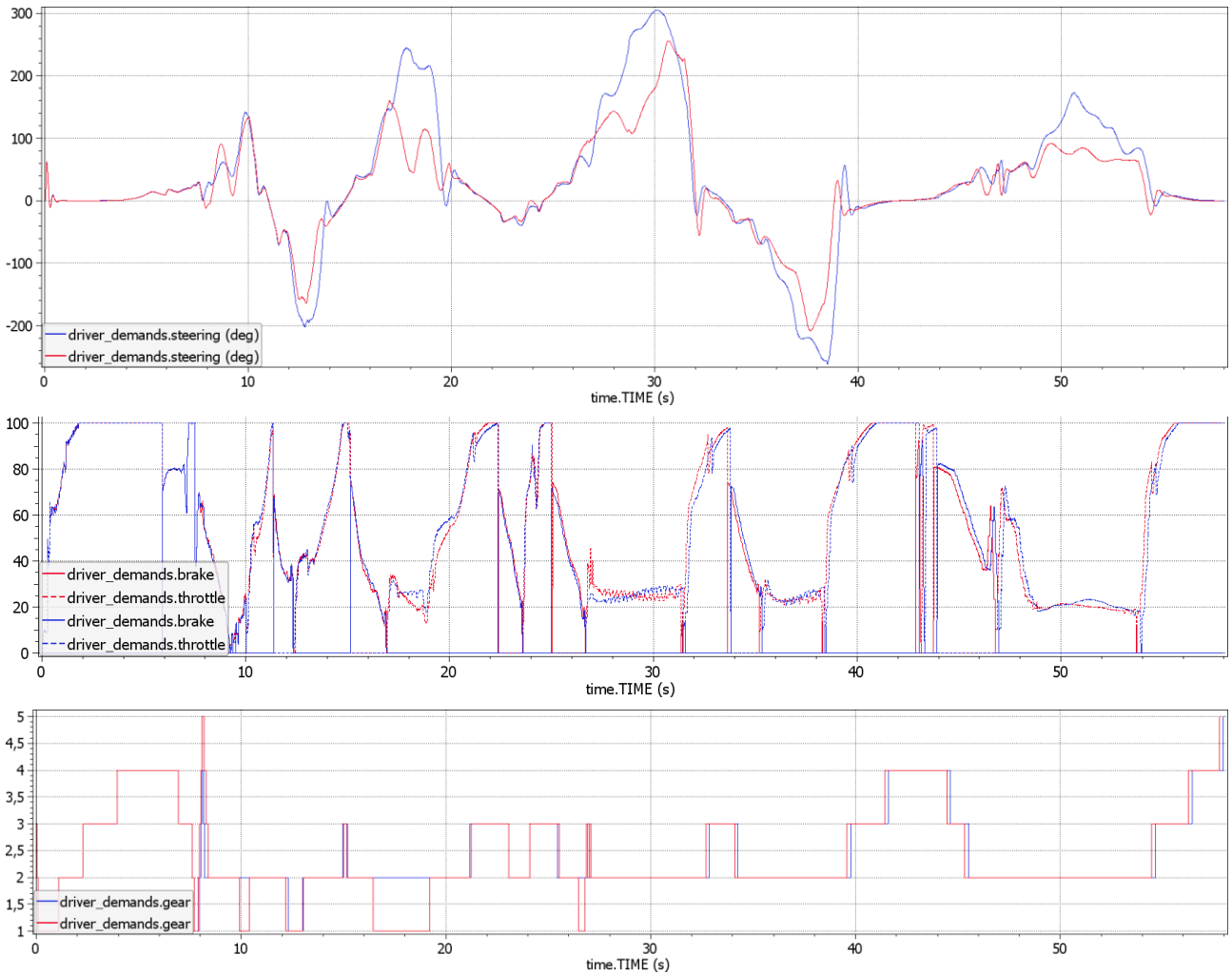
Figure 4.68 Driver inputs: above the steering wheel angle (interc – base).

116
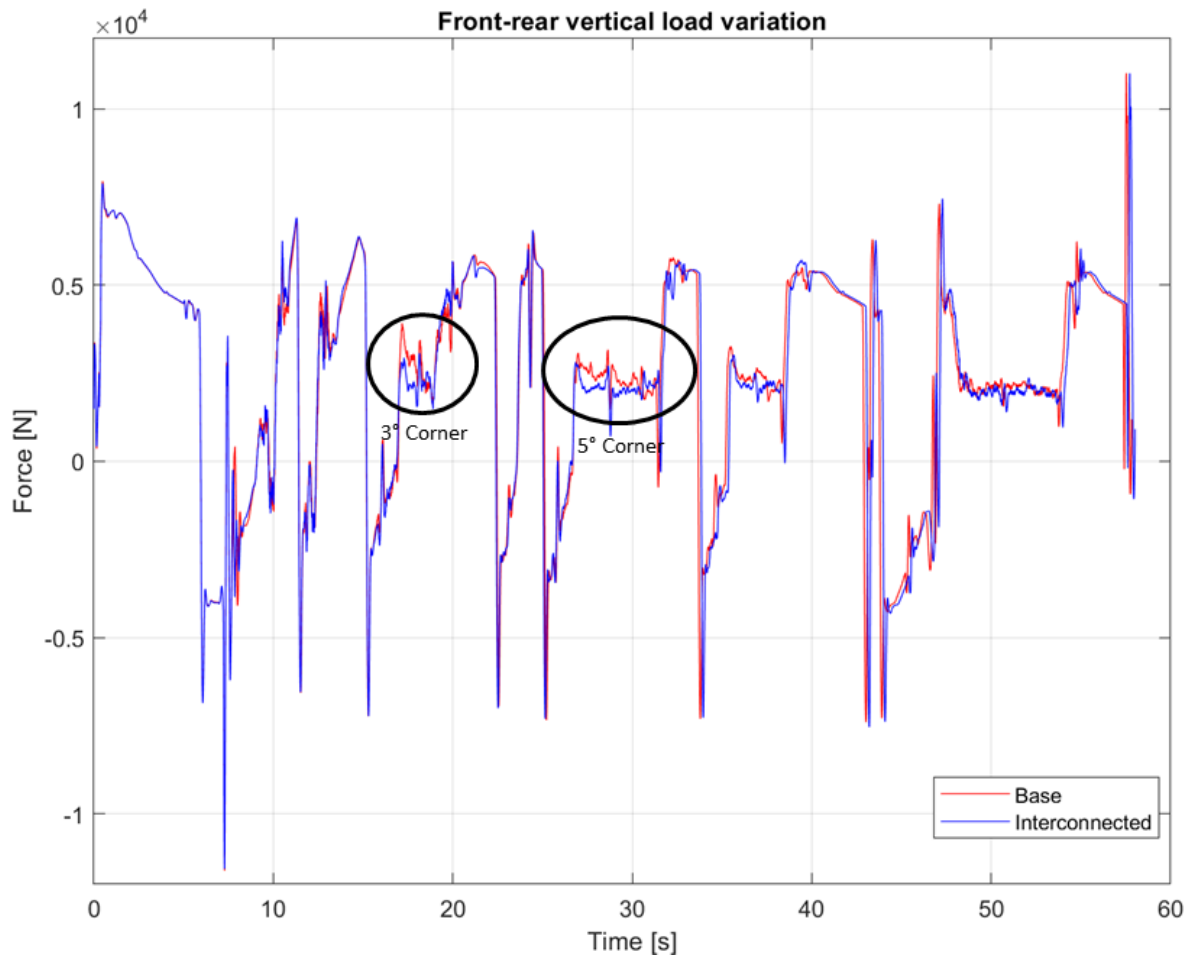
Figure 4.69 Difference between the rear vertical load and the front. It is possible to affirm that in the third and fifth corner the interconnected vehicle has more front load distribution with respect the standard, that enhances an understeering behaviour (interc − base).
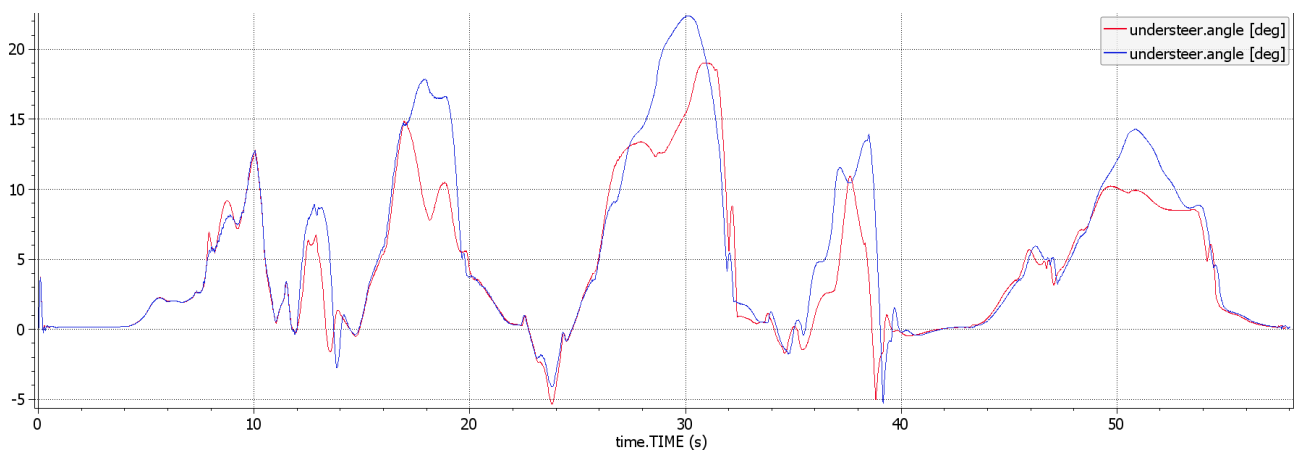
Figure 4.70 Understeering angle [deg] (interc − base).
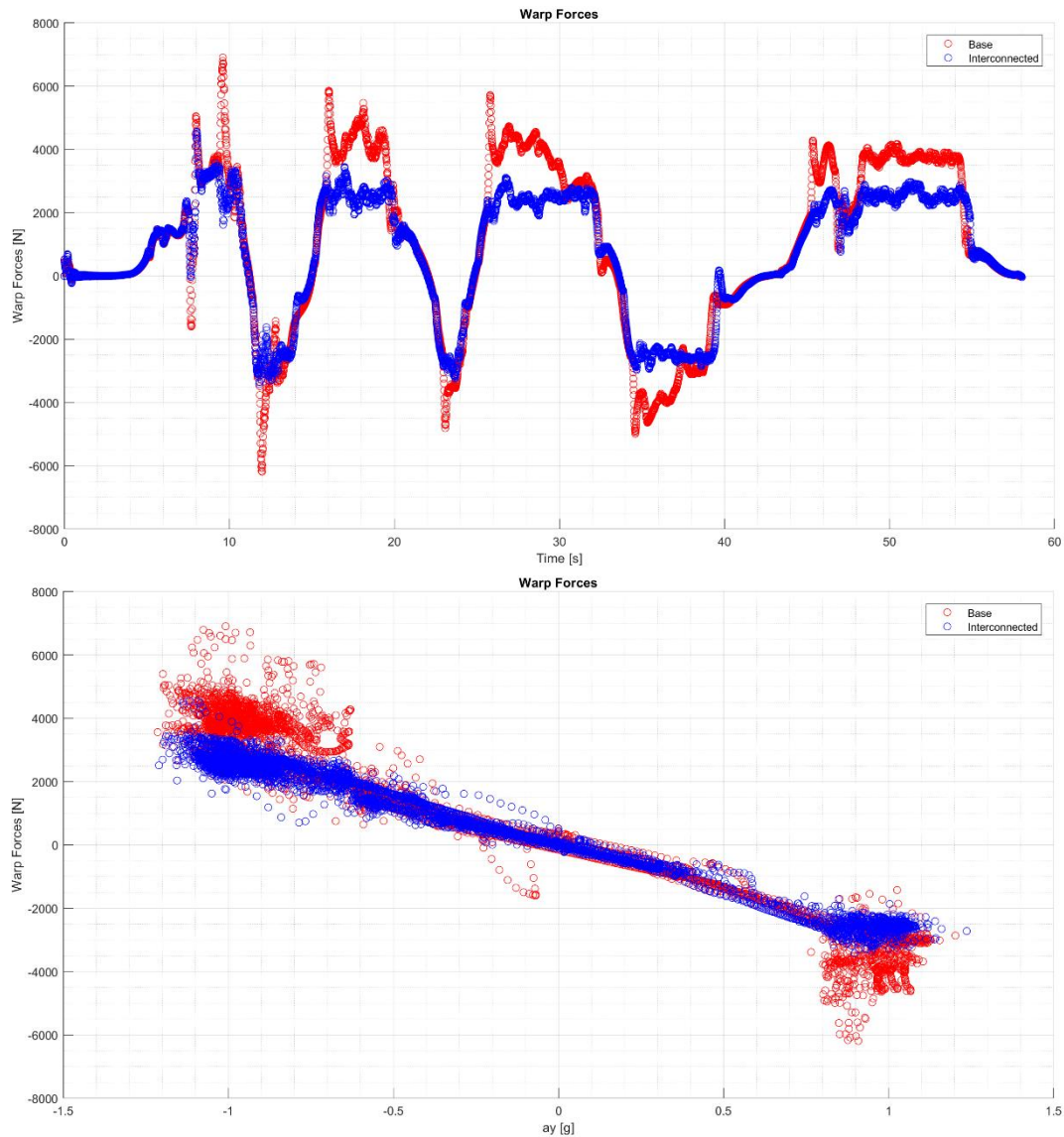
*Figure 4.71 Warp force as function of the time (above) and as function of the lateral acceleration (*interc* −*
base).*

The understeer behaviour has consequently the effect that the interconnected vehicle is not able to generate the same amount of lateral forces as the standard vehicle. This effect is clearly visible looking at the g-g plot in the Fig. 4.72, where are shown the combination of lateral and longitudinal accelerations.

For what concern the other parameters, the previous results obtained in the standard manoeuvre are confirmed, in fact the interconnected vehicle demonstrate a higher stability, as revealed by the sideslip angle that is systematically lower with respect the standard vehicle (Fig. 4.73).
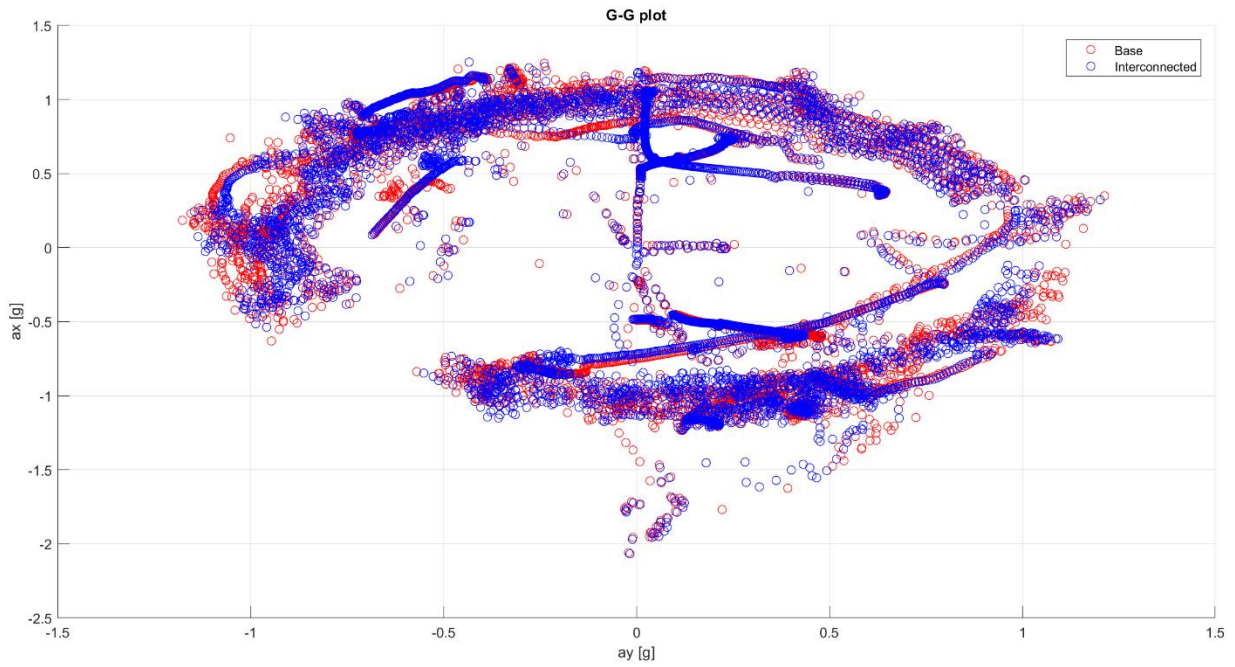
Figure 4.72 G-G plot (interc – base).
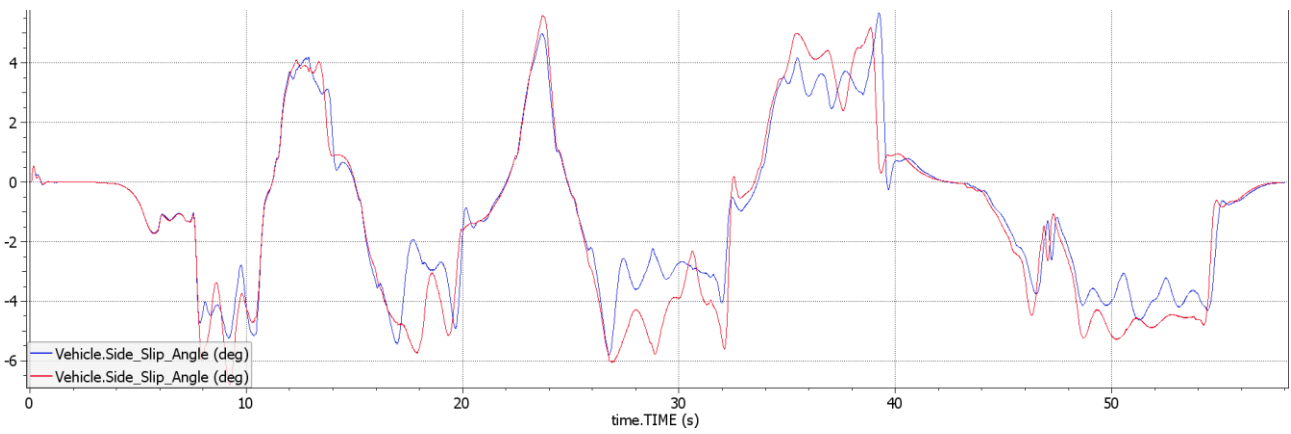
Figure 4.73 Vehicle side slip (interc – base).
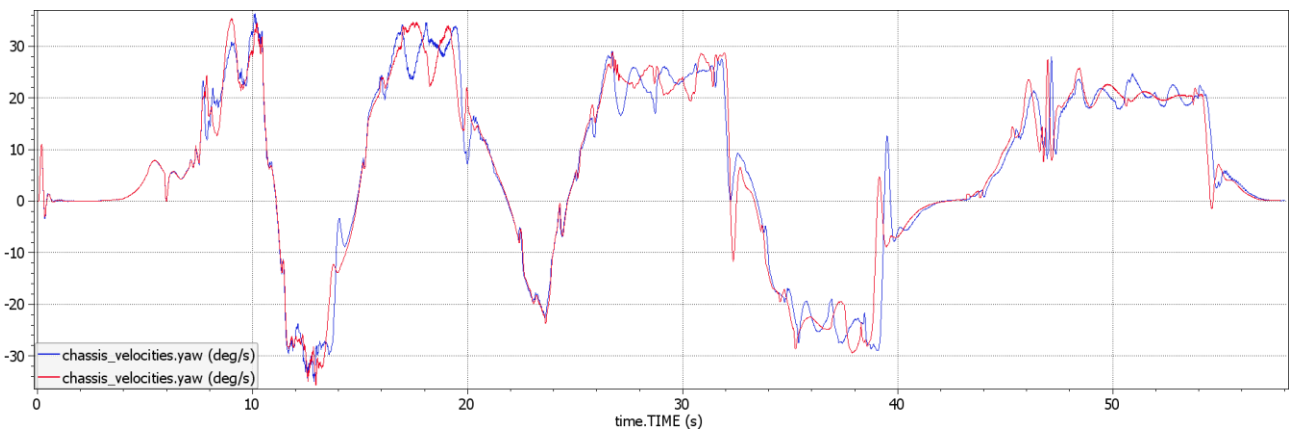
Figure 4.74 Yawrate (interc – base).

119

The parameters involved with the comfort also confirm the previous results, indeed the trends of the vertical acceleration are almost overlapped, despite the presence of kerbs and changes in the vertical slope as it is possible to note at time instants 5.4s and 57.5s (Fig. 4.75). In the Figure 5.76 it is shown the behaviour of the roll acceleration: also in this case the trends are almost overlapped excluding some peaks more pronounced for the interconnected vehicle, related to the higher roll stiffness; the high frequency oscillations around the zero values are caused by the passage over the kerbs in the corners.
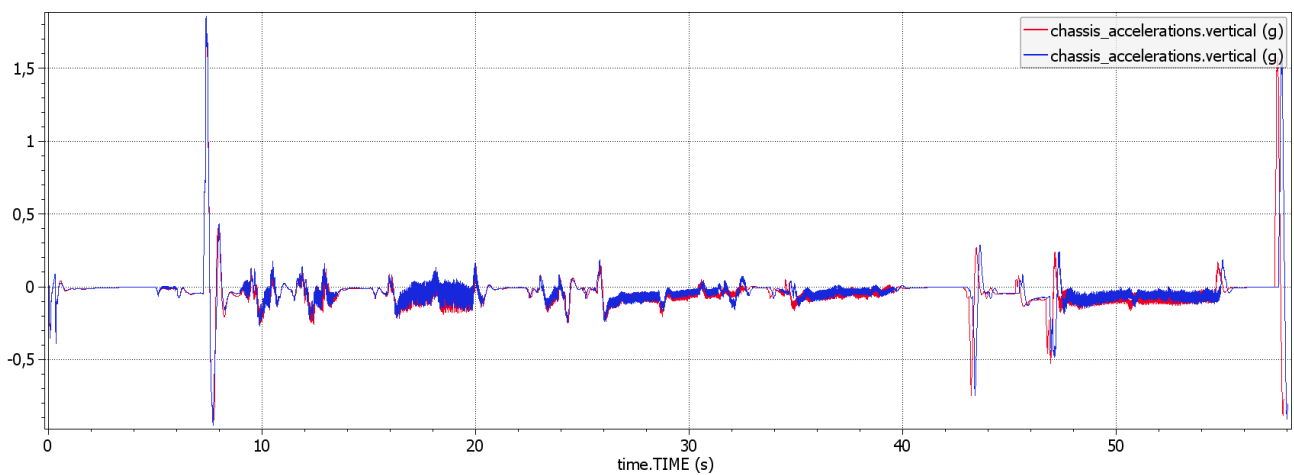
Figure 4.75 Vertical acceleration (interc – base).
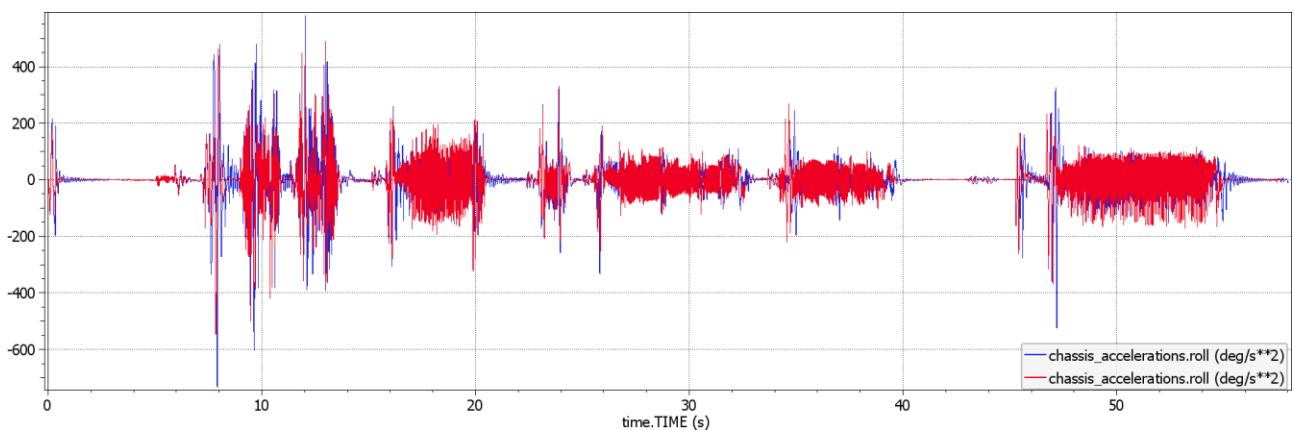
Figure 4.76 Roll acceleration of the sprung mass (interc – base).

5 Conclusions

The suspension system is one of the main subsystems involved in the definition of the vehicle handling and ride performances. Generally, for the conventional suspension systems present in the marked, to improve the vehicle performances it is required a stiffer system, while to improve the comfort of the occupants, a softer setting. The aim of this thesis has been to propose a not conventional suspension system with the purpose to decouple the two effect and optimize both the dynamics and the ride.

The proposed interconnection is constituted by a completely passive fluid-mechanic system capable to uncouple the roll and the warp mode. The suspension system has been modelled in Simscape, following a physical approach, which include the hydraulic actuators, accumulators, springs and dampers; big part of the work regarded the integration between the suspension model and the vehicle model.

The analysis of the effects on the vehicle dynamics have been carried out in co-simulation environment between Simscape and Vi-CarRealTime, where a high-performance vehicle has been selected for the study.

To compare the standard vehicle and the interconnected one, have been selected five events: a steep steer test, a Fishhook, an acceleration on a sinusoidal road profile, a passage over a right-side bump and a lap-time simulation.
The first two test have demonstrated that the interconnected vehicle, provided with higher roll stiffness with respect the standard one, is more stable and have a better dynamic response to the steering inputs; also, the reduction of the roll angle has as advantage the better exploiting of the suspension kinematic, reducing the wheels' camber variation and the roll steer effect, increasing the contact patch area between the road and the tires and the directional stability of the vehicle. Furthermore, the fishhook test has highlighted the fact that in an emergency manoeuvre, the interconnected vehicle is capable to follow a tighter path, indication of more stability and improved obstacle avoidance capability. In these tests, the sideslip angle of the interconnected vehicle is systematically lower with respect that of the standard vehicle.

The acceleration on a sinusoidal road profile (only in the right side of the vehicles, the left is maintained flat) and the passage over the right-side bump have been done to evaluate the ride performance of the interconnected vehicle. The results confirm the initial premises, indeed, the interconnection system is able to free the warp mode, allowing to reduce the wheels' elasticity and as a consequence of that, the wheel travels increase, enabling to the tires to not lose the contact with the road on the irregularities and improve the grip and the longitudinal acceleration. Another important effect of the soft warp mode is the reduction of the tires' vertical load variation; it too gives an important contribution in the improvement of tire grip capabilities. The study of the vertical and roll accelerations has shown that, despite the higher roll stiffness, the interconnected vehicle as ride performance similar and, in some intervals, better than the standard vehicle. On the other hand, these tests revealed the presence of oscillations in the tire vertical loads and in the wheel vertical movements in the range of the unsprung resonance frequency, probable indication of the fact that this system is not able to properly damp this kind of oscillations activated by road irregularities, and for which are necessary further investigations.

Finally, the lap time simulation has been carried out on a dedicated track in which have been included kerbs, bank angles in the corner and an elevation profile, to make the track more realistic and to make possible to evaluate the effects of the soft warp mode.
The simulation has revealed that the interconnected vehicle has a pronounced understeering behaviour in the middle-corner travel, since the soft warp mode tries to equalize the vertical load between the wheel corners, transferring more load on the front axle. Because of that, the standard vehicle is 0.19 s faster, that it means the 0.33% with respect the total time, while all the other observations done before are confirmed.

At the end of the work, is possible to affirm that the initial premises have been confirmed and that this system presents different advantages that can justify the rising in complexity and costs. In particular, it is reasonably to affirm that this system could be very interesting if applied on SUVs: nowadays the market is focused on this segment of vehicle, also for high performance applications, and as how well known, this types of vehicles suffer of a marked rollover tendency due to the higher centre of mass that in case of incidents, is one of the most lethal for the occupants. For these reason, the interconnection scheme proposed can represent a win-win strategy: on one side it allows to increase the roll stiffness, determining a better anti-rollover capability and an enhanced dynamic behaviour, and on the other side, to maintain a high level of ride performance and to improve the off-road abilities, that is the reason for which this type

of vehicles, initially, have been introduced; as a final remark, all of these improvements can be reached with the proposed system that is completely passive, avoiding the applications of complex and heavy active systems.

APPENDIX A

System Modelling

In this chapter will be illustrated a different approach to model an interconnected suspension system, in order to propose a simplified solution that can increase the computation efficiency of simulations and make available the model for HIL or DIL interfaces. The comparison of this simplified model with the physical one, has revealed the fact that this approach is not enough accurate, leading to results that not correspond to which of the physical model and that underestimate the dynamics of the system; but it is chosen to show this different approach to give a spark to the curious lector that want to examine in deep the argument and propose modifications that can contribute to improve the model accuracy. The main problem regards the definition of the warp stiffness, that has a crucial importance in the results and from which it was not possible to associate a univocal formulation.

The starting point of the work take inspiration by the formulation proposed by J. Fontdecaba in [13] and already illustrated in the 1.3.1 section.

The simplifying assumptions done regarding the parametrization of the interconnection scheme, so that the hydraulic circuit and the central lever arm are not more described by physics law, as in the previous modelling solution. The first ideal assumption is that the hydraulic system behaves as ideal levers, so inertia, elasticity and damping effects are neglected, and it is evaluated only the kinematics of the system; this assumption is like that did by Smith et Walker in [14]. Furthermore, the accumulators are not considered, and it is assumed a direct link between the wheels' actuators and central hydraulic cylinders.

The model is constituted by three subsystems (Fig. A.1):

- *Kinematic subsystem*, to define the motion of the point O (actuation of the roll-spring damper) as function of rockers' displacement and the values of the front and rear warp stiffness.
- *Stiffness subsystem*, to define the elastic force components at each wheel;
- *Damping subsystem*, where are evaluated the wheels' damping force contribution.
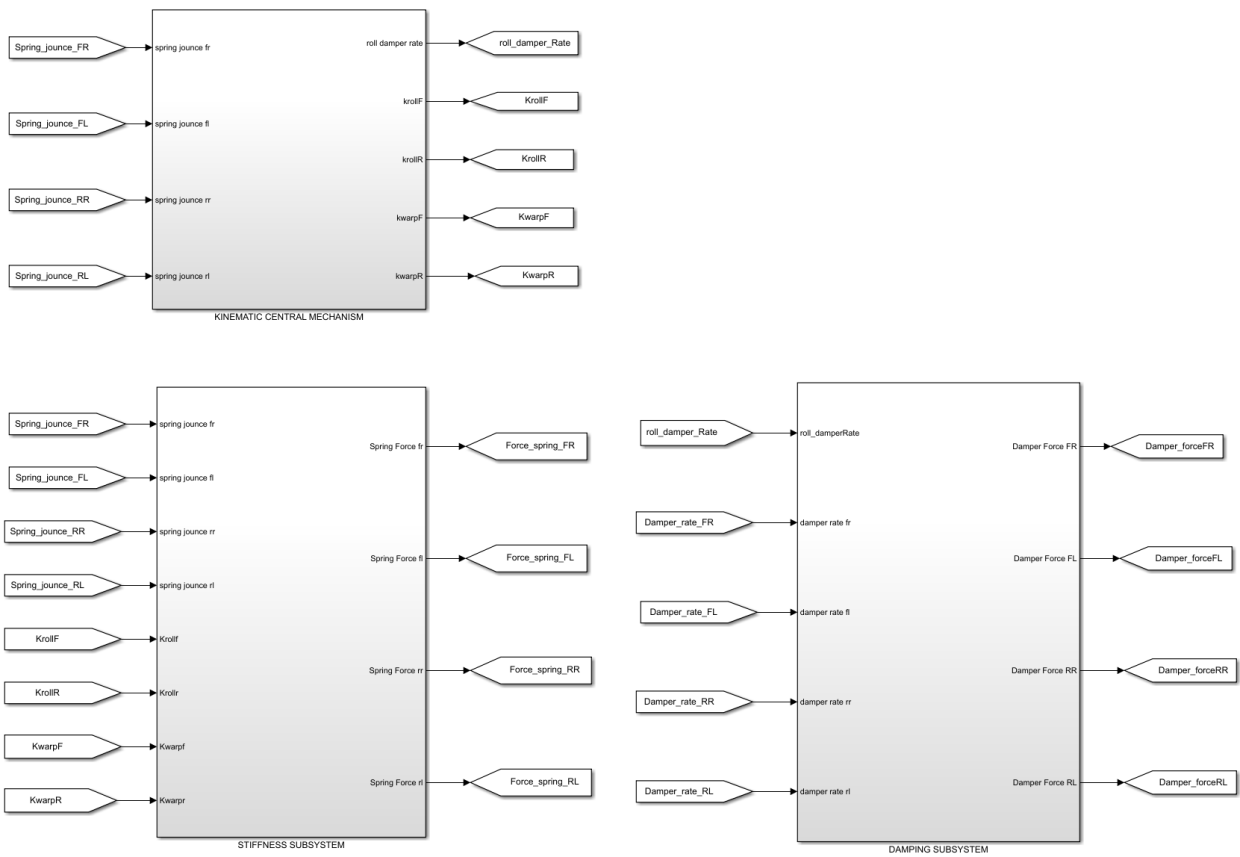
Fig. A.1 Simplified model composition.

A.1 Kinematic subsystem

Referring to the assumption that the hydraulic system can be described as ideal mechanical levers the transmission ratio between the wheels' actuators and the central double acting cylinders depends only by the area ratio. In fact, referring to the Fig. A.2 it is possible to evaluate the mathematical formulation below.
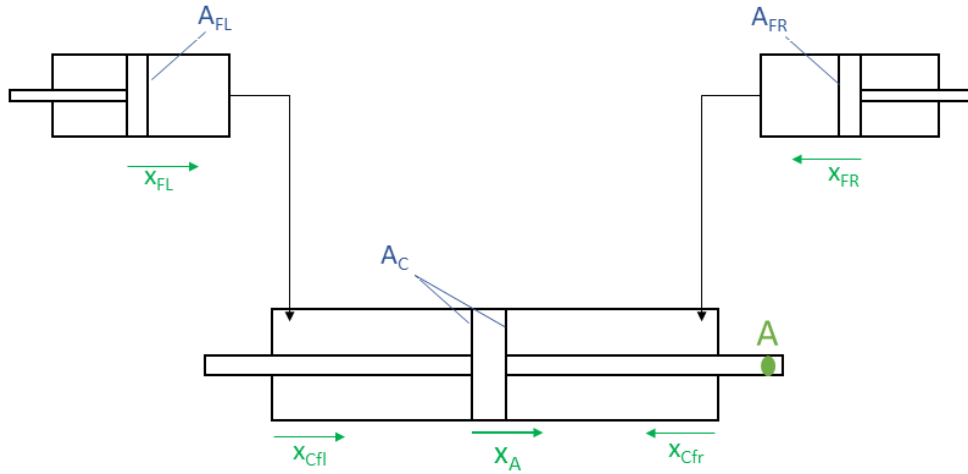
Fig. A.2 Front hydraulic system with front actuators and the double acting cylinder. The areas of the cylinder's chambers are highlighted. The accumulator's function is neglected in this description.

For the flow conservation law, it is possible to affirm:

$$x_{fl} \cdot A_{fl} = A_c \cdot x_{cfl} x \qquad \rightarrow \qquad x_{cfl} = \frac{Afl}{Ac} \, x_{fl}$$

$$x_{fr} \cdot A_{fr} = A_c \cdot x_{cfr} x \qquad \rightarrow \qquad x_{cfr} = \frac{Afr}{Ac} \, x_{fr}$$

Therefore, the motion of the point A, representing the axial displacement of the piston inside the double acting hydraulic cylinder is:

$$x_A = x_{cfl} - x_{cfr} = \left(\frac{Afl}{Ac}\right) x_{fl} - \left(\frac{Afr}{Ac}\right) x_{fr} = \alpha \, (x_{fl} - x_{fr}) \qquad \text{(A.1)}$$

With:

$\alpha = \left(\frac{Afl}{Ac}\right) = \left(\frac{Afr}{Ac}\right)$ because $A_{fl} = A_{fr}$, where α representing the transmission ratio.

Holds the same considerations for the rear axle, so:

$$x_B = x_{crl} - x_{crr} = \left(\frac{Arl}{Ac}\right) x_{rl} - \left(\frac{Arr}{Ac}\right) x_{rr} = \alpha \, (x_{rl} - x_{rr}) \qquad \text{(A.2)}$$

For this description it is assumed that α is equal to 0.5 in order to have the same displacements between the wheels' actuators and the piston inside the central cylinders, so a transmission ratio equal to 1 for the roll spring actuation.

Then, referring to the Fig. A.3, the roto-translational motion of the point O it is described by the equations A.3 and A.4.

Fig. A.3 Roll actuation system.

$$x = \frac{x_A \cdot b + x_B \cdot a}{a + b} \qquad (A.3)$$

$$\vartheta = \arctan\left(\frac{x_B - x_A}{a + b}\right) \qquad (A.4)$$

A.2 Stiffness subsystem

A.2.1 Matrix Formulation

The modelling proposed, as said, is based on the ideal formulation proposed by J. Fontdecaba in [13] and arranged for this type of real interconnection.

Considering what said in the chapter 1.3.1, it is possible to decouple the stiffness contribution for each mode with the matrix system 1.1, that is valid where the front and the real stiffnesses are the same.

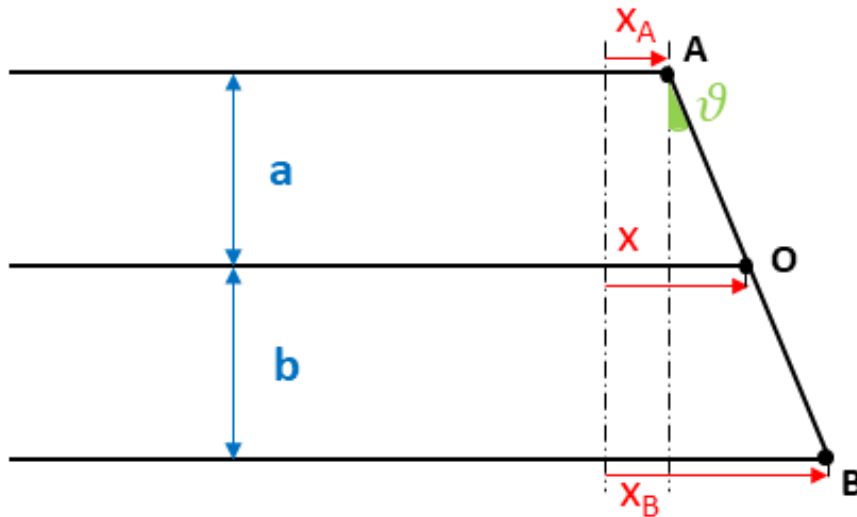Generally, a conventional vehicle has different stiffness for the front and the rear axle, so that the matrix system 1.1 became:

$$\begin{bmatrix} Ffr \\ Ffl \\ Frr \\ Frl \end{bmatrix} = \begin{bmatrix} 1 & 1 & 1 & 1 \\ 1 & 1 & -1 & -1 \\ 1 & -1 & 1 & -1 \\ 1 & -1 & -1 & 1 \end{bmatrix}^{-1} \begin{bmatrix} K_{H(f+r)} & K_{H(f-r)} & 0 & 0 \\ K_{P(f-r)} & K_{P(f+r)} & 0 & 0 \\ 0 & 0 & K_{R(f+r)} & K_{R(f-r)} \\ 0 & 0 & K_{W(f-r)} & K_{W(f+r)} \end{bmatrix} \begin{bmatrix} 1 & 1 & 1 & 1 \\ 1 & 1 & -1 & -1 \\ 1 & -1 & 1 & -1 \\ 1 & -1 & -1 & 1 \end{bmatrix} \begin{bmatrix} xfr \\ xfl \\ xrr \\ xrl \end{bmatrix}$$

(A.5)

Where K_H, K_P, K_R, K_W represent respectively the stiffness for heave, pitch, roll and warp; the subscript in bracket *(f+r)* indicate the sum of front and rear contributions, while *(f-r)* the difference.

For a conventional suspension system, the warp and the roll contribution are the same, so:

$$\begin{bmatrix} Ffr \\ Ffl \\ Frr \\ Frl \end{bmatrix} = \begin{bmatrix} 1 & 1 & 1 & 1 \\ 1 & 1 & -1 & -1 \\ 1 & -1 & 1 & -1 \\ 1 & -1 & -1 & 1 \end{bmatrix}^{-1} \begin{bmatrix} a & b & 0 & 0 \\ b & a & 0 & 0 \\ 0 & 0 & c & d \\ 0 & 0 & d & c \end{bmatrix} \begin{bmatrix} 1 & 1 & 1 & 1 \\ 1 & 1 & -1 & -1 \\ 1 & -1 & 1 & -1 \\ 1 & -1 & -1 & 1 \end{bmatrix} \begin{bmatrix} xfr \\ xfl \\ xrr \\ xrl \end{bmatrix}$$

(A.6)

With:

$$a = \frac{1}{2}(K_{sf} + K_{sr}) \qquad\qquad b = \frac{1}{2}(K_{sf} - K_{sr})$$

(A.7)

$$c = \frac{1}{2}[(K_{sf} + 2K_{ARBf}) + (K_{sr} + 2K_{ARBr})] \qquad d = \frac{1}{2}[(K_{sf} + 2K_{ARBf}) - (K_{sr} + 2K_{ARBr})]$$

With K_{sf} and K_{sr} the stiffness of front and rear coil springs, and K_{ARBf} and K_{ARBr} the stiffness of the front and the rear anti-roll bars.

A.2.2 Roll stiffness

The equation A.7 valid for a standard vehicle is not more appropriate for the proposed suspension system because to control the roll motion there are not the conventional coil springs and the torsion-bars, but a single spring actuated by a lever arm.

The central lever arm's equations seen into the 2.2.3 section and valid for the forces at points A, B, C can be transferred to the stiffness, so that the front-rear roll stiffness distribution depends on the relation between the length a and b of the lever arms:

$$K_{rollF} = \left(\frac{b}{a+b}\right) K_{rollTOT} \qquad (A.8)$$

$$K_{rollR} = \left(\frac{a}{a+b}\right) K_{rollTOT} \qquad (A.9)$$

Where $K_{rollTOT}$ is the stiffness of the roll spring, expressed in N/mm. The calculation of this value for the vehicle chosen will be shown in the next chapter.

A.2.3 Stiffness matrix

The stiffness matrix is obtained from A.5, A.8, A.9 equations:

$$\begin{bmatrix} Ffr \\ Ffl \\ Frr \\ Frl \end{bmatrix} = \begin{bmatrix} 1 & 1 & 1 & 1 \\ 1 & 1 & -1 & -1 \\ 1 & -1 & 1 & -1 \\ 1 & -1 & -1 & 1 \end{bmatrix}^{-1} \begin{bmatrix} a & b & 0 & 0 \\ b & a & 0 & 0 \\ 0 & 0 & c & d \\ 0 & 0 & f & e \end{bmatrix} \begin{bmatrix} 1 & 1 & 1 & 1 \\ 1 & 1 & -1 & -1 \\ 1 & -1 & 1 & -1 \\ 1 & -1 & -1 & 1 \end{bmatrix} \begin{bmatrix} xfr \\ xfl \\ xrr \\ xrl \end{bmatrix} \qquad (A.10)$$

Where,

$$c = \frac{1}{2}(K_{rollF} + K_{rollR})$$

$$d = \frac{1}{2}\left(K_{rollF} - K_{rollR}\right)$$

$$e = \frac{1}{2}\left(K_{warpF} + K_{warpR}\right)$$

$$f = \frac{1}{2}\left(K_{warpF} - K_{warpR}\right)$$
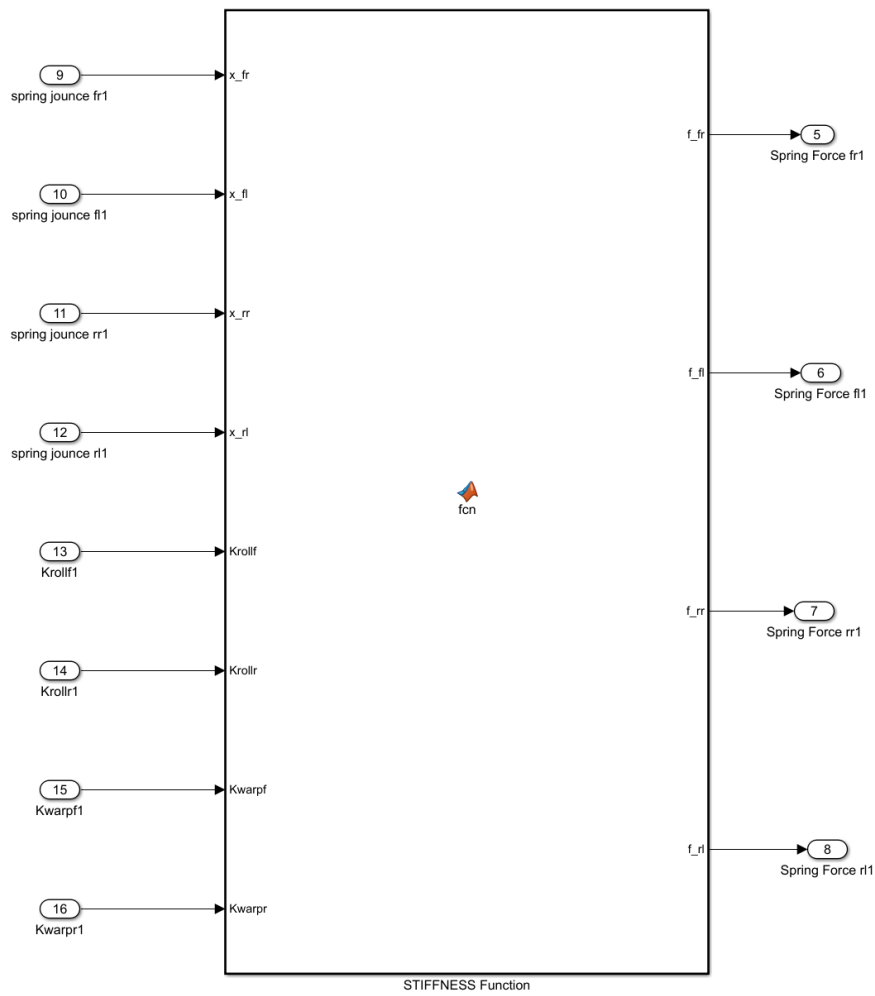
Fig. A.4 The Stiffness subsystem is described by a MATLAB function; it is possible to observe the input and the output of the system.

A.3 Damping subsystem

A.3.1 Damping matrix

The proposed suspension system provides the application of three dampers, divided in:

- A double acting damper on the front axle to control the pitch and the heave mode at front (*element 4* in Fig. A.5);

- A double acting damper to control the pitch and the heave on the rear axle (*element 10* in Fig. A.5)

- A single acting damper with a linear characteristic to control the roll of the whole sprung mass (*element 7*).
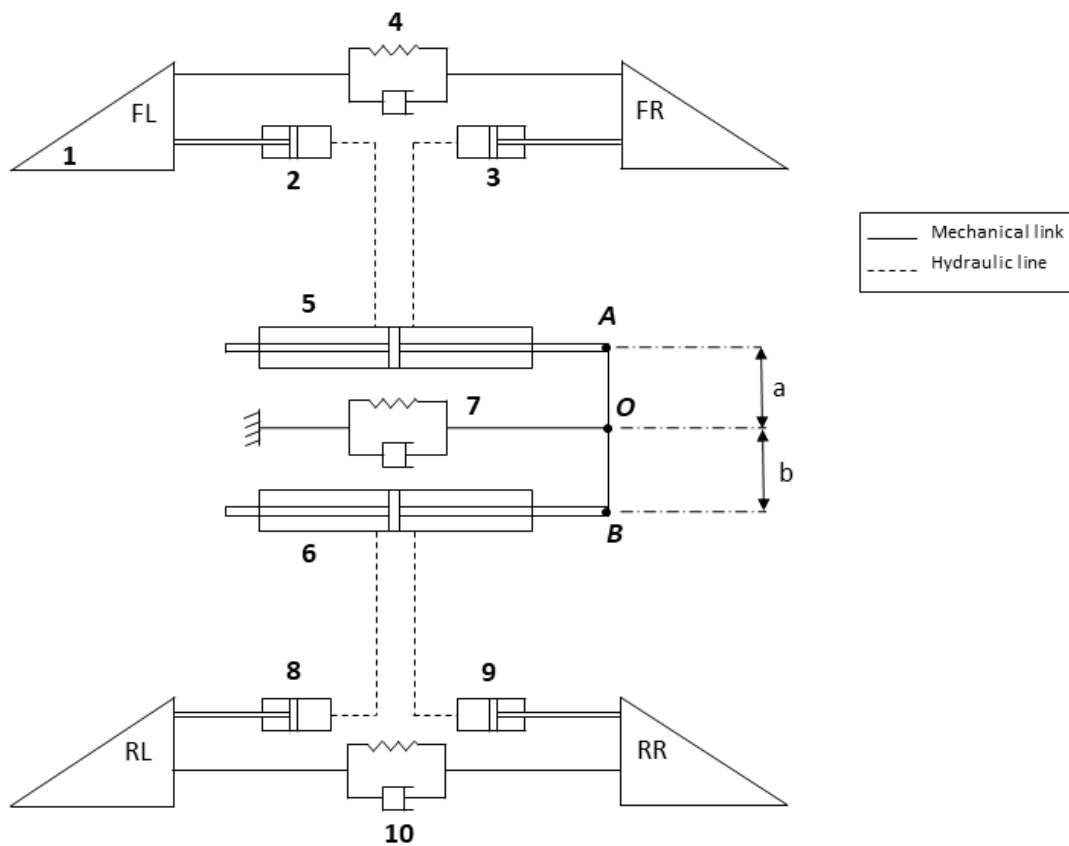
Figure A.5 Overall suspension architecture with interconnection mechanism for the simplified model: 1 Rockers – 2 – 3 – 8 – 9 hydraulic actuators – 4 front heave spring-damper – 5 front double hydraulic cylinder actuator –6 rear double hydraulic actuator – 7 roll spring-damper – 10 rear heave spring-damper.

The warp motion is not provided of a dedicated damper. The present configuration has the advantage to manage the damping curve in an independent way between the pitch and the roll mode, increasing the capability of the suspension to handle the trade-off between handling and

comfort, due the fact that the pitch mode is more involved in the filtering action of road irregularities and the roll mode is more decisive for the performance in handling.

The damper matrix is similar to the one illustrated for the stiffness but it highline an important difference: the nonlinear trend of the damping curves generally employed in the dampers installed in automotive applications; in fact, other the nonlinearity in the bounce and rebound working area, almost always, the curves are not symmetric, so that the behaviour in bounce and rebound are different.

Assuming the case in which, for the damping, we use the same formulation described in the matrix system A.5, substituting the stiffnesses for each suspension mode with the damping coefficients; now, assuming the case in which only the right wheel of the front axle it is subjected to a bump at high speed: the nonlinear curve of the damper gives the fact that the left wheel work in a low damper rate's area while the right wheel in the high speed region, and this is the cause of the fact that the two damping coefficient of the front axle are different (generally the right that impacts the obstacle at higher rate is lower than the left). If we use the formulation A.5 for model the damping systems, because of the matrix formulation we get only one damping coefficient for axle, that is the mean of the left and right damper: this would be wrong and not a realistic representation of the real properties of the automotive dampers.

To overcame this problem, a different solution it is proposed: instead of include the damping coefficients into the matrix system, they are considered at the exit, so that at input of the matrix system we have the damper rate, while at exit a corrected damper rate that takes into account the contribution at each wheel for the suspension mode involved (Fig. A.6).

The damping forces are calculated multiplying the corrected rate exiting from the matrix system with the damping coefficient described as function of dampers' rate through look up table, in order to obtain the same damping curves of the original dampers of the original model of Vi-CarRealTime.

The damping matrix is substituted by an identity matrix:

$$
\begin{bmatrix} vcorr\_fr \\ vcorr\_fl \\ vcorr\_rr \\ vcorr\_rl \end{bmatrix} = \begin{bmatrix} 1 & 1 & 1 & 1 \\ 1 & 1 & -1 & -1 \\ 1 & -1 & 1 & -1 \\ 1 & -1 & -1 & 1 \end{bmatrix}^{-1} \begin{bmatrix} 1 & 0 & 0 & 0 \\ 0 & 1 & 0 & 0 \\ 0 & 0 & 1 & 0 \\ 0 & 0 & 0 & 1 \end{bmatrix} \begin{bmatrix} 1 & 1 & 1 & 1 \\ 1 & 1 & -1 & -1 \\ 1 & -1 & 1 & -1 \\ 1 & -1 & -1 & 1 \end{bmatrix} \begin{bmatrix} vfr \\ vfl \\ vrr \\ vrl \end{bmatrix} \quad (A.11)
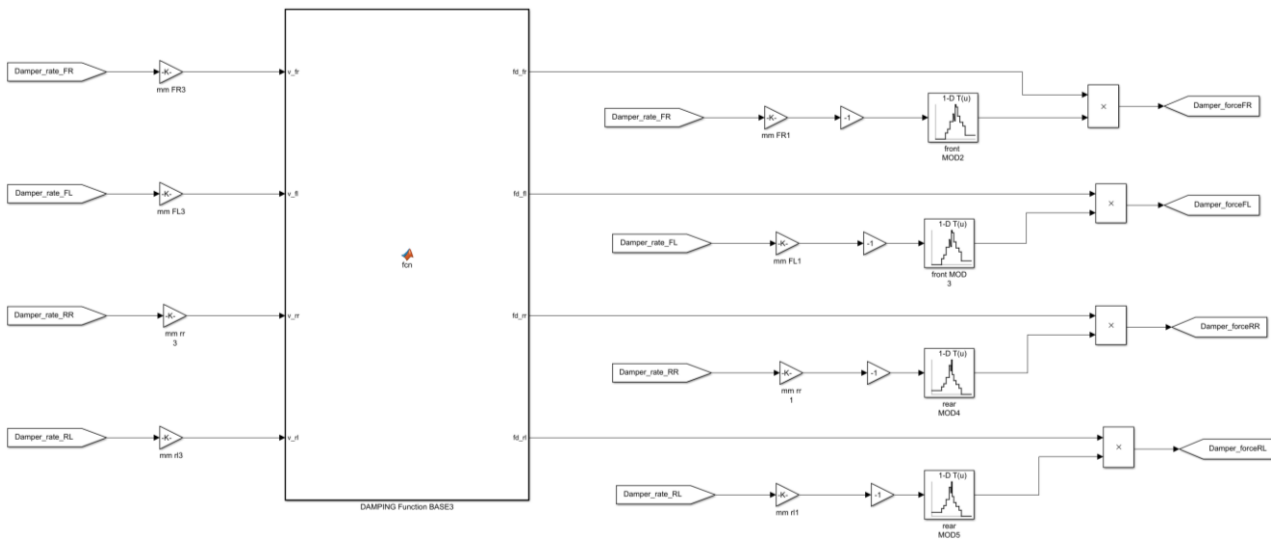$$

Figure A.6 Damping matrix system implementation in Simulink environment.

A.3.2 Interconnected damping matrix

To insert the roll damper effect in the damping modelling it is decided to add its contribution outside of the damping system: in this way the matrix system evaluate only the damping forces due to pitch and heave mode while the roll contribution it is separated and there is no more the uncertainty related to the formulation of the warp damping forces, as for the stiffness.

Furthermore, the roll damping characteristic need to be symmetric so that the different contribution in bounce and rebound in the roll mode disappears; but, it can be nonlinear yet, reason for which it is implemented with a Look-up table as function of the rate of the point O of the central lever arm mechanism (Fig. A.7a).

The way in which this characteristic is evaluated for the vehicle model chosen it is explained in the next chapter.

Based on what it is said above, in the damping matrix we put ' 0 ' instead to ' 1 ' in the roll and warp rows:

$$
\begin{bmatrix} vcorr\_fr \\ vcorr\_fl \\ vcorr\_rr \\ vcorr\_rl \end{bmatrix} = \begin{bmatrix} 1 & 1 & 1 & 1 \\ 1 & 1 & -1 & -1 \\ 1 & -1 & 1 & -1 \\ 1 & -1 & -1 & 1 \end{bmatrix}^{-1} \begin{bmatrix} 1 & 0 & 0 & 0 \\ 0 & 1 & 0 & 0 \\ 0 & 0 & \mathbf{0} & 0 \\ 0 & 0 & 0 & \mathbf{0} \end{bmatrix} \begin{bmatrix} 1 & 1 & 1 & 1 \\ 1 & 1 & -1 & -1 \\ 1 & -1 & 1 & -1 \\ 1 & -1 & -1 & 1 \end{bmatrix} \begin{bmatrix} vfr \\ vfl \\ vrr \\ vrl \end{bmatrix} \quad \text{(A.12)}
$$

And the damping force evaluation became:

$$
F_{d,fi} = F_{p,h} + F_{r,w} = c_{p,h}(v_{fi}) \cdot v_{corr,fi} + \%front \cdot c_{r,w}(v_o) \cdot v_o \quad \text{(A.13)}
$$

$$
F_{d,ri} = F_{p,h} + F_{r,w} = c_{p,h}(v_{ri}) \cdot v_{corr,ri} + \%rear \cdot c_{r,w}(v_o) \cdot v_o \quad \text{(A.14)}
$$

With $i= l, r$ to indicate the left or right vehicle's side; $F_{p,h}$ is the damping force due to pitch and heave mode, $F_{r,w}$ the damping force associated to the roll and warp motion; $c_{p,h}(v_i)$ the damping coefficient for pitch/heave mode, evaluated as function of the four wheels rate v_i ; $v_{corr,i}$ the corrected wheels rate in pitch/heave suspension mode; $c_{r,w}(v_o)$ the roll/warp damping coefficient as function of v_o , the rate of the point O in the central lever arm; finally, the coefficients $\%front$ and $\%rear$, indicate the front and rear roll distribution that represent also the ratio of the rates of the points A and B with respect the point O.
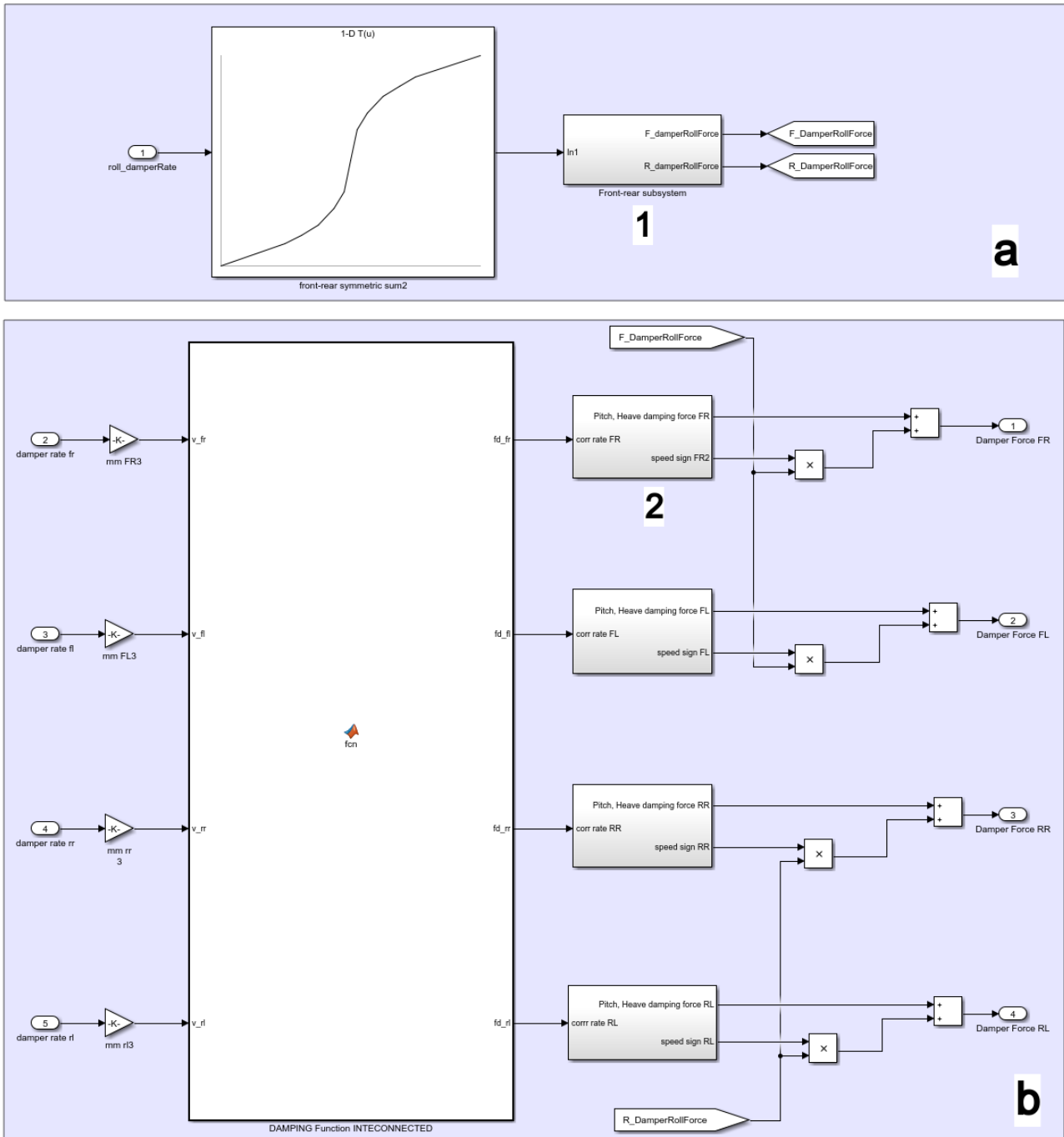
*Fig. A.7 **a)** Front and Rear axle damping force evaluation as a function of the rate of the point O, by means of a Look-Up table that describe the roll damper curve; the subsystem 1 is used to define the front and rear damping force distribution. **b)** Overall damping system integration: the MATLAB function include the matrix system A.12, the subsystems 2 allow to calculate the pitch/heave damping forces multiplying the corrected wheel's rate with the pitch/heave damping coefficient and the sign to attribute at the roll damping forces*

Bibliography

1. M.C. Smith and G.W. Walker, *"Interconnected vehicle suspension"*, Proc. Inst. Mech. Eng. D, J.Automob. Eng.219 pp. 295–307, 2005.

2. W.A. Smith, N. Zhang, *"Recent developments in passive interconnected vehicle suspension"*, Frontiers of Mechanical Engineering in China, 2007.

3. E. Zapletal, *"Balanced suspension"*, SAE Technical Papers, 2000.

4. Toyota Land Cruiser 150 KDSS - https://www.youtube.com/watch?v=NLF6n3nMwww.

5. M. Ortiz, *"Principles of Interconnected Suspensions"* in RaceCar Engineering, vol. 7, 1997.

6. N. Amati, *"Chassis Design A course slides"*, a.y. 2018-2019.

7. C. Scarborough, ScrabTech Twitter - https://twitter.com/scarbstech/status/1151867328189128704

8. https://www.racedepartment.com/threads/setup-confusion-third-spring-lateral.51649/

9. Newton, *"The Motor Vehicle"*, ISBN 0408010827, London; Boston: Butterworths, 1989

10. William D Allison, *US Patent US3419101A. Washington*, DC: U.S, 1968

11. Moulton A E, Best A. *"Hydragas suspension"*, SAE Technical Paper Series, SAE 790374, 1979

12. J. B. Hawley Jr, *US Patent US1647518A*. Washington, DC: U.S, 1927

13. J. Fontdecaba, *"Integral Suspension System for Motor Vehicles Based on Passive Components"*, SAE Technical Paper Series, SAE 2002-01-3105, 2002

14. Smith M C, Walker G W. *"Interconnected vehicle suspension"*, Proc IMechE, Part D. Journal of Automobile Engineering, 2005, 219: 295–307

15. AMZ hydraulic decoupled suspension MathWorks blog - https://blogs.mathworks.com/racing-lounge/2018/02/01/hydraulic-decoupled-suspension-part1/

16. AMZ hydraulic decoupled suspension video - https://www.youtube.com/watch?v=Wxtf-LDbiEM&feature=youtu.be

17. Y. Wu, N. Zhang, "Modelling and performance analysis of a vehicle with kinetic dynamic suspension system", J. of Automobile Engineering, 2017

18. https://www.sae.org/binaries/content/gallery/cm/articles/news/2018/07/lead-image-mclaren-suspension---cropped.jpg

19. W.A. Smith, *An Investigation into the Dynamics of Vehicles With Hydraulically Interconnected Suspensions*, Ph.D Thesis, University of Technology, Sydney, 2009

20. P. Liu, *An analytical study of ride and handling performance of an interconnected vehicle suspension*, Master Thesis, Concordia University, Montreal, 1994.

21. D. Gao, S. Rakheja, Su C Y., *Property Analysis of an X-Coupled Suspension for Sport Utility Vehicles*, SAE Technical Paper Series, SAE 2008-01-1149, 2008

22. W.A. Smith, N. Zhang, W. Hu, *Hydraulically interconnected vehicle suspension: handling performance*, Vehicle System Dynamics, 2010.

23. N. Zhang, W.A. Smith, J. Jeyakumaran, *Hydraulically interconnected vehicle suspension: Background and modelling*, Vehicle System Dynamics, 2010.

24. A. Tkachev, *Vehicle Ride and Handling Control Using Active Hydraulically Interconnected Suspension*, Ph.D Dissertation, University of Technology, Sydney, 2018.

25. J.R. Wilde, G.J. Heydinger, D.A. Guenther, T. Mallin, A.M. Devenish, *Experimental Evaluation of Fishhook Maneuver Performance of a Kinetic Suspension System*, SAE Technical Papers series 2005-01-0392, 2005.

26. J.R. Wilde, G.J. Heydinger, D.A. Guenther, *ADAMS Simulation of Ride and Handling Performance of the Kinetic™ Suspension System*, SAE Technical Papers series 2006-01-1972, 2006.

27. L. Wang, N. Zhang, *Experimental Investigation of a Hydraulically Interconnected Suspension in Vehicle Dynamics and Stability Control*, SAE Technical Papers serie 2012-01-0240, 2012.

28. P. Peiffer, C. Heierli, *Hydraulic Suspension for a Formula SAE Race Car*, ATZextra Worldw 24, 26-29, 2019. https://doi.org/10.1007/s40111-019-0005-z.

29. https://www.motor1.com/photo/1920509/mercedes-amg-project-one-underpinnings/

30. Vi-Grade, '*Vi-CarRealTime 19.2 Documentation*', Vi-Grade Gmbh, 2020.

31. J. Segers, 'Analysis Techniques for Racecar Data Acquisition', second edition, SAE International.

32. Matt Giaraffa, 'Tech Tip: Springs & Dampers, Part One – The Phantom Knowledge', OptimumG –https://optimumg.com/springsdampers1/

33. https://it.motor1.com/features/252529/dossi-artificiali-ecco-quando-sono-legali/

Acknowledgements

È difficile dire quello che provo, perché se da un lato termina un cammino duro, di cui ne ho sempre sognato il termine, ora che l'ho raggiunto rimane la nostalgia di doverlo lasciare per intraprenderne uno totalmente diverso. La vita universitaria mi ha richiesto tanto, tenendomi lontano dai miei affetti, ma dall'altro lato mi ha fatto crescere, mi ha fatto conoscere tante belle persone e vivere tante splendide esperienze che mi hanno reso quello che sono oggi. Di tutto questo conserverò per sempre un dolce ricordo indelebile.

Vorrei ringraziare il Professore Vigliani per la sua enorme disponibilità e per avermi spronato a dare il meglio in questo lavoro di tesi: tutti gli studenti meriterebbero un relatore così. Ringrazio anche il Prof. Galvagno per gli ottimi spunti che mi ha fornito per la riuscita del lavoro.

Un ringraziamento a Vi-Grade nella persona dell'Ing. Ambrogi, da subito pronto a supportarmi nel lavoro e a concedermi uno strumento grazie al quale ho potuto sviluppare una mia idea.

Ma se son arrivato qui, è soprattutto merito di due delle persone più importanti per me, i miei Genitori. Vi ringrazio per il supporto e l'amore che mi avete sempre dato. Vorrei che sentiste questo traguardo anche un po' vostro.

Ringrazio mio fratello, Mario, ha dato un colore diverso a questi tre anni trascorsi insieme.

Un pensiero di ringraziamento a Pietro, Domenico, Francesco, Pierluigi, Salvatore e Vincenzo: avete reso tutto più leggero ed è grazie a voi se avrò un bel ricordo di questi anni.

Un ringraziamento voglio farlo a Luca e Marco, con cui più di tutti ho condiviso quella che è stata una delle esperienze più belle della mia vita e che di più di tutte mi ha messo alla prova: la Squadra Corse. È stato un piacere conoscervi e lavorare insieme.

Ed infine lasciare l'ultimo ringraziamento per una persona speciale: Katia. Averti al mio fianco, nonostante la distanza, è una delle cose che più mi dato certezze. Grazie per esserci sempre stata.